Bioinspired Surface Modification for Antifouling and Antibacterial Applications

by

Anika Benozir Asha

A thesis submitted in partial fulfillment of the requirements for the degree of

Doctor of Philosophy

in

CHEMICAL ENGINEERING

Department of Chemical and Materials Engineering
University of Alberta

Abstract

Biofouling is a serious problem in the medical, marine, and several other industrial fields as it poses significant health risks and financial losses. Therefore, there is a great need to endow surfaces with antifouling and antimicrobial properties to mitigate biofouling. For long-term biofouling resistance, a unifunctional antimicrobial or non-adhesive surface is insufficient for preventing biofilm formation. To overcome this limitation, non-adhesive and antimicrobial dual-functional surfaces are highly desirable. Zwitterionic polymers have been used extensively as one of the best antifouling materials for surface modification. Being a super hydrophilic polymer, zwitterionic polymers need a strong binding agent to maintain attachment to the surface for long-term applications. In this thesis work, new strategies have been explored for surface modification to covalently graft zwitterionic polymers using mussel-inspired dopamine chemistry and prebiotic chemistry for long-term antifouling and antimicrobial applications.

In the first project, a facile surface modification technique using dopamine chemistry was developed to prepare a super hydrophilic coating with both antifouling and antimicrobial properties. Catechol containing adhesive monomer dopamine methacrylamide (DMA) was copolymerized with bioinspired zwitterionic 2-methacryloyloxyethyl phosphorylcholine (MPC) monomer, and the synthesized copolymers were covalently grafted onto the amino ($-NH_2$) rich polyethylenimine (PEI)/polydopamine (PDA) codeposited surface to obtain a stable antifouling surface. The resulting surface was used for *in situ* deposition of antimicrobial silver nanoparticles (AgNPs), facilitated by the presence of catechol groups of the coating. This dual functional coating significantly reduced the adhesion of both Gram-negative *Escherichia coli* and Gram-positive *Staphylococcus aureus* bacteria and showed excellent resistance to bovine serum albumin

adsorption. This bioinspired and efficient surface modification strategy with dual functional coating promises its potential application in implantable biomedical devices.

In the second project, a smart surface was developed which can not only kill the attached microbials but also can release the dead cells and foulants from the surface under a particular incitement on demand. In this project, sugar responsive self-cleaning coating was developed by forming covalent boronic ester bonds between catechol groups from polydopamine and benzoxaborole pendant from zwitterionic and cationic polymers. To incorporate antifouling property and enhance biocompatibility of the coating, zwitterionic compound MPC was chosen and benzoxaborole pendant containing zwitterionic polymer poly (MPC-st-MAABO) (MAABO: 5-Methacrylamido-1,2-benzoxaborole) was synthesized. Additionally, to impart antibacterial properties to the surface, quaternary ammonium containing cationic polymer poly (2-(methacryloyloxy)ethyl trimethylammonium (META)-st-MAABO)) was synthesized. These synthesized polymers were covalently grafted to PDA coated surface by forming a strong cyclic boronic ester complex with catechol group of PDA layer endowing the surface with bacteria contact-killing property and capturing specific protein. After the addition of cis-diol containing competitive molecules i.e. sugars, this boronic ester complex with catechol group of PDA was replaced and attached polymer layer cleaved from the surface resulting in the release of both absorbed protein and live/killed bacteria electrostatically attached to the polymer layer. This dynamic self-cleaning surface can be a promising material for biomedical applications avoiding the gathering of dead cells and debris which is typically encountered on traditional biocidal surfaces.

In practice macro or micro scratches or damages can happen to the coating which can act as an active site for microbial deposition and destroy the antifouling or antibacterial functionality of the

coating. In the third project, an excellent biocompatible and multifunctional coating with antifouling, antibacterial and self-healing property was developed. Prebiotic chemistry inspired self-polymerization of AMN was used as a primary coating layer which act as a primer to graft vitamin B5 analogous methacrylamide polymer poly(B5AMA) and zwitterionic compound MPC containing polymer poly (MPC-st-B5AMA) by forming strong hydrogen bond. B5AMA having multiple polar groups into the structure acted as an intrinsic self-healing material and showed excellent antifouling property against protein and bacteria maintaining a good hydration layer. To impart the antibacterial property into the coating AgNps has also been incorporated which showed more that 90% killing efficiency against both gram-positive and gram-negative bacteria with significant reduction of their adhesion on the surface. Incorporation of self-healing property into the fouling repelling and antibacterial coating can significantly extend the durability of the multifunctional coating making it promising for biomedical applications.

Three different surface modification techniques explored in this thesis, not only demonstrates excellent antifouling and antibacterial property but also provides fundamental insights into the facile development of multifunctional coating in various biomedical applications.

Preface

This thesis is an original work of Anika Benozir Asha under the supervision of Dr. Ravin Narain (Department of Chemical and Materials Engineering) at the University of Alberta.

A part of Chapter 1 of this thesis has been published as Anika Benozir Asha, Yangjun Chen, Ravin Narain, Bioinspired dopamine and zwitterionic polymers for non-fouling surface engineering Bioinspired dopamine and zwitterionic polymers for non-fouling surface engineering in *Chemical Society Reviews*, 2021, 50, 11668-11683. I was responsible for the manuscript composition. Prof. Ravin Narain helped with manuscript writing, revisions and edits.

Chapter 2 of this thesis has been published as Anika Benozir Asha, Yangjun Chen, Huixin Zhang, Sina Ghaemi, Kazuhiko Ishihara, Yang Liu, Ravin Narain, Rapid mussel-inspired surface zwitteration for enhanced antifouling and antibacterial properties in *Langmuir*, 2018, 35(5), 1621-1630. I was responsible for materials synthesis, experimental design, data collection and analysis, as well as manuscript composition. Dr. Yangjun Chen helped with polymer characterization manuscript revision. Dr. Huixin Zhang, Dr. Yang Liu and Prof. Ravin Narain helped with manuscript writing, revisions and edits.

Chapter 3 of this thesis has been published as Anika Benozir Asha, Yi-Yang Peng, Qiuli Cheng, Kazuhiko Ishihara, Yang Liu, Ravin Narain, Dopamine Assisted Self-cleaning, Antifouling and Antibacterial Coating via Dynamic Covalent Interactions in *ACS Applied Materials & Interfaces,* 2022. I was responsible for materials synthesis, experimental design, data collection and analysis, as well as manuscript composition. Dr. Yi-Yang Peng and Dr. Qiuli Cheng helped with polymer characterization and cytotoxicity assay. Prof. Kazuhiko Ishihara and Prof. Ravin Narain helped with manuscript writing, revisions and edits.

Chapter 4 of this thesis has been submitted to Advanced Functional Materials as Anika Benozir Asha, Yi-Yang Peng, Mohammad Reza Gholipour, Kazuhiko Ishihara, Yang Liu, Ravin Narain, Bioinspired Antifouling and Antibacterial Coating with Intrinsic Self-healing Property. I was responsible for materials synthesis, experimental design, data collection and analysis, as well as manuscript composition. Dr. Yi-Yang Peng and helped with polymer characterization and cytotoxicity assay. Dr. Mohammad Reza Gholipour helped with AFM imaging and nano scratch tests. Prof. Ravin Narain helped with manuscript writing, revisions and edits.

Chapter 5 of this thesis is about the overall discussions and conclusions. It contains sections published by me and unpublished literature review, discussion and future studies that result from my PhD studies.

Dedicated to My Beloved Parents

Acknowledgement

First and foremost, I would like to thank and praise almighty Allah who has granted me with countless blessings and given me strength to successfully accomplish this Ph.D. thesis work. I would like to express my heartfelt gratitude to my supervisor Prof. Ravin Narain for providing me this great opportunity. I cannot say thank you enough for his tremendous support. Though I had an unconventional background in my bachelor study, his immeasurable guidance and mentoring helped to overcome all the challenges throughout this arduous journey. He provided me enthusiastic support and encouragement to apply my own ideas which have helped me to broaden my knowledge in the field of polymer chemistry and surface modification. I am honored to have had the opportunity to work with him.

I am grateful to our vibrant research team, my colleague and my friends Dr. Yangjun Chen, Dr. Yi-Yang Peng, Dr. Wenda Wang, Dr. Diana Diaz Dussan and to all current and previous students of Dr. Narain´s research laboratory. My special thanks to Dr. Yangjun Chen and Dr. Yi-Yang Peng for their unconditional support and patience to train me in research work from the first day of my Ph.D. Their constructive comments and guidance helped me a lot to improve my research projects.

I am also thankful to Prof. Yang Liu and her research group for allowing me in her lab to conduct research with gram-positive and gram-negative bacteria. Sincere thanks Dr. Huixin Zhang for providing me with her strong insight into microbiological duties.

I would also like to thank Prof. Michael Serpe and Prof. Larry Unsworth for the help with the use of the goniometer and mechanical shaker throughout my Ph.D. research project. I am also grateful to Dr. Thomas Gengenbach (CSIRO Manufacturing, Melbourne, Australia) for the help with the XPS analysis.

I would like to convey my deepest indebtedness to my respected father and mother who are always the pillar of my every success. Without their support this thesis would never be possible to be finished. I am also thankful to my adorable younger brother and sister for their continuous inspiration towards my higher studies and taking care of my parents while I am away from the family. Last but not least, I would like to thank my beloved husband for his love, patience and understanding during my graduate studies. His continuous encouragement helped me to be focused on my aim and finished my research work smoothly. Thank you for supporting me in everything.

I would like to acknowledge the research funding supported by the Natural Sciences and Engineering Research Council of Canada (NSERC).

Table of Content

List of Figures

List of Tables

List of Schemes

List of Abbreviation

ACVA	4,4’-Azobis(4-cyanovaleric acid)
AEMA	2-aminoethyl methacrylamide hydrochloride
AFM	Atomic force microscope
AgNO3	Silver nitrate
AgNPs	Silver nanoparticles
AMN	Aminomalononitrile
ARGET-ATRP	Activators regenerated by electron transfer atom transfer radical polymerization
ATRP	Atom transfer radical polymerization
BCA	Bicinchoninic acid
BE	Binding Energy
BSA	Bovine serum albumin
CFU	Colony forming unit
DMA	Dopamine methacrylamide
DMAEMA	2-(dimethylamino)-ethyl methacrylate
DMEM	Dulbecco's Modified Eagle Medium

DMF	Dimethylformamide
E. coil	*Escherichia coli*
eV	Electron volt
FT-IR	Fourier-transform infrared spectroscopy
FBS	Fetal bovine serum
GPC	Gel permeation chromatography
HCN	Hydrogen cyanide
LB	Luria-Bertani broth
LBL	Layer by layer
MAABO	5-Methacrylamido-1,2-benzoxaborole
MCT^3	Micro Combi Tester
META	2-(methacryloyloxy)ethyl trimethylammonium
MPC	2-methacryloyloxyethyl phosphorylcholine
MTT	Thiazolyl blue tetrazolium bromide
MW	Molecular weight
NMR	Nuclear magnetic resonance

OD	Optical density
PBS	Phosphate-buffered saline
PC	Phosphorylcholine
PDA	Polydopamine
PEG	Poly(ethylene glycol)
PEI	Polyethylenimine
QA	Quaternary ammonium
RAFT	Reversible addition–fragmentation chain transfer
S. aureus	*Staphylococcus aureus*
SBMA	Sulfobetaine methacrylate
SEM	Scanning electron microscopy
SI-ATRP	Surface-initiated atom transfer radical polymerization
TBT	Tributyltin
TSB	Tryptic soy broth
WCA	Water contact angle
XPS	X-ray photoelectron spectroscopy

List of Publications

1. **Anika Benozir Asha**, Yi-Yang Peng, Qiuli Cheng, Kazuhiko Ishihara, Yang Liu, Ravin Narain, “Dopamine assisted self-cleaning, antifouling and antibacterial coating via Dynamic Covalent Interactions”. ***ACS Applied Materials & Interfaces,*** 2022, 14 (7), pp 9557–9569.
2. **Anika Benozir Asha**, Yangjun Chen, Ravin Narain, “Bioinspired Dopamine and Zwitterionic Polymers for Nonfouling Surface Engineering” ***Chemical Society Reviews***, 2021, 50, pp 11668-11683.
3. Qiuli Cheng, Yi-Yang Peng, **Anika Benozir Asha**, Leitang Zhang, Junbo Li, Zuosen Shi, Zhanchen Cui, Ravin Narain, “Construction of Antibacterial Adhesion Surfaces Based on Bioinspired Borneol-Containing Glycopolymers,” ***Biomaterials Science,*** 2022.
4. Qiuli Cheng, **Anika Benozir Asha**, Yang Liu, Yi-Yang Peng, Diana Diaz-Dussan, Zuosen Shi, Zhanchen Cui, Ravin Narain, "Antifouling and Antibacterial Polymer-Coated Surfaces Based on the Combined Effect of Zwitterions and the Natural Borneol”, ***ACS Applied Materials & Interfaces***, 2021, 13 (7), pp 9006−9014.
5. Wagih Abu Rowin, **Anika Benozir Asha**, Ravin Narain, and Sina Ghaemi, “A Novel Approach for Drag Reduction Using Polymer Coating”, ***Ocean Engineering,*** 2021, 240, pp 109895.
6. Pengtao Gao, Pengrui Jin, Ruben Dumas, Jianjun Huang, **Anika Benozir Asha**, Ravin Narain, Bart Van der Bruggen, Xing Yang “Prebiotic Chemistry Inspired One-step Functionalization of Zwitterionic Nanofiltration Membranes for Efficient Molecular Separation” ***Journal of Membrane Science Letters,*** 2022, 2(1), pp 100013.
7. Wenda Wang, Zicheng Zeng, Li Xiang, Cong Liu, Diana Diaz-Dussan, Zunguo Du, **Anika Benozir Asha**, Wenshuai Yang, Yi-Yang Peng, Mingfei Pan, Ravin Narain, Jifang Liu

"Injectable Self -Healing Hydrogel via Biological Environment-Adaptive Supramolecular Assembly for Gastric Perforation Healing", ***ACS Nano***, 2021, 15(6), pp 9913–9923.

8. Caitlyn Shum**, Anika Benozir Asha**, Ravin Narain, "Carbohydrate Biosensors and Applications", ***Comprehensive Glycoscience 2nd Edition***. Elsevier,2021.
9. **Anika Benozir Asha**, Ravin Narain, "Nanomaterials Properties", ***Polymer Science and Nanotechnology***. Elsevier, 2020. pp 343-359.
10. **Anika Benozir Asha**, Yangjun Chen, Huixin Zhang, Sina Ghaemi, Kazuhiko Ishihara, Yang Liu, Ravin Narain, "Rapid Mussel-Inspired Surface Zwitteration for Enhanced Antifouling and Antibacterial Properties", ***Langmuir***, 2019, *35* (5), pp 1621–1630.
11. Wenda Wang, Li Xiang, Lu Gong, Wenjihao Hu, Weijuan Huang, Yangjun Chen, **Anika Benozir Asha**, Shruti Srinivas, Lingyun Chen, Ravin Narain, Hongbo Zeng , "Injectable, Self-healing Hydrogel with Tunable Optical, Mechanical and Antimicrobial Properties", ***Chemistry of Materials***, 2019, 31 (7), pp 2366–2376.
12. **Anika Benozir Asha**, Shruti Srinivas, Xiaojuan Hao, Ravin Narain, "Enzyme-responsive polymers: properties, synthesis and applications", ***Smart polymers and their applications***. Elsevier, 2019. pp 155-189.
13. Yangjun Chen, Diana Diaz-Dussan, Di Wu, Wanda Wang, Yi-Yang Peng, **Anika Benozir Asha**, Dennis Hall, Kazuhiko Ishihara, Ravin Narain, "Bioinspired Self-Healing Hydrogel Based on Benzoxaborole-Catechol Dynamic Covalent Chemistry for 3D Cell Encapsulation", ***ACS Macro Letters***, 2018, 7(8), pp 904-908.
14. **Anika Benozir Asha**, Yi-Yang Peng, Yang Liu, Ravin Narain, "Rapid Self-Healing, Antibacterial and Antifouling Coating Using Vitamin B5 Analogous Polymer and Prebiotic Chemistry", **Chemistry of Materials**, 2022. (Submitted)

Chapter 1 General Introduction

A portion of this chapter was published in

Journal of Chemical Society Reviews

Reproduced from "A. B. Asha, Y. Chen and R. Narain, *Chem. Soc. Rev*., 2021, 50, 11668 DOI: 10.1039/D1CS00658D" with permission from the Royal Society of Chemistry.

1.1 Why Non-fouling?

Biofouling is highly undesirable to many applications which has become a worldwide costly and serious problem in medical, marine and industrial fields. Biofouling arises from non-specific interaction between wetted surfaces and foulants such as micro- and macro-organisms, biomolecules, plants or algae[1]. Prosthetic implants, biosensors, catheters, vascular stents, dental implants and other medical equipment are prone to surface biofouling due to adhesion of microbial or thrombotic agents[2]. Infection from these biomedical devices and implants can lead to death of the patient. Severe biofouling of ships and underwater structure, ultimately resulting in failure, has become a common threat in marine industry. Increased drag, corrosion, loss of speed and increased fuel consumption etc. are the resulting problems of marine biofouling which also responsible for significant financial losses in this sector[3]. Power plants, textile industries, water-treatment systems and food/beverage industries are the mostly affected industrial sectors because of biofilm formation[4,5]. Production loss, damage to materials, pipe blockage, decreased membrane flux, contaminated water and reduced heat-exchanger efficiency etc. are the resulting problems of industrial fouling. The annual total costs associated with biofouling in the marine industry is nearly $1 billion[6] . The costs associated with infections from biofouling in the medical industry in the United States alone is $6 billion per year[7]. Therefore, endowing surfaces with antifouling and antimicrobial properties to mitigate the biofouling has become a great demand. The surface chemistry and physical properties of the material are both crucial in preventing the recruitment of biofouling organisms. Antifouling commonly refers to all systems that prevent an organism from attaching to a surface. Natural antifouling surfaces exhibit both chemical and physical attributes. Shark, mussel, lotus leaf and crab are common examples of marine organisms who possess natural antifouling defenses[6]. They offer many physical and chemical mechanisms such as low drag,

adhesion and wettability (water repellency and attraction) etc. to control fouling. Inspired by nature, researchers are currently designing antifouling surfaces to combat biofouling which is more environmentally friendly and nontoxic than previously reported approaches. Earlier, the term antifouling was associated only with incorporating biocidal agents such as copper, zinc and tributyltin (TBT) etc. on surface coating with gradual release system[6,8] . The excess release of biocidal compounds is detrimental to non-target organisms and the surrounding environment. A potential alternative approach towards combating biofouling is to alter the characteristics of the material surface to less favorable biological attachment. In this regard, polymers are considered as one of the most prospective materials because of its wide range of antifouling and antimicrobial properties with excellent biocompatibility. A broad range of antifouling strategies are currently employed ranging from coatings to cleaning techniques. Among them, maintaining a strong hydration layer on top of the surface is believed to be the best approach to mitigate surface fouling[9].

1.2 Zwitterion

Among all the approaches for developing novel antifouling surfaces for non-specific protein repulsion, incorporation of hydrophilic polymer layer is the most promising one[10]. Highly hydrated chemical groups with optimized physical properties of the surface, along with appropriate surface coating methods, are the effective strategies for developing stable non-fouling materials for long-term applications**.** Chen *et al.* have classified these non-fouling materials into two major categories, polyhydrophilic and polyzwitterionic[11]. Non-fouling mechanisms of both polyhydrophilic and polyzwitterionic materials are based on creating a hydration layer near the surface and steric repulsion[11–13]. Hydration layer formed by hydrophilic polymers such as PEG and their derivatives, is maintained by weak hydrogen bonds[14]. On the other hand, the hydration layer formed by zwitterionic polymers is more tightly bound through electrostatic interactions

which makes these polymers more effective in resisting the adhesion of fouling agents[15]. PEG based polymers are composed of one oxygen atom in each repeat unit (–CH_2CH_2O–) which can bind only one water molecule through a hydrogen bond, while zwitterions can bind up to eight water molecules by forming electrostatic forces which is stronger than the hydrogen bonding in PEG/water systems[16]. Moreover, reports have shown that PEG based hydrophilic polymers degrade by oxidation, especially in complex media which limits their long-term applications[10]. Zwitterionic polymers have an equimolar number of homogeneously distributed anionic and cationic groups on their polymer chains. Non-fouling zwitterionic polymers can be of two types: Polybetaines with positively and negatively charged moieties on the same monomer unit and polyampholytes with positively and negatively charged moieties on different monomer units[11]. Polybetaines can be further classified into three major groups based on the negatively charged groups: sulfonate-betaines (SB), carboxylate-betaines (CB), and phosphonate-betaines (PB). Among them phosphobetaine-based zwitterionic polymers are considered as biomimetic fouling resistant material as they have phosphorylcholine headgroups which are usually found in the outside layer of cell membranes[17]. Polyampholyte polymer is another class of antifouling polymers which is called *pseudo-zwitterionic* polymer and composed of a pair of separate monomers with uniformly distributed two opposite charge moieties respectively[18]. Polyampholytes with a perfect balance of positive and negative moieties mimic zwitterionic materials and exhibit excellent antifouling properties[19,20]. Uniform charge distribution and charge neutrality of two closely connected opposite charge moieties on the zwitterionic materials are the main reasons for forming maximum electrostatically induced hydration layer and avoiding favorable interaction with proteins [11,16]. Because of the simplicity of synthesis, ease of applicability and availability of functional groups zwitterionic polymers are considered one of the promising

non-fouling biomaterials. Some of the common zwitterionic functional groups are shown in Figure 1.1.

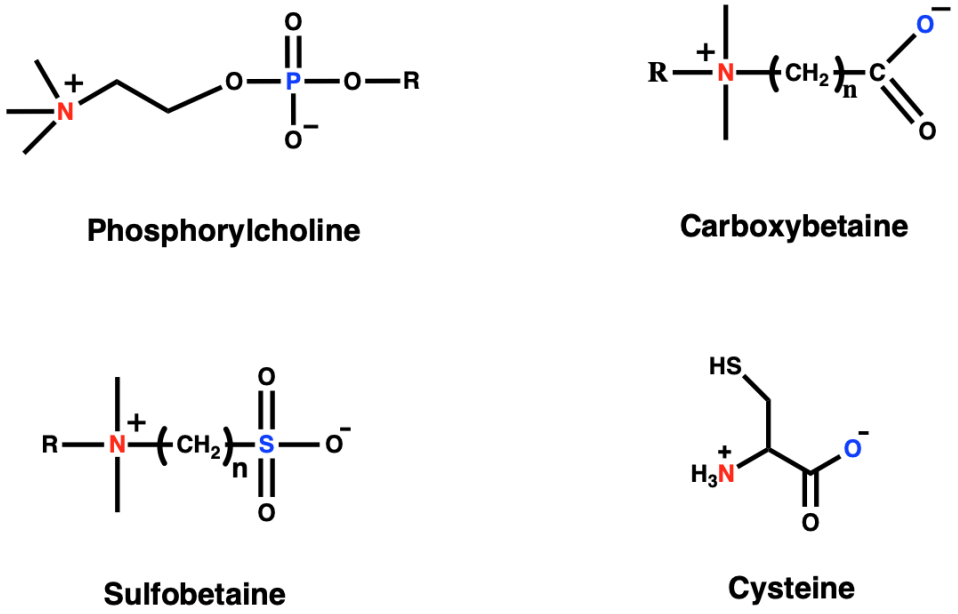

Figure 1.1: Zwitterionic functional groups: phosphorylcholine, sulfobetaine, carboxybetaines, and cysteine. Redrawn with permission from ref 21[21]. Copyright 2014 American Chemical Society.

1.3 Dopamine

Since first reported by Messersmith and co-workers in 2007[22], mussel-inspired dopamine chemistry has been increasingly used for surface modification due to its simplicity, versatility and strong reactivity for secondary functionalization[23,24]. Messersmith and co-workers reported that under oxidative condition dopamine with functional catechol and amino groups, can be self-

polymerized to form a single-step thin coating of polydopamine (PDA) on a wide range of substrates[22]. This approach is mainly inspired by the wet adhesive biomolecules-foot proteins secreted by mussels for attachment to all types of inorganic and organic surfaces[22,25]. Amino acid composition of these foot proteins that found near the plaque-substrate interface, has two key features that inspired PDA: (i) high catechol (3,4-dihydroxybenzene) content due to the presence of 3,4-dihydroxy-L-phenylalanine (DOPA); and (ii) high primary and secondary amine content due to lysine (Lys) and histidine residues[26,27]. Messersmith and co-workers hypothesised that coexistence of catechol and amine functional groups is responsible for strong adhesion to a wide spectrum of materials and identified dopamine as a small-molecule compound that contains both functionalities[22]. They reported that dopamine acts as a powerful building block for spontaneous deposition of thin polymer films of polydopamine on virtually any bulk material surface and the deposited films can easily be adapted for a wide variety of functional uses[22,28].

1.3.1 Polydopamine Structure and Formation

Understanding the chemistry of polydopamine formation is a challenging subject and the details of this mechanism still remain an active area of investigation. A consensus in polydopamine chemistry begins with spontaneous deprotonation of hydroxyl groups under oxidative condition and formation of dopamine-quinone[29]. This oxidation product dopamine-quinone undergoes a nucleophilic intramolecular cyclization and later turns into leukodopaminechrome which subsequently forms 5,6 dihydroxyindole or 5,6 indolequinone through further oxidation and rearrangement[30,31]. At this point there are different proposed chemical pathways leading to final PDA structure and the polymerization mechanism of dopamine. The proposed mechanism includes intermolecular crosslinking of 5,6-dihydroxyindole or 5,6-indolequinone through branching reactions at positions 2, 3, 4, and 7 finally leads to eumelanin like polymer polydopamine[31]. Lee

and coworkers suggested that dimers and trimers formed via oxidation coupling and then assembled to the PDA[32]. It has also been proposed that PDA is composed entirely of noncovalent assemblies of dopamine, dopamine-quinone and 5,6-dihydroxyindole[33], whereas Beck and coworkers hypothesised that these molecules polymerize to form a heteropolymer composed of catecholamine, quinone and indole repeat units[34]. Possible polymerization mechanisms and structures of polydopamine proposed by researchers are shown in Figure 1.2.

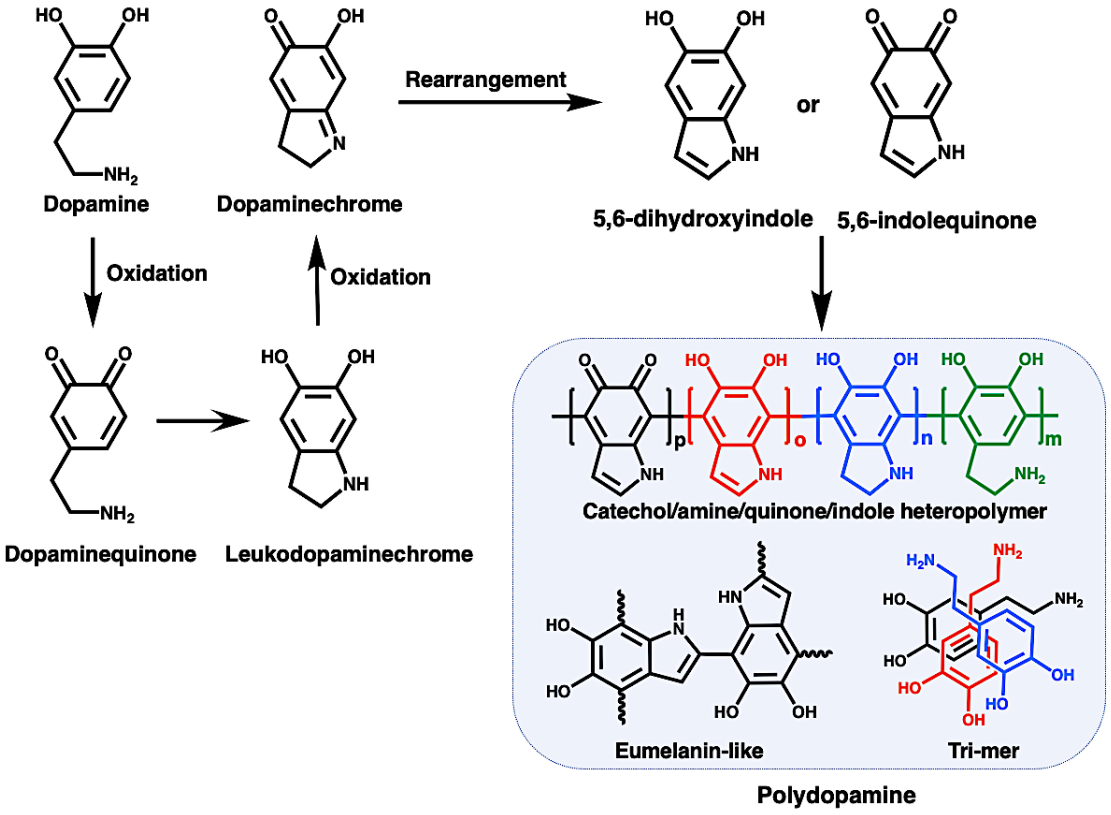

Figure 1.2 : Possible polymerization mechanism of dopamine. Auto-oxidation of dopamine leads to the formation of dopamine-quinone which undergoes further oxidation and rearrangement to form 5,6-dihydroxyindole and 5,6 indolequinone. Proposed possible structures of final product polydopamine ranges from non-covalent trimer assemblies,

eumelanin-like oligo-indoles and covalent coupling of subunits to yield a catechol/amine/quinone/indole heteropolymer.

Thus, a firmly adherent PDA layer can be formed on the surface of a substrate that is immersed in the dopamine solution for a certain time. PDA layer can be tightly attached to any kind of substrate by covalent or non-covalent interactions (such as π-π interaction, charge transfer interactions). PDA coating thickness depends on concentration of dopamine in solution, deposition time, pH and supplied oxygen in the solution[28]. This primary PDA coating can be used without further modification or used as a "primer" onto which a subsequent secondary coating can be applied. The PDA-coated surface layers contain amino groups and phenolic groups, which can react with a variety of molecules via Schiff-base and Michael addition chemistries to facilely immobilize thiol or amine containing molecules and directly reduce metal cations to metal nanoparticles[22,35] (Figure 1.3). Due to great adhesion of PDA with a wide range of polymers, one step PDA coating has been explored as a surface modifier. PDA also serve as a linker for initiators for both atom transfer radical polymerization (ATRP) and reversible addition−fragmentation chain-transfer polymerization (RAFT) techniques (Figure 1.3)[28]. By connecting with these initiators various polymer chains can be grafted onto the PDA modified surfaces via surface-initiated ATRP (SI-ATRP) or RAFT. In the last decade, PDA coating has been utilized in various sectors such as energy storage device, anti-biofouling, antimicrobial surface, drug delivery, cancer nanomedicine, membrane separation technologies, tissue engineering, artificial spore, mechanically tough hydrogels, photonic materials, bone regenerations and so on[33,36]. Among these applications, in most cases PDA coating played the role as an intermediate linker to immobilize other chemical components onto the surface to impart the desired property.

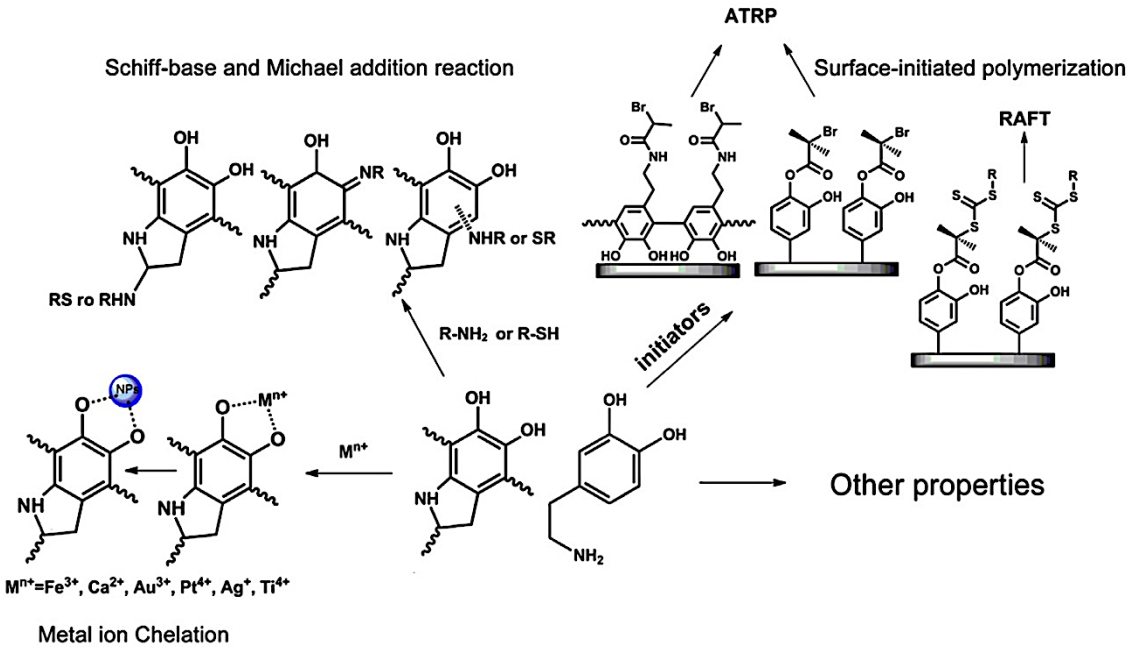

Figure 1.3 Chemical properties of dopamine and PDA as representatives of catecholamine and catecholamine-based materials. Reprinted with permission from ref 28[28]. Copyright 2015 Elsevier.

1.3.2 Comparison of PDA Coating with Other Coating Techniques

Prior to the invention of PDA coating, for polymer coating, three major techniques have been utilized in surface modification chemistry and they are - self-assembled monolayer (SAM)[37–39], layer-by-layer (LbL) assembly[40,4142], and plasma treatment[43,44]. All these methods have specific advantages along with some drawbacks but share a certain surface specificity. Self-assembled monolayers can only be developed on the noble metal (i.e. Cu, Pt, Ag, Au) surfaces[45] using molecules carrying thiol groups through highly specific metal–thiolate bonds[38] or can be deposited on the surface of oxides using alkylsilanes[45] and therefore require matching surface–adsorbate chemistries. On the other hand, robust PDA coating can be deposited onto any kind of surface

with secondary reactivity, whether organic or inorganic, whether hydrophilic or hydrophobic; whether blocky, filamentous or granular; whether metal, polymer or even a living cell[46]. Another interesting surface functionalization technique is polymer thin films assembly via sequential deposition of interacting polymers or layer-by-layer deposition of polyelectrolyte multilayer films of charged surfaces[47]. Though LBL assembly is flexible in terms of substrate choice for deposition and allows post modification, it involves multiple deposition steps using interacting polymers and requires modification of polymers for crosslinking or (bio)functionalization[48]. Therefore, polymers, used in LBL assembly, need to be synthesized specifically with a view toward LBL use or to provide a new function. In contrast, PDA in its simplest form is a synthesis-free method in which the coating with intrinsic chemical reactivity[28] can be built in only one step without the requirement of synthesizing sophisticated polymers or other coating components[33]. As the LBL assembly mostly involves many coating cycles, the formation of multilayers approaching thermodynamic equilibrium is relatively time-consuming process[49] and labor intensive. In terms of costs of the instrumentation, production procedures, number and variety of materials that can be assembled, and surfaces to be coated, it is generally accepted that polydopamine coating is a more suitable, simple, and versatile surface modification method for the fabrication of robust functional multilayer assemblies[33].

1.4 Dopamine and Zwitterion Conjugation

Conjugation of zwitterionic polymer with dopamine is a very promising approach to obtain a non-fouling surface where dopamine serves as surface anchoring motif and zwitterionic polymer serve as antifouling motif. Surface coating with biomimetic zwitterionic polymer has been extensively explored to endow the surface with antifouling properties for medical devices, biosensors and marine coatings applications[10]. Because of the high resistance to the nonspecific adsorption of

proteins and the irreversible adhesion of microorganisms, zwitterionic polymers have been considered as a new generation of antifouling materials[50]. Polydopamine (PDA) layer on the surface is one of the best candidates as a precursor layer to effectively immobilize zwitterionic polymers on the surface. Zwitterionic polymers can be immobilized onto the surface by either 'graft to' or 'graft from' method using dopamine chemistry[51,52]. 'Graft to' method commonly includes synthesis of an end-functionalized polymers and then subsequently adsorbed onto a surface by forming a chemical bond (i.e., chemisorption) or a physical adsorption of polymers via specific interactions of the polymers with the surface (i.e., hydrophobic or electrostatic interactions, hydrogen bonds, antibody-antigen, and geometrical complementary match)[51]. In 'graft to' strategies, polymers may be conveniently characterized prior to grafting but it can be difficult to achieve high grafting density due to steric effects, particularly as the chain length increases. In the case of the 'graft from' method, either an initiator is immobilized or generated on a surface and then *in situ* surface-initiated polymerization with monomers initiated by the immobilized initiators[51]. Compared to the 'graft to' method, "graft from" approach is more promising for synthesizing the polymer brushes on the surface with a high grafting density[10] and well-controlled film thickness. Therefore, dopamine or catechol derivatives can serve as a versatile grafting agent or 'primer' for the convenient and stable anchoring of the zwitterionic polymers onto surfaces by either 'graft to' or 'graft from' approaches.

Based on the recent studies, for zwitterion and dopamine conjugation, these two approaches can be divided into four more methods which are summarized into Figure 1.4. In brief, we have categorized that zwitterionic polymers can be conjugated with dopamine by mostly four methods (Figure 4) : a) Direct modifications by zwitterions with dopamine group, b) Co-deposition of dopamine with zwitterionic polymers, c) Zwitterionic post modification of PDA coated surface,

and d) Surface initiated polymerization of zwitterionic polymer. Here, the first three methods - direct modification, co-deposition and post modification fall under 'graft to' approach and surface initiated polymerization method mainly refers to 'graft from' approach. The details of each method has been discussed later under section 2 and 3.

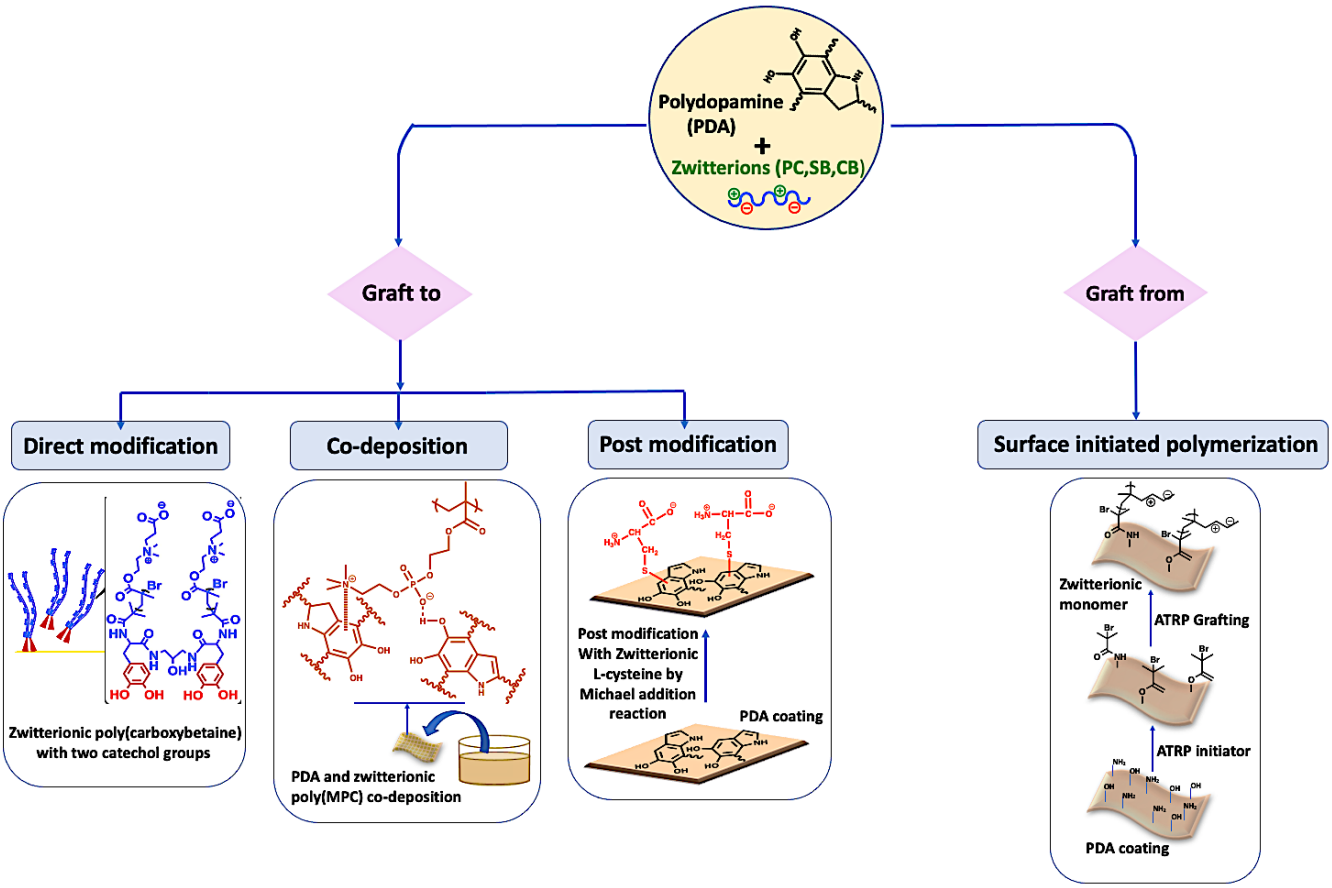

Figure 1.4 Categorization of dopamine zwitterion conjugation into 'Graft to' and 'Graft from' approaches. Examples of four different conjugation methods - direct modification, co-deposition post modification and surface-initiated polymerization which fall under the two major categorization 'Graft to' and 'Graft from' approaches.

Researchers have explored extensively both 'graft to' and 'graft from' method using dopamine derivatives to conveniently anchor zwitterionic polymers on the surfaces for achieving ultra-low

fouling. Jiang and co-workers have developed a series of efficient surfaces modification techniques with dopamine derivatives to anchor zwitterionic polymers such as poly(sulfobetaine methacrylate) (PSBMA)[53–55] and poly(carboxybetaine methacrylate) (PCBMA)[56–58] to obtain super low fouling surfaces in complex media. Their studies were mostly based on grafting or growing zwitterionic polymer brushes on the surface from a synthesized catecholic atom transfer radical polymerization (ATRP) initiator. Elimelech and coworkers developed PDA assisted dual functional zwitterionic and cationic polymer brush coating via activators regenerated by electron transfer atom transfer radical polymerization (ARGET-ATRP) to obtain both antifouling and antibacterial property[59]. All these techniques required multiple step treatment to functionalize the surface which would be costly and time consumable. To simplify the surface modification process, Chen *et al.* developed adhesive monomer dopamine methacrylamide (DMA) containing terpolymers with MPC and cationic monomer by a conventional free radical polymerization and constructed a self-assembled antifouling and contact killing antibacterial surface by a simple one-step dip coating method[60]. Following this one-step dip coating technique, Xu *et al.* utilized the non-covalent interaction between dopamine and zwitterionic polymers and developed dopamine triggered one step co-deposition of zwitterionic monomers (SBMA, MPC and CMA) to fabricate non-fouling surface[61]. They were the first to report that dopamine can act as an initiator for the polymerization of acrylate monomers. Previously, they also fabricated antifouling membrane surface and underwater superoleophobic meshes for oil/water separation by poly(SBMA)/PDA one-step codeposition[50,62]. Emrick *et al*. also utilized this method and co-deposited poly(MPC)/PDA to construct a super hydrophilic antifouling surface using the hydrogen bonding and cation π interpolymer interaction between poly(MPC) and PDA[63]. Later, Xu *et al.* improved this co-deposition time by increasing the oxidation rate of dopamine[64]. As co-deposition rate is

completely dependent on the oxidation of dopamine, they added $CuSO_4$ /H_2O_2 into the solution to produce reactive oxygen free radicals which accelerated the polymerization and deposition rate of PDA with zwitterionic polymers. As PDA coated layer always contains some reactive catechol or amine group, thiol-containing zwitterionic polymers can be easily covalently grafted to PDA coated surface via click chemistry[65,66]. Kang,[65] Lin[66] and coworkers recently utilized this thiol-ene "click" photopolymerization strategy to graft MPC polymer brush from the PDA coated surface to mitigate the surface fouling. Other researchers also utilized dopamine assisted surface initiator immobilization and subsequent surface initiated polymerization of zwitterionic monomer to fabricate antifouling zwitterionic polymer brush[67–69].

1.5 Antifouling Strategies with Zwitterions and Dopamine Using 'Graft to' Approaches

1.5.1 Direct Modification by Zwitterions with Dopamine Group:

To achieve non-fouling surface coating with higher packing density, direct attachment of zwitterionic polymer chains with adhesive groups to the surface in one step is highly desirable because of its simplicity in approach. As zwitterionic polymer is highly water soluble, it is essential to have a strong surface binding group on the zwitterionic polymer to achieve higher packing density and stability. Catechol containing dopamine is a promising candidate as a surface binding group because of its stable surface anchoring property to a wide range of surfaces[22]. With this in mind, in 2008, Jiang *et al.* first developed catecholic ATRP initiator (Figure 1.5) for grafting zwitterionic polymers on gold surface to obtain ultralow fouling surface in complex media[53]. Catecholic oxygens of this initiator were protected by the reaction of dopamine hydrochloride and t-butyldimethylsilyl (TBDMS) chloride. With the help of this protected initiator - bromo-2-methyl-N-[2-(3,4-di(t-butyldimethylsilyloxy)-phenyl) ethyl] propionamide the polymerization of SBMA was carried out via ATRP method. Catechol containing poly(SBMA) polymer was then grafted to

the surface with high packing density by simply flowing the polymer solution over the surface and an excellent antifouling surface was achieved.

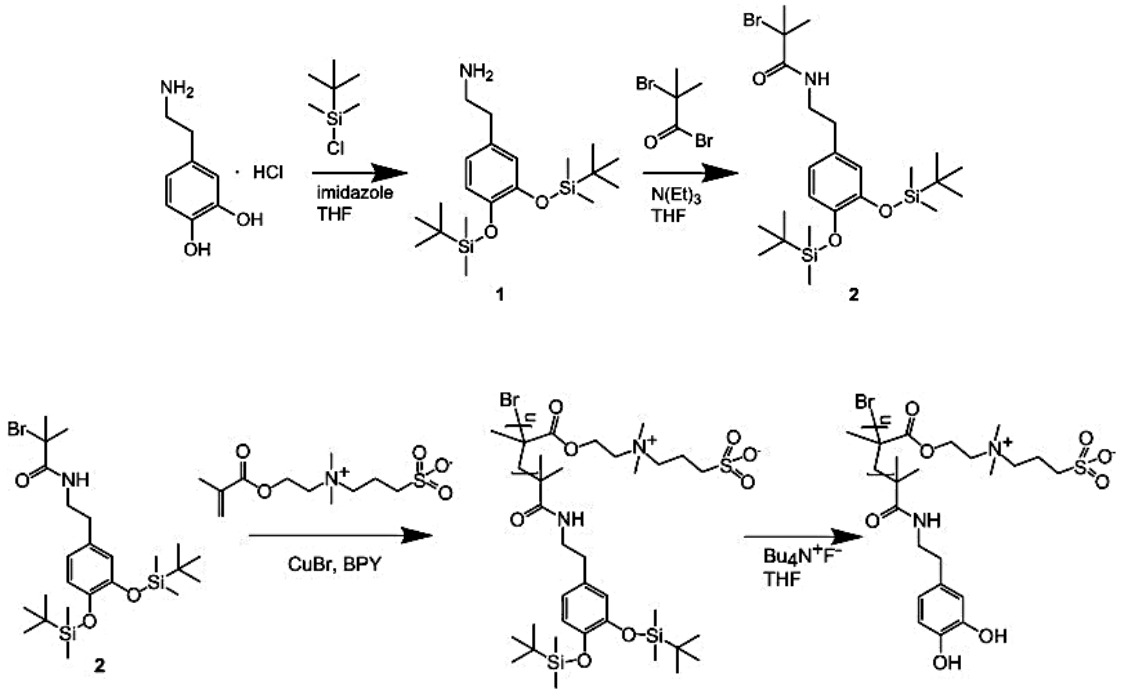

Figure 1.5 Reaction steps for the grafting of poly(SBMA) from the catechol initiator via ATRP, followed by the deprotection of hydroxyl groups before surface adhesion. Reprinted with permission from ref 53[53]. Copyright 2008 Elsevier.

Jiang *et al.* applied this universal one-step dip-coating method to obtain the antifouling property of both hydrophilic and hydrophobic surfaces[54,70]. Zwitterionic sulfobetaine (poly(SBMA)) and extremely hydrophilic carboxybetaine methacrylate (poly(CBMA)) polymers with one catechol chain end from adhesive 3,4-dihydroxyphenyl-l-alanine (DOPA) (i.e. DOPA-poly(SBMA),

DOPA-poly(CBMA)) were applied to a variety of surfaces such as hydrophilic metal oxides (silica) and hydrophobic polymer sheets and fibers (nylon, polystyrene, polypropylene, polyvinyl chloride and teflon etc.). To improve more grafting density of the catechol containing polymer, Gao *et al.* synthesized two catechol groups containing polymer (pCB_2-$catechol_2$) with two zwitterionic poly(carboxybetaine) (pCB) arms[57]. Due to increased surface anchoring group DOPA in the polymer chain, pCB_2-$catechol_2$ showed the best non-fouling properties on the grafted surface with strong surface binding and increased surface coverage (Figure 1.6).

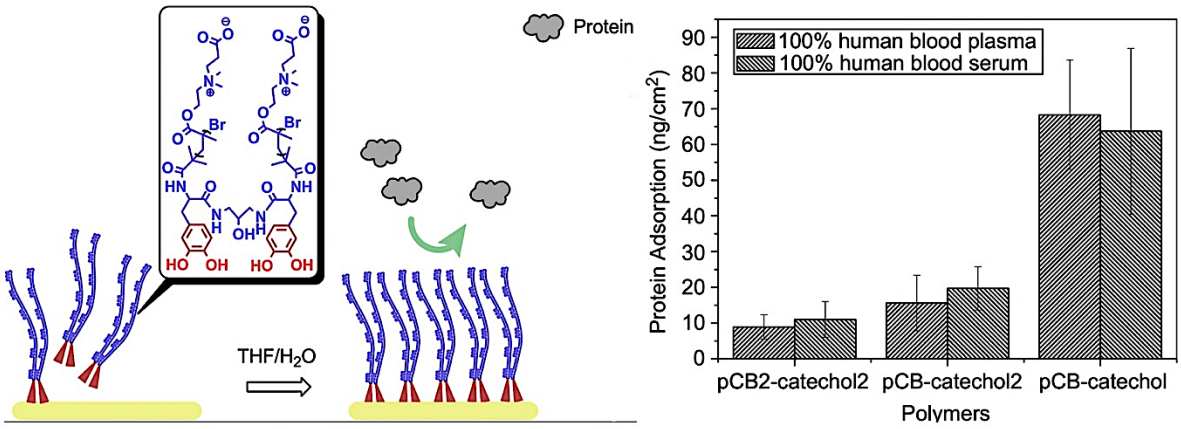

Figure 1.6 Schematic diagram of an antifouling Au surface grafted with pCB_2-$catechol_2$ in THF/H_2O. Reprinted with permission from ref 57 [57]. Copyright 2010 Elsevier.

To increase the coating binding affinity, Sun *et al.* introduced four adhesive L-3,4-dihydroxyphenylalanine (DOPA) groups in poly(CBMA) polymer chain[71]. The presence of four surface binding group in one polymer chain (poly(CBMA)-$DOPA_4$) increased the surface binding affinity along with the antifouling property of coated cellulose paper. Because of the high water

solubility of poly(CBMA)-DOPA, it showed weaker binding to hydrophobic surfaces which led to high fouling. To overcome this solubility problem Subdaram *et al.* included dopamine along with poly(CBMA)-DOPA to promote the attachment of this polymer to any kind of surface[70]. Dopamine can easily polymerize to polydopamine and the catechol group of poly(CBMA)-DOPA polymer chain can react with the amine group present on polydopamine and thus this mixed polymer solution can easily be grafted to any kind of surface with higher surface coverage. In 2014, Zhao *et al*. developed a series of synthetic bifunctional polymers with catechol conjugation to construct self-cross-linked nanolayers on polymeric substrates via the pH induced catechol cross-linking and immobilization[52]. Several bio-functional polymers, i.e., poly(sodium 4-vinylbenzenesulfonate)-co-poly(acrylic acid) (P(SS-co-AA)), poly((2-(methacryloyloxy)ethyl) dimethyl-(3-sulfopropyl)ammonium hydroxide)-co-poly(acrylic acid) (P-(SBMA-co-AA)), poly(poly(ethylene glycol) methyl ether methacrylate)-co-poly(acrylic acid) (P(EGMA-co-AA)), poly-(1-vinyl-2-pyrrolidone)-co-poly(acrylic acid) (P(VP-co-AA)), and poly((2 (methacryloyloxy)ethyl) trimethylammonium chloride)-co-poly(acrylic acid) (P(MTAC-co-AA)), were first synthesized via reversible addition-fragmentation chain transfer (RAFT) polymerization, and then the catecholic molecules (dopamine) were conjugated to these polymers by the facile carbodiimide reaction with acrylic acid units. This mussel adhesion protein inspired dopamine chemistry helped to develop several stable biointerfaces with versatile biological functionalities due to easy immobilization of catechol containing polymers[52]. Ye *et al.* also utilized this carbodiimide chemistry between hyaluronic acid (HA) and dopamine to make a polyanion of the HA-dopamine conjugate for low fouling surface[72]. Chen *et al.* prepared terpolymer containing dopamine, zwitterionic polymer MPC and cations to construct a recycle antibacterial and antifouling surface[60]. This terpolymer of dopamine containing dopamine methacrylamide (DMA),

cationic 2-(dimethylamino)-ethyl methacrylate (DMAEMA) and MPC was synthesized by conventional free-radical polymerization. Pendent DMA of this terpolymer served as a surface adhesive to successfully coat the polymer solution onto the surface by a simple one-step self-assembly method. Instead of a larger polymer chain, Huang *et al.* employed small molecules of zwitterions and dopamine[73]. Without any complex polymerization reactions, they conjugated dopamine molecules with zwitterionic sulfobetaine moiety to obtain a highly packed adhesive thin film through pH transition approach for an antifouling biointerface.

1.5.2 Co-deposition of Dopamine with Zwitterionic Polymers

Compared to traditional 'grafting to' method for zwitterionic polymer immobilization, dopamine-assisted co-deposition is more robust, controllable and can be easily adjusted by changing the pH, deposition time, concentration and atmosphere. Dopamine-assisted co-deposition can greatly simplify the procedure of zwitterionic polymer grafting and enrich possible coating functionality by integrating the deposition and functionalization in a single simultaneous step. In 2012, Lee *et al.* first proposed the concept of dopamine-assisted co-deposition by dissolving dopamine with molecules of a wide range in sizes (10^2 to 10^6 Da) and with various chemistries containing carboxyl, amine, thiol, quaternary ammonium, and/catechol groups[74]. Later inspired by this dopamine assisted co-deposition concept and to avoid complicated multistep procedure for grafting zwitterionic polymer, Xu *et al.* first reported one-step dopamine-assisted co-deposition method for constructing antifouling membrane surface with poly(SBMA)[50,62]. This one step deposition using one-pot mixture of dopamine alkaline solution with polymer, greatly simplifies the coating process and provides an ultrathin composite coating on a variety of surfaces, including glass, silicon, nanofiber, polystyrene, perfluorinated silicon, steel, and microporous polypropylene membranes. Dopamine-assisted co-deposition involves a second component during the deposition

of dopamine, including synthetic polymers or monomers, small organic molecules and nanomaterials.

The mechanism of dopamine-assisted deposition involves single or multiple covalent/non-covalent interactions between dopamine and second component[75]. Compared to the non-covalent co-deposition, the covalent co-deposition provides a robust network to promote the coating stability. Emrick *et al.* utilized dopamine assisted non covalent co-deposition technique to fabricate biocompatible, hydrophilic, and fouling-resistant surfaces via the co-deposition of dopamine and poly(MPC)[63,76,77]. Both poly(SBMA) and poly(MPC) interact with PDA through non-covalent linkages, including electrostatic interaction and hydrogen bonding. Poly(SBMA) interacts with PDA through local electrostatic interactions between deprotonated phenols groups of dopamine and the quaternary ammonium of poly(SBMA)[62]. Poly(MPC) interacts with PDA through phenol-phospholipid hydrogen bonding and cation-π interactions (Figure 1.7)[63].

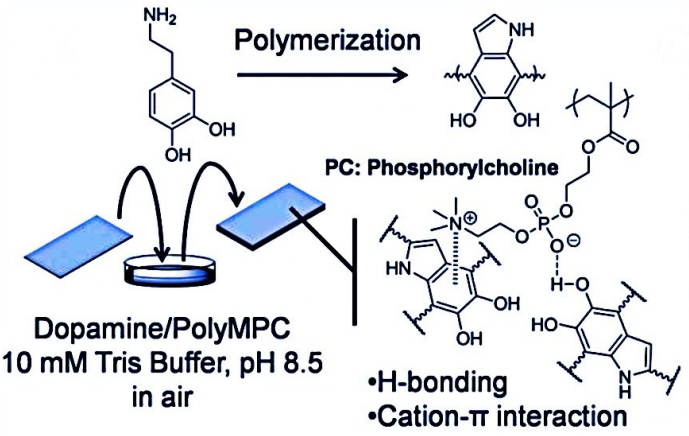

Figure 1.7. Schematic illustration of PDA and poly(MPC) co-deposition coating and the mechanism of the PDA-poly(MPC) non-covalent interactions. Reprinted with permission from ref 63[63].Copyright 2016 Wiley Online.

Coating conditions, deposition time, oxidation of dopamine and solution concentration control the coating thickness of PDA assisted coating. Oxygen diffusion barrier was still a problem for oxidative dopamine polymerization which has been further solved by Xu *et al*.[64,78]. They accelerated the polymerization of dopamine and the deposition rate of PDA coatings by using $CuSO_4/H_2O_2$ as a trigger. Cu^{2+} and H_2O_2 produce a great deal of reactive oxygen free radicals in an alkaline medium which play a key role in rapid polymerization of dopamine and improve the deposition rate of PDA coatings. In this way, they reduced the PDA based co-deposition time from 18 hrs to 1 hr only. PDA based co-deposited coating can also be used for secondary functionalization of the surface because of the presence of some unreacted catechol group in PDA. Unreacted –OH group of PDA based coating can be utilized to incorporate metal nanoparticles into the coating which can impart some antibacterial activities as well. Zhao *et al*. recently reported, novel antibacterial and antifouling membrane via co-deposition of PDA and PEI-SBMA, followed by incorporating bactericidal silver nanoparticles (AgNPs)[79]. One catechol group of PDA can lose two electrons and reduce the diffused Ag^+ ion to Ag^0 and transformed itself into stable 1,2-benzoquinone as shown in Figure 1.8. Thus, the catechol group of PDA can reduce metal ions, including silver and gold ions, into metallic nanoparticles without any reducing agent.

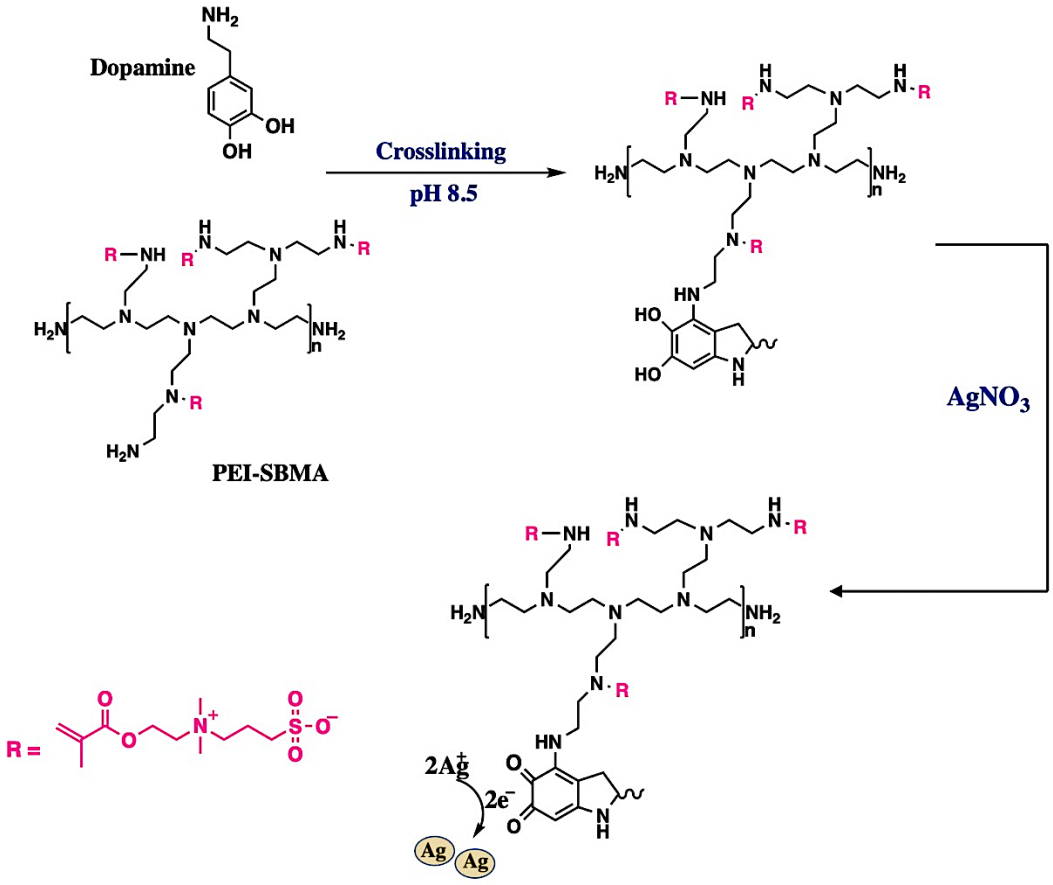

Figure 1.8. Schematic presentation of PDA/PEI-SBMA co-deposition and AgNPs incorporation. Redrawn with permission from ref 78[78]. Copyright 2016 Wiley Online.

1.5.3 Zwitterionic Post Modification of PDA Coated Surface

The catechol motif of polydopamine is more beneficial when it comes to post modification strategies, especially in the context of conjugation with thiol or amine containing molecules. To be specific, the oxidized quinone form of catechol of PDA can undergo reactions with nucleophilic amine or thiol groups via Michael addition or Schiff-base reaction (Figure 1.9) to form covalently grafted functional polymer layer[80]. In a Michael addition reaction between amine terminated polymer and polydopamine, an amine is attached to the catechol ring at the 4- or 5-position, and

in a Schiff base reaction the amine attacks the 2-position of the catechol ring and an imine is created[81]. This reaction mechanism between oxidized quinone of PDA and amine containing polymer depends on the type of amine. Generally, aromatic amines favor the Michael- addition reaction, whereas aliphatic amines favor the Schiff base reaction[81]. Similarly, the electrophilic oxidized quinone of PDA is highly reactive towards nucleophilic thiol groups and can react with thiol terminated polymer via the Michael addition reaction to form catechol–thiol adducts.

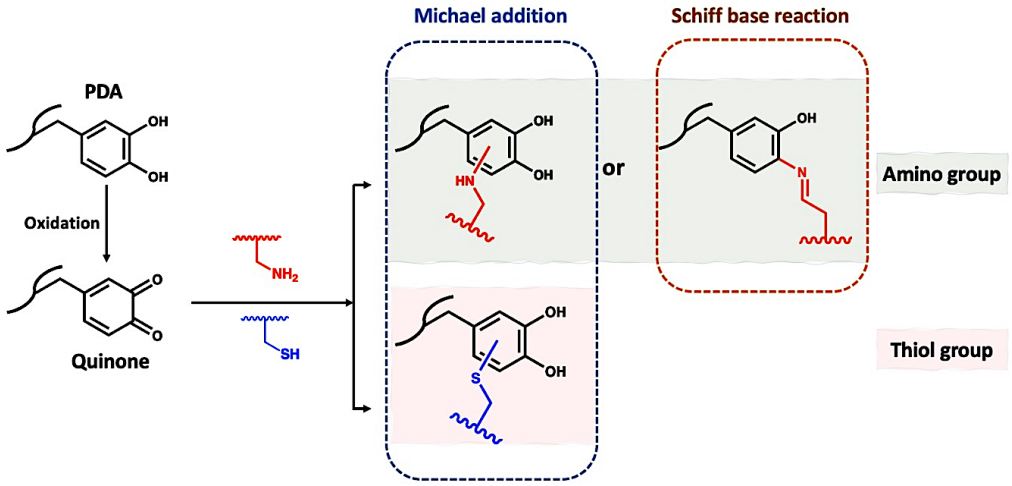

Figure 1.9. Reactions of oxidized quinone of PDA with amines and thiols via Michael addition and Schiff base reaction. In a Michael addition reaction both amino group and thiol group attacks the catechol ring at the 4- or 5-position, whereas in a Schiff base reaction the amino group attacks the 2-position of the catechol ring of PDA.

1.5.3.1 PDA and Thiol Group Containing Zwitterionic Polymer Conjugation

Catechol–thiol adducts have been detected in many different systems. Inspired by this dopamine chemistry, in 2013, Jian Shen *et al.* covalently grafted thiol and amino group containing

zwitterionic material cysteine to the PDA coated PET sheets via thiol-ene Michael addition reaction to improve the antifouling and hemocompatibility property[82]. Being pH responsive, the post modified surface with cysteine coating can act as a self-cleaning surface which was further investigated by Shevate *et al.* by anchoring cysteine on the PDA coated membranes via Michael-addition reaction at 50°C to alleviate the antifouling ability of the membrane with foulants solution.[83] Cui et al. also immobilized zwitterionic glutamic acid and lysine-based peptides onto PDA coated noble metals, metal oxides, polymers and semiconductors via Michael-addition reaction between thiol of peptides and quinone of PDA groups to obtain surface-independent low fouling surfaces[84]. For long-term application and to overcome the high water solubility of zwitterionic polymer this two-step PDA assisted coating technique is convenient and effective. To prove this concept, Lin *et al.* grafted dithiol-containing poly(MPC-co-2-(methacryloyloxy)ethyl lipoate (MAEL)) copolymer to PDA coated via Michael addition reaction[66] [44]. They first modified the membrane with a thin layer of PDA coating in Tris-buffer solution. Then covalently grafted the dithiol containing poly(MPC-co-MAEL) copolymer synthesized by RAFT polymerization technique. Thiol-functional group containing zwitterionic copolymers grafting showed increased hydrophilicity and superior long term antifouling properties[66]. Xu *et al.* utilized click chemistry to assemble zwitterionic and cationic binary polymer brushes onto PDA-anchored stainless steel (SS) surfaces[65]. Zwitterionic poly(MPC) was first polymerized grafting from the PDA functionalized SS surface via thiol−ene "click" reaction. Alkynyl-modified cationic poly(2-(methacryloyloxy) ethyl trimethylammonium chloride) (alkynyl-poly(META)) was then grafted to the surface via azide−alkyne "click" reaction. This poly(MPC)/poly(META) binary polymer brushes grafted via click chemistry to the PDA modified surface showed very stable (more than 30 days) and durable antifouling and antibacterial properties[65].

1.5.3.2 PDA and Amine Group Containing Zwitterionic Polymer Conjugation

Similar to these 'thiol-functional' groups containing zwitterionic polymer grafting, PDA layer also can act as an intermediate layer to immobilize 'amine-containing' molecules via Michael addition or Schiff- base reaction. Shen *et al.* successfully immobilized small zwitterionic molecule lysine (contains two amine $–NH_2$ groups) to the pre coated PDA layer via amino-ene Michael addition reaction and obtained excellent biocompatible and antifouling surface[85]. To avoid the selectivity of only amine functional group containing zwitterionic molecule grafting on PDA coated surface, Wang *et al.* synthesized a copolymer of acrylate zwitterionic molecule SBMA with 2-aminoethyl methacrylate (AEMA) named as poly(SBMA-co-AEMA)[86]. The amino groups ($–NH_2$) of AEMA segment reacted with PDA-modified surface by Michael addition or Schiff base reactions and opened a new possibilities of grafting zwitterionic copolymers with amino group pendant chain. Besides, by controlling the content of $–NH_2$ in the copolymers through adjusting the ratio of Zwitterion/AEMA the interaction of the copolymer with PDA coating can also be enhanced.

Instead of utilizing the amine functional group from zwitterionic molecule/polymer, researchers had also employed the amine groups in the bulk PDA layer and grafted amine free zwitterionic molecule/polymer on the PDA coated surface covalently. Using this two-step post modification approach, Liu *et al.* developed a new conjugation technique to the formation of *β*-amino carbonyl linkages between the amine functional group of PDA and acrylate/acrylamide zwitterionic molecules (Sulfobetaine acrylamide (SBAA) and SBMA) via the aza-Michael reaction (Figure 1.10) for developing the multifunctional antifouling interfaces in a substrate-independent fashion[87]. The aza-Michael addition is of synthetic importance, in which the nucleophilic amine groups of PDA coating attach to the α,β-unsaturated carbonyl compounds.

To enhance the interaction between PDA coating and zwitterionic compound, by utilizing amine groups of PDA coated surface, recently Narain and coworkers have developed a robust strategy by covalently grafting adhesive monomer DMA and zwitterionic MPC containing copolymer poly(MPC-co-DMA) onto amino ($-NH_2$) rich polyethylenimine (PEI)/PDA co-deposited surface[88]. Co-deposition of PEI and PDA helped to decorate the surface with more anchoring sites (more nucleophilic amine groups on the surface) available for zwitterionic compound grafting. The resulting surface was also treated for *in situ* deposition of antimicrobial silver nanoparticles (AgNPs), facilitated by the presence of catechol groups of the coating to impart antibacterial property.

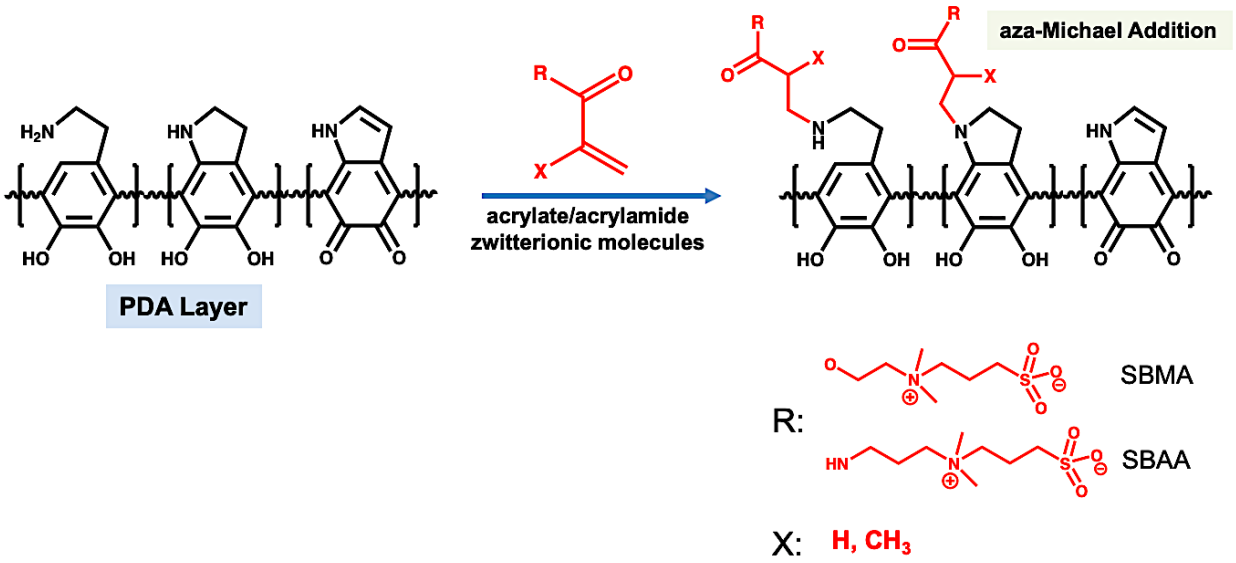

Figure 1.10. PDA and acrylate/acrylamide zwitterionic molecule conjugation by the formation of β-amino carbonyl linkages via aza-Michael addition reaction. Redrawn with permission from ref 87[87]. Copyright 2016 American Chemical Society.

1.6 Antifouling Strategies with Zwitterions and Dopamine Using 'Graft from' Approach

1.6.1 Surface Initiated Polymerization of Zwitterionic Polymers

One of the most effective methods to prevent biofouling are grafting the zwitterionic monomers from a surface via surface-initiated atom transfer radical polymerization (SI-ATRP). Due to its controlled/living feature, this SI-ATRP has been widely developed to generate non-fouling polymer brushes with high packing densities and controllable film thicknesses[89]. One of the challenges of the conventional SI-ATRP method are the selectivity of chemically reactive surfaces for covalent immobilization of ATRP initiators[90]. The most conventionally used ATRP initiators that can assemble on a substrate surface are thiol, chlorosilane and alkoxysilane-based[91–93]. The binding chemistries of these ATRP initiators are substrate-dependent. For example, the thiol-based initiator is only effective on gold and some noble metal substrates, and the chlorosilane or alkoxysilane-based initiators are effective on oxides surfaces[94].

To overcome this limitation of SI-ATRP for the selective substrate surface, mussel-inspired robust adhesive dopamine chemistry has been extensively studied to deposit the PDA layer onto a wide range of surfaces and thereby acts as an efficient platform for further surface immobilization of ATRP initiators[67,95–97]. To show the efficiency of dopamine for the immobilization ATRP initiators, Chang *et al.* compared catecholic dopamine and organosilane as the respective anchor site for subsequent immobilization of ATRP initiator onto stainless steel surface and poly(SBMA) polymerization[68]. In their study, poly(SBMA) brushes grown from the respective dopamine and silane-assembly layers were compared for the effectiveness in resisting the adhesion of plasma protein, blood cells, mammalian cells, and bacteria. Results showed that poly(SBMA) grafted from polydopamine interfacial layers achieved better bioadhesion resistance than from silane-based assembly layers. Such dopamine-initiated ATRP can be applied to nearly any substrate to achieve

the desired surface chemical characteristics, shapes and sizes for growing antifouling polymer brushes from the surface. This dopamine-initiated ATRP method can be divided into two approaches. In the first approach, most of the researchers first coated the surface with dopamine followed by immersing that PDA coated substrate into ATRP initiator aqueous solution for cross linking the PDA oligomers with the ATRP initiator and then grew zwitterionic polymer brushes from the modified surface[95–98](Figure 1.11). The amount of initiators immobilized on surfaces determines the graft ratio of zwitterionic polymers on membrane surfaces[56] . Usually in SI-ATRP, the initiator's primary concentration on a surface remains very low compared to that used for bulk or solution ATRP[99]. Therefore, to obtain thicker polymer brushes at a faster growth rate and to establish an equilibrium between dormant and active chains during SI-ATRP, an excess amount of deactivating Cu(II) complex in the form of CuBr is usually added.

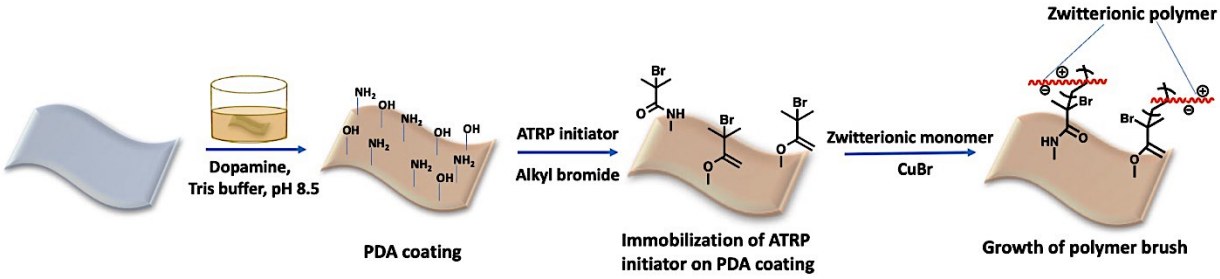

Figure 1.11. Schematic illustration for surface initiated ATRP for generating zwitterionic polymer brush on PDA coated surface through immobilization of ATRP initiator onto the PDA coated surface.

In another approach, the researchers studied modified polydopamine as an initiator layer for SI-ATRP, which was synthesized by reacting dopamine with ATRP initiator before

deposition[67,100,101]. This ATRP initiator modified dopamine film subsequently act as initiator to initiate polymerization of antifouling monomers from the surface using activators regenerated by electron transfer (ARGET) – ATRP. As the conventional SI-ATRP has few limitations including the use of relatively high concentration of catalyst complexes, rigorous removal of oxygen and the purification of polymers, the newly developed ATRP initiating system ARGET-ATRP can help to mitigate these limitations by introducing reducing agent (i.e., ascorbic acid) and reducing the concentration of the catalyst[90,98]. Recently, Gong *et al.* reported an universal strategy of preparing stable zwitterionic polymer brushes by integrating the advantages of both PDA chemistry and ARGET-ATRP[90]. In their study, a PDA adhesive layer was first dip-coated on a substrate, followed by covalent immobilization of 3-trimethoxysilyl propyl 2-bromo-2-methylpropionate (SiBr, ATRP initiator) on the PDA coated surface via condensation reaction between the silicon hydroxyl and the PDA hydroxyl groups. Then, SI-ARGET-ATRP was performed in a zwitterionic monomer solution catalyzed by the parts per million level of $CuBr_2$ without deoxygenation (Figure 1.12). This conveniently fabricated zwitterionic polymer brush coatings were demonstrated to have stable, ultralow fouling, and extremely blood compatibility.

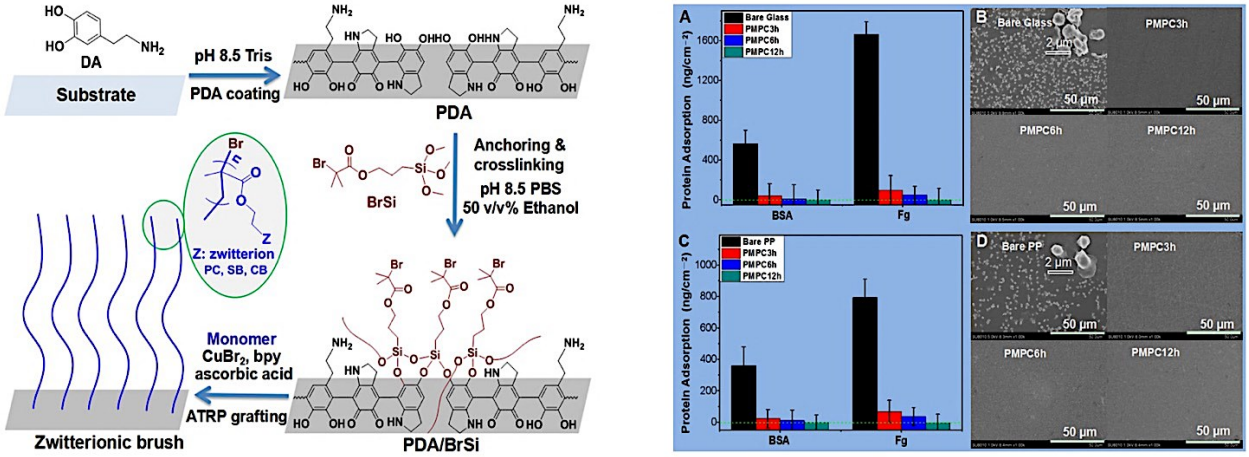

Figure 1.12. Schematic illustration of zwitterionic polymer brush construction on a material-independent substrate by PDA universal adhesion, trimethoxysilyl group cross-link, and ATRP initiator covalent immobilization (left), (A, C) Protein adsorption and (B, D) platelet adhesion results on (A, B) glass and (C, D) polypropylene (PP) surfaces grafted with PMPC brushes for different hours. The graft polymerization was carried out in aqueous solution containing 20 mg mL^{-1} MPC, 0.0036 mg mL^{-1} $CuBr_2$, 0.0152 mg mL^{-1} bipyridine (bpy), and 0.14 mg mL^{-1} ascorbic acid at 50 °C. Protein adsorption amount was measured by the BCA assay (right). Reprinted with permission from ref 90[90]. Copyright 2020 American Chemical Society.

1.7 Applications

In the past few years, polydopamine and zwitterion conjugation has attracted considerable interest for various types of applications ranging from marine to biomedical industries. Because of the unique molecular structure of zwitterionic compounds, they have been widely used as promising candidates to tune the interface properties of materials in various fields. In conjunction with adhesive domain dopamine or dopamine derivatives, these zwitterionic compounds are broadly utilized in biomedical applications due to their dual capabilities for fouling resistance and

functionalization. In most of the applications polydopamine based simple and versatile surface modification techniques play three common roles: surface coatings, interlayers for better compatibility and interlayers for further functionalization. Apart from antifouling application, this dopamine-zwitterion novel conjugation has been employed to waste water treatment, drug carriers, wound healing and biosensors etc. In Table 1, we have summarized the recent advances in the dopamine and dopamine derivatives mediated surfaces in conjugation with zwitterions for various applications.

Table 1.1. Summary of the recent applications of dopamine-zwitterion conjugation

Substrate	Antifouling zwitterionic compound	Conjugation mechanism with dopamine/dopamine derivatives	Applications	Refs.
Stainless steel	SBMA	ATRP	General anti-bio adhesive against plasma protein, blood cells, mammalian cells, and bacteria.	[68]
Commercial thin-film composite (TFC) membranes	SBMA	ARGET-ATRP	Mitigate biofouling on TFC membranes used in desalination technology for global water production	[59]
Cellulose nanofibers	MPC	Sequential deposition and co deposition	Antifouling nanofiber mats for tissue engineering scaffolds and water purification technologies.	[76]
_	1,3-propane sultone	Ring opening reaction	Scarless wound healing	[102]

Electrospun poly (L - lactic) acid (PLLA) film	SBMA	ATRP	Ultra low fouling in complex media for biomedical application	[55]
Sensor chip of surface plasma resonance (SPR) instrument.	MPC	Amidation reaction with intermediate PDA layer	Advanced antifouling surfaces for clinical catheters, vascular stent, artificial lung, hemodialyzer, biomedical devices and long circulating nanocarriers	[103]
Polydimethylsiloxane (PDMS) membranes	CBMA	ATRP	Anticoagulant biomaterials with reduced platelet fouling	[58]
Silicon wafer, glass and stainless steel mesh	MPC, SBMA	Hydrogen bonding, cation- π interaction and electrostatic interaction	Underwater super oleophobic surface for oil/water separation	[62,63]
Cellulose paper, Gold and silica	CBMA	ATRP	Functionalized biosensor for sensing and detection in complex media	[57,71,104]
Titanium Surface	MPC	ATRP	For improved hemocompatibility of cardiovascular stent and some other biomaterials.	[95]
Stainless steel	MPC	SI-ATRP	Marine antifouling	[96]
Polypropylene	SBMA	SI-ATRP	Oriented antibody immobilization and immunoassay	[105]
Poly(ethylene terephthalate) (PET)	Cysteine, Lysine	Michael addition reaction	Hemocompatible anti-biofouling	[82,85]

Ultrafiltration (UF) membranes	SBMA	Michael addition reaction	Waste water reuse in water treatment	106
Polyethersulfone ultrafiltration membrane	SBMA	Schiff-base and Michael addition	Ultrafiltration membranes for reduced biofouling in skim milk filtration	107
PVDF membrane	MPC	Amidation reaction	Oil/Water separation	108
Poly(lactic acid) membrane	SBMA	ATRP	Hemodiafiltration for hemodialysis	109
Poly(lactic-co-glycolic acid) nanoparticles	CBMA	Schiff-base	Nano drug carriers	23
Mesoporous silica nanoparticles	CBMA	ATRP	Stealth multifunctional biocarriers for drug delivery / diagnostics	110
Glass, mica, and gold	SBMA	Crosslinking	antifouling , anti- freezing and antifogging	111

1.8 Challenges of Dopamine – Zwitterion Conjugation

Though most of the dopamine-zwitterion conjugation strategies have shown excellent results in combating the problem of fouling, some of them are also associated with shortcomings related to stability, and complexity of the method of fabrication.

Superhydrophilic zwitterionic polymers have been extensively used as a promising antifouling material for surface modification. However, it remains challenging to form a thick layer with high zwitterion content on the surfaces with different degrees of hydrophilicity. Since the zwitterionic polymer brush chain non-covalently attached to the surface often suffer stability problems, researches have widely exploited mussel-inspired polydopamine (PDA) adhesive functional layer

to attach zwitterion layer stably via thiol and amine chemistry. Due to material-independent coating ability, simplicity of the deposition process, and the unique and broad ranging capabilities for donating sufficient binding sites for antifouling agents PDA coating has become the most convenient and universal coating material to graft other polymers. The conjugation of PDA and zwitterionic polymer act as one of the most effective antifouling systems with durable performance. The key to graft zwitterionic polymers using dopamine is to optimize the functional groups of the zwitterionic monomers that can react with PDA to achieve uniform layers and high zwitterion content on the surface for maximum antifouling properties. Despite several notable achievements on PDA-zwitterion conjugation, there are still some challenges in this field including better understanding of PDA formation mechanisms, enhancement of mechanical robustness of PDA coating, and extension of the PDA coating approach to large scale industrial applications.

1.9 Prebiotic Chemistry-Inspired Aminomalononitrile (AMN) Coating:

Hydrogen cyanide (HCN) derived polymers in the research of prebiotic chemistry have been widely explored as a possible building block to the origin of life [112]. Among them AMN – a trimer of HCN has recently been reported as cross linked nitrogenous coating for simple and biocompatible surface modification purposes[112]. Similar to polydopamine and polyphenol based versatile coating mechanism, AMN polymerizes spontaneously when the commercially available *p*-toluenesulfonate is neutralized in basic buffer solution [113,114]. The adhesive AMN film can be deposited as a brown colored coating to a wide range of surfaces at room temperature[112]. The polymerization and deposition mechanism of AMN film is still under investigation. However in a recent study Vincent *et al.* proposed a possible chemical structure (Figure 1.13) of self-polymerized AMN through investigating the polymeric material obtained at the solid-liquid

interface from an AMN based solution at pH = 8.6 [114]. AMN contains a primary amine group, an active methylene and two activated nitrile groups in its structure.

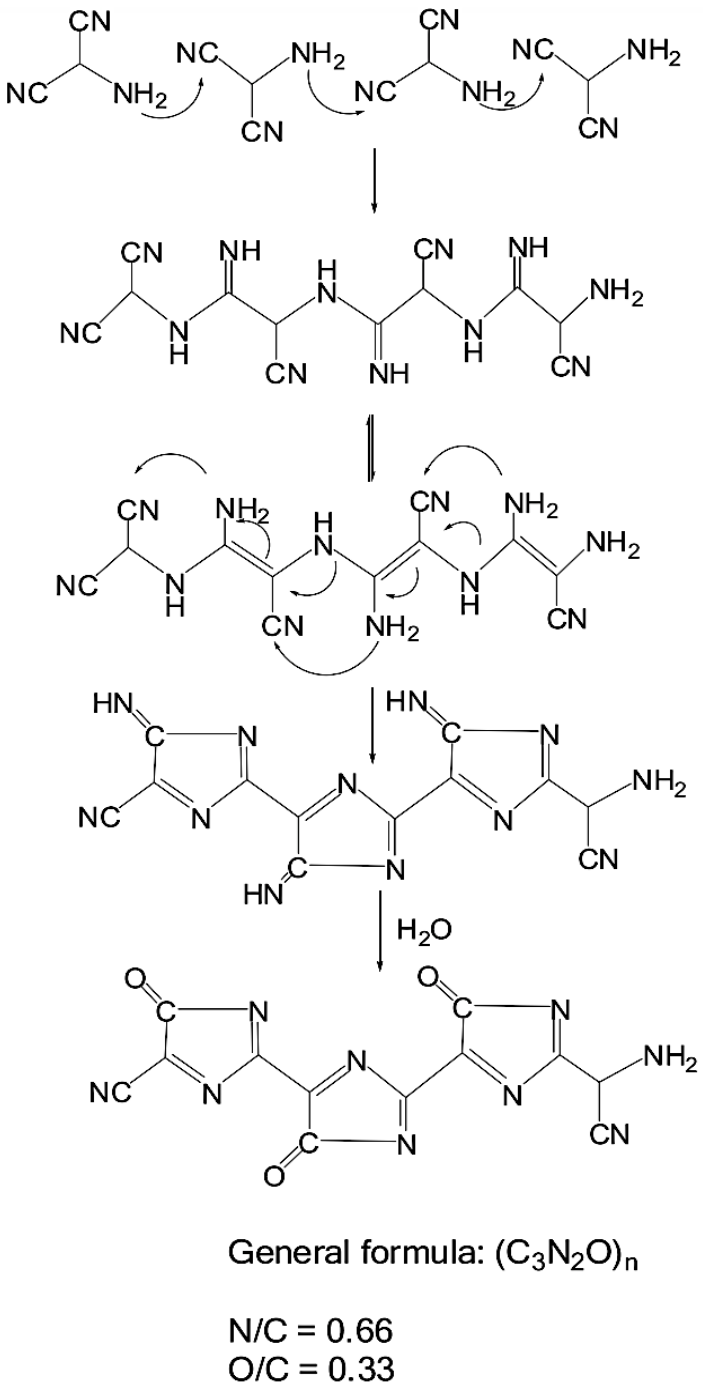

Figure 1.13. Proposed chemical structure of self-polymerized AMN film formed at solid-liquid interface. Reprinted with the permission from ref 114[114].

As shown in the Figure 1.13, the coating formation self-polymerization reaction mostly involves the active methylene and nucleophilic primary amine groups through attacking reactive nitrile groups of another AMN molecule and finally forms an amidine. Thus for every AMN amine reacting with a nitrile, there will be one unreacted nitrile. Furthermore studies revealed that AMN coating can successfully functionalize a surface by incorporating small organic molecule or polymer containing suitable functional group such as aldehydes and amines[112,113,115]. The unreacted nitrile of AMN after polymerization can take part in reaction with an exogenous amine from secondary molecule as shown in Figure 1.14 (a)[112]. Richard *et al*. proposed two possible reaction mechanisms of aldehydes with HCN polymers. Either amine groups from the HCN polymers can react with aldehydes and form imine or active methyl hydrogen available in AMN can be expected to react with aldehyde by nucleophilic reaction (Figure 1.14 (b)). Apart from amines and aldehydes, AMN coating can possibly incorporate thiol containing small molecule or polymer as reported by Raulin *et al.*[116]. Nitrile groups available in AMN can be readily attacked by the nucleophilic thiol group and can form iminothioester as shown in Figure 1.14 (c). Along with reactions with secondary molecules, highly nitrogenous AMN coating has proven ability to incorporate metal nanoparticles such as Silver nanoparticles via in situ deposition into the coating which provides the opportunity for the fabrication of antibacterial surface[112]. As AMN coating provides several electron donors such as amines and nitriles, these nucleophiles can take part in metal coordination.

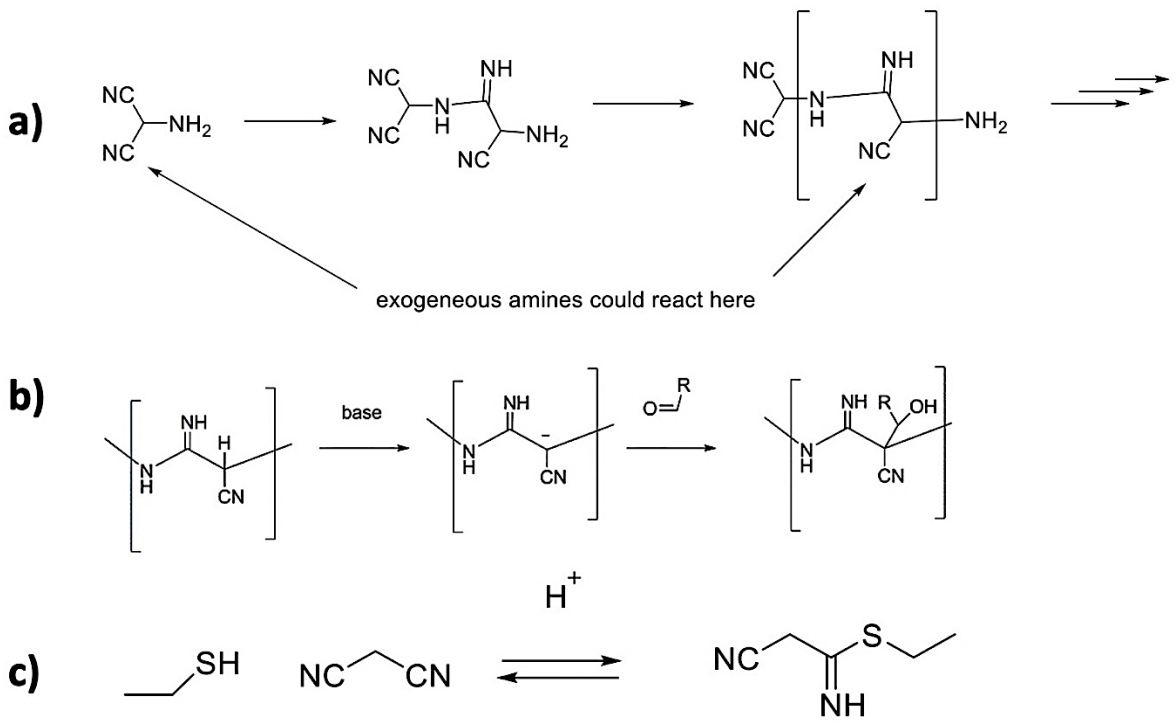

Figure 1.14. Possible chemical reaction mechanisms of AMN with a) amines, b) aldehydes and c) thiol containing molecules. Reprinted with the permission from ref 112[112].

The biocompatible AMN coating provides an outstanding cell attachment platform with negligible cytotoxicity which makes it suitable for a wide range of biomedical applications. Any surface coating produced either from AMN or dopamine are highly biocompatible. Mostly, the application fields of PDA and AMN-based surface modifications are very similar even though the chemical pathways leading up to these coatings are different.

1.10 Bacteria characterization:

Bacterial biofilm is one of the main causes of biofouling in most industrial sectors[117]. So, it is important to understand the bacteria cell structure and how it influences bacteria's adhesion to a

variety of surfaces. The most studied characteristics of bacteria cell can be divided into two key areas: structural characteristics and physicochemical characteristics. Based on the morphology (size and shape), all the bacteria available in nature are commonly defined as elongated rod-shaped cell (bacillus), spherical cell (coccus) or spiral shaped cell (spirillum)[118]. The cell volume of bacteria varies from ~0.4–3 μm^3. Most of the rod-shaped bacteria are found between 0.25 μm and 4 μm wide and less than 10 μm long, while coccus-shaped bacteria have an average diameter of about 0.5–1.0 μm. Depending on the nutrient available in the media, the cell length and width of the same shaped bacteria can vary[119]. For example, rod-shaped *E. coli* bacterial cells can readily adapt their lengths and widths in response to environmental changes. Another fundamental aspect to characterize bacteria is the cell wall. Depending on the cell wall structure bacteria can be divided into two distinct groups: gram positive and gram negative. Bacteria with a thick peptidoglycan layer surrounding the plasma membrane are called Gram-positive and bacteria with a thin peptidoglycan layer between the outer membrane and the inner plasma membrane are called Gram-negative. Gram staining is an effective technique to identify and distinguish certain bacteria. This method developed in 1882 involves the use of crystal violet or methylene blue as the primary colour[120]. The thick cell wall of gram-positive bacteria retains the primary colour and appear purple-brown under a microscope whereas the thin peptidoglycan layer of gram-negative bacteria cannot take up primary stain and appear red under a microscope. An overview of structural characteristics of gram negative and gram-positive bacteria is listed in Table 1.2. Some cell surface appendages such as flagella, cilia, and fibrils are also present on some bacteria species, and which can also influence bacterial adhesion to surfaces. Electron microscopy is a particularly powerful tool for visualizing adhesion structures of bacteria cell.

Table 1.2 Summary of gram-positive and gram-negative bacteria

	Gram-positive	**Gram-negative**
Color after Gram staining	Dark blue/violet	Red/pink
Characteristics of cell wall	Thick peptidoglycan layer	Thin peptidoglycan layer
	No outer membrane	Outer membrane with lipopolysaccharides and proteins
	Negatively charged teichoic acids are often present	No teichoic acids
Examples	*Staphylococcus aureus* *Streptococcus mutans* *Staphylococcus epidermidis*	*Pseudomonas aeruginosa* *Escherichia coli* *Salmonella typhimurium*

This basic bacteria cell wall structure may not influence the adhesion of bacteria on the surfaces directly, however, differences between the adhesion of Gram-positive and Gram-negative species of bacteria to surfaces have been reported[121]. Researchers have found that positively charged surfaces attract more bacteria, but this effect can be counterbalanced by the absence of any growth, at least for the Gram-negative strains[121]. Surface charge of bacteria also play a significant role on the adhesion or interaction of bacteria with varies surfaces, ions or particles. Surface charge is mostly related to their envelope structure composition and interactions with surfaces in natural environments. Bacteria cell surface possess net negative charge under physiological condition due to the presence of peptidoglycan, which is rich in carboxyl and amino groups[122]. A variety of methods has been used to characterize bacterial cell surfaces for the determination of the cell-surface charge[123]. Among them the most reliable technique to measure this physicochemical

parameter is micro electrophoresis or electrokinetic or zeta (ζ) potential measurement, which can be estimated from the electrophoretic mobility of cells. A cellular dispersion with a determined ionic strength is placed into an electrophoresis chamber that is subjected to a potential difference. After applying voltage, the time that cells spend migrating under a constant electric field is related to their electrophoretic mobility. The ζ potential and electrophoretic mobility of cells is dependent on variety of factors i.e. the cell surface charge, electric field, temperature and ionic conditions of the cellular dispersion[124].

1.11 Objective:

'Graft to' and 'graft from' these two methods have been exploited so far to fabricate nonfouling polymer coating. Compared to 'graft to' methods, 'graft from' methods are more complicated and need multiple steps with special conditions such as no water, no oxygen and an inert atmosphere. This limits its large-scale practical application. 'Graft to' method is the most adopted coating strategy since it is very convenient and simple to employ. Nevertheless, there are some major challenges in this modification such as short-term efficiency and limited stability in complex environments. Most of the approaches explored by researchers for 'graft to' method include weak physical adsorption or hydrogen bond which are weaker than other chemical bond. That is why, a strong covalent bond between polymer and surface is highly desired to graft hydrophilic polymer onto the surface for maintaining a strong hydration layer. A strong hydration layer can keep the foulant away and make the surface unfavorable for any microbial attachment for long-term application. But developing a dual functional surface with both antifouling and antimicrobial property with high biocompatibility in a facile way is challenging.

The main objective of this thesis was to establish facile surface modification techniques using dopamine chemistry and prebiotic chemistry to prepare a zwitterionic polymer coating with both

antifouling and antimicrobial properties. Different types of molecular interactions have been explored to graft the synthesized zwitterionic polymers and prepare a stable multifunctional coating for biomedical application. The following three types of surface modifications strategies has been developed:

1) In the first project of this thesis, catechol containing adhesive monomer Dopamine methacrylamide (DMA) has been copolymerized with MPC monomer and resultant copolymers covalently grafted onto the amino ($-NH_2$) rich polyethylenimine (PEI)/PDA co-deposited surface. The purpose of incorporation of PEI of low molecular weight (M_w = 600 Da) was to accelerate the deposition process and covalent network between PEI and PDA and improve the coating stability under both strong acidic and alkaline environments. To improve antibacterial activity of the surface silver nanoparticles (AgNPs) have also been introduced into the surface. Unreacted catechol groups can reduce Ag^+ ions effectively from the $AgNO_3$ solution and help to prepare a stable dual functional antifouling and antibacterial surface. To understand the effect of adhesive catechol content for anchoring the zwitterionic copolymer onto the PDA/PEI coated substrate, three different polymers containing different percentages of adhesive DMA monomer content have been synthesized. The covalently grafted polymer coated surface demonstrated to be stronger and more stable than any other weak physical adsorption such as electrostatic forces and hydrogen bonds.
2) Rapid accumulation of dead bacteria or protein on a bactericidal surface can reduce the effectiveness of the modified surface and alter its biocidal activity by shielding the surface biocide functional groups, promoting microbial attachment and subsequent biofilm formation. Therefore, developing a smart self-cleaning surface is of great interest. In the

second project of this thesis, sugar responsive self-cleaning surface has been developed by utilizing covalent boronic ester bonds between catechol groups from polydopamine (PDA) layer and benzoxaborole pendant from zwitterionic and cationic polymers. This distinctive boronic ester complex is reversible and sugar responsive. To impart surface hydration zwitterion and for incorporating biocidal activity cationic quaternary ammonium moieties was utilized to prepare a dynamic dual-functional surface based on the unique property of boronic ester. Thus, the modified surface has been endowed with bacteria contact-killing property. However, after the addition of cis-diol containing sugar such as fructose solution onto the modified surface, this boronic ester complex with PDA could be cleaved and the attached copolymer layer removed from the surface resulting in the release of all attached dead bacteria from the surface. After sugar treatment, more than 85% of attached bacteria on the surface has been released. As this benzoxaborole-catechol complexation is reversible, after sugar treatment, the copolymer grafted PDA surface can be regenerated by simply adding freshly prepared polymer solution onto the sugar treated surface to form the benzoxaborole-catechol complexation again at physiological pH 7.4 which is higher than pKa value (~7.2) of benozoxaborole. The resultant sugar responsive self-cleaning surface can be used as a non-leaching, self-sterilizing surface for potential applications in biomedical implants.

3) Multifunctional coating decorated with antifouling and antibacterial property is widely used to combat this biofouling related infections. But in practice, during storage, transport, and clinical use accidental mechanical damage, such as scratching, and abrasion can happen which significantly affect and alter the coating properties exposing the underlying substrate. This scratched area acts as an active site for microbial colonization and

subsequently diminishes the antifouling or antibacterial functionality of the coating. To overcome this challenge, introduction of intrinsic self-healing property into the antifouling and antibacterial coating can be a promising solution. Considering this fact, in the third project of this thesis an excellent biocompatible coating with intrinsic self-healing property along with antifouling and antibacterial functionality have been developed. In this project, prebiotic chemistry inspired self-polymerization of aminomalononitrile (AMN) has been used as a primary coating layer which act as a primer to graft vitamin B5 analogous methacrylamide polymer poly(B5AMA) and zwitterionic compound 2-methacryloyloxyethyl phosphorylcholine (MPC) containing polymer poly (MPC-st-B5AMA) by forming strong hydrogen bond. B5AMA having multiple polar groups into the structure act as an intrinsic rapid self-healing material. Moreover, being hygroscopic in nature, B5AMA based coating has shown excellent antifouling property against protein and bacteria maintaining a good hydration layer similar to MPC containing polymer. In addition, incorporation of silver nanoparticles into the coating by *in situ* deposition, has provided excellent antibacterial properties.

1.12 References:

(1) Park, J.; Gill, G. A.; Strivens, J. E.; Kuo, L. J.; Jeters, R. T.; Avila, A.; Wood, J. R.; Schlafer, N. J.; Janke, C. J.; Miller, E. A.; et al. Effect of Biofouling on the Performance of Amidoxime-Based Polymeric Uranium Adsorbents. *Ind. Eng. Chem. Res.* **2016**, *55* (15), 4328–4338.

(2) Harding, J. L.; Reynolds, M. M. Combating Medical Device Fouling. *Trends Biotechnol.* **2014**, *32* (3), 140–146.

(3) Lindner, E. A Low Surface Free Energy Approach in the Control of Marine Biofouling.

Biofouling **1992**, *6* (2), 193–205.

(4) Bixler, G. D.; Bhushan, B. Review Article: Biofouling: Lessons from Nature. *Philosophical Transactions of the Royal Society A: Mathematical, Physical and Engineering Sciences*. **2012**, *270,* 2381–2417.

(5) Yu, Q.; Ista, L. K.; López, G. P. Nanopatterned Antimicrobial Enzymatic Surfaces Combining Biocidal and Fouling Release Properties. *Nanoscale* **2014**, *6* (9), 4750–4757.

(6) Magin, C. M.; Cooper, S. P.; Brennan, A. B. Non-Toxic Antifouling Strategies. *Materials Today*. **2010**, *13,* 36–44.

(7) O'Toole, G. A. A Resistance Switch. *Nature*. **2002**, *416,* 695–696.

(8) Yebra, D. M.; Kiil, S.; Dam-Johansen, K. Antifouling Technology - Past, Present and Future Steps towards Efficient and Environmentally Friendly Antifouling Coatings. *Progress in Organic Coatings*. **2004**, *50,* 75–104.

(9) Damodaran, V. B.; Murthy, S. N. Bio-Inspired Strategies for Designing Antifouling Biomaterials. *Biomater. Res.* **2016**, *20* (1).

(10) He, M.; Gao, K.; Zhou, L.; Jiao, Z.; Wu, M.; Cao, J.; You, X.; Cai, Z.; Su, Y.; Jiang, Z. Zwitterionic Materials for Antifouling Membrane Surface Construction. *Acta Biomaterialia*. **2016**, *40*, 142–152.

(11) Chen, S.; Li, L.; Zhao, C.; Zheng, J. Surface Hydration: Principles and Applications toward Low-Fouling/Nonfouling Biomaterials. *Polymer*. **2010**, *51*, 5283–5293.

(12) Zheng, J.; Li, L.; Tsao, H. K.; Sheng, Y. J.; Chen, S.; Jiang, S. Strong Repulsive Forces between Protein and Oligo (Ethylene Glycol) Self-Assembled Monolayers: A Molecular Simulation Study. *Biophys. J.* **2005**, *89* (1), 158–166.

(13) Zhao, J.; Shi, Q.; Luan, S.; Song, L.; Yang, H.; Shi, H.; Jin, J.; Li, X.; Yin, J.; Stagnaro, P. Improved Biocompatibility and Antifouling Property of Polypropylene Non-Woven Fabric Membrane by Surface Grafting Zwitterionic Polymer. *J. Memb. Sci.* **2011**, *369* (1–2), 5–12.

(14) Yu, Q.; Wu, Z.; Chen, H. Dual-Function Antibacterial Surfaces for Biomedical

Applications. *Acta Biomaterialia*. **2015**, *16*, 1–13.

(15) Zhao, Y. H.; Zhu, X. Y.; Wee, K. H.; Bai, R. Achieving Highly Effective Non-Biofouling Performance for Polypropylene Membranes Modified by UV-Induced Surface Graft Polymerization of Two Oppositely Charged Monomers. *J. Phys. Chem. B* **2010**, *114* (7), 2422–2429.

(16) Shahkaramipour, N.; Tran, T. N.; Ramanan, S.; Lin, H. Membranes with Surface-Enhanced Antifouling Properties for Water Purification. *Membranes*. **2017,** *7*(1), 13.

(17) Jiang, S.; Cao, Z. Ultralow-Fouling, Functionalizable, and Hydrolyzable Zwitterionic Materials and Their Derivatives for Biological Applications. *Adv. Mater.* **2010**, *22* (9), 920–932.

(18) Bernards, M.; He, Y. Polyampholyte Polymers as a Versatile Zwitterionic Biomaterial Platform. *Journal of Biomaterials Science, Polymer Edition*. **2014**, *25*, 1479–1488.

(19) Zhang, L.; Tang, M.; Zhang, J.; Zhang, P.; Zhang, J.; Deng, L.; Lin, C.; Dong, A. One Simple and Stable Coating of Mixed-Charge Copolymers on Poly(Vinyl Chloride) Films to Improve Antifouling Efficiency. *J. Appl. Polym. Sci.* **2017**, *134* (12), 44632.

(20) Jhong, J. F.; Venault, A.; Liu, L.; Zheng, J.; Chen, S. H.; Higuchi, A.; Huang, J.; Chang, Y. Introducing Mixed-Charge Copolymers as Wound Dressing Biomaterials. *ACS Appl. Mater. Interfaces* **2014**, *6* (12), 9858–9870.

(21) Schlenoff, J. B. Zwitteration: Coating Surfaces with Zwitterionic Functionality to Reduce Nonspecific Adsorption. *Langmuir*. **2014**, *6,* 9625–9636.

(22) Lee, H.; Dellatore, S. M.; Miller, W. M.; Messersmith, P. B. Mussel-Inspired Surface Chemistry for Multifunctional Coatings. *Science (80-.).* **2007**, *318* (5849), 426–430.

(23) Park, J.; Brust, T. F.; Lee, H. J.; Lee, S. C.; Watts, V. J.; Yeo, Y. Polydopamine-Based Simple and Versatile Surface Modification of Polymeric Nano Drug Carriers. *ACS Nano* **2014**, *8* (4), 3347–3356.

(24) Chen, Y.; Feng, X.; Zhao, Y.; Zhao, X.; Zhang, X. Mussel-Inspired Polydopamine Coating Enhances the Intracutaneous Drug Delivery from Nanostructured Lipid Carriers

Dependently on a Follicular Pathway. *Mol. Pharm.* **2020**, *17* (4), 1215–1225.

(25) Waite, J. H.; Tanzer, M. L. Polyphenolic Substance of Mytilus Edulis: Novel Adhesive Containing L-Dopa and Hydroxyproline. *Science (80-.).* **1981**, *212* (4498), 1038–1040.

(26) Waite, J. H.; Qin, X. Polyphosphoprotein from the Adhesive Pads of Mytilus Edulis. *Biochemistry* **2001**, *40* (9), 2887–2893.

(27) Silverman, H. G.; Roberto, F. F. Understanding Marine Mussel Adhesion. *Marine Biotechnology*. **2007**, pp 661–681.

(28) Yang, H. C.; Luo, J.; Lv, Y.; Shen, P.; Xu, Z. K. Surface Engineering of Polymer Membranes via Mussel-Inspired Chemistry. *J. Memb. Sci.* **2015**, *483*, 42–59.

(29) Lee, H. A.; Ma, Y.; Zhou, F.; Hong, S.; Lee, H. Material-Independent Surface Chemistry beyond Polydopamine Coating. *Acc. Chem. Res.* **2019**, *52* (3), 704–713.

(30) Jiang, J.; Zhu, L.; Zhu, L.; Zhu, B.; Xu, Y. Surface Characteristics of a Self-Polymerized Dopamine Coating Deposited on Hydrophobic Polymer Films. *Langmuir* **2011**, *27* (23), 14180–14187.

(31) Bernsmann, F.; Ball, V.; Addiego, F.; Ponche, A.; Michel, M.; Gracio, J. J. D. A.; Toniazzo, V.; Ruch, D. Dopamine-Melanin Film Deposition Depends on the Used Oxidant and Buffer Solution. *Langmuir* **2011**, *27* (6), 2819–2825.

(32) Hong, S.; Na, Y. S.; Choi, S.; Song, I. T.; Kim, W. Y.; Lee, H. Non-Covalent Self-Assembly and Covalent Polymerization Co-Contribute to Polydopamine Formation. *Adv. Funct. Mater.* **2012**, *22* (22), 4711–4717.

(33) Ryu, J. H.; Messersmith, P. B.; Lee, H. Polydopamine Surface Chemistry: A Decade of Discovery. *ACS Applied Materials and Interfaces*. **2018**, *10,* 7523–7540.

(34) Liebscher, J.; Mrówczyński, R.; Scheidt, H. A.; Filip, C.; Haìdade, N. D.; Turcu, R.; Bende, A.; Beck, S. Structure of Polydopamine: A Never-Ending Story? *Langmuir* **2013**, *29* (33), 10539–10548.

(35) Zeng, Y.; Liu, W.; Wang, Z.; Singamaneni, S.; Wang, R. Multifunctional Surface

Modification of Nanodiamonds Based on Dopamine Polymerization. *Langmuir* **2018**, *34* (13), 4036–4042.

(36) Schanze, K. S.; Lee, H.; Messersmith, P. B. Ten Years of Polydopamine: Current Status and Future Directions. *ACS Applied Materials and Interfaces*. **2018**, *10,* 7521–7522.

(37) Nuzzo, R. G.; Allara, D. L. Adsorption of Bifunctional Organic Disulfides on Gold Surfaces. *Journal of the American Chemical Society*. **1983**, *105,* 4481–4483.

(38) Love, J. C.; Estroff, L. A.; Kriebel, J. K.; Nuzzo, R. G.; Whitesides, G. M. Self-Assembled Monolayers of Thiolates on Metals as a Form of Nanotechnology. *Chemical Reviews*. **2005**, *105,* 1103–1169.

(39) Ulman, A. Formation and Structure of Self-Assembled Monolayers. *Chem. Rev.* **1996**, *96* (4), 1533–1554.

(40) Kirkland, J. J. Porous Thin-Layer Modified Glass Bead Supports for Gas Liquid Chromatography. *Anal. Chem.* **1965**, *37* (12), 1458–1461.

(41) Iler, R. K. Multilayers of Colloidal Particles. *J. Colloid Interface Sci.* **1966**, *21* (6), 569–594.

(42) Richardson, J. J.; Cui, J.; Björnmalm, M.; Braunger, J. A.; Ejima, H.; Caruso, F. Innovation in Layer-by-Layer Assembly. *Chemical Reviews*. **2016**, *116,* 14828–14867.

(43) Liston, E. M.; Martinu, L.; Wertheimer, M. R. Plasma Surface Modification of Polymers for Improved Adhesion: A Critical Review. *J. Adhes. Sci. Technol.* **1993**, *7* (10), 1091–1127.

(44) Chu, P. K.; Chen, J. Y.; Wang, L. P.; Huang, N. Plasma-Surface Modification of Biomaterials. *Materials Science and Engineering: R: Reports*. **2002**, *36*(5-6), 143–206.

(45) Ball, V.; Del Frari, D.; Michel, M.; Buehler, M. J.; Toniazzo, V.; Singh, M. K.; Gracio, J.; Ruch, D. Deposition Mechanism and Properties of Thin Polydopamine Films for High Added Value Applications in Surface Science at the Nanoscale. *BioNanoScience*. **2012**, *2* 16–34.

(46) Tan, X.; Gao, P.; Li, Y.; Qi, P.; Liu, J.; Shen, R.; Wang, L.; Huang, N.; Xiong, K.; Tian, W.; et al. Poly-Dopamine, Poly-Levodopa, and Poly-Norepinephrine Coatings: Comparison of Physico-Chemical and Biological Properties with Focus on the Application for Blood-Contacting Devices. *Bioact. Mater.* **2021**, *6* (1), 285–296.

(47) Borges, J.; Mano, J. F. Molecular Interactions Driving the Layer-by-Layer Assembly of Multilayers. *Chemical Reviews*. **2014**, *114,* 8883–8942.

(48) Lynge, M. E.; Van Der Westen, R.; Postma, A.; Städler, B. Polydopamine - A Nature-Inspired Polymer Coating for Biomedical Science. *Nanoscale* **2011**, *3* (12), 4916–4928.

(49) Zhao, S.; Caruso, F.; Dahne, L.; Decher, G.; De Geest, B. G.; Fan, J.; Feliu, N.; Gogotsi, Y.; Hammond, P. T.; Hersam, M. C.; et al. The Future of Layer-by-Layer Assembly: A Tribute to ACS Nano Associate Editor Helmuth Mohwald. *ACS Nano* **2019**, *13* (6), 6151–6169.

(50) Zhou, R.; Ren, P. F.; Yang, H. C.; Xu, Z. K. Fabrication of Antifouling Membrane Surface by Poly(Sulfobetaine Methacrylate)/Polydopamine Co-Deposition. *J. Memb. Sci.* **2014**, *466*, 18–25.

(51) Yu, B. Y.; Zheng, J.; Chang, Y.; Sin, M. C.; Chang, C. H.; Higuchi, A.; Sun, Y. M. Surface Zwitterionization of Titanium for a General Bio-Inert Control of Plasma Proteins, Blood Cells, Tissue Cells, and Bacteria. *Langmuir* **2014**, *30* (25), 7502–7512.

(52) Liu, X.; Deng, J.; Ma, L.; Cheng, C.; Nie, C.; He, C.; Zhao, C. Catechol Chemistry Inspired Approach to Construct Self-Cross-Linked Polymer Nanolayers as Versatile Biointerfaces. *Langmuir* **2014**, *30* (49), 14905–14915.

(53) Li, G.; Cheng, G.; Xue, H.; Chen, S.; Zhang, F.; Jiang, S. Ultra Low Fouling Zwitterionic Polymers with a Biomimetic Adhesive Group. *Biomaterials* **2008**, *29* (35), 4592–4597.

(54) Sundaram, H. S.; Han, X.; Nowinski, A. K.; Ella-Menye, J. R.; Wimbish, C.; Marek, P.; Senecal, K.; Jiang, S. One-Step Dip Coating of Zwitterionic Sulfobetaine Polymers on Hydrophobic and Hydrophilic Surfaces. In *ACS Applied Materials and Interfaces*; **2014**; *6*, 6664–6671.

(55) Yang, W.; Sundaram, H. S.; Ella, J. R.; He, N.; Jiang, S. Low-Fouling Electrospun PLLA Films Modified with Zwitterionic Poly(Sulfobetaine Methacrylate)-Catechol Conjugates. *Acta Biomater.* **2016**, *40*, 92–99.

(56) Cheng, G.; Li, G.; Xue, H.; Chen, S.; Bryers, J. D.; Jiang, S. Zwitterionic Carboxybetaine Polymer Surfaces and Their Resistance to Long-Term Biofilm Formation. *Biomaterials* **2009**, *30* (28), 5234–5240.

(57) Gao, C.; Li, G.; Xue, H.; Yang, W.; Zhang, F.; Jiang, S. Functionalizable and Ultra-Low Fouling Zwitterionic Surfaces via Adhesive Mussel Mimetic Linkages. *Biomaterials* **2010**, *31* (7), 1486–1492.

(58) Amoako, K. A.; Sundaram, H. S.; Suhaib, A.; Jiang, S.; Cook, K. E. Multimodal, Biomaterial-Focused Anticoagulation via Superlow Fouling Zwitterionic Functional Groups Coupled with Anti-Platelet Nitric Oxide Release. *Adv. Mater. Interfaces* **2016**, *3* (6).

(59) Ye, G.; Lee, J.; Perreault, F.; Elimelech, M. Controlled Architecture of Dual-Functional Block Copolymer Brushes on Thin-Film Composite Membranes for Integrated "Defending" and "Attacking" Strategies against Biofouling. *ACS Appl. Mater. Interfaces* **2015**, *7* (41), 23069–23079.

(60) Wang, B. L.; Jin, T. W.; Han, Y. M.; Shen, C. H.; Li, Q.; Lin, Q. K.; Chen, H. Bio-Inspired Terpolymers Containing Dopamine, Cations and MPC: A Versatile Platform to Construct a Recycle Antibacterial and Antifouling Surface. *J. Mater. Chem. B* **2015**, *3* (27), 5501–5510.

(61) Zhang, C.; Ma, M. Q.; Chen, T. T.; Zhang, H.; Hu, D. F.; Wu, B. H.; Ji, J.; Xu, Z. K. Dopamine-Triggered One-Step Polymerization and Codeposition of Acrylate Monomers for Functional Coatings. *ACS Appl. Mater. Interfaces* **2017**, *9* (39), 34356–34366.

(62) Ren, P. F.; Yang, H. C.; Jin, Y. N.; Liang, H. Q.; Wan, L. S.; Xu, Z. K. Underwater Superoleophobic Meshes Fabricated by Poly(Sulfobetaine)/Polydopamine Co-Deposition. *RSC Adv.* **2015**, *5* (59), 47592–47598.

(63) Chang, C. C.; Kolewe, K. W.; Li, Y.; Kosif, I.; Freeman, B. D.; Carter, K. R.; Schiffman, J. D.; Emrick, T. Underwater Superoleophobic Surfaces Prepared from Polymer

Zwitterion/Dopamine Composite Coatings. *Adv. Mater. Interfaces* **2016**, *3* (6), 1500521.

(64) Zhang, C.; Li, H. N.; Du, Y.; Ma, M. Q.; Xu, Z. K. CuSO4/H2O2-Triggered Polydopamine/Poly(Sulfobetaine Methacrylate) Coatings for Antifouling Membrane Surfaces. *Langmuir* **2017**, *33* (5), 1210–1216.

(65) Xu, G.; Liu, P.; Pranantyo, D.; Xu, L.; Neoh, K. G.; Kang, E. T. Antifouling and Antimicrobial Coatings from Zwitterionic and Cationic Binary Polymer Brushes Assembled via "Click" Reactions. *Ind. Eng. Chem. Res.* **2017**, *56* (49), 14479–14488.

(66) Shahkaramipour, N.; Lai, C. K.; Venna, S. R.; Sun, H.; Cheng, C.; Lin, H. Membrane Surface Modification Using Thiol-Containing Zwitterionic Polymers via Bioadhesive Polydopamine. *Ind. Eng. Chem. Res.* **2018**, *57* (6), 2336–2345.

(67) Kuang, J.; Messersmith, P. B. Universal Surface-Initiated Polymerization of Antifouling Zwitterionic Brushes Using a Mussel-Mimetic Peptide Initiator. *Langmuir* **2012**, *28* (18), 7258–7266.

(68) Sin, M. C.; Sun, Y. M.; Chang, Y. Zwitterionic-Based Stainless Steel with Well-Defined Polysulfobetaine Brushes for General Bioadhesive Control. *ACS Appl. Mater. Interfaces* **2014**, *6* (2), 861–873.

(69) Liu, C.; Lee, J.; Ma, J.; Elimelech, M. Antifouling Thin-Film Composite Membranes by Controlled Architecture of Zwitterionic Polymer Brush Layer. *Environ. Sci. Technol.* **2017**, *51* (4), 2161–2169.

(70) Sundaram, H. S.; Han, X.; Nowinski, A. K.; Brault, N. D.; Li, Y.; Ella-Menye, J. R.; Amoaka, K. A.; Cook, K. E.; Marek, P.; Senecal, K.; et al. Achieving One-Step Surface Coating of Highly Hydrophilic Poly(Carboxybetaine Methacrylate) Polymers on Hydrophobic and Hydrophilic Surfaces. *Adv. Mater. Interfaces* **2014**, *1* (6).

(71) Sun, F.; Wu, K.; Hung, H. C.; Zhang, P.; Che, X.; Smith, J.; Lin, X.; Li, B.; Jain, P.; Yu, Q.; et al. Paper Sensor Coated with a Poly(Carboxybetaine)-Multiple DOPA Conjugate via Dip-Coating for Biosensing in Complex Media. *Anal. Chem.* **2017**, *89* (20), 10999–11004.

(72) Ye, H.; Xia, Y.; Liu, Z.; Huang, R.; Su, R.; Qi, W.; Wang, L.; He, Z. Dopamine-Assisted

Deposition and Zwitteration of Hyaluronic Acid for the Nanoscale Fabrication of Low-Fouling Surfaces. *J. Mater. Chem. B* **2016**, *4* (23), 4084–4091.

(73) Huang, C. J.; Wang, L. C.; Shyue, J. J.; Chang, Y. C. Developing Antifouling Biointerfaces Based on Bioinspired Zwitterionic Dopamine through PH-Modulated Assembly. *Langmuir* **2014**, *30* (42), 12638–12646.

(74) Kang, S. M.; Hwang, N. S.; Yeom, J.; Park, S. Y.; Messersmith, P. B.; Choi, I. S.; Langer, R.; Anderson, D. G.; Lee, H. One-Step Multipurpose Surface Functionalization by Adhesive Catecholamine. *Adv. Funct. Mater.* **2012**, *22* (14), 2949–2955.

(75) Qiu, W. Z.; Yang, H. C.; Xu, Z. K. Dopamine-Assisted Co-Deposition: An Emerging and Promising Strategy for Surface Modification. *Advances in Colloid and Interface Science*. **2018**, *256,* 111–125.

(76) Kolewe, K. W.; Dobosz, K. M.; Rieger, K. A.; Chang, C. C.; Emrick, T.; Schiffman, J. D. Antifouling Electrospun Nanofiber Mats Functionalized with Polymer Zwitterions. *ACS Appl. Mater. Interfaces* **2016**, *8* (41), 27585–27593.

(77) Kirschner, A. Y.; Chang, C. C.; Kasemset, S.; Emrick, T.; Freeman, B. D. Fouling-Resistant Ultrafiltration Membranes Prepared via Co-Deposition of Dopamine/Zwitterion Composite Coatings. *J. Memb. Sci.* **2017**, *541*, 300–311.

(78) Zhang, C.; Ou, Y.; Lei, W. X.; Wan, L. S.; Ji, J.; Xu, Z. K. CuSO4/H2O2-Induced Rapid Deposition of Polydopamine Coatings with High Uniformity and Enhanced Stability. *Angew. Chemie - Int. Ed.* **2016**, *55* (9), 3054–3057.

(79) Xie, Y.; Tang, C.; Wang, Z.; Xu, Y.; Zhao, W.; Sun, S.; Zhao, C. Co-Deposition towards Mussel-Inspired Antifouling and Antibacterial Membranes by Using Zwitterionic Polymers and Silver Nanoparticles. *J. Mater. Chem. B* **2017**, *5* (34), 7186–7193.

(80) Ding, Y. H.; Floren, M.; Tan, W. Mussel-Inspired Polydopamine for Bio-Surface Functionalization. *Biosurface and Biotribology* **2016**, *2* (4), 121–136.

(81) Yang, J.; Cohen Stuart, M. A.; Kamperman, M. Jack of All Trades: Versatile Catechol Crosslinking Mechanisms. *Chemical Society Reviews*. **2014**, 8271–8298.

(82) Li, P.; Cai, X.; Wang, D.; Chen, S.; Yuan, J.; Li, L.; Shen, J. Hemocompatibility and Anti-Biofouling Property Improvement of Poly(Ethylene Terephthalate) via Self-Polymerization of Dopamine and Covalent Graft of Zwitterionic Cysteine. *Colloids Surfaces B Biointerfaces* **2013**, *110*, 327–332.

(83) Shevate, R.; Kumar, M.; Karunakaran, M.; Hedhili, M. N.; Peinemann, K. V. Polydopamine/Cysteine Surface Modified Isoporous Membranes with Self-Cleaning Properties. *J. Memb. Sci.* **2017**, *529*, 185–194.

(84) Cui, J.; Ju, Y.; Liang, K.; Ejima, H.; Lörcher, S.; Gause, K. T.; Richardson, J. J.; Caruso, F. Nanoscale Engineering of Low-Fouling Surfaces through Polydopamine Immobilisation of Zwitterionic Peptides. *Soft Matter* **2014**, *10* (15), 2656–2663.

(85) Zhi, X.; Li, P.; Gan, X.; Zhang, W.; Shen, T.; Yuan, J.; Shen, J. Hemocompatibility and Anti-Biofouling Property Improvement of Poly(Ethylene Terephthalate) via Self-Polymerization of Dopamine and Covalent Graft of Lysine. *J. Biomater. Sci. Polym. Ed.* **2014**, *25* (14–15), 1619–1628.

(86) Chen, L.; Tan, L.; Liu, S.; Bai, L.; Wang, Y. Surface Modification by Grafting of Poly(SBMA-Co-AEMA)-g-PDA Coating and Its Application in CE. *J. Biomater. Sci. Polym. Ed.* **2014**, *25* (8), 766–785.

(87) Liu, C. Y.; Huang, C. J. Functionalization of Polydopamine via the Aza-Michael Reaction for Antimicrobial Interfaces. *Langmuir* **2016**, *32* (19), 5019–5028.

(88) Asha, A. B.; Chen, Y.; Zhang, H.; Ghaemi, S.; Ishihara, K.; Liu, Y.; Narain, R. Rapid Mussel-Inspired Surface Zwitteration for Enhanced Antifouling and Antibacterial Properties. *Langmuir* **2019**, *35* (5), 1621–1630.

(89) Gillich, T.; Benetti, E. M.; Rakhmatullina, E.; Konradi, R.; Li, W.; Zhang, A.; Schlüter, A. D.; Textor, M. Self-Assembly of Focal Point Oligo-Catechol Ethylene Glycol Dendrons on Titanium Oxide Surfaces: Adsorption Kinetics, Surface Characterization, and Nonfouling Properties. *J. Am. Chem. Soc.* **2011**, *133* (28), 10940–10950.

(90) Li, N.; Li, T.; Qiao, X. Y.; Li, R.; Yao, Y.; Gong, Y. K. Universal Strategy for Efficient Fabrication of Blood Compatible Surfaces via Polydopamine-Assisted Surface-Initiated

Activators Regenerated by Electron Transfer Atom-Transfer Radical Polymerization of Zwitterions. *ACS Appl. Mater. Interfaces* **2020**, *12* (10), 12337–12344.

(91) Ma, H.; Hyun, J.; Stiller, P.; Chilkoti, A. "Non-Fouling" Oligo(Ethylene Glycol)-Functionalized Polymer Brushes Synthesized by Surface-Initiated Atom Transfer Radical Polymerization. *Adv. Mater.* **2004**, *16* (4), 338–341.

(92) Matyjaszewski, K.; Miller, P. J.; Shukla, N.; Immaraporn, B.; Gelman, A.; Luokala, B. B.; Siclovan, T. M.; Kickelbick, G.; Valiant, T.; Hoffmann, H.; et al. Polymers at Interfaces: Using Atom Transfer Radical Polymerization in the Controlled Growth of Homopolymers and Block Copolymers from Silicon Surfaces in the Absence of Untethered Sacrificial Initiator. *Macromolecules* **1999**, *32* (26), 8716–8724.

(93) He, X.; Yang, W.; Pei, X. Preparation, Characterization, and Tunable Wettability of Poly(Ionic Liquid) Brushes via Surface-Initiated Atom Transfer Radical Polymerization. *Macromolecules* **2008**, *41* (13), 4615–4621.

(94) Edmondson, S.; Vo, C. D.; Armes, S. P.; Unali, G. F. Surface Polymerization from Planar Surfaces by Atom Transfer Radical Polymerization Using Polyelectrolytic Macroinitiators. *Macromolecules* **2007**, *40* (15), 5271–5278.

(95) Ma, W.; Yang, P.; Li, J.; Li, S.; Li, P.; Zhao, Y.; Huang, N. Immobilization of Poly(MPC) Brushes onto Titanium Surface by Combining Dopamine Self-Polymerization and ATRP: Preparation, Characterization and Evaluation of Hemocompatibility in Vitro. *Appl. Surf. Sci.* **2015**, *349*, 445–451.

(96) Wang, J.; Wei, J. Hydrogel Brushes Grafted from Stainless Steel via Surface-Initiated Atom Transfer Radical Polymerization for Marine Antifouling. *Appl. Surf. Sci.* **2016**, *382*, 202–216.

(97) Jiang, J.; Zhang, P.; Zhu, L.; Zhu, B.; Xu, Y. Improving Antifouling Ability and Hemocompatibility of Poly(Vinylidene Fluoride) Membranes by Polydopamine-Mediated ATRP. *J. Mater. Chem. B* **2015**, *3* (39), 7698–7706.

(98) Jin, X.; Yuan, J.; Shen, J. Zwitterionic Polymer Brushes via Dopamine-Initiated ATRP from PET Sheets for Improving Hemocompatible and Antifouling Properties. *Colloids Surfaces*

B Biointerfaces **2016**, *145*, 275–284.

(99) Wang, W. C.; Wang, J.; Liao, Y.; Zhang, L.; Cao, B.; Song, G.; She, X. Surface Initiated ATRP of Acrylic Acid on Dopamine-Functionalized AAO Membranes. *J. Appl. Polym. Sci.* **2010**, *117* (1), 534–541.

(100) Li, G.; Xue, H.; Cheng, G.; Chen, S.; Zhang, F.; Jiang, S. Ultralow Fouling Zwitterionic Polymers Grafted from Surfaces Covered with an Initiator via an Adhesive Mussel Mimetic Linkage. *J. Phys. Chem. B* **2008**, *112* (48), 15269–15274.

(101) Ginic-Markovic, M.; Barclay, T.; Constantopoulos, K. T.; Al-Ghamdi, T.; Blok, A.; Markovic, E.; Ellis, A. V. A Versatile Approach to Grafting Biofouling Resistant Coatings from Polymeric Membrane Surfaces Using an Adhesive Macroinitiator. *RSC Adv.* **2015**, *5* (77), 63017–63024.

(102) Peng, B.; Lai, X.; Chen, L.; Lin, X.; Sun, C.; Liu, L.; Qi, S.; Chen, Y.; Leong, K. W. Scarless Wound Closure by a Mussel-Inspired Poly(Amidoamine) Tissue Adhesive with Tunable Degradability. *ACS Omega* **2017**, *2* (9), 6053–6062.

(103) Xing, C. M.; Meng, F. N.; Quan, M.; Ding, K.; Dang, Y.; Gong, Y. K. Quantitative Fabrication, Performance Optimization and Comparison of PEG and Zwitterionic Polymer Antifouling Coatings. *Acta Biomater.* **2017**, *59*, 129–138.

(104) Brault, N. D.; Gao, C.; Xue, H.; Piliarik, M.; Homola, J.; Jiang, S.; Yu, Q. Ultra-Low Fouling and Functionalizable Zwitterionic Coatings Grafted onto SiO2 via a Biomimetic Adhesive Group for Sensing and Detection in Complex Media. *Biosens. Bioelectron.* **2010**, *25* (10), 2276–2282.

(105) Zhao, J.; Mo, R.; Tian, L. M.; Song, L. J.; Luan, S. F.; Yin, J. H.; Ren, L. Q. Oriented Antibody Immobilization and Immunoassay Based on Boronic Acid-Containing Polymer Brush. *Chinese J. Polym. Sci. (English Ed.* **2018**, *36* (4), 472–478.

(106) Shahkaramipour, N.; Ramanan, S. N.; Fister, D.; Park, E.; Venna, S. R.; Sun, H.; Cheng, C.; Lin, H. Facile Grafting of Zwitterions onto the Membrane Surface to Enhance Antifouling Properties for Wastewater Reuse. *Ind. Eng. Chem. Res.* **2017**, *56* (32), 9202–9212.

(107) Barclay, T. G.; Hegab, H. M.; Michelmore, A.; Weeks, M.; Ginic-Markovic, M. Multidentate Polyzwitterion Attachment to Polydopamine Modified Ultrafiltration Membranes for Dairy Processing: Characterization, Performance and Durability. *J. Ind. Eng. Chem.* **2018**, *61*, 356–367.

(108) Meng, F. N.; Zhang, M. Q.; Ding, K.; Zhang, T.; Gong, Y. K. Cell Membrane Mimetic PVDF Microfiltration Membrane with Enhanced Antifouling and Separation Performance for Oil/Water Mixtures. *J. Mater. Chem. A* **2018**, *6* (7), 3231–3241.

(109) Zhu, L. J.; Liu, F.; Yu, X. M.; Gao, A. L.; Xue, L. X. Surface Zwitterionization of Hemocompatible Poly(Lactic Acid) Membranes for Hemodiafiltration. *J. Memb. Sci.* **2015**, *475*, 469–479.

(110) Zhu, Y.; Sundaram, H. S.; Liu, S.; Zhang, L.; Xu, X.; Yu, Q.; Xu, J.; Jiang, S. A Robust Graft-to Strategy to Form Multifunctional and Stealth Zwitterionic Polymer-Coated Mesoporous Silica Nanoparticles. *Biomacromolecules* **2014**, *15* (5), 1845–1851.

(111) Vatankhah-Varnosfaderani, M.; Hu, X.; Li, Q.; Adelnia, H.; Ina, M.; Sheiko, S. S. Universal Coatings Based on Zwitterionic-Dopamine Copolymer Microgels. *ACS Appl. Mater. Interfaces* **2018**.

(112) Thissen, H.; Koegler, A.; Salwiczek, M.; Easton, C. D.; Qu, Y.; Lithgow, T.; Evans, R. A. Prebiotic-Chemistry Inspired Polymer Coatings for Biomedical and Material Science Applications. *NPG Asia Mater.* **2015**, *7* (11), 1–9.

(113) Menzies, D. J.; Ang, A.; Thissen, H.; Evans, R. A. Adhesive Prebiotic Chemistry Inspired Coatings for Bone Contacting Applications. *ACS Biomater. Sci. Eng.* **2017**, *3* (5), 793–806.

(114) Toh, R. J.; Evans, R.; Thissen, H.; Voelcker, N. H.; D'ischia, M.; Ball, V. Deposition of Aminomalononitrile-Based Films: Kinetics, Chemistry, and Morphology. *Langmuir* **2019**, *35* (30), 9896–9903.

(115) Cheng, Q.; Asha, A. B.; Liu, Y.; Peng, Y. Y.; Diaz-Dussan, D.; Shi, Z.; Cui, Z.; Narain, R. Antifouling and Antibacterial Polymer-Coated Surfaces Based on the Combined Effect of Zwitterions and the Natural Borneol. *ACS Appl. Mater. Interfaces* **2021**, *13* (7), 9006–9014.

(116) Raulin, F.; Lussiana, J.-P. Prebiotic Formation of Iminothioesters. II: Addition of Thiophenols to Malonic Nitriles. *Orig. Life* **1984**, *14* (1), 157–162.

(117) Mittelman, M. W. *Marine Biotechnology*; **1999**.

(118) Harris, L. G. Microbial Cell Structure and Organization: Bacteria. *Encycl. Infect. Immun.* **2022**, *1*, 345–362.

(119) Ojkic, N.; Serbanescu, D.; Banerjee, S. Surface-to-Volume Scaling and Aspect Ratio Preservation in Rod-Shaped Bacteria. *Elife* **2019**, *8*, 1–11.

(120) O'Toole, G. A. Classic Spotlight: How the Gram Stain Works. *J. Bacteriol.* **2016**, *198* (23), 3128–3128.

(121) Bart Gottenbos, Dirk W. Grijpma, Henny C. van der Mei, J. F. and H. J. B. Antimicrobial Effects of Positively Charged Surfaces on Adhering Gram-Positive and Gram-Negative Bacteria. *J. Antimicrob. Chemother.* **2001**, *48*, 7–13.

(122) Vollmer, W.; Blanot, D.; De Pedro, M. A. Peptidoglycan Structure and Architecture. *FEMS Microbiol. Rev.* **2008**, *32* (2), 149–167.

(123) Wilson, W. W.; Wade, M. M.; Holman, S. C.; Champlin, F. R. Status of Methods for Assessing Bacterial Cell Surface Charge Properties Based on Zeta Potential Measurements. *J. Microbiol. Methods* **2001**, *43* (3), 153–164.

(124) Ayala-Torres, C.; Hernández, N.; Galeano, A.; Novoa-Aponte, L.; Soto, C. Y. Zeta Potential as a Measure of the Surface Charge of Mycobacterial Cells. *Ann. Microbiol.* **2014**, *64* (3), 1189–1195.

Chapter 2 Rapid Mussel-Inspired Surface Zwitteration for Enhanced Antifouling and Antibacterial Properties

The content of this chapter was published in

The Journal of ***Langmuir***

2.1 Introduction

Biofouling due to undesirable accumulation of microorganisms on wet surfaces has become a common and serious problem in the medical industry[1]. Prosthetic implants, biosensors, catheters, vascular stents, dental implants and other medical equipment are prone to surface biofouling due to irreversible adhesion of microbial or thrombotic agents[2]. Therefore, endowing surfaces with antifouling and antimicrobial properties to mitigate the biofouling has become a great demand. Currently, researchers are designing a broad range of antifouling strategies to tackle the fouling issues by nature-inspired approaches ranging from coatings to cleaning techniques[3–7]. Bio-passive polymers (PEG-based polymer or zwitterionic polymers) can be considered as one of the most promising materials for combating biofouling because of their retaining a hydration layer near the surface which is believed to be a physical barrier to prevent direct contact between biomolecules and surface by endowing low interfacial energy[8–10]. Hydration layer formed by hydrophilic polymers such as polyethylene glycol (PEG) and their derivatives, is maintained by weak hydrogen bonds[10,11] and they can be easily degraded by oxidation, especially in complex media which limits their long-term applications[12]. On the other hand, zwitterionic polymers having an equimolar number of homogenously distributed anionic and cationic groups on their polymer chains[8,10] can maintain more tightly bound hydration layer through electrostatic interactions[13] which makes these polymers more effective in discouraging biomolecules adsorption.

Zwitterionic polymers can be effectively immobilized onto the surface by either 'grafting to'[14–16] or 'grafting from'[17–19] method using mussel-inspired dopamine chemistry[20]. Alkali-induced autoxidation[21,22] of dopamine into polydopamine (PDA)[23] coatings is the most interesting single step surface functionalization method[24] to obtain nonfouling surface. The PDA-coated surface layers contain amino groups and phenolic hydroxyl groups[25,26], which can react with a variety of

molecules via Schiff-base and Michael addition chemistries to facilely immobilize thiol or amine containing molecules and directly reduce metal cations to metal nanoparticles[24,27]. Jiang and co-workers have developed a series of nonfouling surfaces with zwitterionic polymers such as poly(sulfobetaine methacrylate) (PSBMA)[3,28,29] and poly(carboxybetaine methacrylate) (PCBMA)[14,30,31] through direct modifications[32] by zwitterionic polymer chain with adhesive dopamine group or dopamine assisted surface-initiated polymerization[33]. With the help of catecholic initiator they carried out the polymerization of zwitterionic polymers via atom transfer radical polymerization (ATRP) method[28]. Xu and coworkers utilized the non-covalent interaction between dopamine and zwitterionic polymers and developed dopamine triggered one step codeposition of zwitterionic monomers (SBMA, MPC and CBMA) to fabricate nonfouling surface[34]. Kang *et al.*[35] and Lin *et al.*[4] recently grafted thiol-containing MPC polymer brush on the PDA coated surface via click chemistry to mitigate the surface fouling.

Among all these 'grafting to' or 'grafting from' methods, 'grafting from' methods are more complicated and need multiple steps with special conditions such as no water, no oxygen and inert atmosphere[36] which limits its large-scale practical application. Though the mostly adopted 'graft to' method is very simple to employ, there are some major challenges in this modification such as short-term efficiency and limited stability. By this 'graft to' method most of the polymer coatings are attached to the surface by weak physical adsorption such as electrostatic forces and hydrogen bonds[37] which limits their long-term application. However, strong covalent bond between surface and polymer coating is mostly desired for long-term application. Thus, it is still a great challenge to optimize the surface modification for developing such a stable surface in a facile way with both antifouling and antimicrobial properties.

Hence, we report here a robust simple dip-coating technique for covalently grafting adhesive DMA

residues containing phospholipid bioinspired p(MPC-*co*-DMA) copolymers to the amino rich PEI/ PDA co-deposited surface via amino–ene Michael addition reaction[38]. The unreacted catechol group of the PEI/PDA coated surface was used to incorporate *in situ* AgNPs from the $AgNO_3$ solution to prepare a stable dual functional antifouling and antibacterial surface. To understand the effect of adhesive catechol content for anchoring the zwitterionic copolymer onto the PDA/PEI coated substrate, three different polymers containing different percentage of DMA monomer: p(MPC_{100}), p(MPC_{90}-*co*-DMA_{10}) and p(MPC_{80}-*co*-DMA_{20}) were synthesized.

2.2 Experimental Section

2.2.1 Materials

Dopamine hydrochloride, 4,4′-Azobis (4-cyanovaleric acid) (ACVA), polyethyleneimine (PEI, M_w=600), silver nitrate ($AgNO_3$) and bovine serum albumin (BSA) was purchased from Sigma-Aldrich and used without further purification. Coomassie (Bradford) protein assay kit, standard BSA and LIVE/DEAD BacLight Bacterial Viability Kit L-7012 was purchased from Thermo Fisher Scientific Inc. *Escherichia coli (E. coli)* (ATCC® 25922™) and *Staphylococcus aureus (S. aureus)* (ATCC® 25923™) (ATCC, USA) were used as model bacteria in all bacterial test. Luria-Bertani broth (LB) and Tryptic Soy Broth (TS) (Fisher Scientific, USA) was used as liquid media for *E. coli* and *S. aureus*, respectively.

2.2.2 Synthesis and characterization of PMPC and P(MPC-co-DMA) copolymers

Three different polymers containing different percentage (0%, 10% and 20% respectively) of unprotected DMA monomer: p(MPC_{100}), p(MPC_{90}-*co*-DMA_{10}) and p(MPC_{80}-*co*-DMA_{20}) were synthesized via simple free radical polymerization using ACVA as an initiator. Prior to these copolymers synthesis, DMA monomer was synthesized according to our previously reported

protocol[39] and the purity was confirmed by ^{1}H NMR (Figure S1). For the synthesis of p(MPC$_{100}$) with 0% DMA content, MPC (700 mg, 2.37 mmol) and ACVA (10 mg, 0.036 mmol) were placed in a 50-mL polymerization tube and dissolved with a mixture of methanol and DMF. After degassing with nitrogen for 30 min, the polymerization was carried out at 70 °C in an oil bath for 24 h. The reaction was terminated by rapid cooling in liquid nitrogen and exposure to air and the resultant polymer was purified by precipitating in acetone followed by dialyzing against distilled water (DI) water for 24 h and lyophilized to obtain the polymer as a powder. For the synthesis of p(MPC-*co*-DMA), in a typical procedure, MPC (903.5 mg, 3.06 mmol), DMA (75.14 mg, 0.34 mmol) and ACVA (9.52 mg, 0.034 mmol) were placed in a 50-mL polymerization tube and dissolved with a mixture of methanol and DMF. Rest of the polymerization was carried out following the same procedure as mentioned above. The resulting polymer was characterized by ^{1}H NMR and Viscotek conventional gel permeation chromatography (GPC) to determine the composition and molecular weight, respectively. ^{1}H NMR spectra of the monomers and polymers were recorded on a Varian 500 MHz spectrometer. The number (M_n) and weight (M_w) average molecular weights and polydispersity (PDI = M_w/M_n) of the zwitterionic polymers were determined by GPC system equipped with one G5000PW$_{XL}$ TSK-GEL column using 0.5 M sodium acetate/0.5 M acetic acid buffer as eluent at a flow rate of 1.0 mL/min. The GPC was calibrated by monodisperse pullulan standards (Mw = 5900-404,000 g/mol).

2.2.3 Dip coating protocol

22 × 22 mm^2 glass cover slips were ultrasonically cleaned with ethanol and DI water for 30min and dried with air. 50mL clear polypropylene centrifuge tube was filled with 25 mL of Tris-HCl (50mM, pH 8.5) buffer solution. Dopamine hydrochloride (DA) and PEI was dissolved into that 25mL Tris-HCl buffer solution with a mass ratio of 1:1 and their concentrations were 2mg/mL.

The cleaned glass cover slip was immersed into freshly prepared DA/PEI solution and shaken at 200 rpm with a mechanical shaker for 8 hours at 25 °C. PDA/PEI – modified substrate was washed with DI water several times and dried. Then the synthesized MPC copolymer was dissolved into 25mL Tris-HCl buffer solution at 2mg/mL concentration. The dried as prepared PDA/PEI – modified substrate was immersed into that polymer solution for 7 h and mildly shaken at 25 °C in dark. Modified substrate was then taken out of the solution and rinsed with DI water for three times followed by drying under N_2 gas stream. As catechol group (-OH) of dopamine can go to auto-oxidation in the presence of oxygen all the modified substrates were stored in an inert and dark environment for further characterization. In this inert environment, all the coatings can be stored for a long time ensuring no oxygen is present for further reaction of dopamine. The coated samples were named as PDA, PDA/PEI, PDA/PEI/P(MPC), PDA/PEI/P(MPC_{90}-*co*-DMA_{10}) and PDA/PEI/P(MPC_{80}-*co*-DMA_{20}).

Further an inorganic component, silver nanoparticles (AgNPs) were deposited onto the modified surfaces by simply immersing all the modified substrates in $AgNO_3$ solution (0.1M) for 18 h in dark. The AgNPs incorporated surfaces were then rinsed with DI water; and the corresponding surfaces were named as PDA/Ag, PDA/PEI/Ag, PDA/PEI/P(MPC)/Ag, PDA/PEI/P(MPC_{90}-*co*-DMA_{10})/Ag and PDA/PEI/P(MPC_{80}-*co*-DMA_{20})/Ag respectively. This AgNps loaded surfaces also stored in inert and dark environment for further characterization and to make them stable for long time.

2.2.4 Surface Characterizations

Chemical composition of the polymer modified substrate was determined by X-ray photoelectron spectroscopy (XPS) using an AXIS Nova spectrometer (Kratos Analytical Inc., Manchester, UK) with a monochromated Al Kα source at a power of 180 W (15 kV × 12 mA) and a hemispherical

analyzer operating in the fixed analyzer transmission mode. Survey spectra were collected at a pass energy of 160 eV. The atomic concentrations of the detected elements were calculated using integral peak intensities and the sensitivity factors supplied by the manufacturer. To acquire more detailed information, high-resolution spectra were recorded from individual peaks at 40 eV pass energy, yielding a typical peak width of less than 1.0 eV (polymer C 1s). Each specimen was analyzed at an emission angle of 0° as measured from the surface normal. Binding energies for all spectra were referenced to the aliphatic carbon peak at 285.0 eV. Surface morphology of the modified substrates was examined in a dry state by atomic force microscope (AFM) using a Bruker Dimension Icon, operated in the PeakForce QNM mode with a SNL-10 probe ($k = 0.6\ N \cdot m^{-1}$). The surface morphology of AgNPs loaded surface was observed by field emission scanning electron microscopy (FESEM, Zeiss Sigma 300/VP) and Ag elemental contents on the coated substrate were also tested using Bruker energy dispersive X-ray spectroscopy (EDX).

2.2.5 Surface Wettability

Water contact angle (CA) measurement is a convenient method of characterizing the surface relative hydrophilicity and wetting properties[40]. Smaller contact angle indicates higher hydrophilicity. Water contact angle of all the coated substrates were measured using a model 590 goniometer. All the contact angles were measured with a 4 μL water droplet onto the surface at room temperature. Three contact angles were measured for each substrate at three different locations and their average recorded as a result.

2.2.6 Bacteria adhesion assay

Both gram-negative *Escherichia coli (E. coli)* and gram-positive *Staphylococcus aureus (S. aureus)* were used as the model bacteria to evaluate anti-adhesion performance of pristine and modified substrates. A single bacteria colony of *E. coli* and *S. aureus* was collected from the Luria-

Bertani (LB) and Tryptic Soy (TS) agar plate respectively, to inoculate 25 mL of liquid LB broth and TS broth respectively. After inoculation at 37 °C for 18 h, bacteria cells were washed with sterile PBS solution through centrifugation at 4000 rpm for 5 min and resuspension in PBS for twice. The harvested bacterial cells were resuspended in PBS solution to an optical density (OD) of 0.1 at 670 nm (OD 670) of 0.1, corresponding to ~8×10^9 cells/mL. Coated samples were immersed into that bacterial solution and mildly shaken for 3 h at 37 °C to foul with bacteria. To check the initial adhesion on the surface only 30 min incubation of a sample in bacteria solution in a static condition is enough[41]. But to show the long-term stability of the coating we chose a longer time and non-static mode to foul with bacterial solution. Primarily we immersed all the coated samples for three different hours 3h, 4h and 5h. But we did not find any difference in the number of the adhered bacteria on the modified surface for these three different time intervals. That is why we have chosen 3h culture time following the same procedure as previously reported[42,43]. The bacterial solution was then discarded and coated substrates were gently washed with PBS for 3 times to remove suspended bacterial cells. The PBS buffer was used because it helped maintain a constant pH and a balanced osmotic pressure between the inside and outside of the bacterial cells. The bacterial cells attached on the glass slides were stained with 50 µL of LIVE/DEAD stain in dark for 15min and then washed with PBS gently. After that, each slide was examined by a fluorescence microscope with a magnification of 400x. The number of bacterial cells was obtained through counting the bacterial cells in five areas (4 corners plus the center) of the glass slides and then averaging. The counted number of the attached bacteria was analyzed using an ImageJ software package and shown as cells/cm^2.

2.2.7 Antibacterial Assay

Bactericidal activity of the modified substrates will be qualitatively investigated by conducting an

inhibition zone test. 30 µL of bacteria-containing liquid media were pipetted on the surface of agar plate (LB agar for *E. coli* and TSA for *S. aureus*) and evenly spread over the surface of corresponding agar using a sterile plastic spreader. Glass slides were broken into small pieces and coated following the coating protocol. Then the control and small coated substrates were carefully plated on the top of agar plates in triplicate and incubated at 37 °C for 24 h for the evaluation of growth inhibition. The halo zone formed after 24 h served as an indicator of the antibacterial activity which was recorded using a digital camera.

2.2.8 Protein adhesion

BSA was used as a model protein for protein adsorption test. The coated samples were immersed into 2mg/mL BSA solution in PBS at 37 °C for 3 h. Then the adsorbed protein was detached by washing with 1mL DI water and the concentration of the absorbed protein was measured using the Bradford method[44]. A standard calibration curve following the micro test tube protocol[45] (working range 1-25 µg/mL) was obtained using standard BSA solution and all the absorbance was measured at 595 nm. Using this standard curve protein concentration of each unknown sample was measured.

2.3 Results and Discussion

2.3.1 Polymer synthesis and Characterization

DMA monomer was first synthesized according to our previous report[39] and characterized by ^{1}H NMR (Figure S 2-1). The purity was confirmed by comparing the integrals of the typical benzyl protons in DMA (δ 6.78, 6.61and 6.43 ppm) with integrals of methacrylate peaks (δ 5.58 and 5.27 ppm) for DMA. Then, free radical polymerization of MPC with different DMA content (0%, 10% and 20%) was conducted as illustrated in Scheme 2-1 with a targeted degree of polymerization

(DP) of 100 and listed as: p(MPC_{100}), p(MPC_{90}-*co*-DMA_{10}) and p(MPC_{80}-*co*-DMA_{20}) respectively. The ^1H NMR results of all the synthesized polymers were presented in Figure S 2-2 to Figure S 2-4. The characteristic signals of MPC and DMA units were clearly observed, and all peaks were well assigned with their chemical structures.

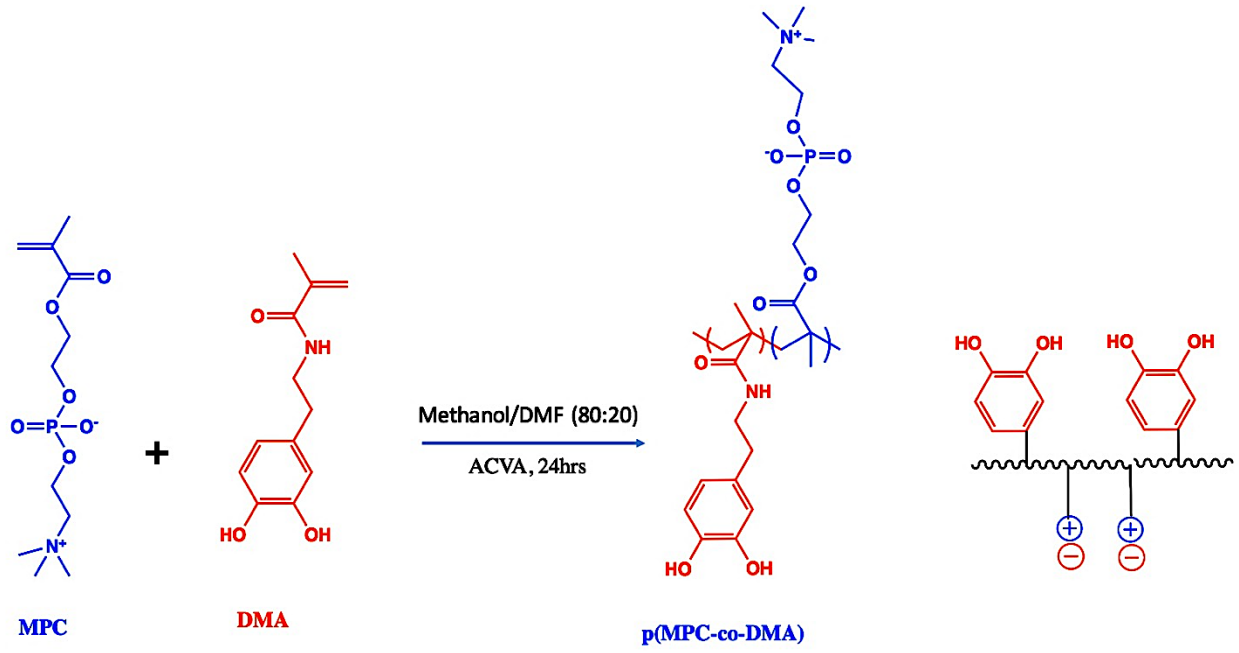

Scheme 2-1. Free-radical copolymerization of MPC with catechol containing DMA monomer

DMA content in the MPC copolymer was calculated by comparison of characteristic peak integrals of MPC (δ 4-4.35 and 3.2-3.7 ppm) and DMA (δ 6.71, 2.68 and 3.1 ppm). The calculated results of DMA content from ^1H NMR and the weight-average molecular weight (M_w) and number-

average molecular weight (M_n) of the MPC copolymers determined by aqueous GPC are shown in Table 2.1. The polydispersity index (PDI) of the synthesized polymers was found quite high which is mostly because of the polymer synthesis method. As there is no control during free radical polymerization, the PDI could be very random and high. But this high PDI won't have any significance in changing surface properties.

Table 2.1. Chemical composition and molecular weights of the synthesized polymers

	Composition[a] (mol%)		Molecular Weight[b]	
Polymers	**MPC**	**DMA**	**M_n (g/mol)**	**M_w (g/mol)**
p(MPC_{100})	100	_	36900	218200
p(MPC_{90}-*co*-DMA_{10})	90.9	9.1	43200	198900
p(MPC_{80}-*co*-DMA_{20})	84.75	15.25	39360	161800

[a] Calculated from ^{1}H NMR results using D_2O or D_2O/DMSO-d_6 mixture as solvent. [b] Obtained from aqueous GPC using 0.5 M sodium acetate/acetic acid buffer as eluent.

2.3.2 Surface Characterization

According to the coating protocol, five coated glass coverslips were prepared and the surface morphology of these modified surfaces were investigated by AFM. As shown in Figure 2.1 the bare glass slide was relatively smooth with a root mean square (RMS) roughness of 6.4 nm. In comparison, the RMS roughness increased remarkably to 30.3 nm for the PDA deposited surface

due to self-polymerized large PDA aggregates[46]. But after introducing PEI into the coating, for PDA/PEI codeposited surfaces, no large aggregates were observed because of the destruction of noncovalent interactions between PDA aggregates[47]. PDA/PEI surface showed lower surface roughness of 16.1 nm only due to the absence of particle aggregation which also proves the successful crosslinking of PDA with PEI. After introducing MPC copolymers no significant change in surface roughness was observed. PDA/PEI/P(MPC), PDA/PEI/P(MPC_{90}-*co*-DMA_{10}) and PDA/PEI/P(MPC_{80}-*co*-DMA_{20}) modified surface showed surface roughness of 16.2, 16.5 and 16.6 nm respectively. As the AFM experiment was conducted in air, slightly increased roughness may indicate increased polymer attachment to the surface. DMA content in polymer did not show any effect on surface roughness.

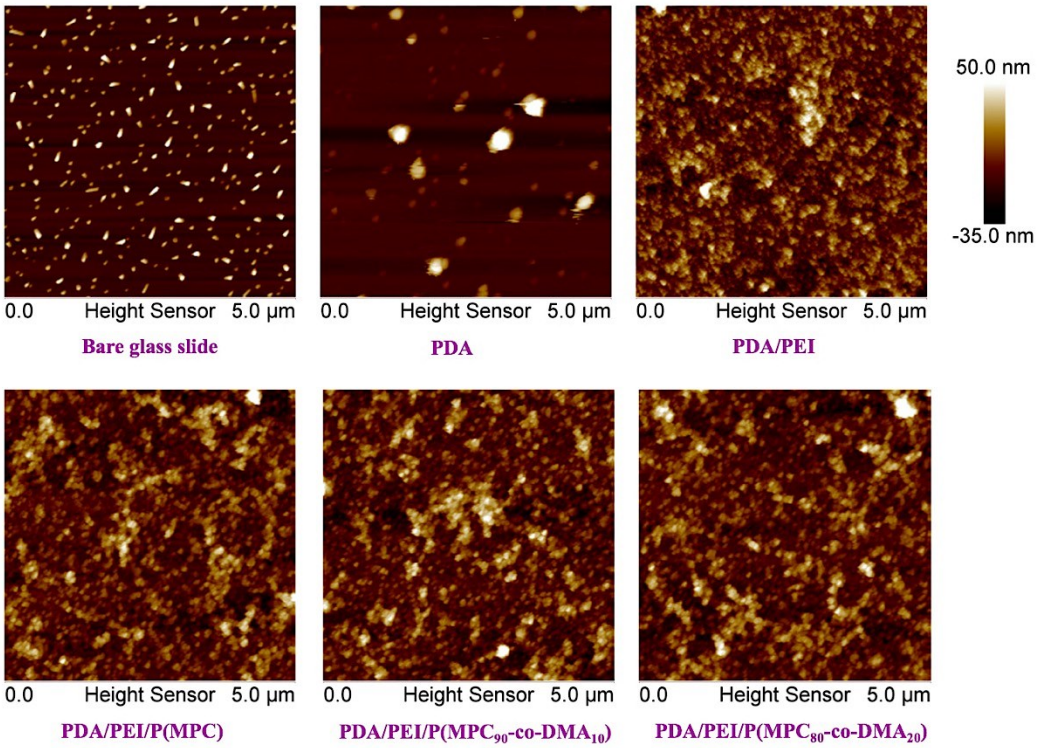

Figure 2.1. QNM-mode Atomic Force Microscopy images of the bare glass, PDA, PDA/PEI, PDA/PEI/P(MPC), PDA/PEI/P(MPC_{90}-co-DMA_{10}) and PDA/PEI/P(MPC_{80}-co-DMA_{20}) modified surfaces in dry state. The dimension of each scan image is 5×5 µm.

The surface elemental compositions of the modified surface were determined by XPS spectra (Figure 2.2). Successful attachment of the MPC copolymer on the PDA/PEI codeposited surface was confirmed by the characteristic phosphorus P 2p signal at 133.7 eV, which was absent in both pure PDA and PDA/PEI coating. High resolution of XPS showed phosphorus to carbon ratio (P/C) increased from 0.009 to 0.013 (Table S1) with the increase of the DMA content in MPC copolymer, which indicates higher grafting of MPC to the surface. A possible amino-ene Michael addition chemical reaction between DMA and PEI can be considered as one of the mechanisms for grafting MPC copolymer to the PDA/PEI surface[38]. This covalent bond between MPC

copolymer and PDA/PEI surface is responsible to make it a promising stable coating. Messersmith *et al.* also reported that the initial pull-off force of this covalent bond to surface-bound amine is 2.2nN which is very high magnitude pull-off force[48] and indicates the strong bond between DMA containing MPC copolymer and amino rich PDA/PEI surfaces. The presence of unique phosphorylcholine (PC) groups also confirmed by the quaternary ammonium N 1s peak at 403.60 eV which was only present in PDA/PEI/P(MPC_{90}-*co*-DMA_{10}) and PDA/PEI/P(MPC_{80}-*co*-DMA_{20}).

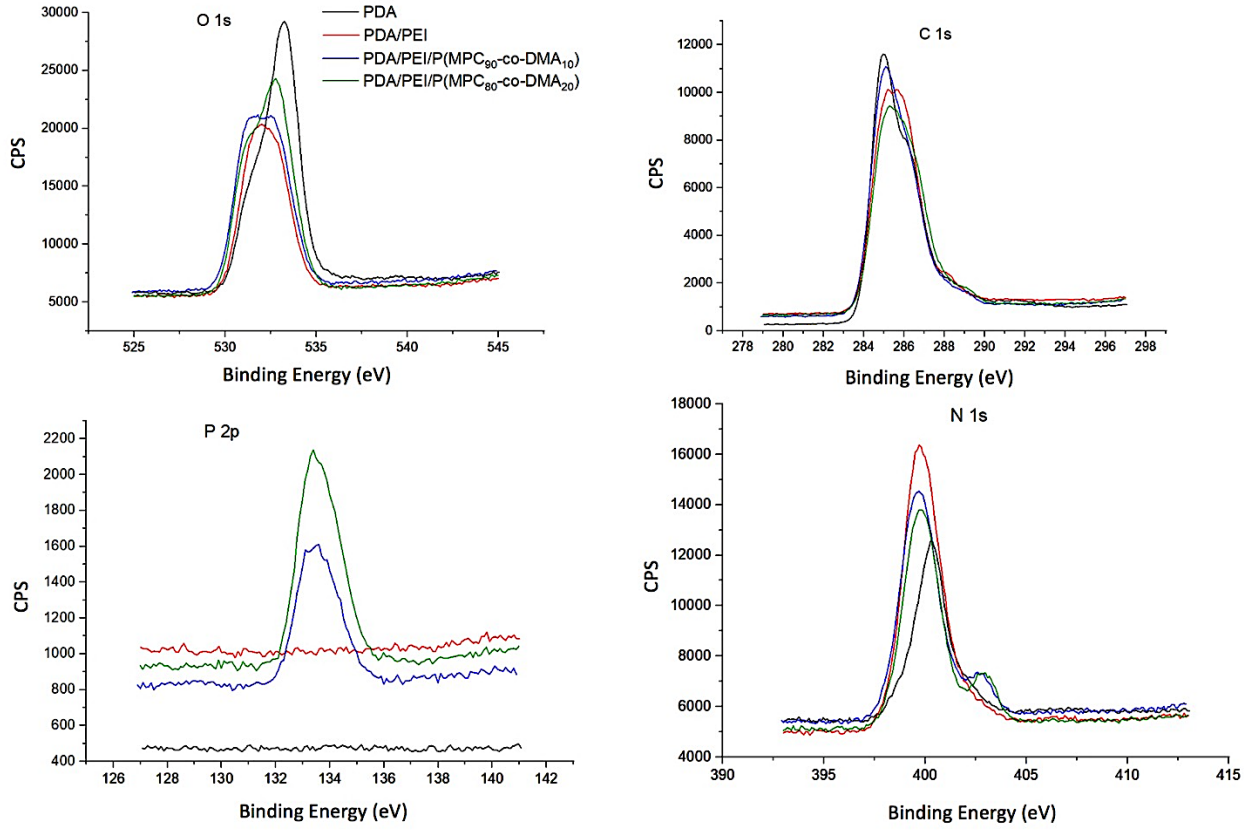

Figure 2.2. XPS spectra of the modified substrates; High-resolution O 1s, C 1s, N 1s, and P 2p narrow scans as a function of electron binding energy

The strong signal of O 1s with highest intensity at 533.16 eV is related to the auto oxidation of the PDA layer. High resolution N 1s spectra also demonstrated the highest nitrogen to carbon (N/C) ratio of 0.209 indicating successful crosslinking of PEI with PDA. For both PDA/PEI/P(MPC$_{90}$-*co*-DMA$_{10}$) and PDA/PEI/P(MPC$_{80}$-*co*-DMA$_{20}$) surfaces N/C ratio (0.172) was almost unchanged indicating homogenous grafting of MPC copolymer to the surface.

To investigate the surface wettability, the static water contact angle (WCA) of the pristine glass slides and modified surfaces were measured in air. As shown in Figure 2.3, WCA of pristine glass substrate was 64.5°. All the other modified glass substrates showed lower WCA than pristine glass due to their improved hydrophilicity. Among them PDA/PEI/P(MPC$_{90}$-*co*-DMA$_{10}$) coated glass substrate showed lowest WCA: 6.8°- indicating the presence of a stronger surface hydration.

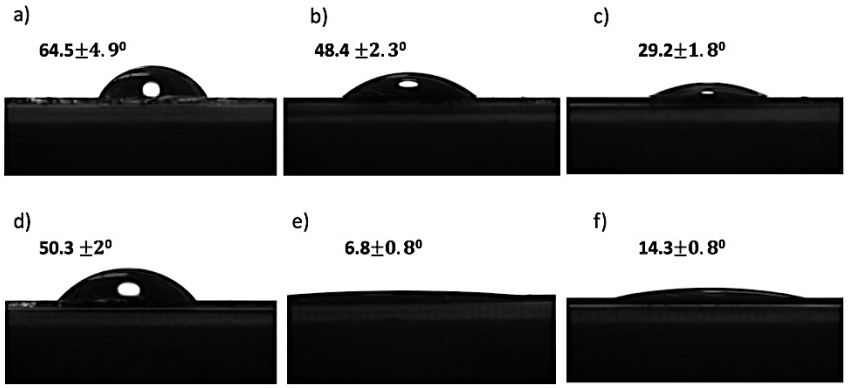

Figure 2.3. Water contact angle of a) bare glass, b) PDA coated glass, c) PDA/PEI coated glass, d) PDA/PEI/P(MPC), e) PDA/PEI/P(MPC$_{90}$-co-DMA$_{10}$) and f) PDA/PEI/P(MPC$_{80}$-co-DMA$_{20}$) coated glass slides.

2.3.3 Bacteria Adhesion Assay

Bacterial adhesion on the medical devices is the primary cause for biofilm formation which leads to medical-device related infection. The initial attachment of a single bacterial cell to a surface is considered as the key preliminary step in the biofilm formation processes[49], as such, the number of initially attached bacteria on the surface is one of the most important factors for evaluating antifouling properties of the surface. In this study, to evaluate bacteria antifouling properties of the modified substrates quantitatively, gram positive *S. aureus* and gram-negative *E. coli* bacteria was selected. After 3 h incubation with bacteria solution containing 8×10^9 cell/mL, all the coated samples were rinsed with PBS to remove loosely bound bacteria and stained using LIVE/DEAD stain for microscopic examination under fluorescence microscopy. As shown in Figure 2.4 many green spots (live bacteria) with only a few red spots (dead bacteria) were observed for PDA coated glass substrate for both *E. coli* and *S. aureus* adhesion indicating the insignificant anti-adhesion efficiency of the PDA coated glass surface. PDA/PEI coated substrate showed less number of adhered bacteria than both bare glass and PDA coating because of a more hydrophilic amino rich surface[46]. After introducing zwitterionic MPC (without any DMA content) onto the surface, the number of *E. coli* bacteria adhesion was significantly reduced (about 85.6%) for PDA/PEI/P(MPC) coating indicating high antiadhesion efficiency as strong hydration layer induced by the zwitterionic copolymers. But for *S. aureus* adhesion no significant reduction was observed for PDA/PEI/P(MPC) coating. Whereas MPC copolymer with DMA content showed dramatically reduced bacteria adhesion for both *E. coli* and *S. aureus* confirming highest grafting density and stability of MPC copolymer on the PDA/PEI coated surface. Both PDA/PEI/P(MPC_{90}-*co*-DMA_{10}) and PDA/PEI/P(MPC_{80}-*co*-DMA_{20}) coating showed less than 92% reduction in bacterial adhesion. Percentage of DMA in their coating did not significantly affect the bacterial adhesion. With

increasing the DMA content bacterial adhesion was slightly reduced. So, a little amount of DMA in an MPC copolymer is enough to graft them more firmly to the PDA/PEI coated surface.

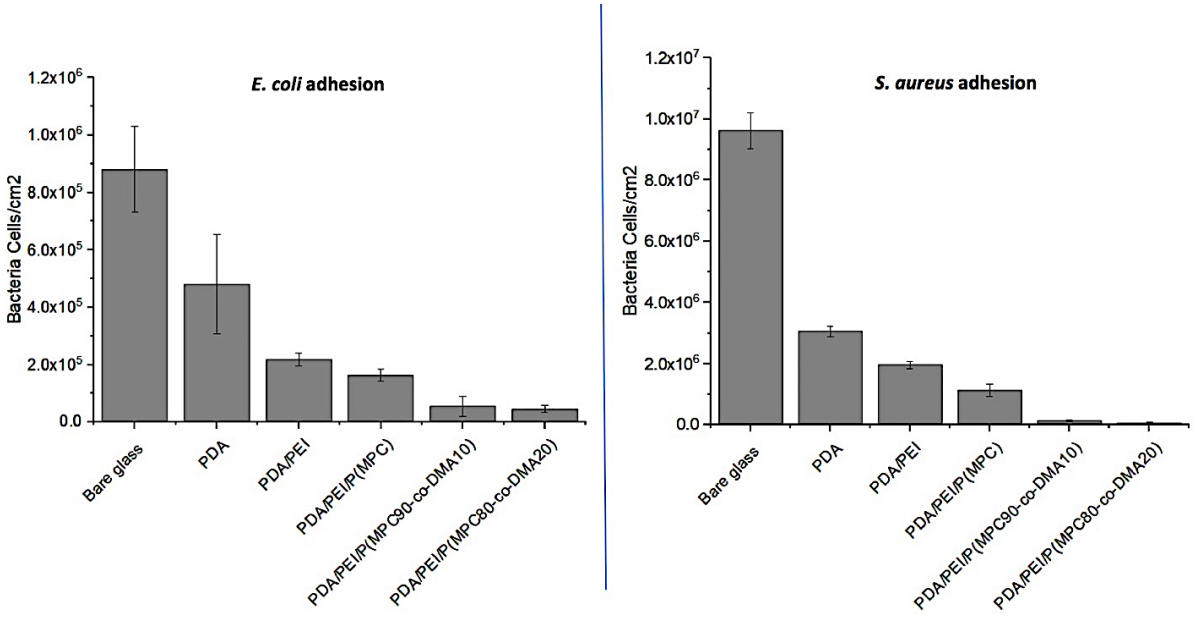

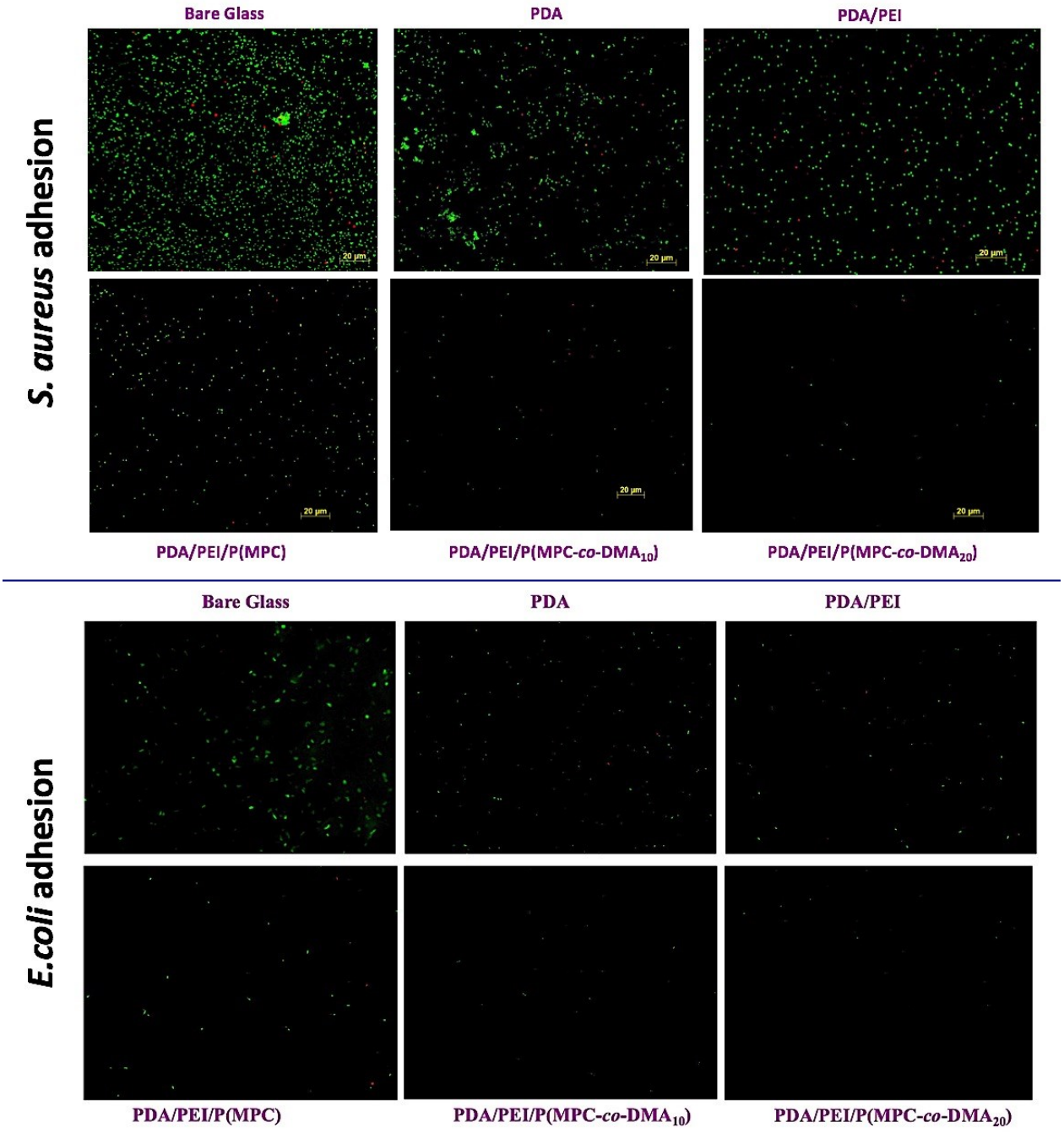

Figure 2.4. E. coli and S. aureus bacterial adhesion on the different polymer coated surfaces

2.3.4 Protein adhesion

The data of the amount of protein adsorbed on the surface is considered one of the most important factors for evaluating biocompatibility and antifouling property of materials[50]. Because adsorption of protein is considered to be the first step of biofouling in biomaterials. Figure 2.5 has shown that the amount of absorbed protein percentage on the MPC copolymer grafted surface was significantly less than without MPC polymer on the surface. Among them PDA/PEI/P(MPC_{80}-*co*-DMA_{20}) showed lowest amount of protein adsorption indicating highest grafting density of MPC copolymer on the surface due to increased anchoring DMA content. But it did not vary much with other MPC copolymer grafted surfaces ensuring that only a small amount of DMA residues in the polymer chain is enough to maintain a strong antifouling surface. As zwitterionic polymers contain both positive and negative charge moieties, they can create a diffusion resistant layer by maintaining a strong hydration layer on the top of their surface. So the increased amount of MPC on the surface is responsible for lowest protein adhesion on the materials[51].

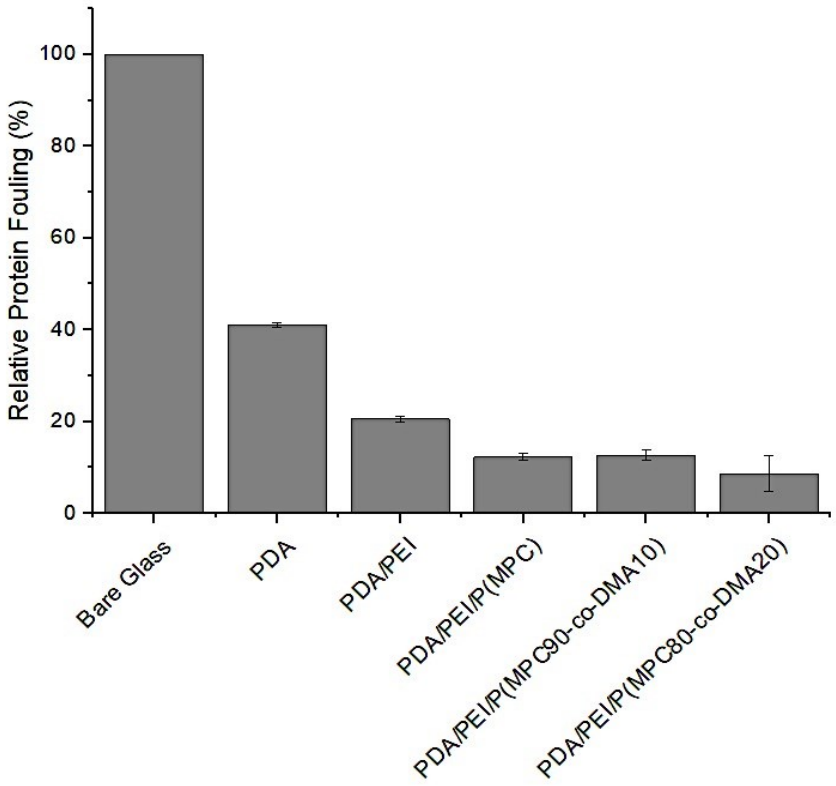

Figure 2.5. Relative protein fouling levels for different coating

2.3.5 Antibacterial Activity

After the *in-situ* formation of AgNPs on all the modified surfaces, different morphological structures were investigated using SEM and the elemental percentage of the AgNPs loaded surfaces was investigated using EDX. SEM images (Figure 2.6) showed cluster-like distribution of round-like AgNPs on a PDA coated surface. But after introducing MPC polymer the AgNPs were uniformly distributed with less size in diameter. More clusters of AgNPs were observed in PDA coating only because of the presence of the high amount of reducing catechol groups in the PDA layer which is mainly responsible for the *in-situ* AgNPs formation[52]. After grafting both PEI and MPC copolymer, the amount of catechol groups was reduced which consequently also

decreased the amount and size of AgNPs on the surface. EDX analysis (Table S2) also demonstrated the same phenomena. Compared to all three MPC copolymer grafted surface PDA/PEI/P(MPC_{80}-*co*-DMA_{20}) showed the highest amount of AgNPs presence on the surface because of the presence of more catechol groups in DMA content.

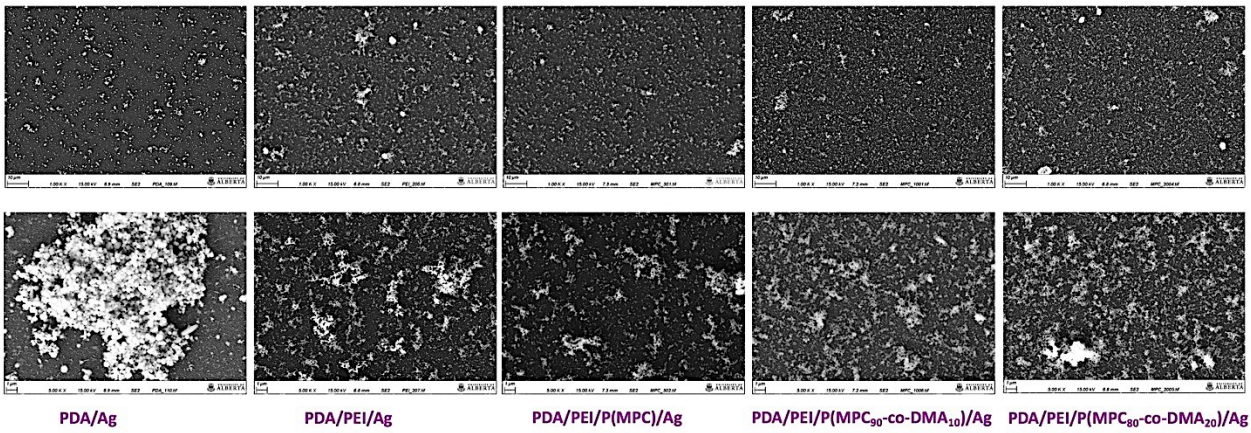

Figure 2.6. SEM images of the surface morphology of AgNPs loaded surfaces

Bactericidal activity of the AgNPs loaded surfaces were studied via a bacterial inhibition zone towards *E. coli* and *S. aureus*, respectively. As shown in Figure 2.7. no apparent bacterial growth under the surface was observed for all the silver incorporated surfaces. Though PDA/Ag coated surface showed highest amount of the AgNPs (Table S2) on the surface, inhibition zone for all the other samples: PDA/PEI/Ag, PDA/PEI/P(MPC)/Ag, PDA/PEI/P(MPC_{90}-*co*-DMA_{10})/Ag and PDA/PEI/P(MPC_{80}-*co*-DMA_{20})/Ag was larger. Release rate of AgNPs from the developed surfaces or the deposited AgNPs sizes can contribute to this inhibition zone formation. This bactericidal activity is attributed to the presence of PEI which can act as a stabilizer for AgNPs[53].

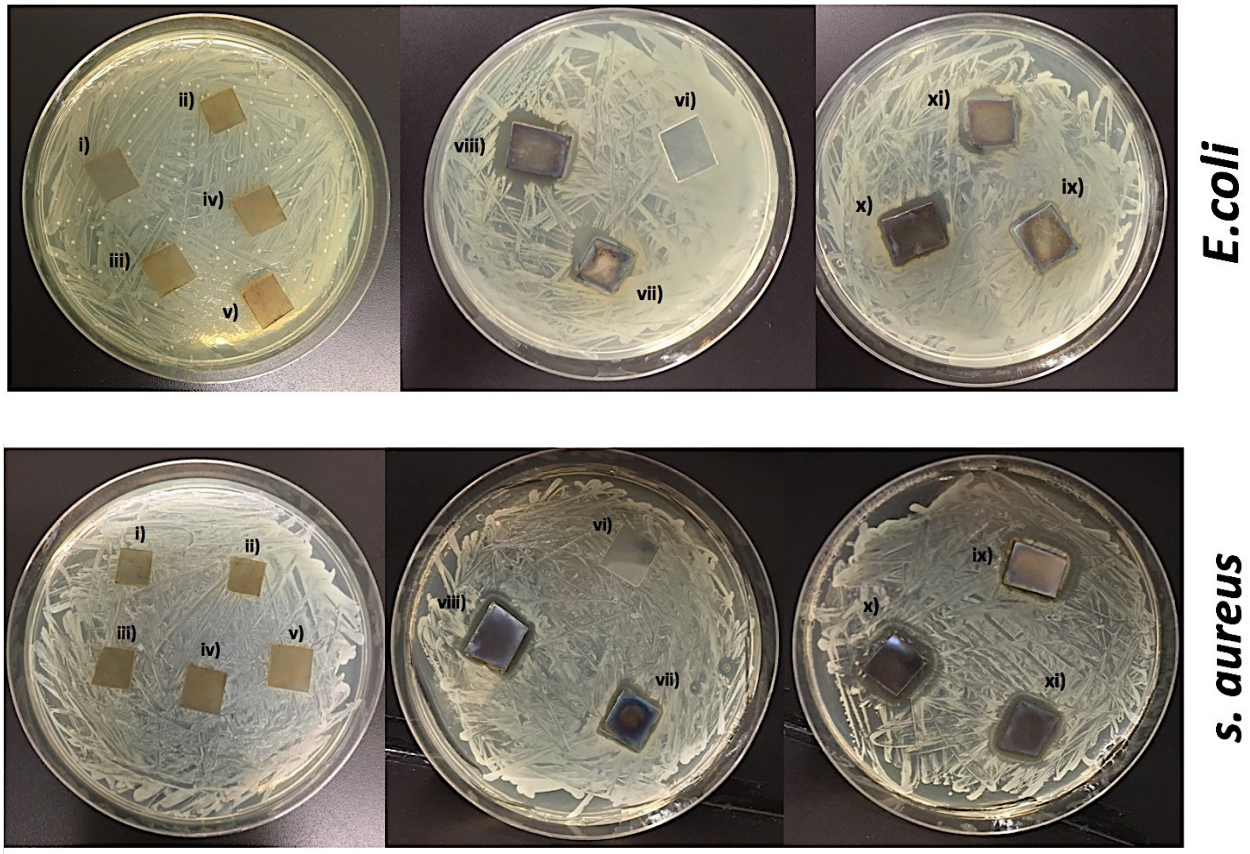

Figure 2.7 Inhibition zone images for E. coli and S. aureus bacteria respectively; i) PDA, ii) PDA/PEI, iii) PDA/PEI/P(MPC), iv) PDA/PEI/P(MPC$_{90}$-co-DMA$_{10}$), v) PDA/PEI/P(MPC$_{80}$-co-DMA$_{20}$), vi) Bare glass slide, vii) PDA/Ag, viii) PDA/PEI/Ag, ix) PDA/PEI/P(MPC)/Ag, x) PDA/PEI/P(MPC$_{90}$-co-DMA$_{10}$)/Ag and xi) PDA/PEI/P(MPC$_{80}$-co-DMA$_{20}$)/Ag.

2.4 Conclusion

A uniform surface coating with PDA/PEI co-deposition and subsequent grafting of P(MPC-*co*-DMA) polymer onto that amino rich modified surface was developed by a facile dip coating method. This coating showed excellent antifouling and antibacterial properties. Here P(MPC-*co*-DMA) copolymer was covalently grafted via possible amino-ene Michael addition reaction with

amino rich PDA/PEI coated surface which demonstrated to be stronger and more stable than any other weak physical adsorption such as electrostatic forces and hydrogen bonds[37]. Small amount of DMA content in the MPC copolymer is enough to enhance hydrophilicity, grafting density and antifouling properties. The outstanding antifouling property of the covalently grafted PDA/PEI/P(MPC-*co*-DMA) surface makes it a promising dual functional coating for application in biomedical devices.

2.5 Supporting Information:

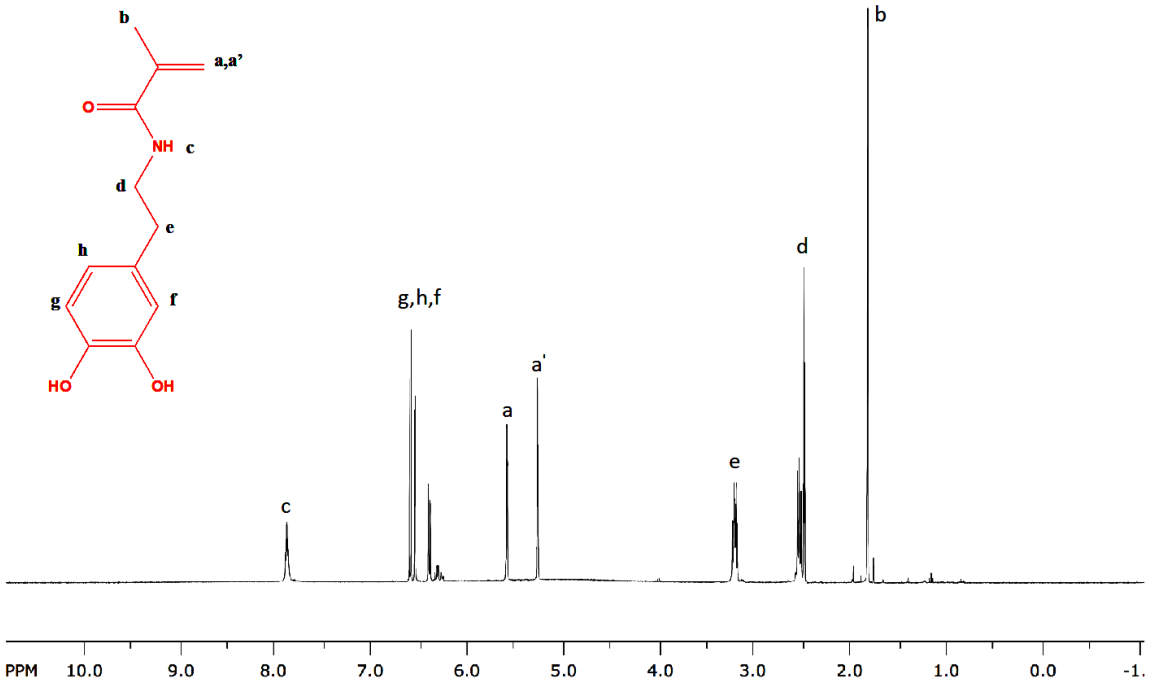

Figure S 2-1. DMA monomer synthesis scheme and ^{1}H NMR spectrum of DMA (DMSO-d_6)

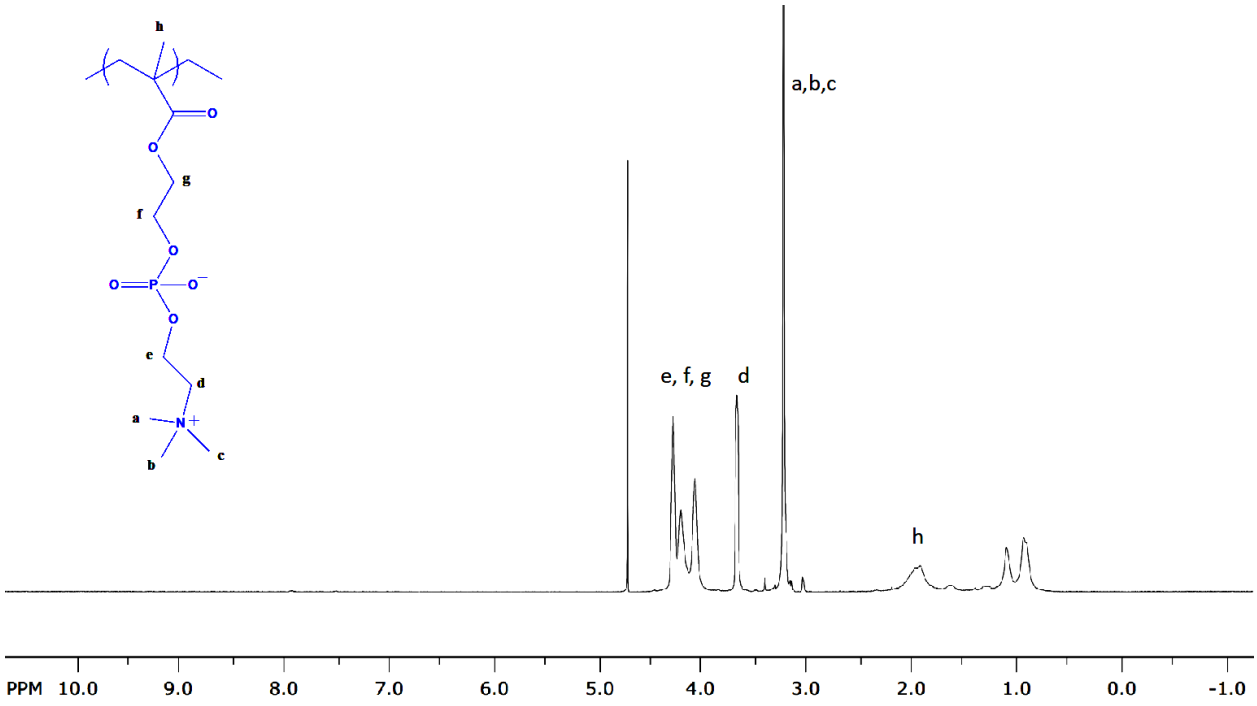

Figure S 2-2. ^{1}H NMR spectrum of p(MPC$_{100}$) (D_2O)

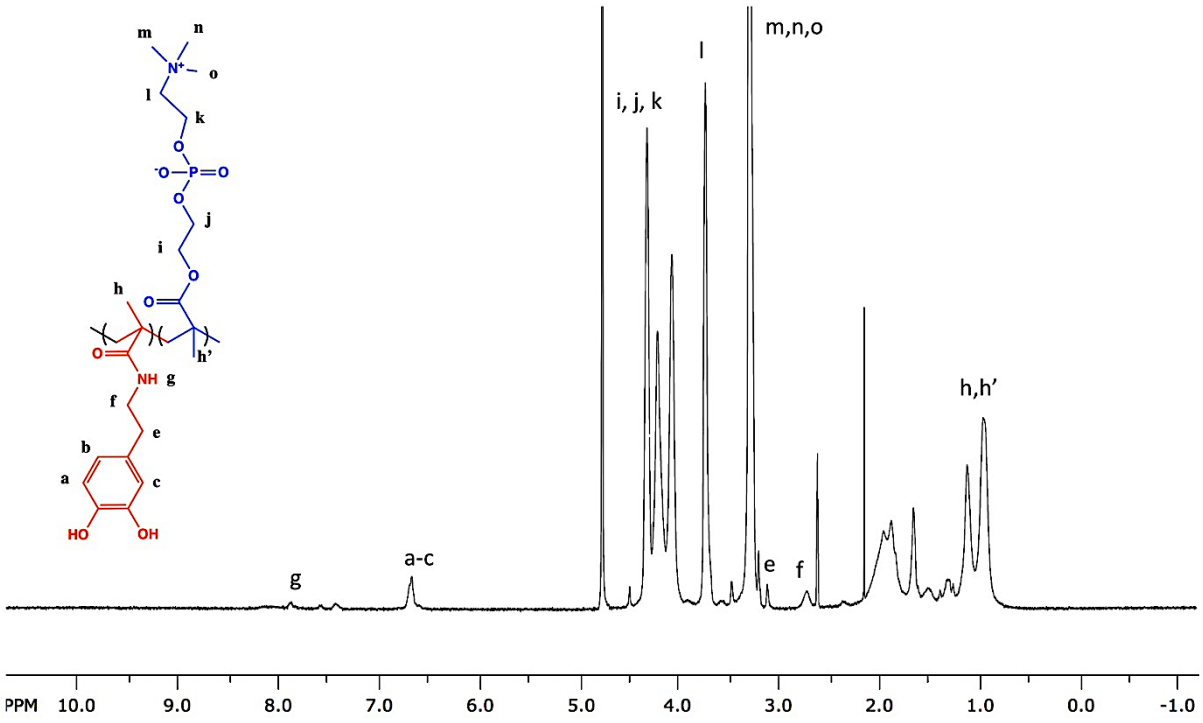

Figure S 2-3. ^{1}H NMR spectrum of p(MPC$_{90}$-*co*-DMA$_{10}$) (CD$_3$OD+DMSO-*d*$_6$)

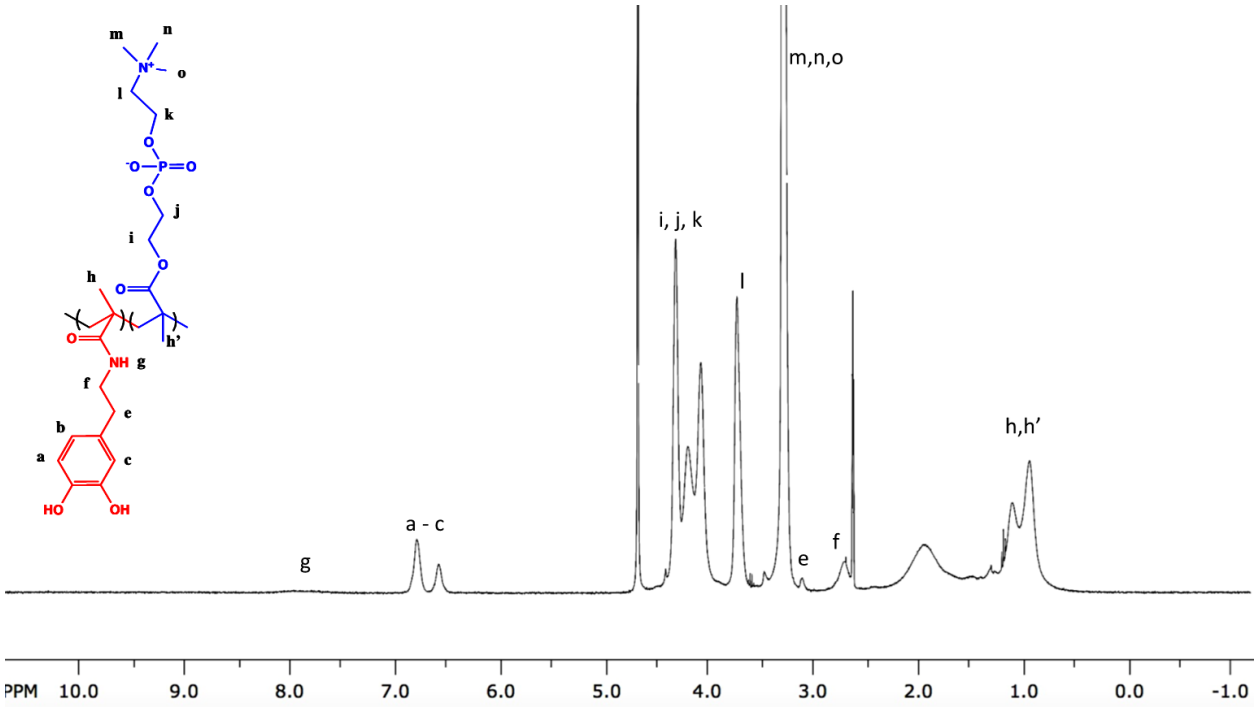

Figure S 2-4. ^{1}H NMR spectrum of p(MPC$_{80}$-*co*-DMA$_{20}$) (CD$_3$OD+DMSO-d_6)

Table S 1 Atomic ratio (X/C) – elemental analysis of the high resolution XPS that provide compositional analysis of the different coated surfaces.

Samples	O/C	N/C	P/C
Bare Glass slides	4.581	0.047	_
PDA	0.235	0.099	_

PDA/PEI	0.200	0.209	_
PDA/PEI/P(MPC$_{90}$-co-DMA$_{10}$)	0.217	0.172	0.009
PDA/PEI/P(MPC$_{80}$-co-DMA$_{20}$)	0.250	0.172	0.013

Table S 2 Surface elemental compositions of the AgNPs loaded surfaces using EDX

Samples	C	O	Na	Mg	Al	Ag	Si	Ca
PDA/Ag	24.50	21.13	6.52	1.77	0.53	14.45	26.56	4.54
PDA/PEI/Ag	15.71	33.04	7.98	2.02	0.58	7.35	29.03	4.29
PDA/PEI/P(MPC)/Ag	27.71	32.69	7.47	1.87	0.54	3.90	27.08	4.07
PDA/PEI/P(MPC$_{90}$-co-DMA$_{10}$)/Ag	33.10	25.96	6.46	1.61	0.54	4.23	24.45	3.64
PDA/PEI/P(MPC$_{80}$-co-DMA$_{20}$)/Ag	22.33	30.52	7.22	1.82	0.59	6.03	27.24	4.24

2.6 References

(1) Bixler, G. D.; Bhushan, B. Review Article: Biofouling: Lessons from Nature. *Philosophical Transactions of the Royal Society A: Mathematical, Physical and Engineering Sciences*. 2012, pp 2381–2417.

(2) Harding, J. L.; Reynolds, M. M. Combating Medical Device Fouling. *Trends Biotechnol.* **2014**, *32* (3), 140–146.

(3) Li, G.; Cheng, G.; Xue, H.; Chen, S.; Zhang, F.; Jiang, S. Ultra Low Fouling Zwitterionic Polymers with a Biomimetic Adhesive Group. *Biomaterials* **2008**, *29* (35), 4592–4597.

(4) Shahkaramipour, N.; Lai, C. K.; Venna, S. R.; Sun, H.; Cheng, C.; Lin, H. Membrane Surface Modification Using Thiol-Containing Zwitterionic Polymers via Bioadhesive Polydopamine. *Ind. Eng. Chem. Res.* **2018**, *57* (6), 2336–2345.

(5) Dang, Y.; Quan, M.; Xing, C. M.; Wang, Y. B.; Gong, Y. K. Biocompatible and Antifouling Coating of Cell Membrane Phosphorylcholine and Mussel Catechol Modified Multi-Arm PEGs. *J. Mater. Chem. B* **2015**, *3* (11), 2350–2361.

(6) Fu, Y.; Wang, Y.; Huang, L.; Xiao, S.; Chen, F.; Fan, P.; Zhong, M.; Tan, J.; Yang, J. Salt-Responsive "Killing and Release" Antibacterial Surfaces of Mixed Polymer Brushes. *Ind. Eng. Chem. Res.* **2018**, *57* (27), 8938–8945.

(7) Selim, M. S.; Yang, H.; Wang, F. Q.; Li, X.; Huang, Y.; Fatthallah, N. A. Silicone/Ag@SiO2core-Shell Nanocomposite as a Self-Cleaning Antifouling Coating Material. *RSC Adv.* **2018**, *8* (18), 9910–9921.

(8) Schlenoff, J. B. Zwitteration: Coating Surfaces with Zwitterionic Functionality to Reduce Nonspecific Adsorption. *Langmuir*. 2014, pp 9625–9636.

(9) Damodaran, V. B.; Murthy, S. N. Bio-Inspired Strategies for Designing Antifouling Biomaterials. *Biomater. Res.* **2016**, *20* (1).

(10) Chen, S.; Li, L.; Zhao, C.; Zheng, J. Surface Hydration: Principles and Applications toward Low-Fouling/Nonfouling Biomaterials. *Polymer*. 2010, pp 5283–5293.

(11) Yu, Q.; Wu, Z.; Chen, H. Dual-Function Antibacterial Surfaces for Biomedical Applications. *Acta Biomaterialia*. 2015, pp 1–13.

(12) He, M.; Gao, K.; Zhou, L.; Jiao, Z.; Wu, M.; Cao, J.; You, X.; Cai, Z.; Su, Y.; Jiang, Z. Zwitterionic Materials for Antifouling Membrane Surface Construction. *Acta Biomaterialia*. 2016, pp 142–152.

(13) Wu, J.; Lin, W.; Wang, Z.; Chen, S.; Chang, Y. Investigation of the Hydration of Nonfouling Material Poly(Sulfobetaine Methacrylate) by Low-Field Nuclear Magnetic Resonance. *Langmuir* **2012**, *28* (19), 7436–7441.

(14) Gao, C.; Li, G.; Xue, H.; Yang, W.; Zhang, F.; Jiang, S. Functionalizable and Ultra-Low Fouling Zwitterionic Surfaces via Adhesive Mussel Mimetic Linkages. *Biomaterials* **2010**, *31* (7), 1486–1492.

(15) Sun, F.; Wu, K.; Hung, H. C.; Zhang, P.; Che, X.; Smith, J.; Lin, X.; Li, B.; Jain, P.; Yu, Q.; et al. Paper Sensor Coated with a Poly(Carboxybetaine)-Multiple DOPA Conjugate via Dip-Coating for Biosensing in Complex Media. *Anal. Chem.* **2017**, *89* (20), 10999–11004.

(16) Wang, B. L.; Jin, T. W.; Han, Y. M.; Shen, C. H.; Li, Q.; Lin, Q. K.; Chen, H. Bio-Inspired Terpolymers Containing Dopamine, Cations and MPC: A Versatile Platform to Construct a Recycle Antibacterial and Antifouling Surface. *J. Mater. Chem. B* **2015**, *3* (27), 5501–5510.

(17) Jin, X.; Yuan, J.; Shen, J. Zwitterionic Polymer Brushes via Dopamine-Initiated ATRP from PET Sheets for Improving Hemocompatible and Antifouling Properties. *Colloids Surfaces B Biointerfaces* **2016**, *145*, 275–284.

(18) Sin, M. C.; Sun, Y. M.; Chang, Y. Zwitterionic-Based Stainless Steel with Well-Defined Polysulfobetaine Brushes for General Bioadhesive Control. *ACS Appl. Mater. Interfaces* **2014**, *6* (2), 861–873.

(19) Kuang, J.; Messersmith, P. B. Universal Surface-Initiated Polymerization of Antifouling Zwitterionic Brushes Using a Mussel-Mimetic Peptide Initiator. *Langmuir* **2012**, *28* (18), 7258–7266.

(20) Lee, H.; Dellatore, S. M.; Miller, W. M.; Messersmith, P. B. Mussel-Inspired Surface

Chemistry for Multifunctional Coatings. *Science (80-.).* **2007**, *318* (5849), 426–430.

(21) Ryu, J. H.; Messersmith, P. B.; Lee, H. Polydopamine Surface Chemistry: A decade of Discovery. *ACS Appl. Mater. Interfaces* **2018**, 10, 7523−7540.

(22) Jiang, J.; Zhu, L.; Zhu, L.; Zhu, B.; Xu, Y. Surface Characteristics of a Self-Polymerized Dopamine Coating Deposited on Hydrophobic Polymer Films. *Langmuir* **2011**, *27* (23), 14180–14187.

(23) Bernsmann, F.; Ball, V.; Addiego, F.; Ponche, A.; Michel, M.; Gracio, J. J. D. A.; Toniazzo, V.; Ruch, D. Dopamine-Melanin Film Deposition Depends on the Used Oxidant and Buffer Solution. *Langmuir* **2011**, *27* (6), 2819–2825.

(24) Yang, H. C.; Luo, J.; Lv, Y.; Shen, P.; Xu, Z. K. Surface Engineering of Polymer Membranes via Mussel-Inspired Chemistry. *J. Memb. Sci.* **2015**, *483*, 42–59.

(25) Yang, H. C.; Waldman, R. Z.; Wu, M. B.; Hou, J.; Chen, L.; Darling, S. B.; Xu, Z. K. Dopamine: Just the Right Medicine for Membranes. *Adv. Funct. Mater.* **2018**, *28* (8).

(26) Li, L.; Zeng, H. Marine Mussel Adhesion and Bio-Inspired Wet Adhesives. *Biotribology* **2016**, *5*, 44–51.

(27) Lu, Z.; Xiao, J.; Wang, Y.; Meng, M. In Situ Synthesis of Silver Nanoparticles Uniformly Distributed on Polydopamine-Coated Silk Fibers for Antibacterial Application. *J. Colloid Interface Sci.* **2015**, *452*, 8–14.

(28) Sundaram, H. S.; Han, X.; Nowinski, A. K.; Ella-Menye, J. R.; Wimbish, C.; Marek, P.; Senecal, K.; Jiang, S. One-Step Dip Coating of Zwitterionic Sulfobetaine Polymers on Hydrophobic and Hydrophilic Surfaces. In *ACS Applied Materials and Interfaces*; 2014; Vol. 6, pp 6664–6671.

(29) Yang, W.; Sundaram, H. S.; Ella, J. R.; He, N.; Jiang, S. Low-Fouling Electrospun PLLA Films Modified with Zwitterionic Poly(Sulfobetaine Methacrylate)-Catechol Conjugates. *Acta Biomater.* **2016**, *40*, 92–99.

(30) Cheng, G.; Li, G.; Xue, H.; Chen, S.; Bryers, J. D.; Jiang, S. Zwitterionic Carboxybetaine Polymer Surfaces and Their Resistance to Long-Term Biofilm Formation. *Biomaterials*

2009, *30* (28), 5234–5240.

(31) Amoako, K. A.; Sundaram, H. S.; Suhaib, A.; Jiang, S.; Cook, K. E. Multimodal, Biomaterial-Focused Anticoagulation via Superlow Fouling Zwitterionic Functional Groups Coupled with Anti-Platelet Nitric Oxide Release. *Adv. Mater. Interfaces* **2016**, *3* (6).

(32) Sundaram, H. S.; Han, X.; Nowinski, A. K.; Brault, N. D.; Li, Y.; Ella-Menye, J.-R.; Amoaka, K. A.; Cook, K. E.; Marek, P.; Senecal, K.; et al. Achieving One-Step Surface Coating of Highly Hydrophilic Poly(Carboxybetaine Methacrylate) Polymers on Hydrophobic and Hydrophilic Surfaces. *Adv. Mater. Interfaces* **2014**, *1* (6), 1400071.

(33) Li, G.; Xue, H.; Cheng, G.; Chen, S.; Zhang, F.; Jiang, S. Ultralow Fouling Zwitterionic Polymers Grafted from Surfaces Covered with an Initiator via an Adhesive Mussel Mimetic Linkage. *J. Phys. Chem. B* **2008**, *112* (48), 15269–15274.

(34) Zhang, C.; Ma, M. Q.; Chen, T. T.; Zhang, H.; Hu, D. F.; Wu, B. H.; Ji, J.; Xu, Z. K. Dopamine-Triggered One-Step Polymerization and Codeposition of Acrylate Monomers for Functional Coatings. *ACS Appl. Mater. Interfaces* **2017**, *9* (39), 34356–34366.

(35) Xu, G.; Liu, P.; Pranantyo, D.; Xu, L.; Neoh, K. G.; Kang, E. T. Antifouling and Antimicrobial Coatings from Zwitterionic and Cationic Binary Polymer Brushes Assembled via “Click” Reactions. *Ind. Eng. Chem. Res*. **2017**, 56 (49), 14479−14488.

(36) Zhang, C.; Li, H. N.; Du, Y.; Ma, M. Q.; Xu, Z. K. CuSO4/H2O2-Triggered Polydopamine/Poly(Sulfobetaine Methacrylate) Coatings for Antifouling Membrane Surfaces. *Langmuir* **2017**, *33* (5), 1210–1216.

(37) Chang, C. C.; Kolewe, K. W.; Li, Y.; Kosif, I.; Freeman, B. D.; Carter, K. R.; Schiffman, J. D.; Emrick, T. Underwater Superoleophobic Surfaces Prepared from Polymer Zwitterion/Dopamine Composite Coatings. *Adv. Mater. Interfaces* **2016**, *3* (6).

(38) An, Q.; Huang, T.; Shi, F. Correction: Covalent Layer-by-Layer Films: Chemistry, Design, and Multidisciplinary Applications (Chem. Soc. Rev., (2018) DOI: 10.1039/C7cs00406k). *Chem. Soc. Rev.* **2018**, *47* (14), 5529.

(39) Chen, Y.; Diaz-Dussan, D.; Wu, D.; Wang, W.; Peng, Y. Y.; Asha, A. B.; Hall, D. G.; Ishihara, K.; Narain, R. Bioinspired Self-Healing Hydrogel Based on Benzoxaborole-Catechol Dynamic Covalent Chemistry for 3D Cell Encapsulation. *ACS Macro Lett.* **2018**, *7* (8), 904–908.

(40) Jiang, J. H.; Zhu, L. P.; Li, X. L.; Xu, Y. Y.; Zhu, B. K. Surface Modification of PE Porous Membranes Based on the Strong Adhesion of Polydopamine and Covalent Immobilization of Heparin. *J. Memb. Sci.* **2010**, *364* (1–2), 194–202.

(41) Sun, X.; Shao, Y.; Boluk, Y.; Liu, Y. The Impact of Cellulose Nanocrystals on the Aggregation and Initial Adhesion to a Solid Surface of Escherichia Coli K12: Role of Solution Chemistry. *Colloids Surfaces B Biointerfaces* **2015**, *136*, 570–576.

(42) Liu, C.-Y.; Huang, C.-J. Functionalization of Polydopamine via the Aza-Michael Reaction for Antimicrobial Interfaces. *Langmuir* **2016,** *32*(19), 5019-5028.

(43) Huang, C. J.; Wang, L. C.; Shyue, J. J.; Chang, Y. C. Developing Antifouling Biointerfaces Based on Bioinspired Zwitterionic Dopamine through PH-Modulated Assembly. *Langmuir* **2014**, *30* (42), 12638–12646.

(44) Kruger, N. J. The Bradford Method for Protein Quantitation. In *The Protein Protocols Handbook*; 1996; pp 15–20.

(45) Thermo Scientific, Instructions: Coomassie Plus (Bradford) Assay Kit. *Pub. No. MAN0011203, Rev. B.0, Pub. Part No. 2160229.11*, Pierce Biotechnology: Rockford, IL, USA

(46) Yang, H. C.; Wu, M. B.; Li, Y. J.; Chen, Y. F.; Wan, L. S.; Xu, Z. K. Effects of Polyethyleneimine Molecular Weight and Proportion on the Membrane Hydrophilization by Codepositing with Dopamine. *J. Appl. Polym. Sci.* **2016**, *133* (32).

(47) Yang, H. C.; Liao, K. J.; Huang, H.; Wu, Q. Y.; Wan, L. S.; Xu, Z. K. Mussel-Inspired Modification of a Polymer Membrane for Ultra-High Water Permeability and Oil-in-Water Emulsion Separation. *J. Mater. Chem. A* **2014**, *2* (26), 10225–10230.

(48) Lee, H.; Scherer, N. F.; Messersmith, P. B. Single-Molecule Mechanics of Mussel

Adhesion. *Proc. Natl. Acad. Sci.* **2006**, *103* (35), 12999–13003.

(49) Hwang, G.; Kang, S.; El-Din, M. G.; Liu, Y. Impact of an Extracellular Polymeric Substance (EPS) Precoating on the Initial Adhesion of Burkholderia Cepacia and Pseudomonas Aeruginosa. *Biofouling* **2012**, *28* (6), 525–538.

(50) Horbett Thomas, A.; Brash John, L. Proteins at Interfaces: Current Issues and Future Prospects. In *Proteins at Interfaces: Physicochemical and Biochemical Studies*; 1987; Vol. 343, pp 1–33.

(51) Ishihara, K. Bioinspired Phospholipid Polymer Biomaterials for Making High Performance Artificial Organs. *Sci. Technol. Adv. Mater.* **2000**, *1* (3), 131–138.

(52) Yang, Z.; Wu, Y.; Wang, J.; Cao, B.; Tang, C. Y. In Situ Reduction of Silver by Polydopamine: A Novel Antimicrobial Modification of a Thin-Film Composite Polyamide Membrane. *Environ. Sci. Technol.* **2016**, *50* (17), 9543–9550.

(53) Liu, Z.; Wang, Y.; Zu, Y.; Fu, Y.; Li, N.; Guo, N.; Liu, R.; Zhang, Y. Synthesis of Polyethylenimine (PEI) Functionalized Silver Nanoparticles by a Hydrothermal Method and Their Antibacterial Activity Study. *Mater. Sci. Eng. C* **2014**, *42*, 31–37.

Chapter 3 Dopamine Assisted Self-cleaning, Antifouling and Antibacterial Coating via Dynamic Covalent Interactions

The content of this chapter was published in

The Journal of ***ACS Applied Materials and Interfaces***

3.1 Introduction:

Infections caused by microbial attachment and subsequent biofilm formation has become a serious global threat for public health and industrial sectors[1,2]. Thousands of people have experienced severe illnesses and even death due to biomedical implant related infections. Prevention of initial microbial attachment on biomedical implant is critical because within a few seconds of implantation, the implant's surface is fouled by proteins such as fibronectin, fibrin and fibrinogen which lead to irreversible adhesion of microbials and biofilm formation[3]. Consequently, implant failure occurs followed by early postoperative infection.

Therefore, it is a great demand to endow surfaces with non-fouling and antimicrobial properties to combat biofouling. To reduce the biofilm formation, researchers have adopted a series of approaches[4–8] which can be categorized into two strategies: non-adhesive surface and biocidal surface. For a non-adhesive surface, the surface is functionalized with flexible and water soluble polymers such as poly(ethylene glycol)[9,10], zwitterionic polymers[11,12], and glycopolymers[13,14] that creates a super hydrophilic surface to prevent the bacteria attachment over shorter time periods. These hydrophilic polymers create a strong hydration layer on top of the surface to avoid the initial attachment of bacteria[15]. Depending on the surface hydration, packing density and polymer chain flexibility, sometimes these hydrophilic polymers experience the transition from non-fouling to fouling and fail to provide long-term protection against bacteria colonization[16]. On the other hand, for biocidal surfaces, researchers either incorporate releasable bacteria killing agents such as silver nanoparticles[17], antibiotics[18] and enzymes[19] into the surface or modify the surface with bactericidal functionalities such as quaternary ammonium salts[20], polycations[21], chitosan[22], graphene oxide[23] for contact killing. Most of the contact killing mechanism involves the electrostatic interaction between the positively charged biocides and the negatively charged cell

membranes leading to the damage of the cell by disrupting cellular membrane charge distribution and finally resulting in death [24]. However, most of the biocidal surfaces face the challenge of rapid accumulation of dead cells after they are killed by contact, which can cover the attached biocide functional groups and promote further adhesion of bacteria and biofilm formation[25,26]. Therefore, for long-term resistance, unifunctional biocidal or non-adhesive surfaces are insufficient for preventing biofilm formation. To overcome this limitation, non-adhesive and biocidal dual-functional surfaces are highly desirable, where non-adhesive functionality can help to inhibit the initial microbial adhesion, and the biocidal functionality aids in killing the attached bacteria cells.

Smart self-cleaning surfaces are also promising to solve this issue, from which both live and dead bacteria cells can be easily released. Recently, researchers have investigated many strategies to develop smart antibacterial surfaces with controllable release property[3,24,27–32]. Using surface-initiated atom-transfer radical polymerization (SI-ATRP), Jiang and co-workers developed switchable polymer surface coating by combining the advantages of both nonfouling and cationic antimicrobial materials[27,28]. They synthesized a novel polymer-coated surface through SI-ATRP from thiol initiator. By altering the pH of the environment, that coating could transform reversibly from bacteria cell killing state to a releasing state[28]. For SI-ATRP, convenient determination of the density of grafted initiator and polymer brush along with the efficiency of the initiator is still a challenge[33,34]. Moreover SI-ATRP requires organic solvent which could be an issue for biocompatibility[10]. Lopez and co-workers prepared temperature triggered fouling release hybrid surfaces by grafting nanopatterned poly(N-isopropylacrylamide) (PNIPAAm) brushes utilizing interferometric lithography and surface-initiated polymerization[26,35,36]. To impart antimicrobial property, several biocides (such as quaternary ammonium salts (QAS)[26], antimicrobial enzymes[35], and singlet oxygen sensitizers[36]) were physiosorbed onto the modified surface. Above the lower

critical solution temperature (LCST), these nanopatterned PNIPAAm chains were collapsed and the resulting surfaces became hydrophobic accelerating the initial attachment of bacteria, and exposing the biocides to kill the surface adhered bacteria[26]. On the other hand, decreasing the temperature to below the LCST induces the hydration of PNIPAAm, which promotes hydrophilicity and swelling of the PNIPAAm brushes and consequently the release of dead cells from surface. Although these nanopatterned temperature responsive surfaces showed promising results to effectively release the dead bacteria cells from the surface, formulation of these hybrid surfaces needs sophisticated equipment and involves relatively complex procedures, which limits their practical broad application[24,37].

However, most of the "*smart*" self-cleaning surfaces reported to date require surface pre-treatment and complicated multistep processes to promote polymer adhesion, and they can only be fabricated under laboratory conditions. Simple, economic, biocompatible and scalable fabrication method for dual functional self-cleaning coating is highly desired.

To overcome these challenges, we report herein a facile technique of developing sugar responsive dynamic antifouling and antibacterial coatings by forming covalent boronic ester bonds between catechol groups from dopamine and benzoxaborole pendant from zwitterionic and cationic polymers. This distinctive boronic ester complex is reversible and sugar responsive[38–40]. We have utilized the advantages of the surface hydration of zwitterion and biocidal activity of cationic quaternary ammonium moieties to prepare a dynamic dual-functional surface based on the unique property of boronic ester. To impart antifouling property, we selected a zwitterionic compound 2-methacryloyloxyethyl phosphorylcholine (MPC) and synthesized a copolymer with benzoxaborole pendant poly(MPC-*st*-5-methacrylamido-1,2-benzoxaborole (MAABO)). Additionally, in order to impart antibacterial property to the surface, benzoxaborole pendant containing cationic copolymer

poly(2-(methacryloyloxy)ethyl trimethylammonium (META)-*st*-MAABO)) was synthesized. As illustrated in the Scheme 3-1, these benzoxaborole containing antifouling and antibacterial copolymers were covalently grafted to the catechol rich polydopamine (PDA) coated surface via the formation of a strong cyclic boronic ester complex with catechol group of PDA layer, thus endowing the surface with bacteria contact-killing property. However, after the addition of cis-diol containing sugar such as fructose solution onto the modified surface, this boronic ester complex with PDA could be cleaved and the attached copolymer layer removed from the surface resulting in the release of all attached dead bacteria from the surface. The resultant sugar responsive self-cleaning surface can be used as a non-leaching, self-sterilizing surface for potential applications in biomedical implants.

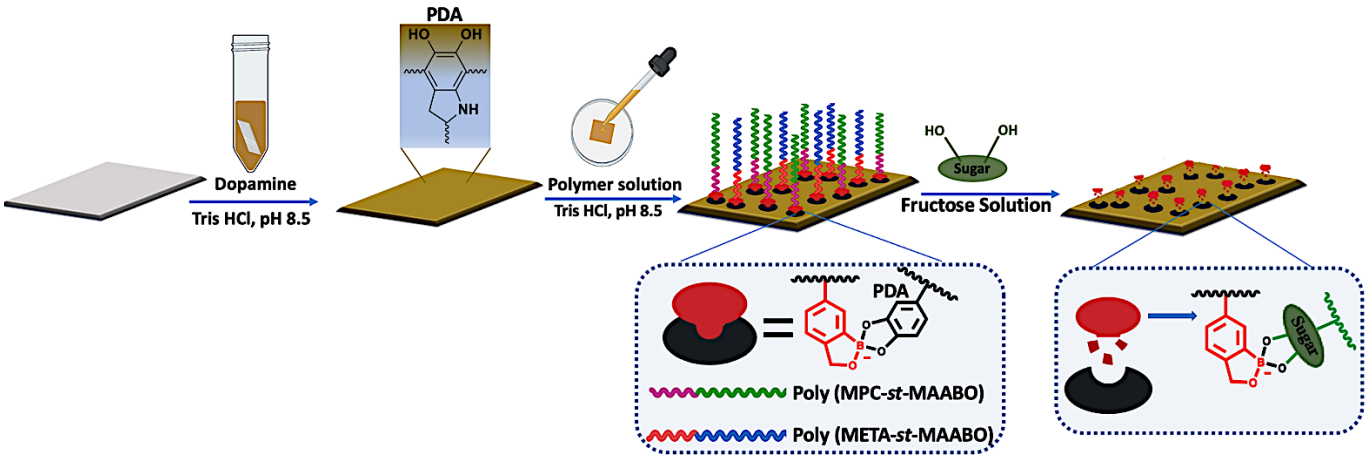

Scheme 3-1. Schematic illustration of PDA coating to subsequently graft benzoxaborole containing cationic polymer poly(META-st-MAABO) and zwitterionic polymer poly(MPC-st-MAABO) on the PDA coated surface by forming boronate ester bond ; dissociation of benzoxaborole-catechol complex in presence of sugar such as fructose solution.

3.2 Experimental:

3.2.1 Materials:

MPC was obtained from Prof. Ishihara's lab (University of Tokyo, Japan). The initiator, 4,4′-azobis(4-cyanovaleric acid) (ACVA), Bovine serum albumin (BSA) and Dopamine hydrochloride were purchased from Sigma-Aldrich and used without further purification. META chloride solution (80 wt. % in H_2O, stabilized with 600 ppm MEHQ) was purchased from Sigma-Aldrich and purified before reaction by passing the monomer through a column of alumina to remove the inhibitor and filtration by a membrane filter. The Live/Dead BacLight Bacterial Viability Kit L-7012 and Micro BCA Protein Assay Kit were obtained from Thermo Fisher Scientific.

3.2.2 Synthesis of Zwitterionic Copolymer:

MAABO was synthesized as previously reported[41] and purity was confirmed by ^{1}H NMR. Benzoxaborole-containing zwitterionic random copolymer poly(MPC-*st*-MAABO) was synthesized via free-radical polymerization. To synthesize poly (MPC-*st*-MAABO), MPC (1.062 g, 3.6 mmol), MAABO (86.8 mg, 0.4 mmol), and ACVA (5.6 mg, 20 μmol) were placed in a polymerization tube and dissolved with a mixture of methanol (3.5 mL), DMF (1.5 mL), and DI water (1 mL) and degassed for 30 mins followed by putting into the oil bath at 70 °C for 18 h After degassing with nitrogen for 30 min, the polymerization was carried out at 70 °C for 18 h. The resultant polymer was further purified dialyzing against DI water for 48 h and freeze-dried to get the purified polymer poly(MPC-*st*-MAABO) as a powder. All the synthesized monomers and polymers were characterized using ^{1}H NMR spectra and gel permeation chromatography (GPC) as reported before[11].

3.2.3 Synthesis of Cationic Copolymer:

Benzoxaborole-containing cationic random copolymer poly (META-*st*-MAABO) was synthesized via free-radical polymerization. To synthesize poly(META-*st*-MAABO), cationic monomer META (1.062 g, 3.6 mmol), benzoxaborole-containing monomer MAABO (86.8 mg, 0.4 mmol), and initiator ACVA (5.6 mg, 20 μmol) were dissolved in a mixture of methanol (3.5 mL), DMF (1.5 mL), and DI water (1 mL) and followed by similar steps as mentioned above for zwitterionic copolymer synthesis. The resulting purified polymer was characterized by ^{1}H NMR and GPC as well.

3.2.4 Surface Preparation:

Cleaned glass substrates were coated with dopamine first following the same protocol as reported in our previous study[11]. After PDA coating, at different weight ratio of synthesized zwitterionic and cationic polymer mixed solution (2mg/ml in Tris buffer at pH 8.5) was added onto the PDA coated surface following the similar procedure [11]. Depending on the different weight percentage of the added polymer solution onto the PDA coated surface, prepared samples were denoted as PDA/(MP50/MT50) , PDA/(MP20/MT80) and PDA/MT100 ; details are listed in Table 3.1.

Table 3.1 Sample details of polymer coating on PDA modified surfaces

Sample name	poly(MPC-*st*-MAABO) Wt.%	poly(META-*st*-MAABO) Wt.%
PDA/(MP50/MT50)	50	50
PDA/(MP20/MT80)	20	80

PDA/MT100	0	100

3.2.5 Surface Analysis:

The chemical composition of all the modified surfaces along with the control glass substrate was determined by X-ray photoelectron spectroscopy (XPS) using either an AXIS Nova or an AXIS Ultra-DLD spectrometer (Kratos Analytical Inc., Manchester, U.K.) with a monochromated Al Kα source.

To confirm the polymer grafting to the surface, the coating was characterized by FTIR using an Agilent Technologies Cary 600 Series FTIR spectrometer (ATR mode) between the wavelength of 600 and 3900 cm^{-1} .

Surface morphology and roughness of the modified surfaces was observed by atomic force microscopy (AFM) in non-contact tapping mode at dry conditions. Surface roughness was expressed as root-mean-square (RMS) value.

To investigate the surface relative hydrophilicity and wetting properties, water contact angles of all the modified surfaces along with bare glass control were measured using a model 590 goniometer with a 4 μL water droplet onto the surface at static condition in air.

3.2.6 Protein Adsorption Assay

To investigate the protein adsorption on the modified surfaces, all sample surfaces (each of 1x1 cm^2 area) were fouled with model protein bovine serum albumin. Following the same protocol of our previous studies[42] absorbed protein on the sample surfaces were quantified by bicinchoninic acid (BCA) protein assay kit consistent with the manufacturer's instructions[43].

For sugar triggered release of protein from the coated surface, the protein-adsorbed initial surfaces were incubated into a fructose solution (60 mM in PBS) for 30 min and gently rinsed with PBS to remove loosely bound one. The amounts of remaining adsorbed protein were quantified using the similar procedure as mentioned above.

3.2.7 Attachment and Detachment of Bacteria

For bacterial attachment, all the sample surfaces were incubated into *Escherichia coli (E. coli)* (ATCC 25922) and *Staphylococcus aureus (S. aureus)* (ATCC 25923) suspension (1×10^8 cells/mL in PBS, pH 7.4) for 3h at 37 °C, followed by 3 times gently rinsing with sterile PBS to remove loosely attached bacteria cells. Bacteria fouled surfaces were then stained with 50 µL of LIVE/DEAD stain in the dark for 15 min and the density of surface adhered bacteria on each sample surface was studied by a fluorescence microscope with a magnification of 400x. To understand the effect of the addition of sugar on the surface and for the predicted detaching of the adhered bacteria cells, all the bacteria fouled sample surfaces were immersed into fructose solution (60 mM in PBS) for 30 min followed by rinsing with sterile PBS. LIVE/DEAD staining assay was then carried out as demonstrated above to determine the density of the remaining bacteria.

3.2.8 Antibacterial Activity Assay:

Two bacteria strains of *E. coli* (Gram-negative) and *S. aureus* (Gram-positive) were used to investigate the anti-bacterial activity of the coating materials. Two different assays were carried out by colony forming unit (CFU) assay (details are listed in the Supporting Information) and LIVE/DEAD assay to study the antibacterial activity of the samples. To examine the non-leaching property of the antibacterial coating, zone-of-inhibition tests were performed. 50µl of *E. coli and S. aureus* solution of 8 x 10^8 cell/ml concentration was uniformly spread onto sterile LB and TS agar plate respectively using a sterile plastic spreader. Then, the samples were placed onto these

agar plates and incubated for 24 h at 37 °C to assess the presence or absence of an inhibition zone. The appearance of an inhibition zone was taken as an indication of cationic polymer leaching from the surfaces.

3.2.9 In Vitro Cell toxicity Assay:

The cytotoxicity of the sample coating extracts was investigated by performing the MTT assay with normal human lung fibroblast cells MRC-5. CCL-171™. The *in vitro* cell toxicity was assessed with both coating extracts and modified sample surfaces. The experimental details are mentioned in the supporting information.

3.3 Results and Discussion:

MAABO was synthesized as previously reported[41] and characterized by ^{1}H NMR (Figure S 3-1). The purity was confirmed by comparing the integrals of the typical phenyl protons in MAABO (δ 7.3, 7.7, and 8.1 ppm) with integrals of methacrylate peaks (δ 5.5 and 5.8 ppm). Then free radical polymerization of MPC and META with 20% MAABO content was conducted as illustrated in Figure 3.1. (a) and 3.1.(b) with a targeted degree of polymerization of 100 and listed as poly(MPC-*st*-MAABO) and poly(META-*st*-MAABO) respectively.

The benzoxaborole pendant MAABO mol contents in the MPC and META copolymer chains were calculated by ^{1}H NMR (Figure S 3-2 and S 3-3 respectively) to be 17.2% and 16.7%, respectively by comparing the integral of the characteristic peak for MAABO (δ 5.01 ppm) with the characteristic peak integral for MPC (δ 3.7-3.4 ppm) and META (δ 4.6-4.27 ppm and δ 4-3.6 ppm) which is quite consistent with the designed ratio. The monomers mol content, number (M_n) and weight (M_w) average molecular weights of poly(MPC-*st*-MAABO) and poly(META-*st*-MAABO) were determined by aqueous GPC and are summarized in Table 3.2.

Table 3.2 Chemical Composition and Molecular Weights of the Synthesized Polymers

Polymer	Composition of Copolymer (mol%)						Molecular weights [b]	
	In Feed			In Polymer [a]			M_n	M_w
	MPC	MAABO	META	MPC	MAABO	META	kDa	
(MPC-*st*-MAABO)	80.0	20.0	_	82.8	17.2	_	14.5	16.0
(META-*st*-MAABO)	_	20.0	80.0	_	16.6	83.3	50.3	73.8

[a] Calculated from ^{1}H NMR signal integration.

[b] Obtained from aqueous GPC

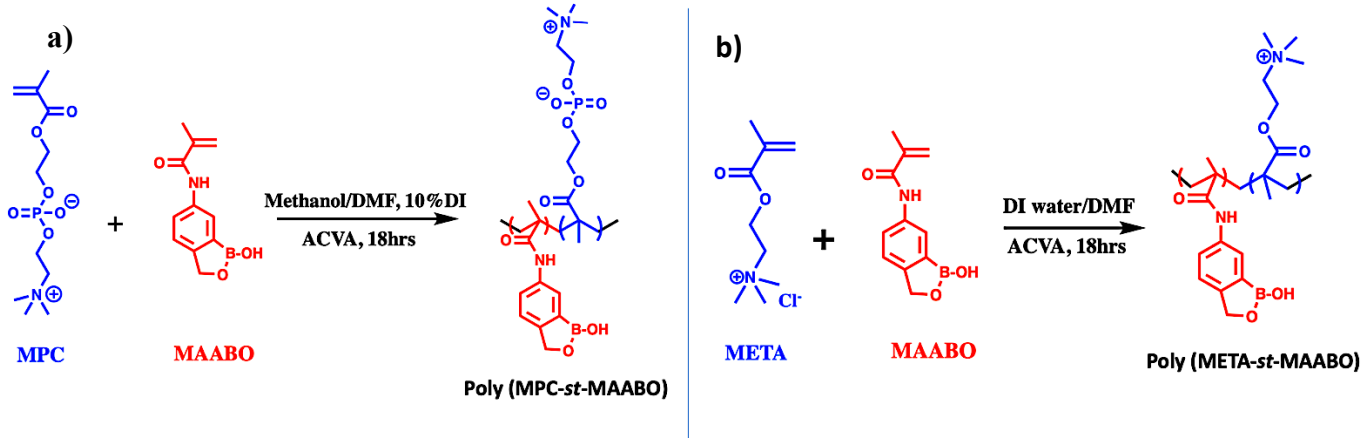

Figure 3.1. a) Reaction scheme of free radical polymerization between MPC and MAABO, and (b) Synthetic route of free radical polymerization between META and MAABO

3.3.1 Surface characterization:

To confirm the presence of the polymeric layer on the substrate and the crosslinking reaction between primary PDA layer and benzoxaborole containing polymers, the surface chemical structures of the modified and unmodified PAN membranes were characterized by attenuated total reflectance Fourier transform infrared (ATR FTIR) spectroscopy. As glass substrates can completely absorb the Infrared radiation, it may be impossible to get a reliable result by ATR FTIR for surface modifications on glass surface. That is why, instead of choosing glass substrates, for FTIR analysis we chose polyacrylonitrile membrane (PAN) as a substrate. Moreover, successful coating on different substrates proves the surface independence of our proposed coating strategy. Absorption band at 2242 cm^{-1} and 1454 cm^{-1} for PAN membrane spectra (Figure 3.2) is mainly attributed to the stretching vibration of nitrile groups (−C≡N) and a bending vibration of methylene[44] (–CH_2–) respectively from PAN membrane[45]. After PDA coating on PAN membrane intensity of these two characteristics peaks of PAN membrane slightly reduced. Though in both PAN and PAN/PDA coated surface a strong peak for nitrile group at 2242 cm^{-1} was observed, this peak was reduced significantly after grafting poly(MPC-*st*-MAABO) and poly(META-*st*-MAABO) polymers on the membrane indicating a good coverage of polymer coating on the membrane surface. In the PAN/PDA spectra (Figure 3.2), the appearance of broad peak at 3342 cm^{-1} is due to the combination of the stretching vibration of O–H and N–H which mostly arises from polydopamine structure [46]. All the spectra displayed absorption peak at around 2854-2958 cm^{-1} wavelength corresponding to -CH_2 stretching which is one of the main building blocks of PAN, PDA and both poly (MPC-*st*-MAABO) and poly (META-*st*-MAABO) polymers. Compared to the control PAN or PAN/PDA spectra, in PAN/PDA/(MP50/MT50) spectra new absorbance peaks at 1722 cm^{-1} and 1483 cm^{-1} were observed. Appearance of these peaks at 1722 cm^{-1} and

1483 cm^{-1} can be attributed to carbonyl group (C=O)[47] of the polymer backbone and the (C-H) bending vibrations of the cationic $N^{+}(CH_3)_3$ group[48] respectively. As all these peaks are aligned with the chemical structure of the poly(MPC-*st*-MAABO) and poly(META-*st*-MAABO) polymers, presence of these characteristic peaks confirms the successful grafting of both polymers on PDA coated PAN membrane. The characteristic peak of P=O bending[47] from MPC content was also identified at 1230 cm^{-1} wavelength in PAN/PDA/(MP50/MT50) spectra. Moreover, after grafting polymers onto the PDA coated surface the intensity of the C-O-C characteristic absorption peak at 1068 cm^{-1} increases which also arises from both MPC and META structure. Most importantly, in PAN/PDA/(MP50/MT50) spectra, appearance of absorption peak at 1338 cm^{-1} characteristic for boronate ester [49,50] and peak of B-C stretching vibration in boronate ester [51] at 1149 cm^{-1} proves that all the MAABO containing MPC and META polymer was grafted into the PAN/PDA coated surface by forming dynamic boronate ester covalent bond with PDA layer successfully.

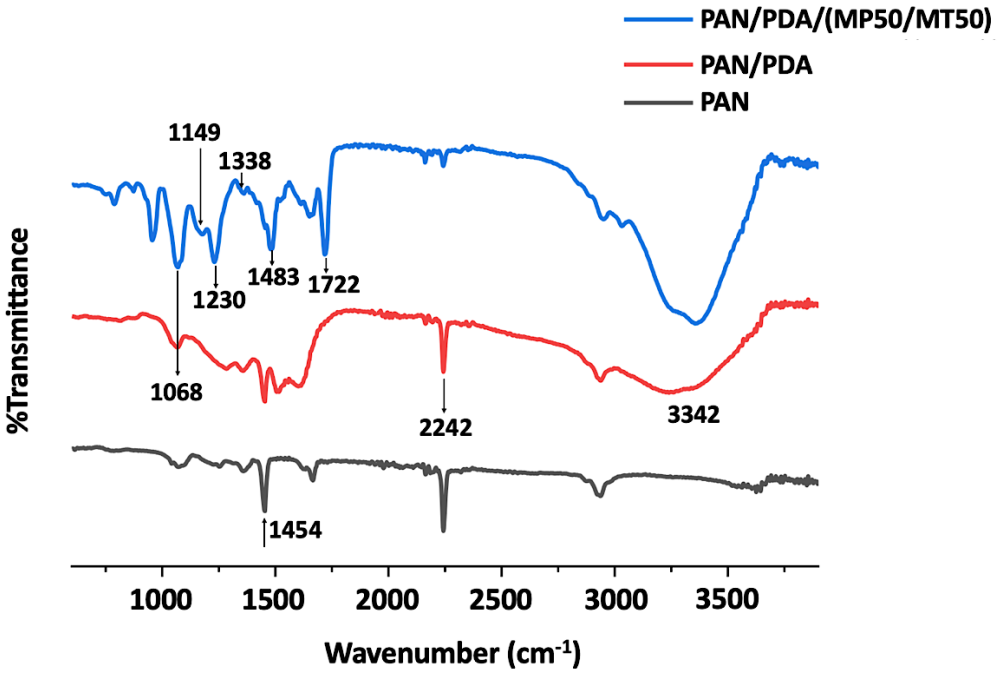

Figure 3.2. FTIR spectra of PAN membrane, PAN with PDA layer (PAN/PDA) and PAN/PDA postdeposition of 50 wt.% poly(MPC-st-MAABO) and 50 wt.% poly(META-st-MAABO) polymers PAN/PDA/(MP50/MT50)

XPS analysis was also performed to investigate the chemical composition of the different surfaces after modifications. Table 3 compiles atomic ratios (normalized to carbon) determined for the main elements; excluded are the minor elements detected in the case of glass (Na, Mg, K, Ca). In addition, high resolution spectra of C 1s, N 1s and P 2p were evaluated qualitatively to confirm the successful grafting of both poly(MPC-*st*-MAABO) and poly(META-*st*-MAABO) polymers on the PDA coated surface. For XPS analysis, the PDA/(MP50/MT50) coating sample was chosen to confirm the presence of both polymers and to compare this polymer-modified surface with PDA and bare glass. Though the main constituent of bare glass was SiO_2, some expected adsorbed organic contamination (adventitious carbon and Nitrogen)[52] was observed (Table 3.3). After introducing the PDA coating, Si was no longer detected, indicating that the glass substrate was completely covered with PDA. The composition of the PDA-coated surface (C, N and O) and the C 1s spectrum were roughly consistent with the polydopamine structure, keeping in mind that PDA is not expected to have a well-defined, regular structure. The high resolution C 1s spectra PDA surface had a broad, pronounced shoulder towards higher binding energy (BE), assigned to functional groups such as C-N and C-O based species. In addition, it displayed a broad signal centered at 290 - 291 eV BE, assigned to the expected shake-up peak of aromatic groups. After introducing poly(MPC-*st*-MAABO) and poly(META-*st*-MAABO) polymers on the PDA coated surface, the overall composition of C, N, O did not change significantly since concentrations of major elements are similar in both surfaces (PDA/(MP50/MT50) and PDA). However, compared

to the control PDA surface, PDA/(MP50/MT50) coating showed the appearance of new spectral peaks, P 2p (Figure 3.3 (e)) and an additional strong N 1s peak at higher BE 402.8eV (Figure 3.3(a)). The strong N 1s signal at 402.8 eV can be attributed to the positively charged nitrogen ($N^+(CH_3)_3$) of MPC and META. The appearance of the characteristic peak of P 2p peak at 133.1 eV (Figure 3.3 (e)) is assigned to the phosphorus atom in MPC. Compared to control ratios of P/C and N^+/C of PDA/(MP50/MT50) coating also increased from 0 to 0.034 and 0 to 0.054 respectively (Table 3.3). The detection of phosphorous (P) and charged nitrogen (N^+) is clear evidence for the presence of the PDA/(MP50/MT50). Moreover, by analyzing the high resolution spectra of C 1s for PDA/(MP50/MT50) coating, successful attachment of both poly(MPC-*st*-MAABO) and poly(META-*st*-MAABO) polymers on the PDA coated surface was confirmed by the appearance of a characteristic peak of C 1s (Figure 3.3 (b)) at 289.1 eV (ester groups) and a strong increase in the peak at 286.6 eV (attributed to C–O and C-N)[53] as would be expected for META and MPC.

Table 3.3. Surface compositions determined by XPS. Concentrations are presented as atomic ratios X/C, i.e., atomic concentration of element X relative to that of Carbon (C).

Surfaces	Composition (X/C)					
	C	Si	P	N	N^+	O
Bare Glass	1.000	0.792	_	0.058	_	2.075
PDA	1.000	_	_	0.102	0.003	0.237
PDA/(MP50/MT50)	1.000	0.011	0.034	0.084	0.054	0.342

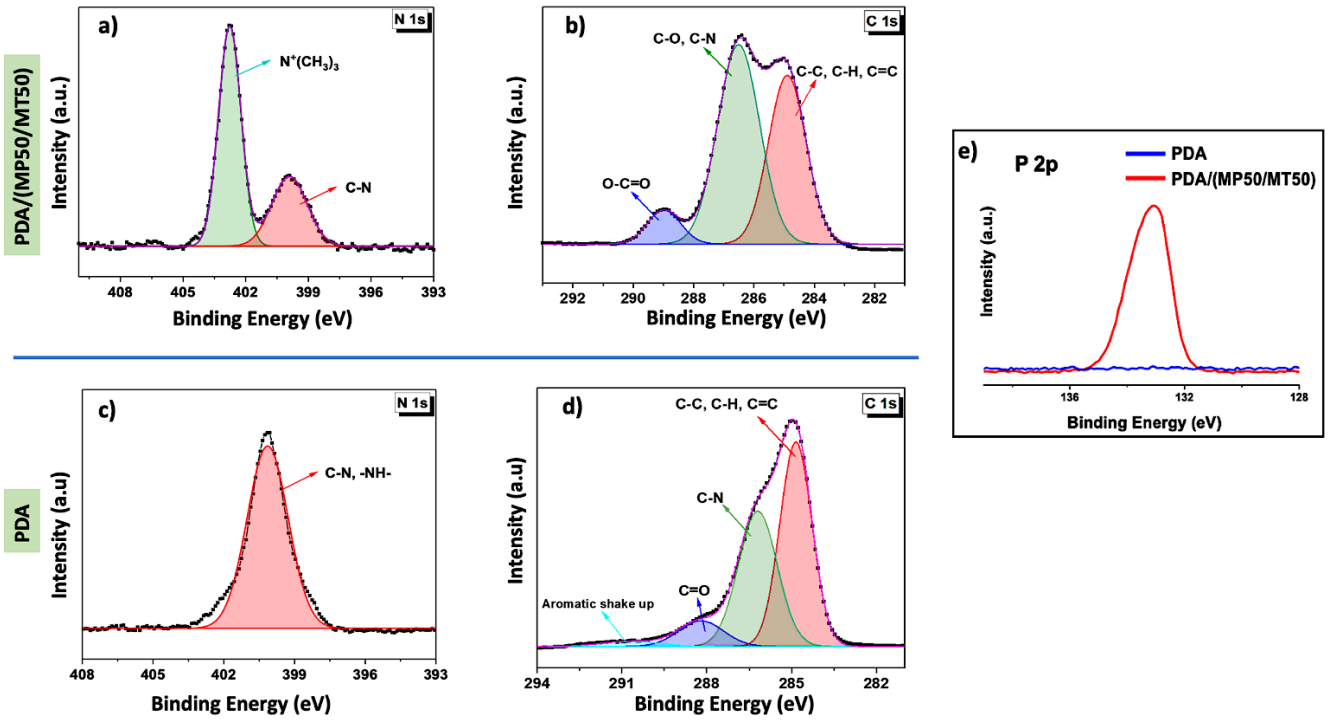

Figure 3.3. XPS high-resolution C 1s, P 2p and N 1s narrow-scan spectra of the modified glass substrates. High resolution a) N 1s spectra for PDA/(MP50/MT50) surface b) C 1s spectra for PDA/(MP50/MT50) surface, c) N 1s spectra for PDA surface d) C 1s spectra for PDA surface, and e) P 2p narrow scan spectra for PDA and PDA/(MP50/MT50) surface

3.3.2 Surface Morphology:

The surface morphology of the modified surfaces was investigated by AFM in non-contact tapping mode and at dry condition. As shown in Figure S 3-4, the control glass surface has shown a smooth surface with a root-mean-square (RMS) roughness of 1.2 nm. Compared to bare glass, PDA coated surface showed significantly higher surface roughness value of 16.3 nm which is mostly because of the deposition of self-polymerized large PDA aggregates[46]. However, after introducing

poly(MPC-st-MAABO) and poly(META-st-MAABO) polymers onto the PDA coated surface, no such aggregates were detected. A homogenous and smooth surface with RMS roughness of 1.6 nm was obtained for PDA/(MP50-MT50) surface confirming a good coverage on PDA aggregates layer. However, after 30 mins of sugar treatment of the PDA/(MP50-MT50) surface, RMS roughness increased to 6.8 nm exposing the PDA aggregates layer again. This phenomenon also confirms the dissociation of boronate ester bond and removal of polymer layer from the PDA coating. However, the surface roughness of sugar treated PDA/(MP50-MT50) surface is very low compared to bare PDA coating.

3.3.3 Surface hydrophilicity:

Water contact angle (WCA) measurement is one of the most reliable techniques of characterization of the surface's relative hydrophilicity and wetting properties[54]. Reduced water contact angle indicates higher hydrophilicity of the surface. As shown in Figure 3.4, the WCA of the pristine glass substrate and control PDA coating was 49.1±3.3°and 40.7±1.9° respectively. All of the other polymer grafted PDA surfaces showed a lower WCA and improved surface hydrophilicity compared to control glass and PDA surfaces. Among them, the PDA/(MP50/MT50) coated sample surface showed the lowest WCA, 11.4±1°, possibly reflecting the presence of a stronger surface hydration due to the presence of a dense zwitterionic polymer content[16] on the surface coating. Decreasing the zwitterionic polymer content on the surface resulted in a slight increase in the water contact angle. Without the presence of poly(MPC-*st*-MAABO) polymer on the PDA surface, sample PDA/MT100 showed increase in WCA suggesting that the zwitterionic groups of the poly(MPC-*st*-MAABO) polymer brushes can interact more strongly with water and create more

effective surface hydration layer[16] than the cationic groups of the poly(META-*st*-MAABO) polymer brushes.

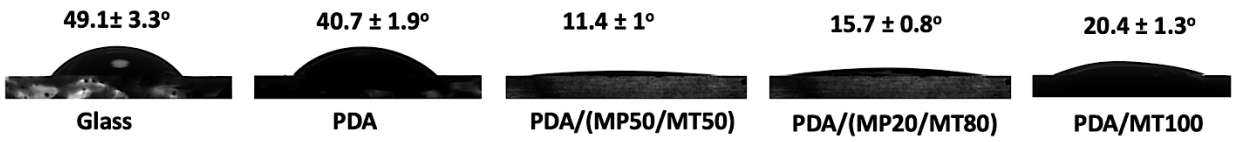

Figure 3.4 Water contact angle of bare glass, PDA, PDA/(MP50/MT50), PDA/(MP20/MT80) and PDA/MT100 coated glass substrates

3.3.4 Antibacterial Activity:

To quantify the percentage of viable bacteria cells attached to coated surfaces, CFU (colony forming unit) counting assay was conducted. The number of CFUs of each sample was determined after an incubation period of 24 hours. Then the viable bacteria cell fraction was calculated using the formula $(N/N_0) \times 100$, where N_0 is the average CFUs number obtained for the control glass surface and N is the average CFUs number for other PDA modified sample surfaces. All the surfaces were challenged with 10^8 cell/ml bacteria solution in PBS. From the results (Figure 3.5 a) it was observed that all coatings with poly(META-*st*-MAABO) polymer showed less than 10% bacteria cell viability for both gram positive *S. aureus* and gram negative *E. coli*. With increasing the poly(META-*st*-MAABO) polymer weight ratio into the coating the killing efficiency also increased. For the sample PDA/MT100 cell viability against *S. aureus* was found to be only 1.1%. META has quaternary ammonium (QA) moiety, which is a commonly used biocide with a permanent, pH-independent positive charge which can damage the negatively charged outer membranes of bacteria. This disruption is usually caused by the cell leakage through destroying

the charge equilibrium of the negatively charged bacteria cells due to the charge transfer between cell membrane and positively charged polymer chain[55] which results in cell death[56]. These results confirm that the biocidal activity is mainly due to the QA component from poly(META-*st*-MAABO) polymer attracting bacteria by electrostatic interaction, then degrading the cell membrane and destabilizing the intracellular matrix through a contact killing mechanism. The fluorescent LIVE/DEAD staining assay was also performed to evaluate the antibacterial adhesion properties of hydrophilic coatings against *E. coli* and *S. aureus*. Results (Figure 3.5) showed that bare glass with and without PDA coating favored the attachment of bacteria cells without compromising their viability which was reduced drastically after introducing zwitterionic and cationic polymer coating on the surface. Such results are evidence for a stable functionalization of glass surface with PDA and benzoxaborole-containing zwitterionic and cationic polymer. As expected, both the *S. aureus* and *E. coli* bacteria were well-kept on the surface of bare glass and PDA coating with very little amount of cell damage but the appearance of dead cells (red in color) increases with increasing weight percentage of poly(META-*st*-MAABO) polymer into the coating. Compared to PDA/(MP50/MT50) and PDA/(MP20/MT80) surfaces, PDA/MT100 showed better antibacterial activity with the highest number of dead cells detected on the surface.

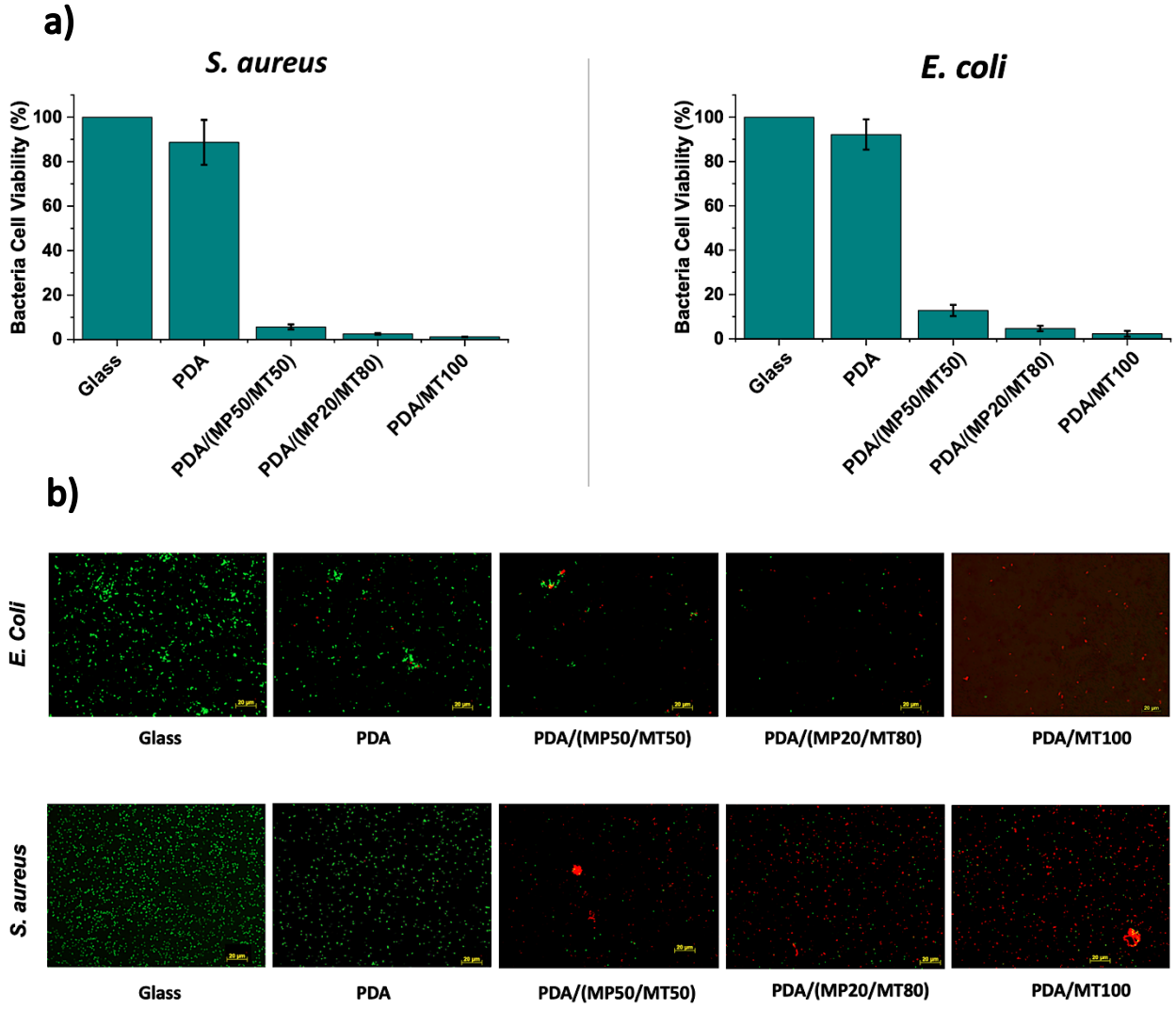

Figure 3.5. a) Cell viability of *E. coli* (left) and *S. aureus* (right) of all sample surfaces. b) Fluorescence images of *E. coli* and *S. aureus* attached on different surfaces (Glass, PDA, PDA/(MP50/MT50), PDA/(MP20/MT80) and PDA/MT100) (Scale bar: 20 µm)

To examine the non-leaching property of the biocide QA containing polymer coating, a zone-of-inhibition test was carried out. From the Figure S 3-6, it is clearly observed that no inhibition zone

was developed against both gram-positive and gram-negative bacteria after placing the polymer coated surfaces on the bacteria containing agar plates. The absence of an inhibition zone confirms the non-leaching property and the stability of our antibacterial coating.

3.3.5 Attachment and Detachment of Bacteria

Conventional contact-killing biocidal surfaces often face critical complications for long-term applications due to the accumulation of attached dead cells and other debris, which leads to secondary contamination and inflammation. Therefore, to maintain effective long-term antibacterial activity it is of great interest to develop a biocidal surface with dead cell release property in a facile way once they are killed[24]. With this objective in mind, we immobilized both zwitterionic and cationic polymers on the PDA coated substrates with the facility to reduce bacterial attachment and increase their cellular membrane disintegration. Compared to bare glass or PDA coating alone, decreased number of *E. coli* (Figure 3.6) and *S. aureus* (Figure S 3-5) cells adhesion were found on the polymer coated PDA surfaces. This low adhesion of bacteria cells may be attributed to the increased hydrophilicity imparted by the presence of poly(MPC-*st*-MAABO) zwitterionic polymer in the coating. In our coating system, both zwitterionic and cationic polymer were attached to the PDA coated surface via dynamic covalent boronate ester bonds with the catechol group of PDA coating. This covalent boronate ester bond can be dissociated after the addition of competitive diol containing molecules such as saccharides / sugars[57]. Thus, it can facilitate the removal of both live and dead bacteria electrostatically attached to the polymer layer avoiding fouling related to the accumulation of dead bacteria. Here, in this project, fructose was selected as the competitive diol containing molecule to dissociate benzoxaborole-catechol complex, because of its higher binding affinity with benzoxaborole than glucose[58]. As shown in Figure 3.6 and Figure S 3-5, more than 85% of attached bacteria on the surface were released after

fructose treatment. The quantities of the bacteria attached initially and after exposure to fructose solution or PBS were calculated using ImageJ software from the fluorescence images of the surfaces. On the other hand, surfaces with no polymer coating such as bare glass and PDA coating showed only around 10% and 12% *E. coli* bacteria release ratio respectively confirming that the release of bacteria from PDA/(MP50/MT50) coated surface was due to the sugar-triggered dissociation of boronate ester bonds. In addition to sugar responsiveness, benzoxaborole-catechol complex is pH responsive and can be dissociated at acidic pH and reconstructed at pH higher than 7.2[59]. Due to the release of metabolites during bacterial growth on the surface, pH of the localized environment can go down to a value of pH 5.5[60,61]. Thus, in an acidic environment due to a large number of bacteria attachments, dissociation of benzoxaborole-catechol complexation can trigger the self-cleaning effect similar to sugar addition.

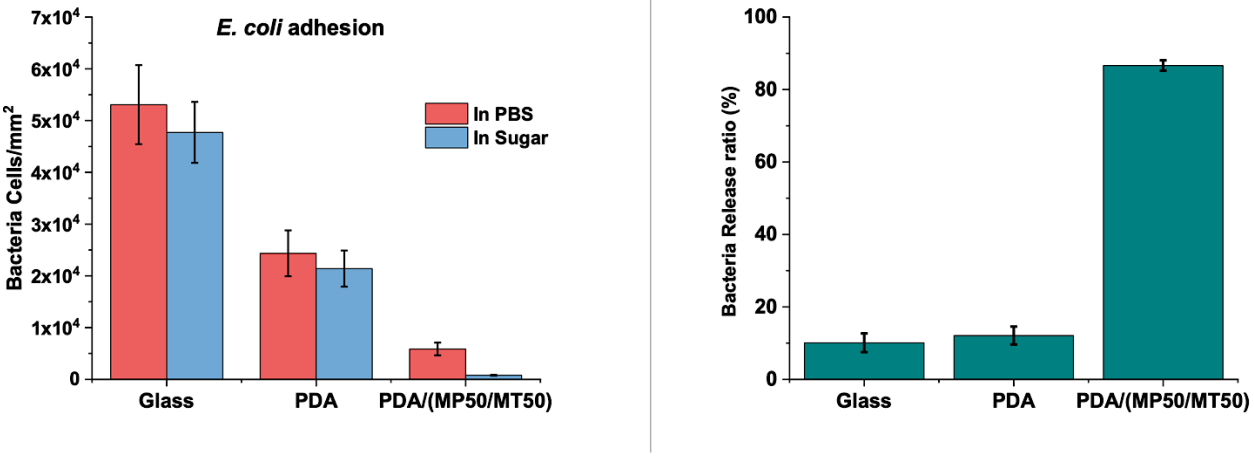

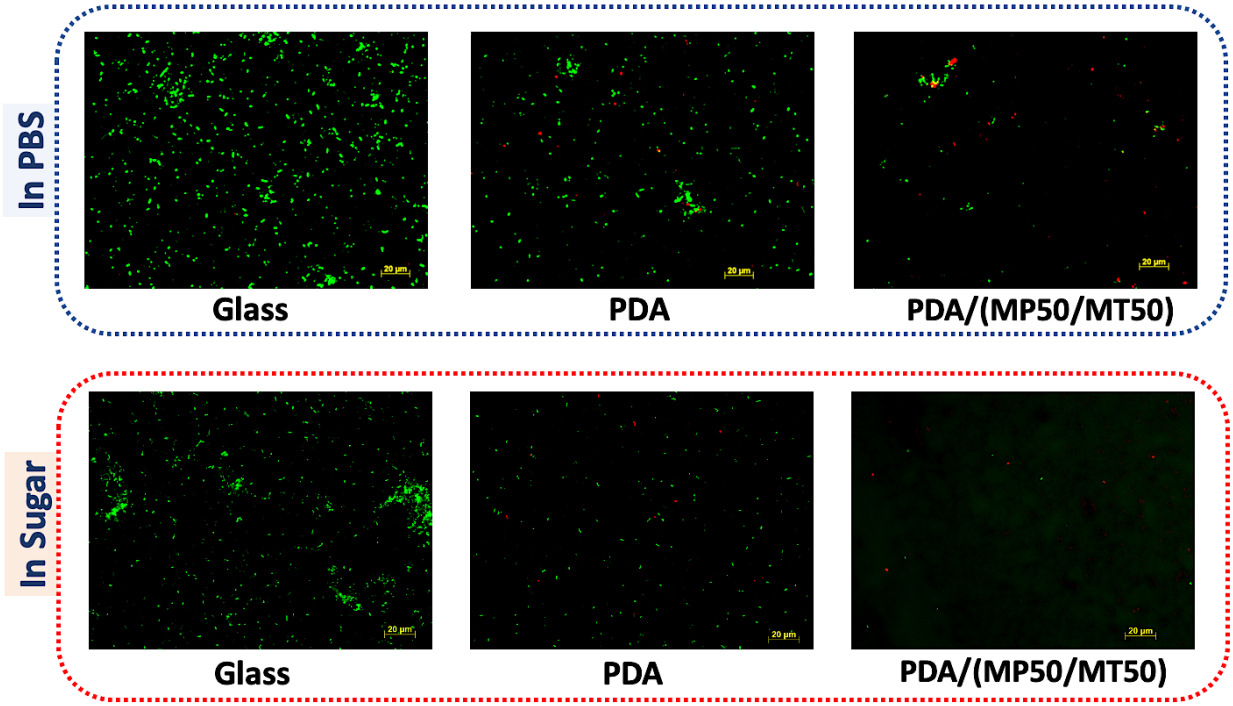

Figure 3.6. *E. coli* bacteria cell attachment to different surfaces (glass, PDA and PDA/(MP50/MT50)) and release ratio of the attached bacteria cells after sugar addition on the surface; fluorescence images of the attached cells on the surface.

As this benzoxaborole-catechol complexation is reversible, after sugar treatment, the PDA/(MP50/MT50) surface can be regenerated by simply adding freshly prepared polymer solution onto the sugar treated surface to form the benzoxaborole-catechol complexation again at physiological pH 7.4 which is higher than pK_a value (~7.2) of benozoxaborole[62]. After sugar treatment, the surface may act as bare PDA coated surface with many catechol functional groups available. Due to high affinity of benzoxaborole towards cis-diol[59] of PDA, after adding freshly prepared bezoxaborole containing polymer solutions onto the sugar treated surface, a new PDA/(MP50/MT50) can be regenerated. This surface regeneration ability as an indication of long-

term performance was also explored against *S. aureus* bacteria. After sugar treatment the PDA/(MP50/MT50) surface was dried and incubated with fresh bacteria solution for 24 hrs. Then LIVE/DEAD assay was conducted to observe bacterial adhesion on the sugar treated surface. As shown in Figure 3.7 (b), after sugar treatment the surface acts as only a PDA surface with few dead cells and many live cells attached. But compared to freshly prepared PDA coating (Figure S 3-4), this sugar treated PDA/(MP50/MT50) surface showed relatively low bacteria adhesion which can be related to reduced surface roughness as shown in Figure S 3-4. Moreover, after adding freshly prepared polymer solutions of poly(MPC-*st*-MAABO) and poly(META-*st*-MAABO) onto the sugar treated PDA/(MP50/MT50) surface, the regenerated PDA/(MP50/MT50) surface (Figure 3.7 (c)) showed similar killing efficiency as before (Figure 3.7(a)) with less amount of attached bacteria on it. Thus the regeneration of this coating makes it a potential candidate for many applications where antibacterial activity maintained overtime is needed.

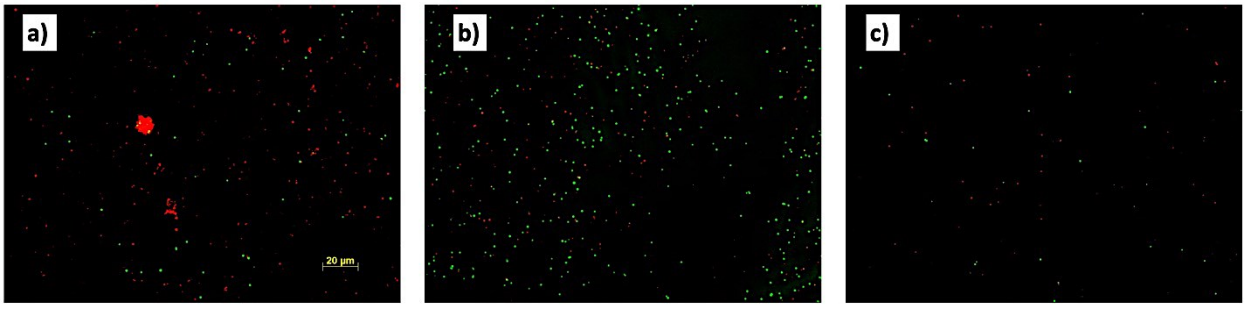

Figure 3.7 Fluorescence images of *S. aureus* bacteria on PDA/(MP50/MT50) surface: (a) before and b) after sugar treatment; c) regenerated PDA/(MP50/MT50) surface.

3.3.6 Adsorption and Release of Protein:

Having confirmed the sugar-responsiveness of the benzoxaborole pendant containing polymer layers on the PDA coating system towards the bacteria release, we further investigated the potential of this system for the absorbance and release of protein. This reversible control of protein adsorption is of great interest for applications such as medical diagnostics, on-demand delivery methods of therapeutics[63] and protein purification[64]. Protein adsorption on the polymer-coated surface was evaluated by the BCA protein assay. As shown in Figure 3.8, a stronger interaction between protein and polymer grafted surfaces (PDA/(MP50/MT50), PDA/(MP20/MT80) and PDA/MT100) was observed. Both bare glass and PDA coating showed relatively low adsorption of protein 36 and 31 μg/cm^2 respectively whereas all the other polymer coated surfaces showed a strong increase of protein adsorption. With the increase of cationic polymer content into the coating the adsorption of protein increased because of the strong interaction between positively charged QA moiety and negatively charged BSA protein[65]. PDA/MT100 surface showed a maximum amount of absorbed protein of 82 μg/cm^2. Reversibility of BSA adsorption on the polymer coated surfaces in response to fructose solution was then explored. After introducing sugar onto the coating the boronate ester bond was dissociated resulting in the cleavage of both cationic and zwitterionic polymer coating from the surface. With the dissociation of boronate ester bond, all of the electrostatically attached protein on the polymer brushes were also released resulting in a significant reduction in adsorbed protein on the surfaces. After sugar (fructose) treatment, the amount of protein adsorption on PDA/(MP50/MT50), PDA/(MP20/MT80) and PDA/MT100 surfaces was reduced to 19, 22 and 20 μg/cm^2 (down from 52, 67, 82 μg/cm^2 respectively). In sugar the release percentage of the absorbed protein was found 63.4 %, 67.2% and 75.6% for PDA/(MP50/MT50), PDA/(MP20/MT80) and PDA/MT100 surfaces respectively.

On the other hand, for PDA coating after sugar treatment, no significant change in the amount of adsorbed protein was observed which confirms that the release of BSA protein was associated with the sugar-triggered dissociation of boronate ester bonds.

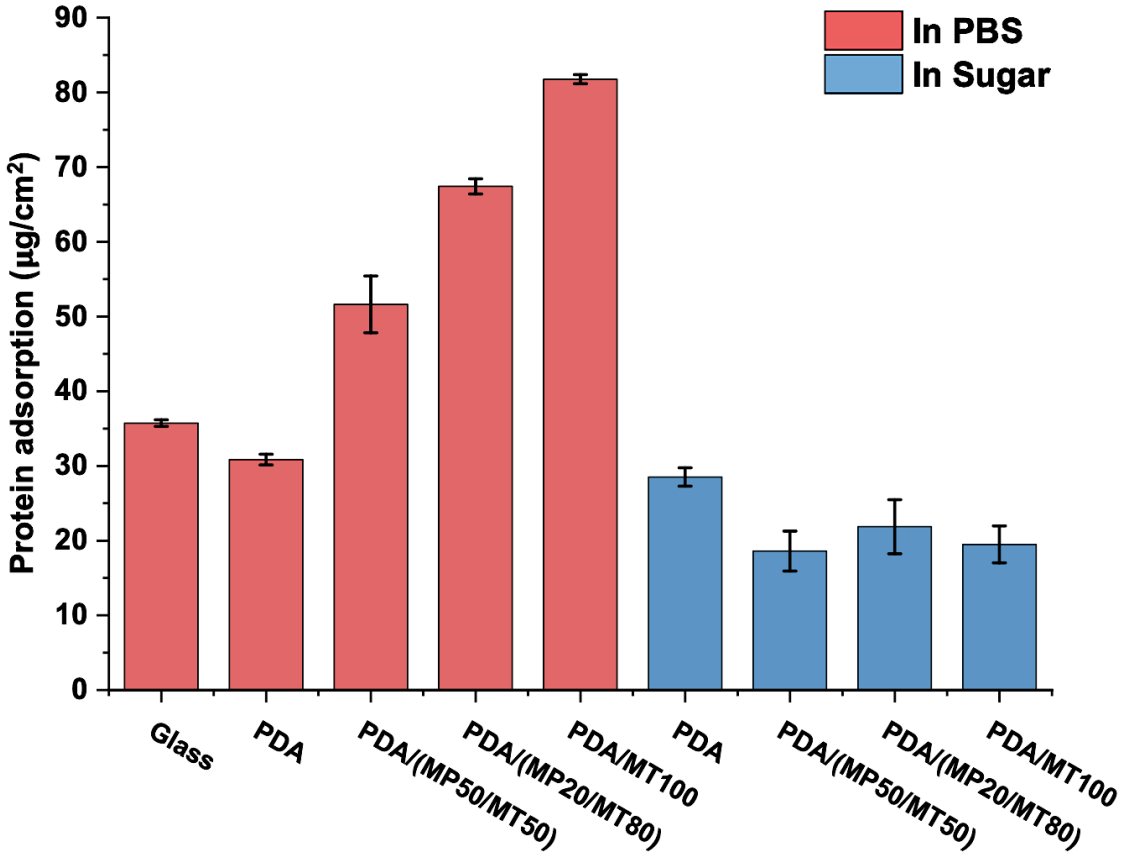

Figure 3.8. BSA protein adsorption on different surfaces (Glass, PDA, PDA/(MP50/MT50), PDA/(MP20/MT80) and PDA/MT100) before and after 30mins immersion into the sugar solution (60mM of Fructose solution in PBS). PDA/(MP50/MT50), PDA/(MP20/MT80) and PDA/MT100 surfaces showed significantly low amount of absorbed protein after sugar treatment.

3.3.7 Cell toxicity:

Biocompatibility of a polymer coating is a crucial requirement for its use in biomedical applications. Therefore, we conducted standard MTT assays to examine the cytotoxicity of all the modified surfaces and polymer coatings (Figure 3.9). Cell toxicity was investigated by incubating MRC-5 cells with culture medium containing the polymer coating extracts for 24 h. From Figure 3.9 (a) we can observe that, after 24h of incubation, all the polymer coatings showed excellent cell viabilities. After comparing all the samples, PDA/(MP50/MT50) exhibited the best cell viability which was 96.8%. This excellent biocompatibility can be ascribed to the fact that the PDA/(MP50/MT50) sample has the highest content of cell membrane biomimetic phosphorylcholine based poly(MPC-*st*-MAABO) polymer. Inspired by the phospholipid bilayer cell membrane structures, MPC-based polymers are widely considered as nontoxic and safe biomaterials[66,67]. An important advantage, associated with the incorporation of poly(MPC-*st*-MAABO) polymer into the coating, is to reduce the overall cell toxicity of the coating, thereby making it more biocompatible. For the coating PDA/MT100, a slightly reduced cell viability of around 88% was noted. The drop in cell viability of MRC-5 cells incubated with poly(META-*st*-MAABO) extract can be explained by the potential cytotoxicity activity of quaternary ammonium[68] moiety from META. In addition to cell viability with coating extract, cell viability and growth was observed onto the PDA, PDA/(MP50/MT50), PDA/(MP20/MT80) and PDA/MT100 coated 96 well plates using the same protocol. Cells were allowed to grow for 24hrs onto the PDA, PDA/(MP50/MT50), PDA/(MP20/MT80) and PDA/MT100 deposited 96 well plate. As shown in Figure 3.9 (b), only PDA/MT100 coated well showed less cell viability compared to other modified surfaces. PDA, PDA/(MP50/MT50) and PDA/(MP20/MT80) coated well showed outstanding cell attachment with more than 100% cell viability. The lack of

cytotoxicity and the cell-adhesive nature of PDA/(MP50/MT50) and PDA/(MP20/MT80) coatings underline their suitability in a broad range of biomedical applications.

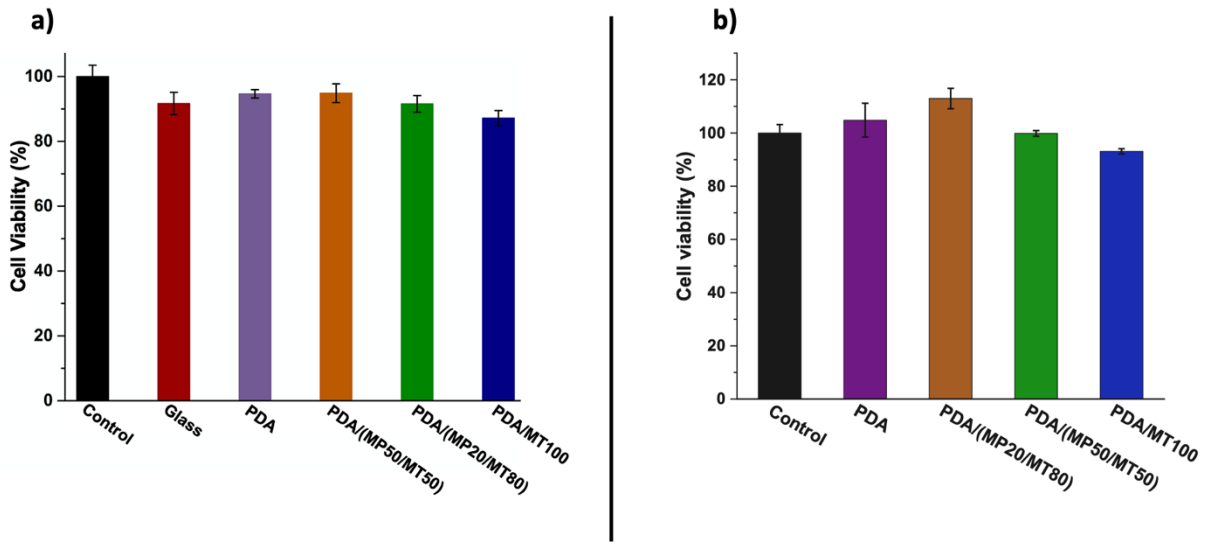

Figure 3.9. Cell viability of MRC-5 cells after 24 h incubation with a) different coating extracts (Glass, PDA, PDA/(MP50/MT50), PDA/(MP20/MT80) and PDA/MT100) and b) cell viability onto the PDA, PDA/(MP50/MT50), PDA/(MP20/MT80) and PDA/MT100 coated surfaces.

3.4 Conclusion:

In summary, a sugar-responsive, self-cleaning surface with dual functional property has been successfully developed. The coating is based on benzoxaborole-catechol complexation and cyclic boronic ester bond. Zwitterionic polymer and quaternary ammonium containing cationic polymer with different weight ratios were successfully grafted to the PDA coated surface. It was observed that presence of a small amount of zwitterionic poly(MPC-*st*-MAABO) polymer into the coating not only helped to reduce the bacteria adhesion but also facilitated the development of a very

hydrophilic surface with excellent biocompatibility. On the other hand, positively charged poly(META-*st*-MAABO) polymer brushes effectively interact with the negatively charged cell membranes of the bacteria, leading to the rupture and lysis of the cellular membrane of bacteria and thus delivering antibacterial properties to the surface. The dead bacteria and negatively charged protein was electrostatically attached to the cationic polymer brushes. After addition of the free sugar molecules to the surface, the benzoxaborole-catechol interactions were cleaved resulting in the release of the polymer chains as well as any attached proteins and bacteria on the surface. This dynamic self-cleaning surface with contact killing and release strategy could have great potential in the field of biomedical applications.

3.5 Supporting Information:

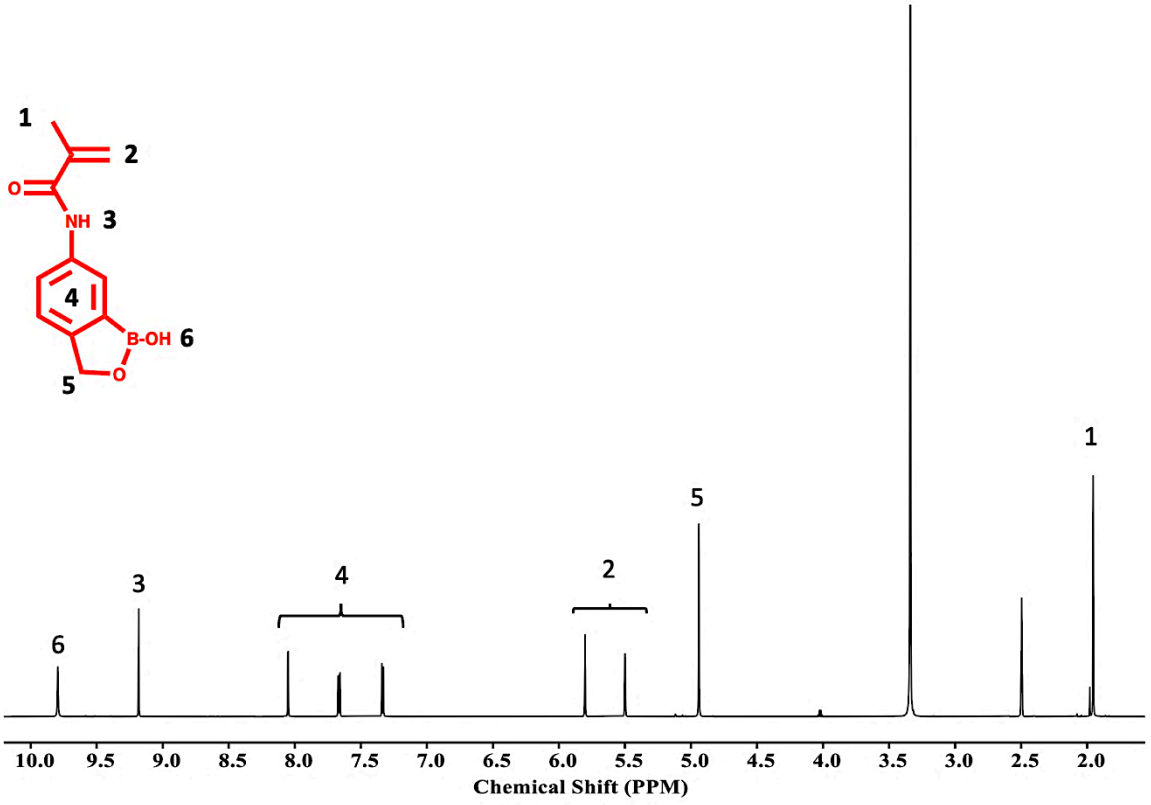

Figure S 3-1. ^{1}H NMR spectrum of 5-methacrylamido-1,2-benzoxaborole (MAABO) in DMSO-d_6.

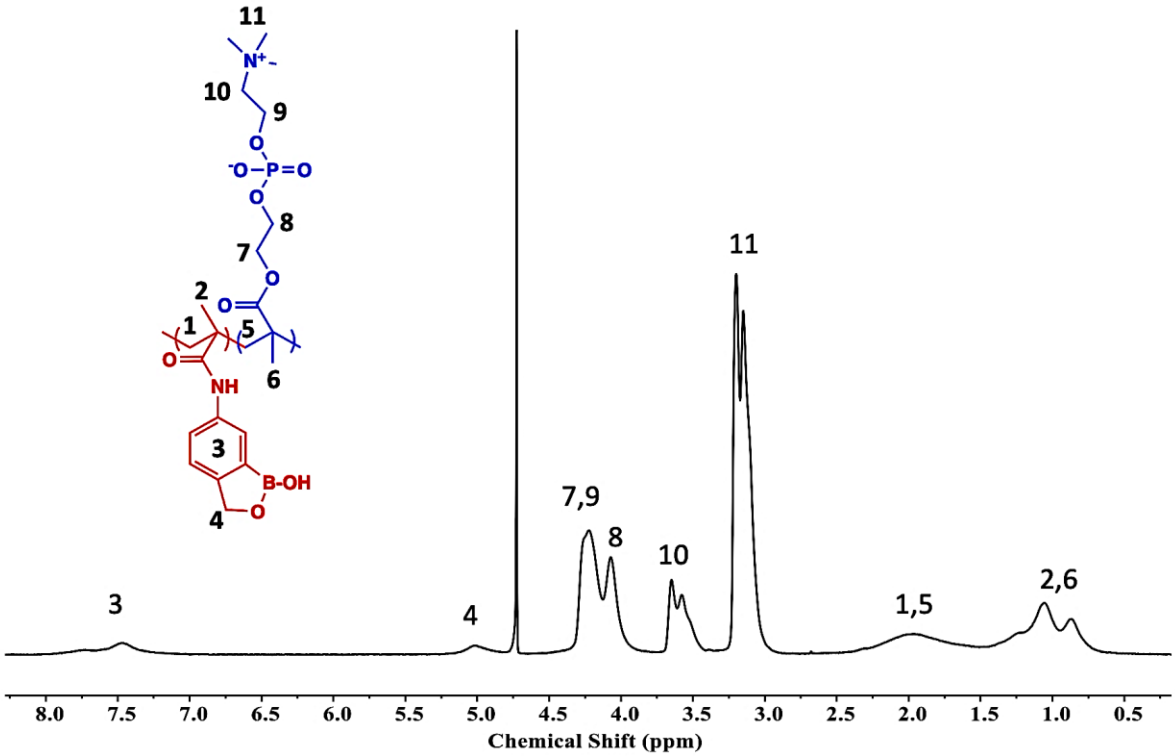

Figure S 3-2. ^{1}H NMR spectrum of benzoxaborole-containing zwitterionic polymer poly(MPC-*st*-MAABO).

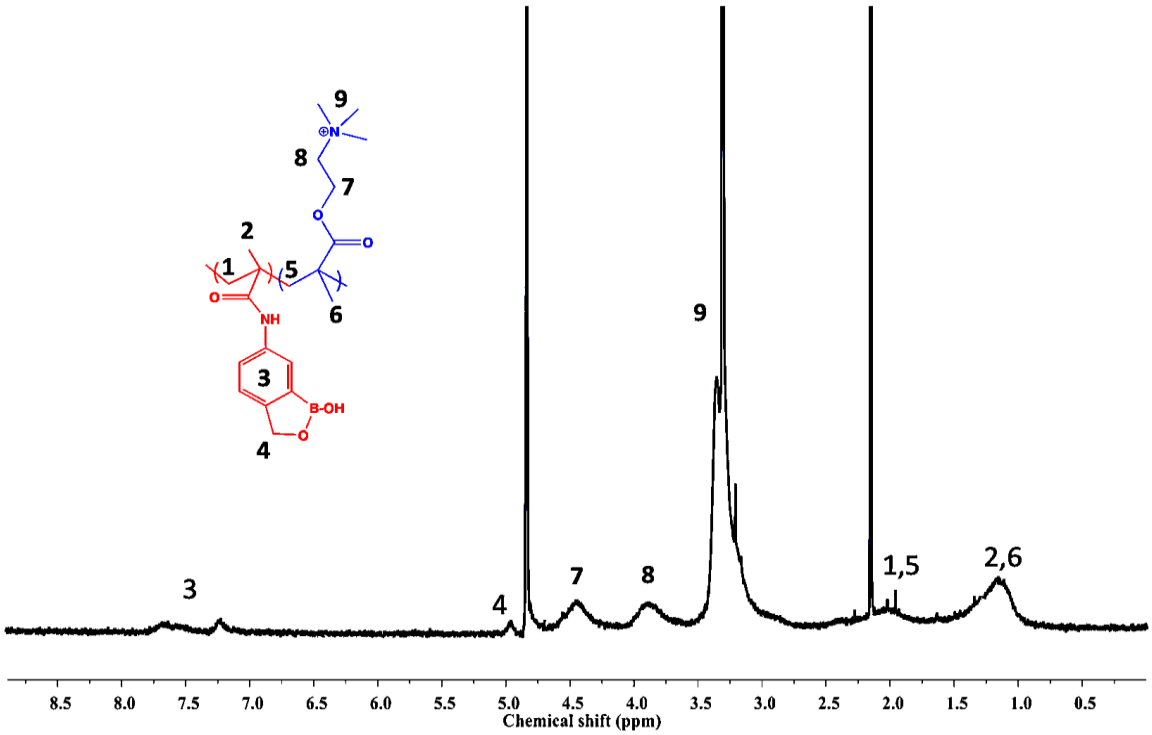

Figure S 3-3. ^{1}H NMR spectrum of benzoxaborole-containing cationic polymer poly(META-*st*-MAABO).

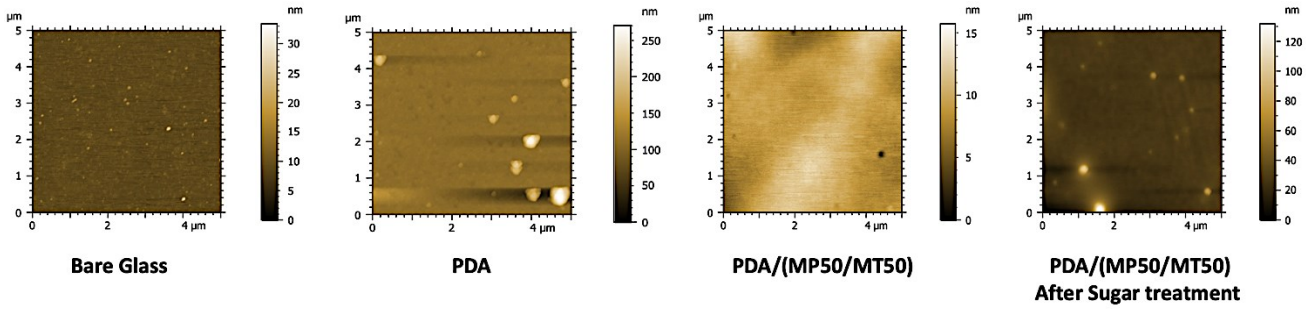

Figure S 3-4 . AFM images of surface morphology with roughness scale for glass, PDA and PDA/(MP50/MT50) and sugar treated PDA/(MP50/MT50) surfaces

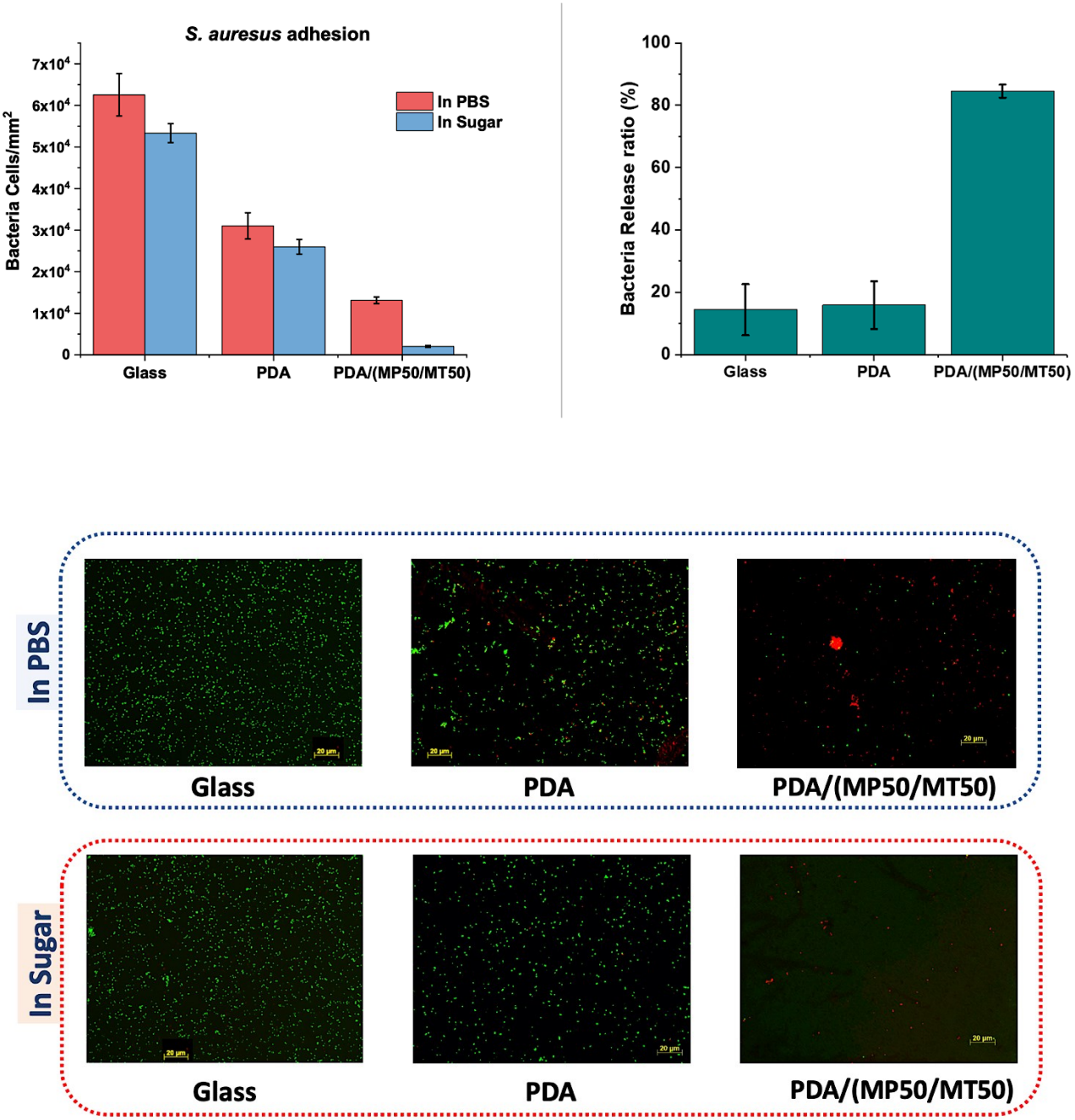

Figure S 3-5. *S. aureus* bacteria cell attachment to different surfaces (glass, PDA and PDA/(MP50/MT50)) and release ratio of the attached bacteria cells after sugar addition on the surface; fluorescence images of the attached cells on the surface.

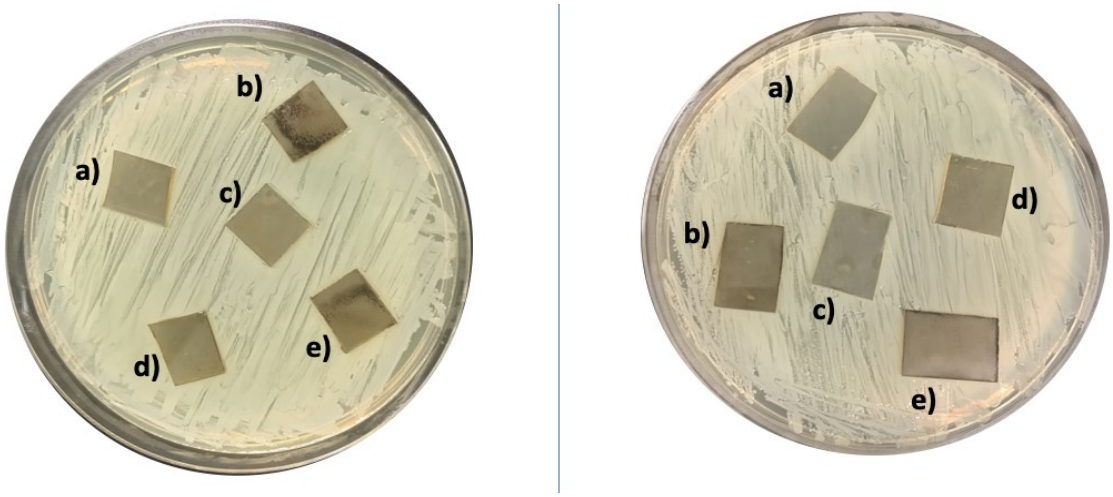

Figure S 3-6. Images of inhibition zone development against *S. aureus* (left) *and E. coli* (right) bacteria for different surfaces: a) bare glass, b) PDA, c) PDA/(MP50/MT50), d) PDA/(MP20/MT80) and e) PDA/MT100

3.5.1 Colony-forming units (CFU) Assay:

A single bacteria colony of *E. coli* and *S. aureus* was collected from the Luria-Bertani (LB) and tryptic soy (TS) agar plate, respectively, to inoculate 25 mL of liquid LB broth and TS broth, respectively. After inoculation at 37 °C for 16 h, bacteria cells were washed with sterile PBS solution through centrifugation at 4000 rpm for 5 min and resuspension in PBS thrice. The harvested bacterial cells were resuspended in PBS solution to an optical density (OD) of 0.1 at 670 nm (OD 670) of 0.1, corresponding to ~8×10^9 cells/mL. The bacteria suspension was adjusted in PBS to a final concentration of approximately 10^8 cell/mL. 100 µL of this bacteria suspended PBS solution was added on top of all the sample surfaces placed in a petri dish. The plate was afterwards sealed and incubated at 37°C under static conditions for 24 hrs. After 24 hrs aliquots were taken

from the top of all treated and control sample surfaces. After serial dilution in phosphate buffer solution, bacteria cells were spread out onto the Luria-Bertani (LB) and tryptic soy (TS) agar plate for *E. coli* and *S. aureus* respectively. Three parallel aliquots were taken for spreading from each diluted cell suspension. The number of CFUs was determined after an incubation period of 24 hours. The viable bacteria cell fraction was calculated using $(N/N_0) \times 100$, where N_0 and N are the average number of CFUs obtained for the control glass substrate and for the investigated sample, respectively.

3.5.2 MTT Assay:

The cell cytotoxicity of all the coated substrates and bare glass was investigated using MRC-5 cells by the standard MTT (3-(4,5-dimethylthiazol-2-yl)-2,5-diphenyltetrazolium bromide) method. Prior to cell seeding, all the samples were sterilized with UV light. Coated samples were placed in 24-well plates and DMEM culture medium (including 10% fetal bovine serum (FBS), 1% penicillin/streptomycin and 1% sodium pyruvate) with a volume fraction of 6 cm^2/mL specimen superficial area was added, and the coating extracts were collected after 48 hrs. MRC-5 cells were seeded in 96-well plates in a density of 6000 cells per well with 100 µL of DMEM medium and incubated at 37 °C for 24 hrs. After 24hrs, the media were substituted with 100 µL of fresh DMEM medium (for blank control) or DMEM medium containing polymer coating extracts, and with these new media MRC-5 cells were incubated for another 24 hrs. The cells were allowed to be further incubated for 3-4 hrs after the addition of MTT solution (20 µL, 5 mg/mL in sterilized PBS). The media were carefully removed, followed by the addition of 100 µL of dimethyl sulfoxide / isopropanol (1:1 v/v) solution to dissolve the formazan crystals. After that the absorbance at 570 nm was obtained via the TECAN Genios pro microplate reader

and percent cell viability was calculated by comparing OD values of cells treated with/without coating extracts.

3.6 References:

(1) Donlan, R. M.; Costerton, J. W. Biofilms: Survival Mechanisms of Clinically Relevant Microorganisms. *Clinical Microbiology Reviews*. **2002**, *15*, 167–193.

(2) Hall-Stoodley, L.; Costerton, J. W.; Stoodley, P. Bacterial Biofilms: From the Natural Environment to Infectious Diseases. *Nature Reviews Microbiology*. **2004**, *2,* 95–108.

(3) Wang, B.; Ye, Z.; Xu, Q.; Liu, H.; Lin, Q.; Chen, H.; Nan, K. Construction of a Temperature-Responsive Terpolymer Coating with Recyclable Bactericidal and Self-Cleaning Antimicrobial Properties. *Biomater. Sci.* **2016**, *4* (12), 1731–1741.

(4) Hou, Z.; Wu, Y.; Xu, C.; Reghu, S.; Shang, Z.; Chen, J.; Pranantyo, D.; Marimuth, K.; De, P. P.; Ng, O. T.; et al. Precisely Structured Nitric-Oxide-Releasing Copolymer Brush Defeats Broad-Spectrum Catheter-Associated Biofilm Infections in Vivo. *ACS Cent. Sci.* **2020**, *6* (11), 2031–2045.

(5) Xing, C. M.; Meng, F. N.; Quan, M.; Ding, K.; Dang, Y.; Gong, Y. K. Quantitative Fabrication, Performance Optimization and Comparison of PEG and Zwitterionic Polymer Antifouling Coatings. *Acta Biomater.* **2017**, *59*, 129–138.

(6) Su, Y.; Feng, T.; Feng, W.; Pei, Y.; Li, Z.; Huo, J.; Xie, C.; Qu, X.; Li, P.; Huang, W. Mussel-Inspired, Surface-Attachable Initiator for Grafting of Antimicrobial and Antifouling Hydrogels. *Macromol. Rapid Commun.* **2019**, *40* (17), 1–8.

(7) Mitra, D.; Kang, E. T.; Neoh, K. G. Polymer-Based Coatings with Integrated Antifouling and Bactericidal Properties for Targeted Biomedical Applications. *ACS Appl. Polym. Mater.* **2021**, *3* (5), 2233–2263.

(8) Xue, C. H.; Guo, X. J.; Ma, J. Z.; Jia, S. T. Fabrication of Robust and Antifouling Superhydrophobic Surfaces via Surface-Initiated Atom Transfer Radical Polymerization. *ACS Appl. Mater. Interfaces* **2015**, *7* (15), 8251–8259.

(9) Ding, X.; Yang, C.; Lim, T. P.; Hsu, L. Y.; Engler, A. C.; Hedrick, J. L.; Yang, Y. Y. Antibacterial and Antifouling Catheter Coatings Using Surface Grafted PEG-b-Cationic Polycarbonate Diblock Copolymers. *Biomaterials* **2012**, *33* (28), 6593–6603.

(10) Zhi, Z.; Su, Y.; Xi, Y.; Tian, L.; Xu, M.; Wang, Q.; Padidan, S.; Li, P.; Huang, W. Dual-Functional Polyethylene Glycol-b-Polyhexanide Surface Coating with in Vitro and in Vivo Antimicrobial and Antifouling Activities. *ACS Appl. Mater. Interfaces* **2017**, *9* (12), 10383–10397.

(11) Asha, A. B.; Chen, Y.; Zhang, H.; Ghaemi, S.; Ishihara, K.; Liu, Y.; Narain, R. Rapid Mussel-Inspired Surface Zwitteration for Enhanced Antifouling and Antibacterial Properties. *Langmuir* **2019**, *35* (5), 1621–1630.

(12) Shahkaramipour, N.; Lai, C. K.; Venna, S. R.; Sun, H.; Cheng, C.; Lin, H. Membrane Surface Modification Using Thiol-Containing Zwitterionic Polymers via Bioadhesive Polydopamine. *Ind. Eng. Chem. Res.* **2018**, *57* (6), 2336–2345.

(13) Yang, Q.; Strathmann, M.; Rumpf, A.; Schaule, G.; Ulbricht, M. Grafted Glycopolymer-Based Receptor Mimics on Polymer Support for Selective Adhesion of Bacteria. *ACS Appl. Mater. Interfaces* **2010**, *2* (12), 3555–3562.

(14) Gu, J. S.; Yu, H. Y.; Huang, L.; Tang, Z. Q.; Li, W.; Zhou, J.; Yan, M. G.; Wei, X. W. Chain-Length Dependence of the Antifouling Characteristics of the Glycopolymer-Modified Polypropylene Membrane in an SMBR. *J. Memb. Sci.* **2009**, *326* (1), 145–152.

(15) Shahkaramipour, N.; Tran, T. N.; Ramanan, S.; Lin, H. Membranes with Surface-Enhanced Antifouling Properties for Water Purification. *Membranes*. **2017**, *7* (1), 13.

(16) Chen, S.; Li, L.; Zhao, C.; Zheng, J. Surface Hydration: Principles and Applications toward Low-Fouling/Nonfouling Biomaterials. *Polymer*. **2010**, *51,* 5283–5293.

(17) Tankhiwale, R.; Bajpai, S. K. Preparation, Characterization and Antibacterial Applications of ZnO-Nanoparticles Coated Polyethylene Films for Food Packaging. *Colloids Surfaces B Biointerfaces* **2012**, *90* (1), 16–20.

(18) Aumsuwan, N.; McConnell, M. S.; Urban, M. W. Tunable Antimicrobial Polypropylene

Surfaces: Simultaneous Attachment of Penicillin (Gram +) and Gentamicin (Gram -). *Biomacromolecules* **2009**, *10* (3), 623–629.

(19) Caro, A.; Humblot, V.; Méthivier, C.; Minier, M.; Salmain, M.; Pradier, C. M. Grafting of Lysozyme and/or Poly(Ethylene Glycol) to Prevent Biofilm Growth on Stainless Steel Surfaces. *J. Phys. Chem. B* **2009**, *113* (7), 2101–2109.

(20) Xu, G.; Liu, P.; Pranantyo, D.; Xu, L.; Neoh, K. G.; Kang, E. T. Antifouling and Antimicrobial Coatings from Zwitterionic and Cationic Binary Polymer Brushes Assembled via "Click" Reactions. *Ind. Eng. Chem. Res.* **2017**, *56* (49), 14479–14488.

(21) Schaer, T. P.; Stewart, S.; Hsu, B. B.; Klibanov, A. M. Hydrophobic Polycationic Coatings That Inhibit Biofilms and Support Bone Healing during Infection. *Biomaterials* **2012**, *33* (5), 1245–1254.

(22) Ye, W.; Leung, M. F.; Xin, J.; Kwong, T. L.; Lee, D. K. L.; Li, P. Novel Core-Shell Particles with Poly(n-Butyl Acrylate) Cores and Chitosan Shells as an Antibacterial Coating for Textiles. *Polymer (Guildf).* **2005**, *46* (23), 10538–10543.

(23) Li, R.; Mansukhani, N. D.; Guiney, L. M.; Ji, Z.; Zhao, Y.; Chang, C. H.; French, C. T.; Miller, J. F.; Hersam, M. C.; Nel, A. E.; et al. Identification and Optimization of Carbon Radicals on Hydrated Graphene Oxide for Ubiquitous Antibacterial Coatings. *ACS Nano* **2016**, *10* (12), 10966–10980.

(24) Wei, T.; Tang, Z.; Yu, Q.; Chen, H. Smart Antibacterial Surfaces with Switchable Bacteria-Killing and Bacteria-Releasing Capabilities. *ACS Applied Materials and Interfaces*. **2017**, *9,* 37511–37523.

(25) Mi, L.; Jiang, S. Integrated Antimicrobial and Nonfouling Zwitterionic Polymers. *Angewandte Chemie - International Edition*. **2014**, *53,* 1746–1754.

(26) Yu, Q.; Cho, J.; Shivapooja, P.; Ista, L. K.; López, G. P. Nanopatterned Smart Polymer Surfaces for Controlled Attachment, Killing, and Release of Bacteria. *ACS Appl. Mater. Interfaces* **2013**, *5* (19), 9295–9304.

(27) Cheng, G.; Xue, H.; Zhang, Z.; Chen, S.; Jiang, S. A Switchable Biocompatible Polymer

Surface with Self-Sterilizing and Nonfouling Capabilities. *Angew. Chemie - Int. Ed.* **2008**, *47* (46), 8831–8834.

(28) Cao, Z.; Mi, L.; Mendiola, J.; Ella-Menye, J. R.; Zhang, L.; Xue, H.; Jiang, S. Reversibly Switching the Function of a Surface between Attacking and Defending against Bacteria. *Angew. Chemie - Int. Ed.* **2012**, *51* (11), 2602–2605.

(29) Děkanovský, L.; Elashnikov, R.; Kubiková, M.; Vokatá, B.; Švorčík, V.; Lyutakov, O. Dual-Action Flexible Antimicrobial Material: Switchable Self-Cleaning, Antifouling, and Smart Drug Release. *Adv. Funct. Mater.* **2019**, *29* (31), 1901880.

(30) Ye, G.; Lee, J.; Perreault, F.; Elimelech, M. Controlled Architecture of Dual-Functional Block Copolymer Brushes on Thin-Film Composite Membranes for Integrated "Defending" and "Attacking" Strategies against Biofouling. *ACS Appl. Mater. Interfaces* **2015**, *7* (41), 23069–23079.

(31) Wu, B.; Zhang, L.; Huang, L.; Xiao, S.; Yang, Y.; Zhong, M.; Yang, J. Salt-Induced Regenerative Surface for Bacteria Killing and Release. *Langmuir* **2017**, *33* (28), 7160–7168.

(32) Qian, W.; Qiu, J.; Su, J.; Liu, X. Minocycline Hydrochloride Loaded on Titanium by Graphene Oxide: An Excellent Antibacterial Platform with the Synergistic Effect of Contact-Killing and Release-Killing. *Biomater. Sci.* **2018**, *6* (2), 304–313.

(33) Li, N.; Li, T.; Qiao, X. Y.; Li, R.; Yao, Y.; Gong, Y. K. Universal Strategy for Efficient Fabrication of Blood Compatible Surfaces via Polydopamine-Assisted Surface-Initiated Activators Regenerated by Electron Transfer Atom-Transfer Radical Polymerization of Zwitterions. *ACS Appl. Mater. Interfaces* **2020**, *12* (10), 12337–12344.

(34) Zoppe, J. O.; Ataman, N. C.; Mocny, P.; Wang, J.; Moraes, J.; Klok, H. A. Surface-Initiated Controlled Radical Polymerization: State-of-the-Art, Opportunities, and Challenges in Surface and Interface Engineering with Polymer Brushes. *Chem. Rev.* **2017**, *117* (3), 1105–1318.

(35) Yu, Q.; Ista, L. K.; López, G. P. Nanopatterned Antimicrobial Enzymatic Surfaces Combining Biocidal and Fouling Release Properties. *Nanoscale* **2014**, *6* (9), 4750–4757.

(36) Ista, L. K.; Yu, Q.; Parthasarathy, A.; Schanze, K. S.; López, G. P. Reusable Nanoengineered Surfaces for Bacterial Recruitment and Decontamination. *Biointerphases* **2016**, *11* (1), 019003.

(37) Zhao, Z.; Ma, X.; Chen, R.; Xue, H.; Lei, J.; Du, H.; Zhang, Z.; Chen, H. Universal Antibacterial Surfaces Fabricated from Quaternary Ammonium Salt-Based Pnipam Microgels. *ACS Appl. Mater. Interfaces* **2020**, *12* (17), 19268.

(38) He, L.; Fullenkamp, D. E.; Rivera, J. G.; Messersmith, P. B. PH Responsive Self-Healing Hydrogels Formed by Boronate-Catechol Complexation. *Chem. Commun.* **2011**, *47* (26), 7497–7499.

(39) Nakahata, M.; Mori, S.; Takashima, Y.; Hashidzume, A.; Yamaguchi, H.; Harada, A. PH- and Sugar-Responsive Gel Assemblies Based on Boronate-Catechol Interactions. *ACS Macro Lett.* **2014**, *3* (4), 337–340.

(40) Chen, Y.; Diaz-Dussan, D.; Wu, D.; Wang, W.; Peng, Y. Y.; Asha, A. B.; Hall, D. G.; Ishihara, K.; Narain, R. Bioinspired Self-Healing Hydrogel Based on Benzoxaborole-Catechol Dynamic Covalent Chemistry for 3D Cell Encapsulation. *ACS Macro Lett.* **2018**, *7* (8), 904–908.

(41) Wu, D.; Wang, W.; Diaz-dussan, D.; Peng, Y.; Chen, Y.; Narain, R.; Hall, D. G. In Situ Forming, Dual-Crosslink Network, Self-Healing Hydrogel Enabled by a Bioorthogonal Nopoldiol − Benzoxaborolate Click Reaction with a Wide PH Range. **2019**. *31* (11), 4092.

(42) Cheng, Q.; Asha, A. B.; Liu, Y.; Peng, Y. Y.; Diaz-Dussan, D.; Shi, Z.; Cui, Z.; Narain, R. Antifouling and Antibacterial Polymer-Coated Surfaces Based on the Combined Effect of Zwitterions and the Natural Borneol. *ACS Appl. Mater. Interfaces* **2021**, *13* (7), 9006–9014.

(43) Wang, B. L.; Jin, T. W.; Han, Y. M.; Shen, C. H.; Li, Q.; Lin, Q. K.; Chen, H. Bio-Inspired Terpolymers Containing Dopamine, Cations and MPC: A Versatile Platform to Construct a Recycle Antibacterial and Antifouling Surface. *J. Mater. Chem. B* **2015**, *3* (27), 5501–5510.

(44) Hung, T.; Fu, C.; Su, C.; Chen, J.; Wu, W.; Lin, Y. Enzyme and Microbial Technology Immobilization of Cellulase onto Electrospun Polyacrylonitrile (PAN) Nanofibrous Membranes and Its Application to the Reducing Sugar Production from Microalgae.

Enzyme Microb. Technol. **2011**, *49* (1), 30–37.

(45) Yalcinkaya, F. Surface Modification of Electrospun Nanofibrous Membranes for Oily Wastewater Separation. *RSC Adv.* **2017**, 56704–56712.

(46) Zangmeister, R. A.; Morris, T. A.; Tarlov, M. J. Characterization of Polydopamine Thin Films Deposited at Short Times by Autoxidation of Dopamine. *Langmuir* **2013**, *29* (27), 8619–8628.

(47) Münch, A. S.; Adam, S.; Fritzsche, T.; Uhlmann, P. Tuning of Smart Multifunctional Polymer Coatings Made by Zwitterionic Phosphorylcholines. *Adv. Mater. Interfaces* **2020**, *1901422* (7), 1–10.

(48) Kozak, M.; Domka, L. Adsorption of the Quaternary Ammonium Salts on Montmorillonite. *J. Phys. Chem. Solids* **2004**, *65*, 441–445.

(49) Yang, G.; Zhao, J.; Cui, L.; Song, S.; Zhang, S.; Yu, L.; Zhang, P. Tribological Characteristic and Mechanism Analysis of Borate Ester as a Lubricant Additive in Di Ff Erent Base Oils. *RSC Adv.* **2017**, *7*, 7944–7953.

(50) Spitler, E. L.; Giovino, M. R.; White, S. L.; Dichtel, W. R. A Mechanistic Study of Lewis Acid-Catalyzed Covalent Organic Framework Formation. *Chem. Sci.* **2011**, *2*, 1588–1593.

(51) Faniran, J. A.; Shurvell, H. F. Infrared Spectra of Phenylboronic Acid (Normal and Deuterated) and Diphenyl Phenylboronate. *Can. J. Chem.* **1968**, *46* (12), 2089–2095.

(52) Sci, J. V.; Gengenbach, T. R.; Major, G. H.; Linford, M. R.; Easton, C. D. Practical Guides for X-Ray Photoelectron Spectroscopy (XPS): Interpreting the Carbon 1s Spectrum Practical Guides for x-Ray Photoelectron Spectroscopy (XPS): Interpreting the Carbon 1s Spectrum. *J. Vac. Sci. Technol. A Vacuum, Surfaces, Film.* **2021**, *39* (1), 013204.

(53) G. Beamson D. Briggs. High Resolution XPS of Organic Polymers: The Scienta ESCA300 Database (Beamson, G.; Briggs, D.). *J. Chem. Educ.* **1993**, *70* (1), A25.

(54) Jiang, J. H.; Zhu, L. P.; Li, X. L.; Xu, Y. Y.; Zhu, B. K. Surface Modification of PE Porous Membranes Based on the Strong Adhesion of Polydopamine and Covalent Immobilization of Heparin. *J. Memb. Sci.* **2010**, *364* (1–2), 194–202.

(55) Wang, H.; Chen, M.; Jin, C.; Niu, B.; Jiang, S.; Li, X.; Jiang, S. Antibacterial [2-(Methacryloyloxy) Ethyl] Trimethylammonium Chloride Functionalized Reduced Graphene Oxide/Poly(Ethylene- Co - Vinyl Alcohol) Multilayer Barrier Film for Food Packaging. *J. Agric. Food Chem.* **2018**, *66* (3), 732–739.

(56) Asri, L. A. T. W.; Crismaru, M.; Roest, S.; Chen, Y.; Ivashenko, O.; Rudolf, P.; Tiller, J. C.; Mei, H. C. Van Der; Loontjens, T. J. A.; Busscher, H. J. A Shape-Adaptive , Antibacterial-Coating of Immobilized Quaternary-Ammonium Compounds Tethered on Hyperbranched Polyurea and Its Mechanism of Action. *Adv. Funct. Mater.* **2014**, *24*, 346–355.

(57) Chen, Y.; Wang, W.; Wu, D.; Nagao, M.; Hall, D. G.; Thundat, T.; Narain, R. Injectable Self-Healing Zwitterionic Hydrogels Based on Dynamic Benzoxaborole-Sugar Interactions with Tunable Mechanical Properties. *Biomacromolecules* **2018**, *19* (2), 596–605.

(58) Pettignano, A.; Grijalvo, S.; Häring, M.; Eritja, R.; Tanchoux, N.; Quignard, F.; Díaz Díaz, D. Boronic Acid-Modified Alginate Enables Direct Formation of Injectable, Self-Healing and Multistimuli-Responsive Hydrogels. *Chem. Commun.* **2017**, *53* (23), 3350–3353.

(59) Chen, Y.; Diaz-Dussan, D.; Wu, D.; Wang, W.; Peng, Y. Y.; Asha, A. B.; Hall, D. G.; Ishihara, K.; Narain, R. Bioinspired Self-Healing Hydrogel Based on Benzoxaborole-Catechol Dynamic Covalent Chemistry for 3D Cell Encapsulation. *ACS Macro Lett.* **2018**, *7* (8), 904–908.

(60) Sánchez-Clemente, R.; Igeño, M. I.; Población, A. G.; Guijo, M. I.; Merchán, F.; Blasco, R. Study of PH Changes in Media during Bacterial Growth of Several Environmental Strains. In *Multidisciplinary Digital Publishing Institute Proceedings*; **2018,** *2 (20),* 1297.

(61) Marsh, P. D. Dental Plaque as a Biofilm and a Microbial Community - Implications for Health and Disease. *BMC Oral Health* **2006**, *6* (SUPPL. 1), 1–7.

(62) Chen, Y.; Diaz-Dussan, D.; Wu, D.; Wang, W.; Peng, Y.-Y.; Benozir Asha, A.; G. Hall, D.; Ishihara, K.; Narain, R. Bioinspired Self-Healing Hydrogel Based on Benzoxaborole-Catechol Dynamic Covalent Chemistry for 3D Cell Encapsulation. *ACS Macro Lett.* **2018**, *7* (8), 904–908.

(63) Cross, M. C.; Toomey, R. G.; Gallant, N. D. Protein-Surface Interactions on Stimuli-Responsive Polymeric Biomaterials. *Biomed. Mater.* **2016**, *11* (2), 022002.

(64) Nagase, K.; Kobayashi, J.; Kikuchi, A.; Akiyama, Y.; Kanazawa, H.; Okano, T. Thermally-Modulated on/off-Adsorption Materials for Pharmaceutical Protein Purification. *Biomaterials* **2011**, *32* (2), 619–627.

(65) Wang, B. L.; Jin, T. W.; Han, Y. M.; Shen, C. H.; Li, Q.; Lin, Q. K.; Chen, H. Bio-Inspired Terpolymers Containing Dopamine, Cations and MPC: A Versatile Platform to Construct a Recycle Antibacterial and Antifouling Surface. *J. Mater. Chem. B* **2015**, *3* (27), 5501–5510.

(66) Matsuno, R.; Ishihara, K. Integrated Functional Nanocolloids Covered with Artificial Cell Membranes for Biomedical Applications. *Nano Today* **2011**, *6* (1), 61–74.

(67) Ishihara, K.; Chen, W.; Liu, Y.; Tsukamoto, Y.; Inoue, Y. Cytocompatible and Multifunctional Polymeric Nanoparticles for Transportation of Bioactive Molecules into and within Cells. *Sci. Technol. Adv. Mater.* **2016**, *17* (1), 300–312.

(68) Joondan, N.; Jhaumeer, S.; Caumul, P.; Marie, D. E. P.; Roy, P.; Hosten, E. Colloids and Surfaces A : Physicochemical and Engineering Aspects Synthesis , Physicochemical Properties and Membrane Interaction of Novel Quaternary Ammonium Surfactants Derived from l -Tyrosine and l -DOPA in Relation to Their Antimicrobial , Hemolytic. *Colloids Surfaces A Physicochem. Eng. Asp.* **2016**, *511*, 120–134.

Chapter 4 Bioinspired Antifouling and Antibacterial Polymer Coating with Intrinsic Self-healing Property

4.1 Introduction:

Surface deposited microorganisms are the critical sources of biofilm formation which has become a serious global health concern due to their resistance to antibiotics and resulting chronic infections [1,2]. Protecting biofilm formation with a recyclable antifouling[3–5] and antimicrobial coating[6,7] is a promising approach to control biofilm related infections [8]. One of the most common strategies adopted by researchers are to functionalize the surface with hydrophilic polymer[9,10] (such as poly(ethylene glycol)[11], zwitterionic polymers[12] and glycopolymers[13]) coating to create a strong hydration layer on top of the surface which usually helps to reduce the adsorption of foulants such as protein and bacteria. But this passive strategy is not effective for long term application and ineffective toward the microbials that had attached to the surface[14]. Researchers have developed many strategies[15–18] to generate dual functional surfaces combining both biocidal or non-adhesive functionalities. Non-adhesive functionality helps to reduce the initial microbial adhesion while the biocidal property helps to simultaneously kill bacterial cells in contact with the surfaces. To impart biocidal property into surfaces, researchers either incorporate releasable bacteria killing agents such as nanoparticles[19], antibiotics[20] and enzymes[21] or modify the surface with antimicrobial functionalities such as quaternary ammonium salts [17], polycations[22] and chitosan[23] etc. for contact killing. Although various concepts to protect surfaces from foulant were introduced, there are still many challenges to be overcome for practical applications. In practice, it was found that during storage, transport, and clinical use accidental mechanical damage, such as scratching, and abrasion can happen which significantly affect and alter the coating properties exposing the underlying substrate [10]. Since bacteria or other microorganisms could invade through the cracks[24,25], a mechanical damage or defect generated during operations might be the origin for surface fouling and accelerated function failure of the coating. One of the promising solutions to overcome this

challenge is to introduce self-healing property into the antifouling and antibacterial coating. Several research on self-healing coatings development have been reported, including multi-layer polymer brushes[24,25], hydrogels[26,27], microspheres[28,29] and nanocomposites[30]. Self-healing mechanisms can be categorized into two approaches such as "extrinsic self-healing" and "intrinsic self-healing" [31]. In 'extrinsic self-healing approach, a large number of microspheres or microcapsules containing a "healing agent" is usually pre-embedded into the material. The crack of the material will cause the release of the healing agent that can reconnect the fractured parts, resulting in the formation of new healed material. The recyclability of extrinsic self-healing is very limited because it allows the material to heal only a limited number of times depending on the amount of healing agent. In contrast, intrinsic self-healing enables the materials to heal infinitely which is more suitable for materials under requirements of long operation lifespans. In an intrinsic self-healing mechanism, healing of the mechanical damage of materials happens by the formation of reversible dynamic covalent bonds[32], non-covalent interactions such as hydrogen bonds[33], electrostatic attractions[34] and so on. This self-healing can also be stimulated by heat or by the action of water.

To functionalize the surface, mussel-inspired dopamine chemistry has been widely used due to its simplicity, versatility and strong reactivity for secondary functionalization[35,36]. Recently, similar to polydopamine coating, prebiotic chemistry inspired another simple, biocompatible and substrate independent functional coating that has been developed by spontaneous polymerization of amine-rich aminomalononitrile (AMN) [37,38]. The adhesive AMN coating has been utilized as a facile and versatile platform for developing multifunctional coating, immobilizing antifouling[39] and antibacterial polymers in a two-step method[40]. In this study, we exploited this unique surface modification technique to develop a rapidly self-healable, anti-fouling and antibacterial surface.

Recently reported vitamin B5 analogous hygroscopic methacrylamide (B5AMA)[41] compound was used to impart the self-healing property by forming amide-amide and amide-hydroxyl multiple hydrogen bonds into the coating. To better understand the self-healing mechanism of the B5AMA, a homopolymer poly(B5AMA) was synthesized and grafted onto the AMN coated surface by hydrogen bonding interactions between poly(B5AMA) and AMN coating. With a zwitterionic compound 2-methacryloyloxyethyl phosphorylcholine (MPC) and B5AMA a statistical copolymer poly (MPC-*st*-B5AMA) was also synthesized to graft onto the AMN coating for developing a biocompatible, antifouling and self-healing coating. As AMN coating can strongly bind silver nanoparticles (AgNPs) from silver nitrate solution[42], AgNPs was also incorporated into the AMN coating to impart antibacterial property into the coating. The developed multifunctional antifouling, antibacterial and self-healing coating is expected to be a promising material for biomedical application.

4.2 Experimental Section:

4.2.1 Materials:

MPC was obtained from Prof. Ishihara's lab (University of Tokyo, Japan). The initiator, 4,4′-azobis (4-cyanovaleric acid) (ACVA), thiazolyl blue tetrazolium bromide (MTT), Bovine serum albumin (BSA), Aminomalononitrile p-toluenesulfonate 98% and D-(−)-Pantolactone were purchased from Sigma-Aldrich and used without further purification. The Live/Dead BacLight Bacterial Viability Kit L-7012 and Micro BCA Protein Assay Kit were obtained from Thermo Fisher Scientific. *Escherichia coli (E. coli)* (ATCC 25922) and *Staphylococcus aureus (S. aureus)* (ATCC 25923) (ATCC, USA) were used as model bacteria in all bacterial tests. Luria-Bertani broth (LB) and tryptic soy broth (TSB) (Fisher Scientific, USA) were used as liquid media for *E.*

coli and *S. aureus* respectively. Normal human lung fibroblast cells MRC-5. CCL-171™ was used for MTT assay.

4.2.2 Synthesis of Polymers:

2-Aminoethyl methacrylamide (AEMA) was synthesized according to previously established procedure of our group[43]. B5AMA monomer was synthesized by simple ring opening chemistry between D-(−)-Pantolactone and synthesized AEMA, as previously reported[41]. The purity of the synthesized monomers was confirmed by ^{1}H NMR. Homo polymer of B5AMA, poly (B5AMA) was synthesized via free-radical polymerization. To synthesize poly (B5AMA), B5AMA (1.55 g, 6 mmol), and initiator ACVA (16.8 mg, 60 µmol) were placed in a 50 mL polymerization tube and dissolved with a mixture of methanol (4.5 mL) and DMF (1.5 mL). After degassing the solution mixture with nitrogen for 30 min, the polymerization reaction was carried out at 70 °C for 18 h. The reaction was terminated by rapid cooling in liquid nitrogen and the resultant copolymer was purified dialyzing against DI water for 48 h. Purified polymer was lyophilized to obtain poly(B5AMA) as a powder. Zwitterionic polymer with B5AMA pendent poly (MPC-*st*-B5AMA) was also synthesized via free-radical polymerization. To synthesize poly (MPC-*st*-B5AMA), B5AMA (774 mg, 3 mmol), MPC (885.8 mg, 3mmol) and initiator ACVA (16.8 mg, 60 µmol) were placed in a 50 mL polymerization tube and dissolved with a mixture of methanol (4.5 mL) and DMF (1.5 mL). After same polymerization and purification steps were carried out as mentioned above. The resulting purified polymers were characterized by ^{1}H NMR and Viscotek conventional gel permeation chromatography (GPC) to determine the composition and molecular weight, respectively. ^{1}H NMR spectra of the monomers and polymers were recorded on a Varian 500 MHz spectrometer. The number (M_n) and weight (M_w) average molecular weights of the synthesized polymers were determined by a GPC system equipped with one G5000PW$_{XL}$ TSK-

GEL column using 0.5 M sodium acetate/0.5 M acetic acid buffer as the eluent at a flow rate of 1.0 mL/min. The GPC was calibrated by monodisperse pullulan standards (M_w = 5900–404000 g/mol).

4.2.3 Surface Coating:

Glass substrates were ultrasonically cleaned with acetone, ethanol and DI water for 30 min respectively and dried with air. To modify the cleaned glass surfaces, first the glass surface was immersed into the 5mg/ml AMN solution in PBS at pH 8.5 and shaken with a mechanical shaker at 200rpm for 24hrs to allow autopolymerisation of AMN and forming a homogenous AMN coating on the glass substrate. After 24hrs shaking, coated glass substrate was gently rinsed with DI water to remove loosely bound AMN aggregates from the surface and air dried. Then polymer solution (10 mg of polymer in 100µl PBS buffer) of either poly(B5AMA) or poly (MPC-*st*-B5AMA) (10 mg of polymer dissolved in 100µl PBS solution) was added dropwise onto the AMN coated surface and placed at room temperature for 12 h. After 12hrs, the resulting coated surfaces were gently rinsed with PBS buffer to remove unreacted polymers and dried with air. The corresponding coated surfaces were denoted as AMN (substrate coated with AMN only), AMN/B5 (AMN coated substrate with poly(B5AMA)) and AMN/B5/MPC (AMN coated substrate with poly(B5AMA)). To incorporate AgNPs into the coating all the modified surfaces were immersed into the 50mM $AgNO_3$ solution for the *in-situ* deposition of the AgNPs onto the surface.

4.2.4 Surface Characterization:

Surface morphology and roughness of all the modified surfaces were observed by atomic force microscopy (AFM) using the Anton Paar Tosca 400 unit in tapping mode at dry condition. Surface roughness was expressed as root-mean-square (RMS) value. The chemical composition of the polymer modified substrate was determined by X-ray photoelectron spectroscopy (XPS) using

either an AXIS Nova or an AXIS Ultra-DLD spectrometer (Kratos Analytical Inc., Manchester, U.K.) with a monochromatic Al Kα source at a power of 180 W (15 kV × 12 mA) and a hemispherical analyzer operating in the fixed analyzer transmission mode. To investigate the surface relative hydrophilicity and wetting properties, static water contact angles of all the modified surfaces were measured using a model 590 goniometer. All the contact angles were measured with a 4 μL water droplet onto the surface at room temperature. Three contact angles were measured for each substrate at three different locations, and their average was recorded as a result. The surface morphology of AgNPs loaded surfaces was observed by field emission scanning electron microscopy (FESEM, Zeiss Sigma 300/VP).

4.2.5 Bacterial adhesion and antibacterial assay:

Gram-negative *Escherichia coli (E. coli)* and Gram-positive *Staphylococcus aureus (S. aureus)* were used as the model bacteria to evaluate both the bacteria adhesion and antibacterial property of the bare glass and modified glass substrates. A single bacteria colony of *E. coli* and *S. aureus* was collected from the cultured Luria-Bertani (LB) and tryptic soy (TS) agar plate, respectively, and cultured into 25 mL of liquid LB broth and TS broth, respectively at 37 °C for 16 hrs. Then the grown bacteria cells were washed with sterile PBS solution through centrifugation at 4000 rpm for 5 min and resuspension in PBS twice. The harvested bacterial cells were resuspended in 1ml of PBS solution to get the concentrated bacteria and later diluted to an optical density reading at 670 nm (OD 670) of 0.15, corresponding to ~8×10^9 cells/mL. For bacterial attachment, all the sample surfaces were incubated into *E. coli* and *S. aureus* suspension (8×10^9 cells/mL in PBS, pH 7.4) for 24hs at 37 °C, followed by 3 times gently rinsing with sterile PBS to remove loosely bound bacteria cells. The bacterial cells attached on the surfaces were stained with 50 μL of LIVE/DEAD stain in the dark for 15 min and then washed with PBS gently. After that, each slide

was examined by a fluorescence microscope with a magnification of 400×. The live bacteria emitted green light and the dead bacteria emitted red light. The number of bacterial cells was obtained through counting the bacterial cells in five different areas (four corners plus the center) of the sample surfaces and then averaging. The counted number of the attached bacteria was analyzed using an ImageJ software package and represented as cells/cm^2. Comparing the number of dead cells to the total number of bacteria cells attached fraction of dead cells were calculated which represented antibacterial ability of the AgNPs loaded surfaces.

4.2.6 Protein adsorption Assay:

The sample surfaces (each of 1x1 cm^2 area) were subjected to the protein adsorption test using Bovine Serum Albumin (BSA) as a model protein and the quantification of the adsorbed protein was performed using a bicinchoninic acid (BCA) protein assay kit according to the manufacturer's instructions. First, the samples were immersed into 2 mg mL^{-1} BSA solution in PBS and incubated at 37 °C for 3 hrs and then rinsed with PBS buffer solution to remove loosely bound protein from the surface. Afterward, samples were placed in a 24-well plate, and 1 mL of 2.0 wt.% sodium dodecyl sulfate solution was added, shaken, and sonicated for 1 h to separate the absorbed protein from the sample surfaces. After the addition of equal volumes of protein solution and BCA reagent, the 96-well plate was incubated at 37 °C for 2 h. The absorbance of the absorbed protein at 570 nm was measured using a Tecan Genios pro microplate reader. The protein absorbance concentration of samples was calculated using the standard curve. The calculated number of absorbed protein was expressed as (μg/cm^2).

4.2.7 Characterization of Self-healing process:

The Nano scratch test (NST) was performed using a sphero-conical diamond indenter (tip radius 200 μm) mounted on a scratch test machine (Anton Paar, Micro Combi Tester, MCT^3). With this

sphero-conical stylus a 2 mm length of scratch was performed on the sample surfaces at constant load of 5N with constant speed. Self-healing properties were characterized by measuring the penetration depth before and after the healing process through performing the cross-scan analysis. After the 2 mm long main scratch, three scanning scratches were done perpendicular to the main scratch with a scanning load of 0.05N in order to scan the profile of the track at several positions. The Pre-scan provides a profile of the surface before scratch. It allows any non-uniformity in the flatness of the samples to borne into consideration when the penetration depth of the indenter is measured during the scratch test. The penetration depth corresponds to the difference between the depth of scratch and the surface profile obtained in the pre-scan step. Comparing the penetration depth of scratch to penetration depth after healing, the percentage of recovery of the coating can be calculated. After the scratching and healing processes reached completion, the scratch-recovered sample was analyzed using an optical microscope. Along with the nano scratch healing observation, macro scratch healing by optical microscope has also been observed. The modified surface was scratched with a sharp knife followed by 5 µl of water added onto the surface for fast healing and the resulting surface was observed under the microscope.

4.2.8 Cytotoxicity:

The cytotoxicity of the sample coating was investigated by performing the MTT assay with normal human lung fibroblast cells MRC-5. CCL-171™. MRC-5 cells were seeded into coated (AMN, AMN/B5 and AMN/B5/MPC coating; following the same procedure as mentioned under surface coating section) 96-well plates in a density of 6000 cells per well with 100 µL of DMEM culture medium (including 10% fetal bovine serum (FBS), 1% penicillin/streptomycin and 1% sodium pyruvate) and incubated at 37 °C for 48 hrs. After 48hrs, the cells were allowed to be further incubated for 3-4 hrs after the addition of MTT solution (20 µL, 5 mg/mL in sterilized PBS). The

media were carefully removed, followed by the addition of 100 µL of dimethyl sulfoxide / isopropanol (1:1 v/v) solution to dissolve the formazan crystals. After that the absorbance at 570 nm was obtained via the TECAN Genios pro microplate reader and percent cell viability was calculated by comparing OD values of cells treated with/without coating.

4.3 Results and Discussion:

Zwitterionic copolymer poly (MPC-*st*-B5AMA) and a homo polymer of B5AMA- poly(B5AMA) was synthesized by free radical polymerization with a targeted degree of polymerization (DP) 100. Prior to that B5AMA monomer was synthesized according to the previous report[41]. The purity of the B5AMA and chemical composition of poly (MPC-*st*-B5AMA) was characterized by ^{1}H NMR (Figure S 4-1 to Figure S 4-3). The mole content of MPC and B5AMA in poly (MPC-*st*-B5AMA) was calculated from ^{1}H NMR and was found to be 61% and 39% respectively by comparing the integral of the characteristic peak for B5AMA (δ 3.97 ppm) with the characteristic peak integral for MPC (δ 3.67 ppm) (Figure S 4-3). The molecular weights of the synthesized polymers are summarized in Table 4.1.

Table 4.1 Chemical Composition and Molecular Weights of the Synthesized Polymers

Polymer	Composition of Copolymer (mol%)				Molecular weights [b]	
	In Feed		In Polymer [a]		M_n	M_w
	MPC	B5AMA	MPC	B5AMA	kDa	
Poly (MPC-*st*-B5AMA)	50	50	61	39	30.2	46.5
Poly (B5AMA)	_	100	_	100	17.5	23.1

Amine rich-AMN coating can strongly graft B5AMA by forming possible hydrogen bond between functional hydroxyl group (-OH) of B5AMA structure and C=O functional group of proposed AMN structure[38]. To evaluate the effect of B5AMA on AMN coated surface, first a cleaned glass substrate was immersed into AMN solution (5 mg/ml in PBS buffer solution, pH 8.5) for 24 hrs to obtain a homogeneous AMN coating and then poly(B5AMA) and poly (MPC-*st*-B5AMA) polymer solution (10 mg of polymer in 100µl PBS solution) was added dropwise onto the AMN coated surface to achieve a homogenous layer of antifouling coating (Figure 4.1). The resultant surfaces are named as AMN/B5 and AMN/B5/MPC respectively.

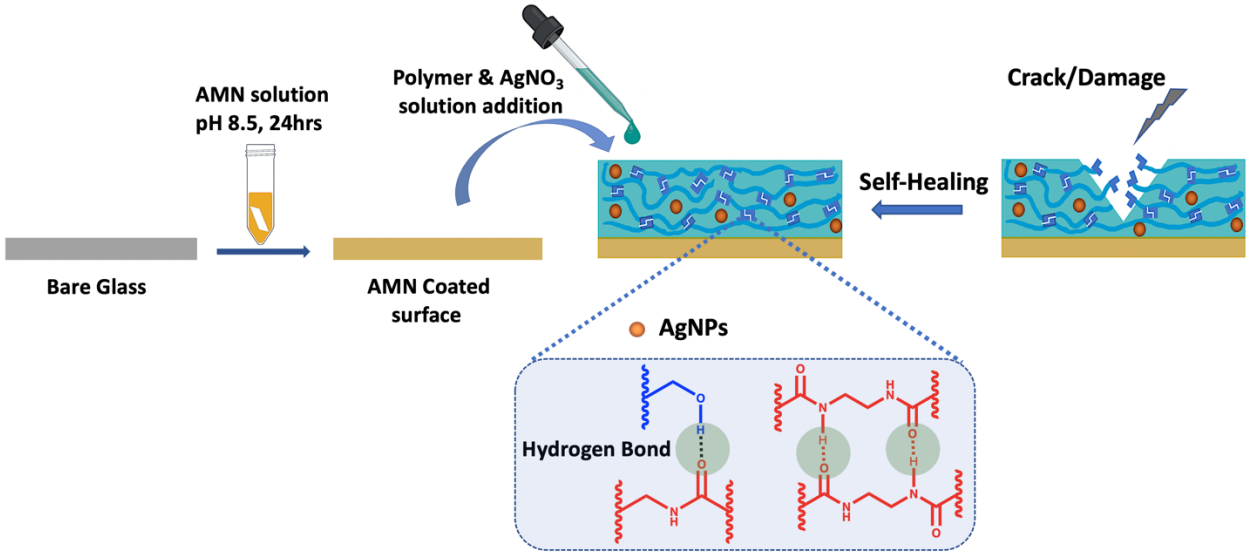

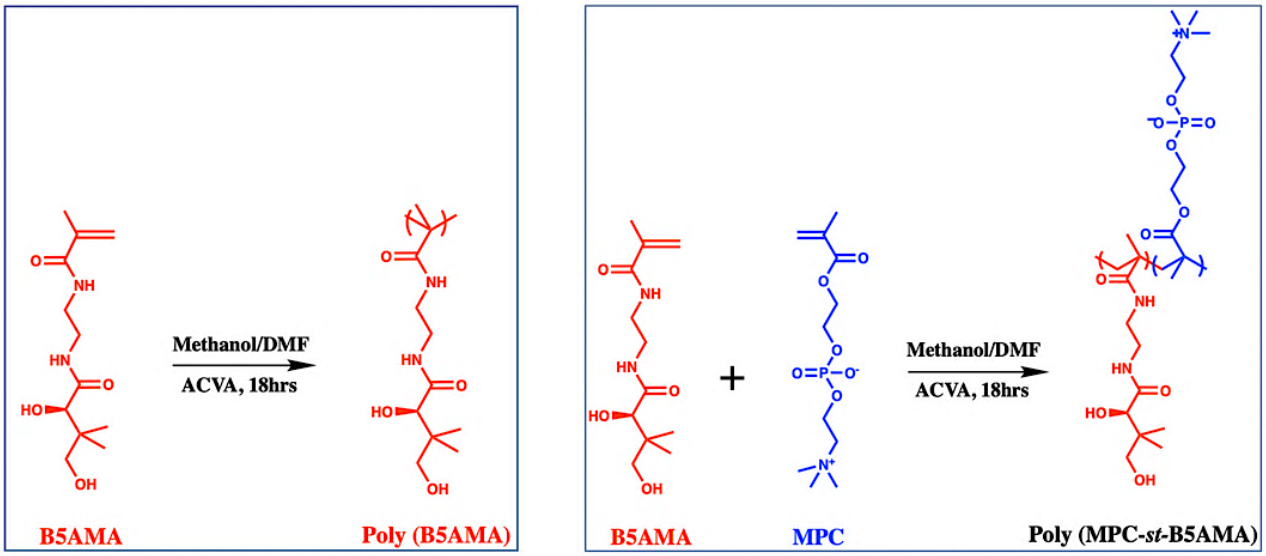

Figure 4.1 Schematic illustration of self-healing coating with possible hydrogen bond responsible for self-healing. Polymerization mechanism of poly(B5AMA) and poly (MPC-st-B5AMA) polymer with chemical structures.

4.3.1 Characterization of Modified Surfaces: Morphology, Composition, and Wettability

The surface morphology of all the coatings on glass substrates was characterized by AFM (Figure 4.2 (a–d)). The AMN surface alone (Figure 4.2 b) was found to contain surface crystallites spherical in shape, roughening the surface morphology. The roughly spherical features observed by AFM represent the AMN-polymer aggregates expected to result from spontaneous polymerization of AMN. However, they are structurally complex polymers where the exact polymerization mechanism and structure are still under investigation[38]. After introducing poly(B5AMA) and poly (MPC-*st*-B5AMA) polymers onto the AMN coated surfaces, all the surface roughness changed significantly (Figure 4.2 c and d), showing lower root mean square

surface roughness values of 0.6 nm and 1.93 nm respectively, which also demonstrated that the polymers were successfully grafted onto the AMN coated surfaces by hydrogen bonding interactions.

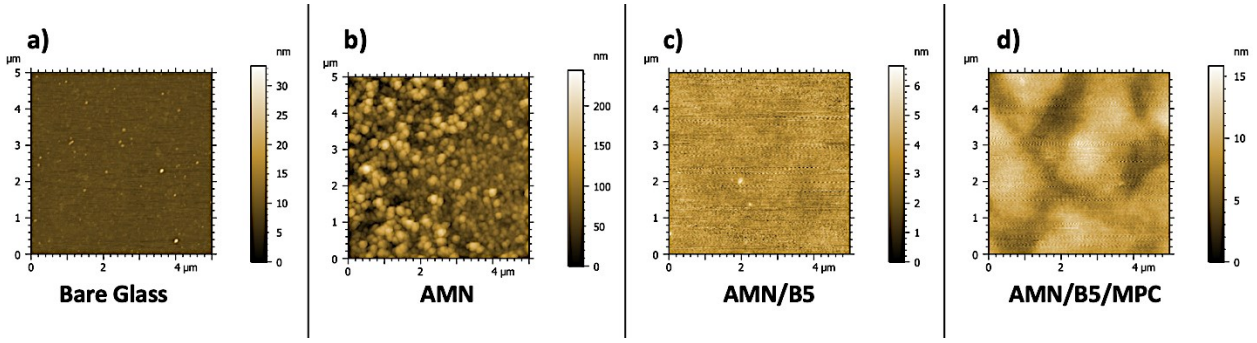

Figure 4.2 AFM images of surface morphology of a) Bare glass, b) AMN, c) AMN/B5 and d) AMN/B5/MPC with surface roughness scale bar.

The elemental compositions of AMN and composite AMN/B5 and AMN/B5/MPC coatings were determined by XPS, with representative spectra presented in Figure 4.3. High resolution spectra of C 1s and N 1s were evaluated qualitatively to confirm the successful grafting of both polymers on the AMN coated glass surface.

Successful AMN coating to the glass surface was indicated by the existence of a strong signal of N 1s peak at 399.2 eV which corresponds to the nitrile and secondary amine groups present in AMN. Whereas in control bare glass no such strong peak was observed. After introducing the zwitterionic copolymer poly (MPC-*st*-B5AMA) another strong signal of N 1s at 402.4 eV has appeared. This characteristic peak was attributed to $N^{+}(CH_3)_3$ of MPC[44] from the polymer brushes of poly(MPC-*st*-B5AMA) which concludes that the zwitterionic copolymer has been successfully grafted to the AMN coated glass surface. In addition, it displayed a broad signal centered at 399.7

– 399.2 eV BE, assigned to the expected amide (-HN-(C=O)-) peak from B5AMA chemical structure and nitrile peak from primary AMN coating. For the AMN/B5 surface this peak was narrowed down a little and mostly appeared at 399.8 eV attributing to the amide peak from B5AMA. Nitrile peak for AMN/B5 surface was not very strong, which confirms a good coverage of AMN surface with poly(B5AMA). As grafting of synthesized polymers on the AMN coated surface was mostly by forming hydrogen bond between B5AMA and AMN, the presence of less amount of B5AMA content in poly (MPC-*st*-B5AMA) led to less coverage on AMN surface. Moreover, by analyzing the high-resolution spectra of C 1s, successful attachment of both poly (MPC-*st*-B5AMA) and poly(B5AMA) polymers on the AMN coated surface was confirmed by the appearance of a characteristic peak of C 1s at 289.1 eV (ester groups) and a strong increase in the peak at 286.4 eV (attributed to C–O and C-N). Appearance of amide peak at 287.8 eV in C 1s also confirms the presence of B5AMA content in the polymer. As previously reported[37], only AMN coating is supposed to be highly nitrogenous. We also found the similar result for AMN coating with higher N/C atomic ratio compared to other two polymer samples (Table 4.2). Moreover, N/C and O/C ratio obtained by XPS for AMN coating was found consistent with the proposed chemical structure of AMN[38]. After anchoring the synthesized polymers this N/C ratio decreased with an increase of oxygen content. The N/C ratio for AMN coating was 0.595 which decreased to 0.285 for AMN/B5 and to 0.323 for AMN/B5/MPC surface. Additionally compared to control, AMN coating and AMN/B5 surfaces P/C ratio of AMN/B5/MPC surface increased from 0 to 0.023 which reflects the native structure of the MPC on the AMN coated surface.

Table 4.2. Surface compositions determined by XPS. Concentrations are expressed as atomic ratios X/C, i.e., atomic concentration of element X relative to that of C.

Surfaces	Composition (X/C)					
	C	Si	P	N	N^+	O
Bare Glass	1.000	0.181	_	0.008	_	0.459
AMN	1.000	0.032	_	0.595	_	0.229
AMN/B5	1.000	0.024	_	0.285	0.006	0.299
AMN/B5/MPC	1.000	0.043	0.023	0.323	0.038	0.379

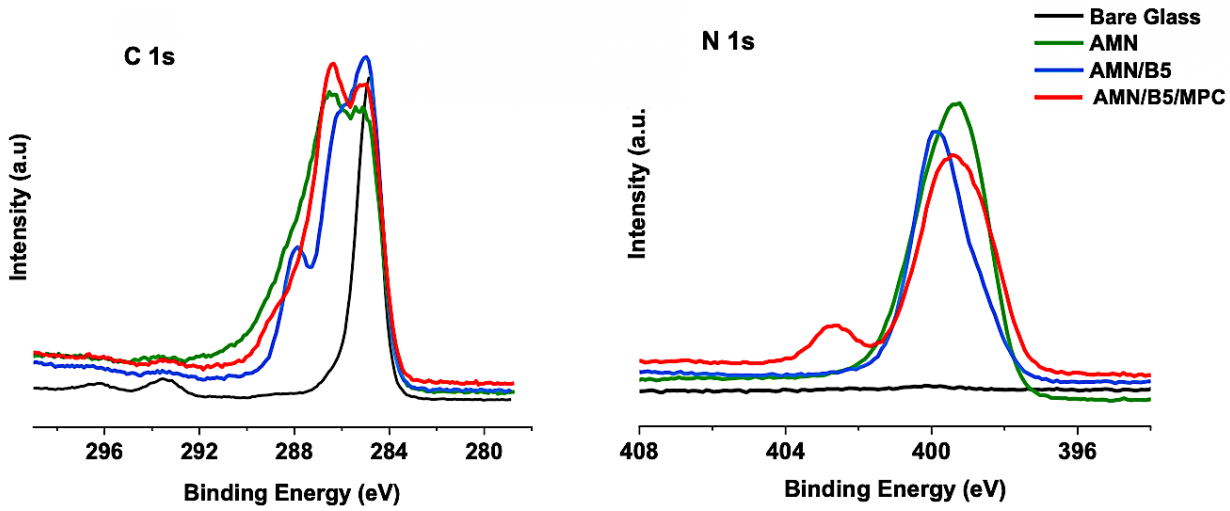

Figure 4.3. XPS high-resolution C 1s, and N 1s narrow-scan spectra of the modified glass substrates

The wetting behavior of AMN and AMN-polymer modified glass surfaces was studied in air with a 4 μL water droplet onto the surface at room temperature. As shown in Figure 4.4, the water contact angle (WCA) of the pristine glass substrate was 47.3±2.0°. It was observed that after introducing AMN coating on the glass substrate the WCA increased to 55.6±1.1° which is consistent with our previous study[45] and can be explained by the higher surface roughness observed by AFM. Both of the polymer grafted on AMN modified glass substrates showed WCA <15° and improved hydrophilicity than pristine glass and AMN coating possibly due to the strong interactions between water molecules and hydrophilic polymer chains of B5AMA and zwitterionic MPC. Among them, the AMN/B5 modified glass substrate showed the lowest WCA, 11.5±1.1°, indicating the presence of a stronger surface hydration. The presence of multiple polar groups (hydroxyl and amide groups) into the B5AMA structure enables the stronger interaction with water and to develop a super hydrophilic surface layer.

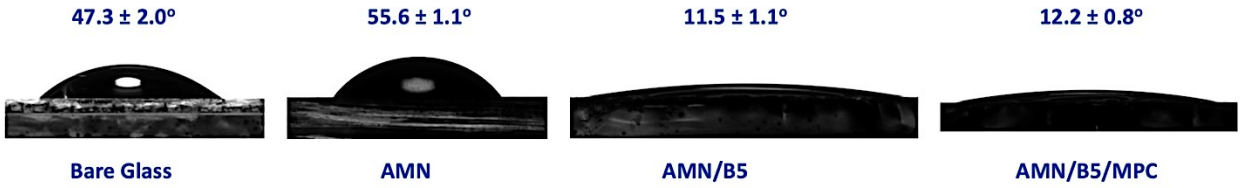

Figure 4.4. Water contact angle of bare glass, AMN, AMN/B5 and AMN/B5/MPC modified glass substrates

4.3.2 Antibacterial adhesion and antifouling property of the coating

We evaluated the antibacterial adhesion characteristics of the coatings using Gram-positive *Staphylococcus aureus* (*S. aureus)* and Gram-negative *Escherichia coli* (*E. coli)* bacteria. The initial attachment of bacterial cells to a surface is considered as the key preliminary step in the biofilm formation processes [46] and plays a vital role for evaluating the antifouling properties of the

surface. In this study, to evaluate antibacterial adhesion properties of the modified substrates quantitatively, all the coated samples were incubated with bacteria solution containing 8×10^9 cells/mL for 24 hrs. After 24 hrs of incubation, all the sample surfaces were rinsed with PBS to remove loosely bound bacteria and stained using LIVE/DEAD stain for microscopic examination under fluorescence microscopy. As shown in Figure 4.5 (a) and Figure S 4-4 (a), many green spots (live bacteria) with only a few red spots (dead bacteria) were observed for AMN coated glass substrate for both *E. coli* and *S. aureus* adhesion, indicating the insignificant anti-adhesion efficiency of the AMN coated glass surface due to the higher surface roughness of AMN surface. After introducing poly(MPC-*st*-B5AMA) and poly(B5AMA) polymers on the surface the amount of bacteria adhesion was significantly reduced for AMN/B5 and AMN/B5/MPC coating, indicating high antiadhesion efficiency. The enhancement of this antiadhesion or antifouling property is due the presence of a strong hydration layer which might be induced by the hygroscopic nature of poly(B5AMA) and zwitterionic poly (MPC-*st*-B5AMA) polymers. Compared to *S. aureus* adhesion, *E. coli* showed higher adhesion on AMN, AMN/B5 and AMN/B5/MPC surfaces (Figure 4.6). Because of the presence of many functional amine groups on the AMN modified surfaces, more negatively charged *E. coli* might be adhered in greater numbers on the surfaces. But no antibacterial activity or no dead cells was found in case of both AMN/B5 and AMN/B5/MPC coating.

a)

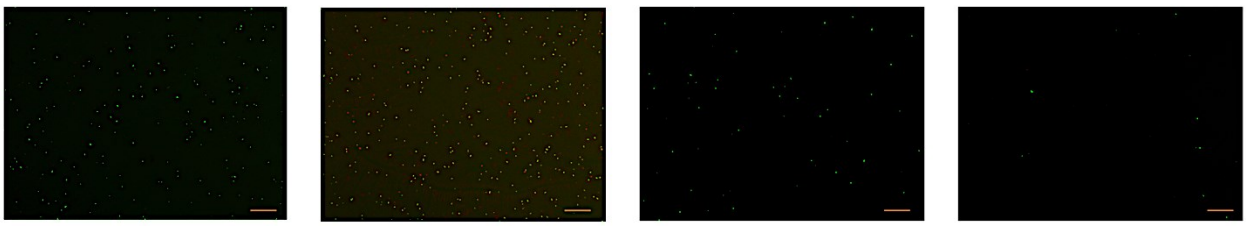

b)

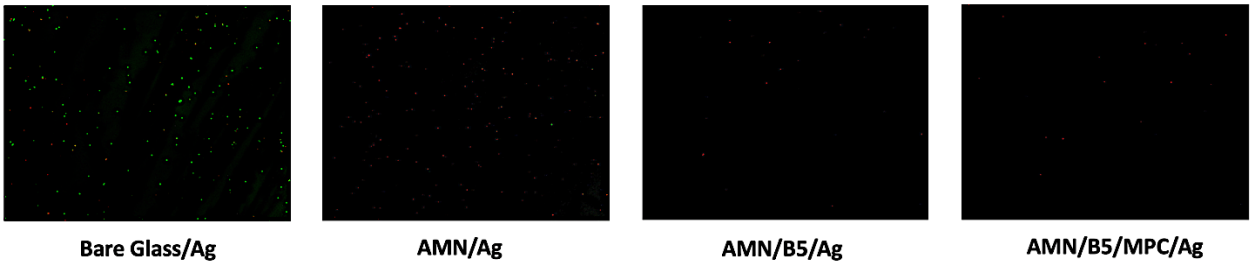

Figure 4.5. Fluorescence images of *S. aureus* adhesion on a) modified surfaces (Bare Glass, AMN, AMN/B5, and AMN/B5/MPC). And b) AgNPs deposited modified surfaces (Bare Glass/Ag, AMN/Ag, AMN/B5/Ag, and AMN/B5/MPC/Ag). Scale bar 20μm.

As surfaces decorated with solely antifouling property cannot achieve long term effectiveness against biofilm formation[40], we incorporated silver nanoparticles (AgNPs) into the coating to impart antibacterial property by simply immersing the modified surfaces into the $AgNO_3$ solution. As AMN has several electron donors such as amines and nitriles for metal coordination[42], it can help to reduce metallic silver and deposit on the surface. After introducing AgNPs into the coating more than 90% bacteria killing efficiency was obtained for both *E. coli* and *S. aureus* due to the release of the Ag^+ bactericide agent. The most evident killing mechanism of Ag^+ bactericide agent is the cell membrane perforation and consequent microbial killing, after its accumulation on negatively charged parts of the cellular membrane. From the fluorescence images (Figure 4.5(b) and S 4-4 (b)) evidently most of the attached bacteria was found dead for all the modified surfaces except bare glass with AgNPs. For bare glass with AgNPs only 9.625% and 13.65% fraction of dead cells for *E. coli* and *S. aureus* respectively was found (Figure 4.6). Compared to other AgNPs

loaded surfaces AMN/B5/MPC surface showed relatively low killing efficiency (85.3%) towards *E. coli* bacteria. Due to the presence of the outer membrane barrier of gram-negative *E. coli,* it tends to be more resistant[47] to the killing agent and the low concentration of killing agent such as AgNPs [48] can also attribute to its lower fraction of dead cells compared to gram-positive *S. aureus* bacteria.

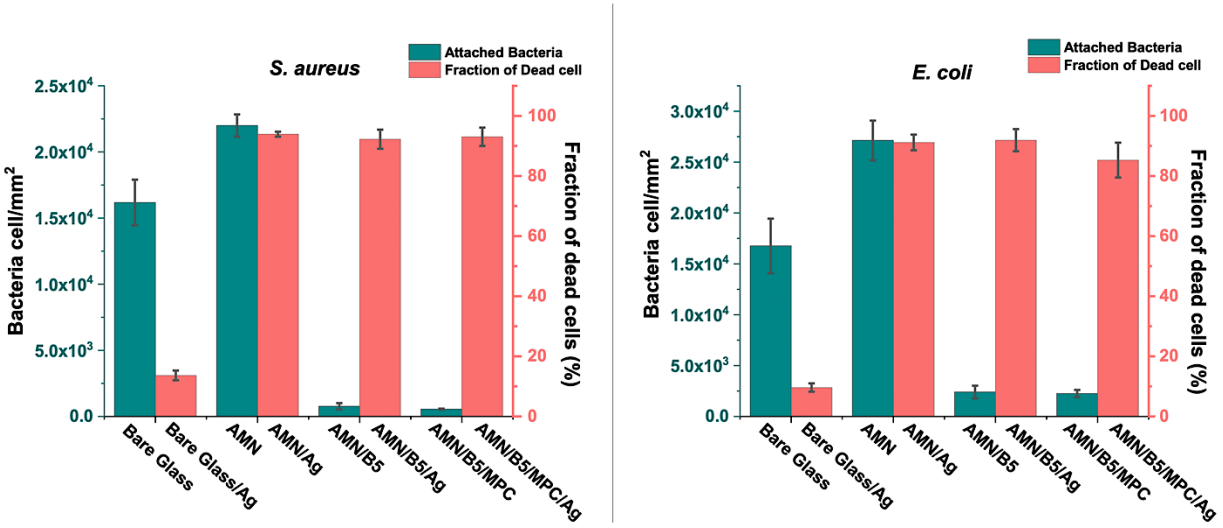

Figure 4.6. Attached number of *S. aureus* (Left) and *E. coli* (right) bacterial on the bare glass and modified surfaces (AMN, AMN/B5, and AMN/B5/MPC); Fraction of dead bacteria cell for AgNPs deposited surfaces (Bare Glass/Ag, AMN/Ag, AMN/B5/Ag, and AMN/B5/MPC/Ag).

To confirm the AgNPs deposition and distribution on the modified surfaces, SEM analysis was conducted (Figure 4.7). From Figure 4.7, it was observed that AMN/Ag surfaces showed clusters of AgNPs aggregates (white phase) onto the surface with very rough surface morphology which supports the high roughness of AMN coating as well. On the other hand, onto the AMN/B5 surface

AgNPs was very homogeneously distributed. Possibly the hydroxyl group of B5AMA can take part into *in situ* deposition of AgNPs along with the functional reducing group of AMN. But compared to AMN/B5 surface AMN/B5/MPC surface showed less amount of AgNPs onto the surface with some aggregates which could explain the low killing efficiency towards the *E. coli* bacteria.

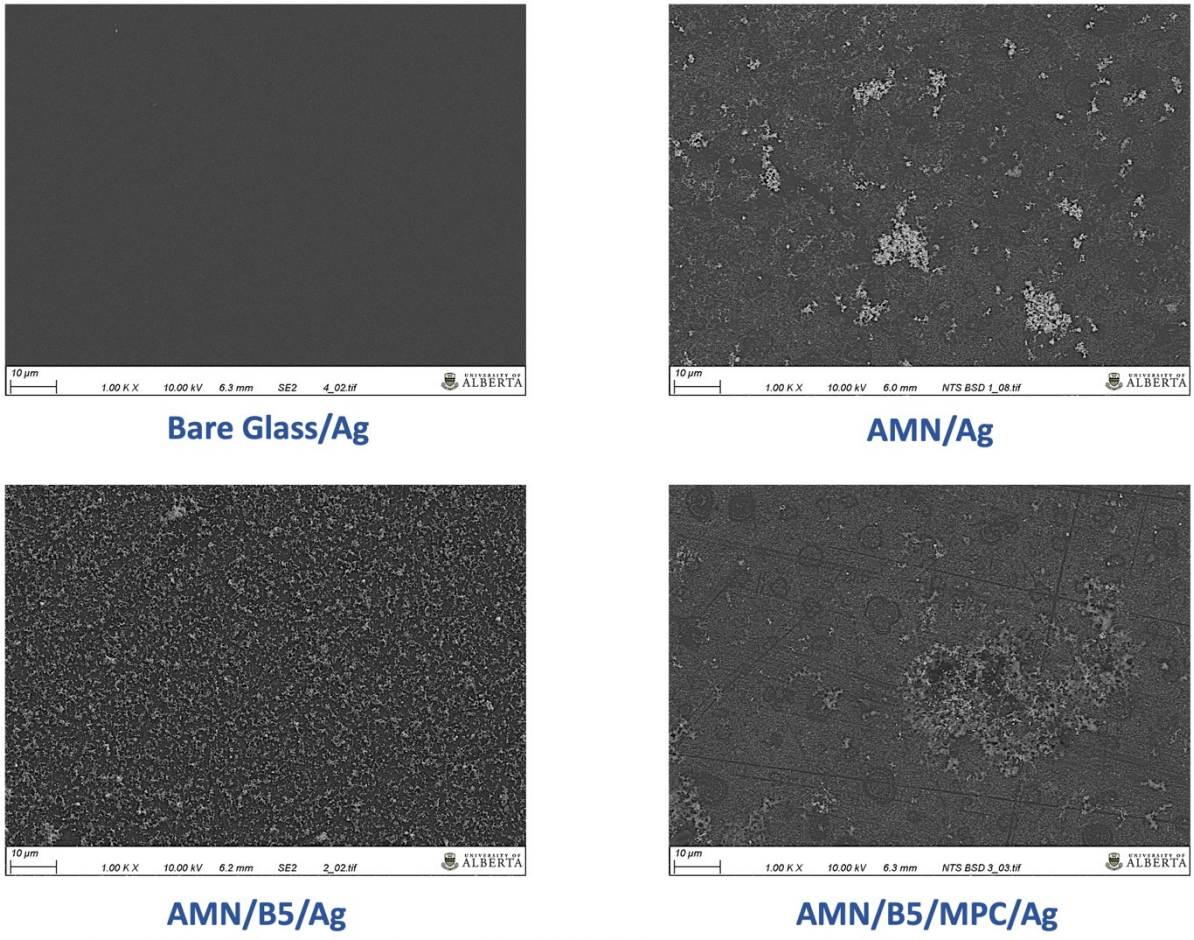

Figure 4.7. SEM images and surface morphology of AgNPs deposited surfaces - Bare Glass/Ag, AMN/Ag, AMN/B5/Ag, and AMN/B5/MPC/Ag. Scale bar 10µm.

To understand more about the antifouling property of the coating, every coated surface was challenged against 2 mg/mL bovine serum albumin (BSA) as a model protein solution. After 3 h incubation of the samples with BSA solution at 37 ^{o}C, the amount of BSA absorbed on the surface was examined using BCA assay kit. As shown in Figure 4.8, compared to bare glass, AMN coating showed higher BSA adsorption. High surface roughness and cationic nature of AMN surface can be attributed to this greater adsorption which also aligns with our previous study[45]. After introducing poly (MPC-*st*-B5AMA) and poly(B5AMA) polymers on the AMN surface, protein adsorption decreased significantly suggesting that both B5AMA and MPC moiety into the polymer contributed almost equally to resist protein adsorption on the surface by maintain a strong hydration layer.

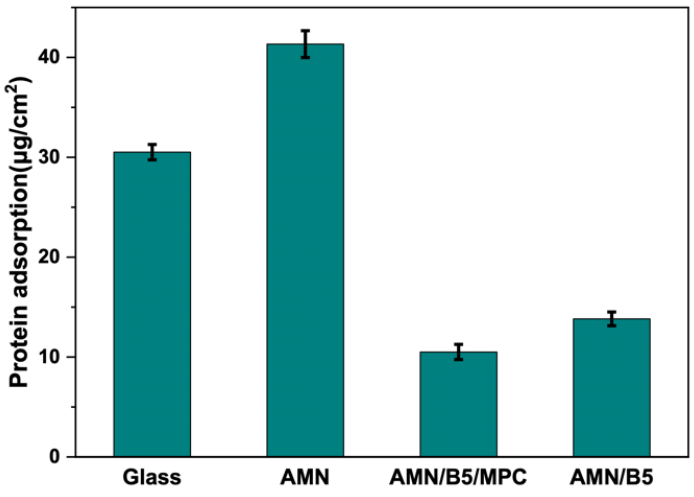

Figure 4.8. BSA protein adsorption on Glass, AMN, AMN/B5, and AMN/B5/MPC surfaces using BCA protein assay.

4.3.3 Self-healing property of the coating:

For long-term practical biomedical application of the surface coating, damage healing property combining with antifouling and antibacterial is highly desirable. In practice, anti-bacterial coatings usually failed as they experienced inevitable damage or scratches leading to the rapid loss or burst release of loaded functional biocides[49]. In our developed coating, it is anticipated that B5AMA mostly takes part in self-healing property by forming amide-amide and amide-hydroxyl multiple hydrogen bonds as demonstrated in Figure 4.1. To characterize the self-healing property of the coating, at constant 5N load, a scratch with a sphero-conical indenter was performed on each sample and the penetration of depth was measured using the Micro Combi Tester (MCT^3). Both penetration depth of as scratched and after healing/elastic recovery of every sample was recorded. It is basically a comparative test where the percentage of recovery of the coating has been determined by comparing the penetration depth of the scratched surface to the healed surface. As shown in Figure 4.9 (b), Bare glass and AMN coating showed negligible percentage of recovery whereas AMN/B5 surface showed more than 90% recovery which proves its outstanding self-healing property. On the other hand, compared to AMN/B5 surface AMN/B5/MPC showed less percentage of self-healing property which can be due to the lower concentration of hydrogen bonding sites. As B5AMA mostly provided active sites for hydrogen bond formation for self-healing, higher concentration of hydrogen bonding sites on AMN/B5 surface might lead to higher possibility of reformation of hydrogen bonds during self-healing[50]. For rapid recovery, 5µl of water droplet was added onto the macro scratch (with a sharp knife random scratch was done on the surface) of the coating which induces the mobility of the polymer chains and resulted in the reconstruction of the damaged coating within a minute. To detect the coating damage and healing, the most reliable microscopic observation was performed. As shown in the Figure 4.9 (c), and 4.9

(d) for AMN/B5 surface, a complete heal of both nano scratch (done by MCT^3) and macro scratch was observed which also aligns with the surface profile of nano scratch test (Figure 4.9(a)).

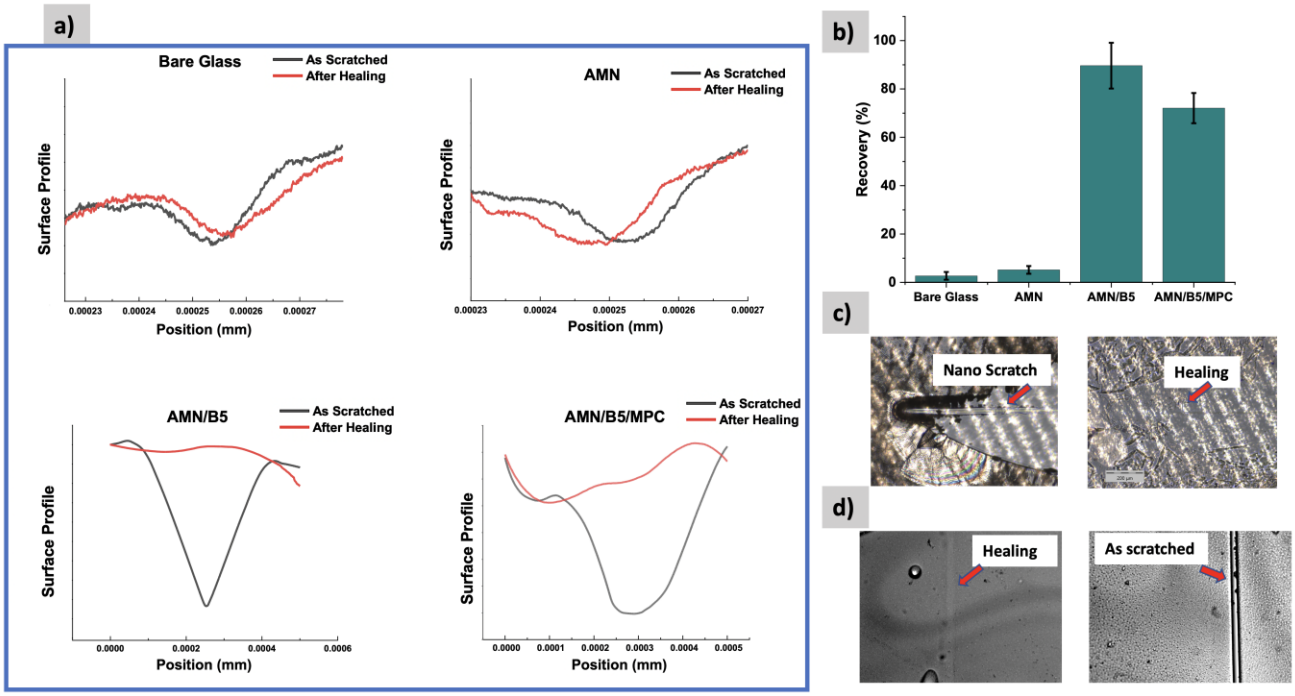

Figure 4.9. a) Penetration depth of the scratch track as scratched and after healing in function of the position of Glass, AMN, AMN/B5, and AMN/B5/MPC surfaces. b) Percentage of recovery of the coating of every surface. c) Optical microscopic images of AMN/B5 surface after nano scratch with Micro Combi Tester and after healing d) Optical microscopic image of macro scratch on AMN/B5 surface with a sharp knife and healing within a minute after adding 5µl water.

4.3.4 Biocompatibility:

As an *in vitro* biocompatibility test, MTT assay was performed on the human fibroblast MRC-5 cells for 48 h to reveal the biocompatibility of the developed surface coatings. As shown in Figure 4.10, all the developed surfaces showed excellent cell viability against normal fibroblast MRC-5

cells. All the AMN coated surfaces showed more than 100% cell viability. It might be explained by the cell proliferating nature of AMN coating[42] which resulted in higher percentage of cell viability. Though we hypothesised that incorporation of MPC residues into the coating might enhance the biocompatibility, from the MTT analysis no such significant change has been found for MPC moiety incorporation. Homopolymer poly (B5AMA) grafted surface - AMN/B5 showed excellent biocompatibility similar to poly (MPC-*st*-B5AMA) grafted AMN/B5/MPC surface. Thus, MTT analysis clearly demonstrated the non-toxic effect and cell adhesive nature of the coating on the human fibroblast cells, qualifying the developed coating for a broad range of biomedical applications.

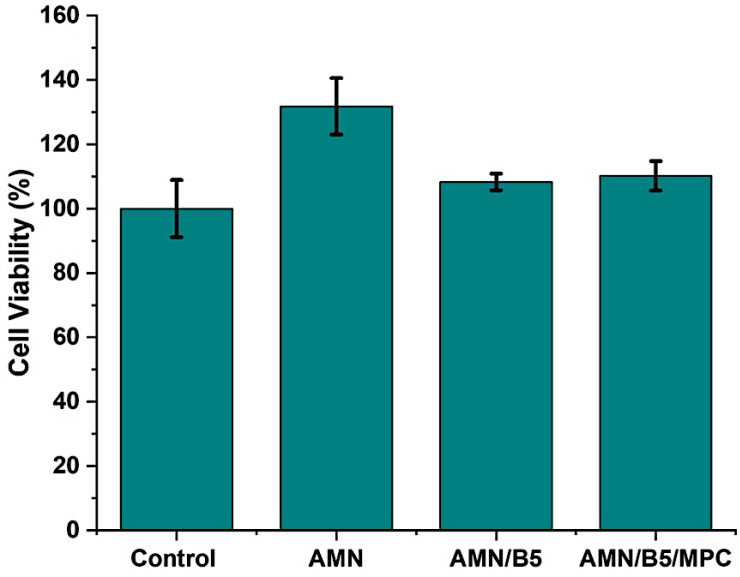

Figure 4.10. Cytotoxicity of coated surfaces after 48hrs incubation with MRC-5 cells

4.4 Conclusion:

In summary, utilizing the multiple hydrogen bond, we have reported a new class of self-healing coating with antifouling and antibacterial properties. In this multifunctional coating, the primary AMN coating layer inspired by prebiotic chemistry not only offered the coating to be universal for a wide range of substrates to strongly graft another functional polymer layer onto the surface but also showed excellent biocompatibility with cell adhesive properties. As the biocompatibility of B5AMA based coating has not been reported before, to understand and to improve the biocompatibility of the coating, we have combined the B5AMA with zwitterionic MPC moiety. But compared to AMN/B5 surface, AMN/B5/MPC surface did not show any significant enhanced biocompatibility. The presence of zwitterionic moiety did not serve any additional advantage. Moreover, AMN/B5 surface showed almost similar outstanding antifouling property as AMN/B5/MPC. So, we can conclude that, only poly (B5AMA) coated surface, being hygroscopic in nature, can act as the best antifouling surface with excellent biocompatibility similar to zwitterionic polymer coated surface. In addition to that, because of the presence of multiple polar functional groups into B5AMA monomer structure, it serves as a promising self-healing material for biomedical application. In our study, we showed the first report of this extraordinary self-healing behaviour of poly (B5AMA) grafted coating. Incorporation of this intrinsic healing material into the antibacterial coating, makes this coating system robust for long operation lifespan of a wide range of biomedical applications such as wound dressing, biomedical implants and optical lenses etc.

4.5 Supporting Information:

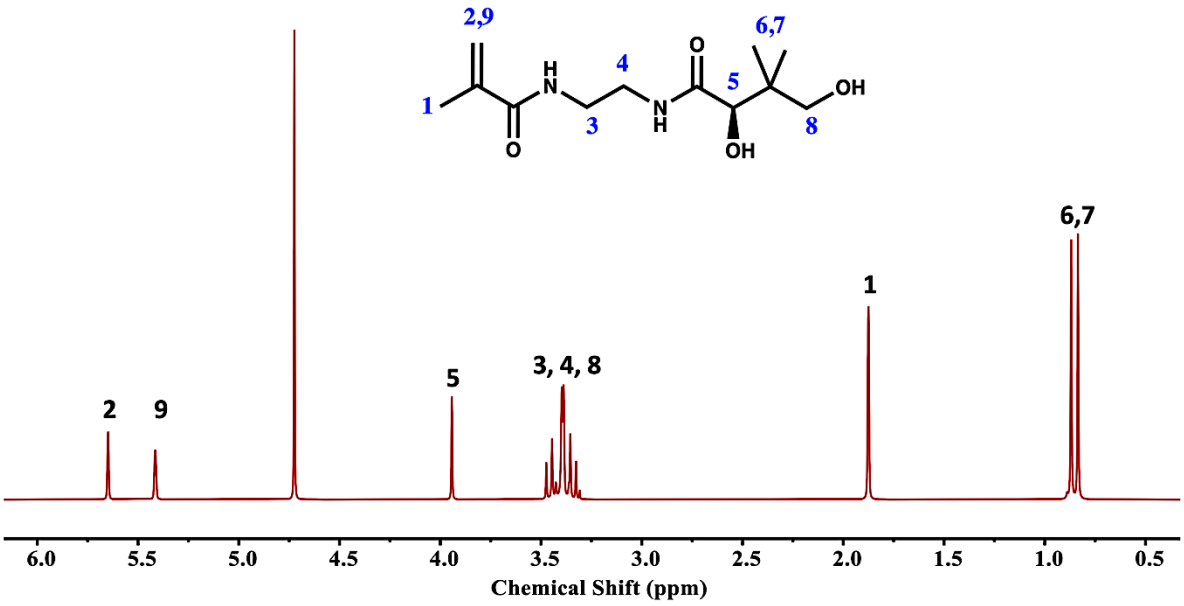

Figure S 4-1. ^{1}H NMR spectrum of the B5AMA monomer

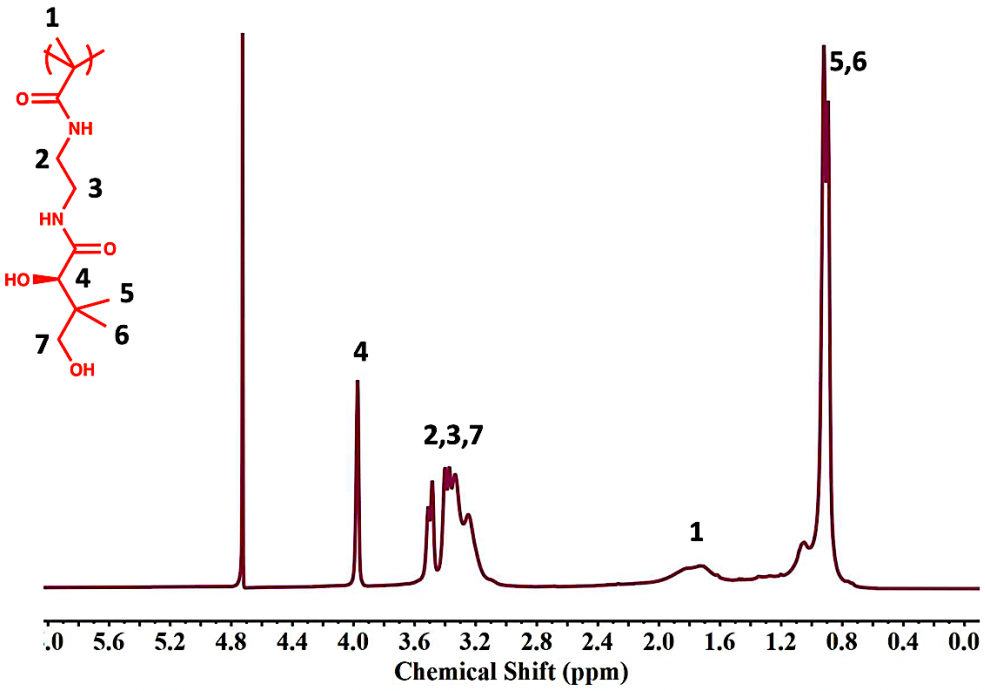

Figure S 4-2 ^{1}H NMR spectrum of the poly (B5AMA) polymer

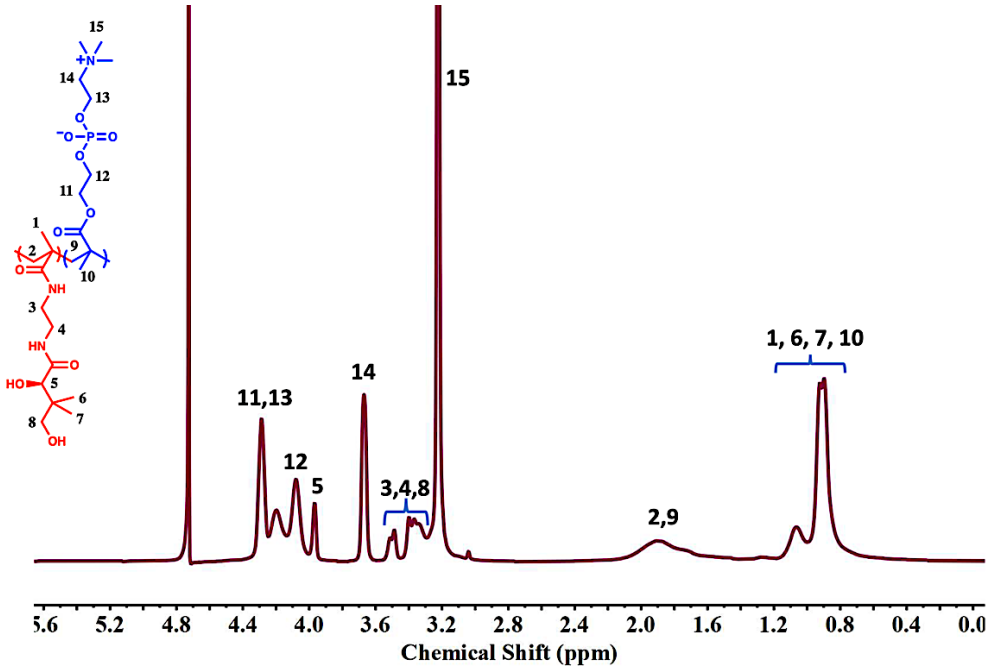

Figure S 4-3. ^{1}H NMR spectrum of the zwitterionic poly (MPC-*st*-B5AMA) polymer

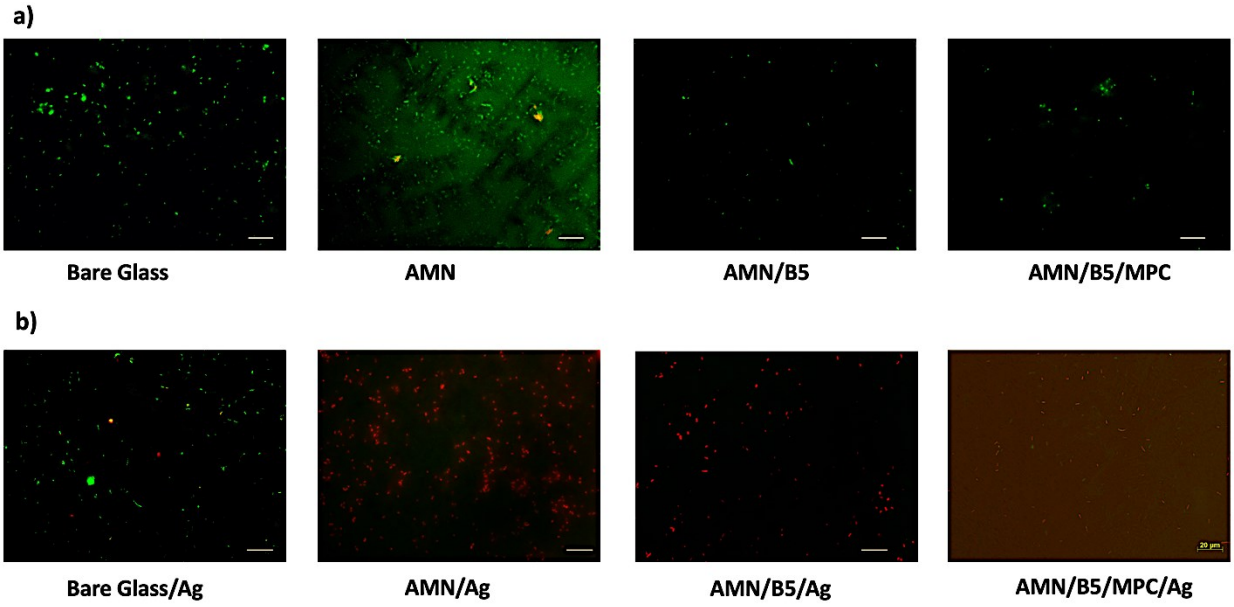

Figure S 4-4. Fluorescence images of *E. coli* adhesion on a) modified surfaces (Bare Glass, AMN, AMN/B5, and AMN/B5/MPC). And b) AgNPs deposited modified surfaces (Bare Glass/Ag, AMN/Ag, AMN/B5/Ag, and AMN/B5/MPC/Ag). Scale bar 20μm.

4.6 Reference:

(1) Elder, M. J.; Stapleton, F.; Evans, E.; Dart, J. K. G. Biofilm-Related Infections in Ophthalmology. *Eye (Basingstoke)* **1995**, *9* (1), 102–109.

(2) Donelli, G. Biofilm-Based Healthcare-Associated Infections: Volume II. *Advances in Experimental Medicine and Biology* **2015**, *831*, 137–146.

(3) Dai, G.; Ai, X.; Mei, L.; Ma, C.; Zhang, G. Kill-Resist-Renew Trinity: Hyperbranched Polymer with Self-Regenerating Attack and Defense for Antifouling Coatings. *ACS Applied Materials and Interfaces* **2021**, *13* (11), 13735–13743.

(4) Voo, Z. X.; Khan, M.; Xu, Q.; Narayanan, K.; Ng, B. W. J.; Bte Ahmad, R.; Hedrick, J. L.; Yang, Y. Y. Antimicrobial Coatings against Biofilm Formation: The Unexpected Balance between Antifouling and Bactericidal Behavior. *Polymer Chemistry* **2016**, *7* (3), 656–668.

(5) Ding, X.; Yang, C.; Lim, T. P.; Hsu, L. Y.; Engler, A. C.; Hedrick, J. L.; Yang, Y. Y. Antibacterial and Antifouling Catheter Coatings Using Surface Grafted PEG-b-Cationic Polycarbonate Diblock Copolymers. *Biomaterials* **2012**, *33* (28), 6593–6603.

(6) Vaishampayan, A.; de Jong, A.; Wight, D. J.; Kok, J.; Grohmann, E. A Novel Antimicrobial Coating Represses Biofilm and Virulence-Related Genes in Methicillin-Resistant Staphylococcus Aureus. *Frontiers in Microbiology* **2018**, *9* (FEB), 1–14.

(7) Jiao, Y.; Tay, F. R.; Niu, L. na; Chen, J. hua. Advancing Antimicrobial Strategies for Managing Oral Biofilm Infections. *International Journal of Oral Science* **2019**, *11* (3), 1–11.

(8) Francolini, I.; Vuotto, C.; Piozzi, A.; Donelli, G. Antifouling and Antimicrobial Biomaterials: An Overview. *Apmis* **2017**, *125* (4), 392–417.

(9) Chen, S.; Li, L.; Zhao, C.; Zheng, J. Surface Hydration: Principles and Applications toward Low-Fouling/Nonfouling Biomaterials. *Polymer*. 2010, pp 5283–5293.

(10) Maan, A. M. C.; Hofman, A. H.; de Vos, W. M.; Kamperman, M. Recent Developments and Practical Feasibility of Polymer-Based Antifouling Coatings. *Advanced Functional Materials* **2020**, *30* (32).

(11) Zhi, Z.; Su, Y.; Xi, Y.; Tian, L.; Xu, M.; Wang, Q.; Padidan, S.; Li, P.; Huang, W. Dual-Functional Polyethylene Glycol-b-Polyhexanide Surface Coating with in Vitro and in Vivo Antimicrobial and Antifouling Activities. *ACS Applied Materials and Interfaces* **2017**, *9* (12), 10383–10397.

(12) Asha, A. B.; Chen, Y.; Zhang, H.; Ghaemi, S.; Ishihara, K.; Liu, Y.; Narain, R. Rapid Mussel-Inspired Surface Zwitteration for Enhanced Antifouling and Antibacterial Properties. *Langmuir* **2019**, *35* (5), 1621–1630.

(13) Gu, J. S.; Yu, H. Y.; Huang, L.; Tang, Z. Q.; Li, W.; Zhou, J.; Yan, M. G.; Wei, X. W. Chain-Length Dependence of the Antifouling Characteristics of the Glycopolymer-Modified Polypropylene Membrane in an SMBR. *Journal of Membrane Science* **2009**, *326* (1), 145–152.

(14) Liang, J.; She, J.; He, H.; Fan, Z.; Chen, S.; Li, J.; Liu, B. A New Approach to Fabricate Polyimidazolium Salt (PIMS) Coatings with Efficient Antifouling and Antibacterial Properties. *Applied Surface Science* **2019**, *478* (September 2018), 770–778.

(15) Xu, G.; Liu, P.; Pranantyo, D.; Xu, L.; Neoh, K. G.; Kang, E. T. Antifouling and Antimicrobial Coatings from Zwitterionic and Cationic Binary Polymer Brushes Assembled via “Click” Reactions. *Industrial and Engineering Chemistry Research* **2017**, *56* (49), 14479–14488.

(16) Cheng, G.; Xue, H.; Zhang, Z.; Chen, S.; Jiang, S. A Switchable Biocompatible Polymer Surface with Self-Sterilizing and Nonfouling Capabilities. *Angewandte Chemie - International Edition* **2008**, *47* (46), 8831–8834.

(17) Wei, T.; Zhan, W.; Yu, Q.; Chen, H. Smart Biointerface with Photoswitched Functions between Bactericidal Activity and Bacteria-Releasing Ability. *ACS Applied Materials and Interfaces* **2017**, *9* (31), 25767–25774.

(18) Mi, L.; Jiang, S. Integrated Antimicrobial and Nonfouling Zwitterionic Polymers. *Angewandte Chemie - International Edition*. 2014, pp 1746–1754.

(19) Tankhiwale, R.; Bajpai, S. K. Preparation, Characterization and Antibacterial Applications of ZnO-Nanoparticles Coated Polyethylene Films for Food Packaging. *Colloids and Surfaces B: Biointerfaces* **2012**, *90* (1), 16–20.

(20) Aumsuwan, N.; McConnell, M. S.; Urban, M. W. Tunable Antimicrobial Polypropylene Surfaces: Simultaneous Attachment of Penicillin (Gram +) and Gentamicin (Gram -). *Biomacromolecules* **2009**, *10* (3), 623–629.

(21) Caro, A.; Humblot, V.; Méthivier, C.; Minier, M.; Salmain, M.; Pradier, C. M. Grafting of Lysozyme and/or Poly(Ethylene Glycol) to Prevent Biofilm Growth on Stainless Steel Surfaces. *Journal of Physical Chemistry B* **2009**, *113* (7), 2101–2109.

(22) Schaer, T. P.; Stewart, S.; Hsu, B. B.; Klibanov, A. M. Hydrophobic Polycationic Coatings That Inhibit Biofilms and Support Bone Healing during Infection. *Biomaterials* **2012**, *33* (5), 1245–1254.

(23) Cado, G.; Aslam, R.; Séon, L.; Garnier, T.; Fabre, R.; Parat, A.; Chassepot, A.; Voegel, J. C.; Senger, B.; Schneider, F.; Frère, Y.; Jierry, L.; Schaaf, P.; Kerdjoudj, H.; Metz-Boutigue, M. H.; Boulmedais, F. Self-Defensive Biomaterial Coating against Bacteria and Yeasts: Polysaccharide Multilayer Film with Embedded Antimicrobial Peptide. *Advanced Functional Materials* **2013**, *23* (38), 4801–4809.

(24) Chen, D.; Wu, M.; Li, B.; Ren, K.; Cheng, Z.; Ji, J.; Li, Y.; Sun, J. Layer-by-Layer-Assembled Healable Antifouling Films. *Advanced Materials* **2015**, *27* (39), 5882–5888.

(25) Wang, Z.; Fei, G.; Xia, H.; Zuilhof, H. Dual Water-Healable Zwitterionic Polymer Coatings for Anti-Biofouling Surfaces. *Journal of Materials Chemistry B* **2018**, *6* (43), 6930–6935.

(26) Li, L.; Yan, B.; Yang, J.; Chen, L.; Zeng, H. Novel Mussel-Inspired Injectable Self-Healing Hydrogel with Anti-Biofouling Property. *Advanced Materials* **2015**, *27* (7), 1294–1299.

(27) Wang, Z.; Yi, B.; Wu, M.; Lv, D.; He, M. L.; Liu, M.; Yao, X. Bioinspired Supramolecular Slippery Organogels for Controlling Pathogen Spread by Respiratory Droplets. *Advanced Functional Materials* **2021**, *31* (34), 1–10.

(28) Sun, D.; Chong, Y. B.; Chen, K.; Yang, J. Chemically and Thermally Stable Isocyanate Microcapsules Having Good Self-Healing and Self-Lubricating Performances. *Chemical Engineering Journal* **2018**, *346* (April), 289–297.

(29) Wu, G.; An, J.; Tang, X. Z.; Xiang, Y.; Yang, J. A Versatile Approach towards Multifunctional Robust Microcapsules with Tunable, Restorable, and Solvent-Proof Superhydrophobicity for Self-Healing and Self-Cleaning Coatings. *Advanced Functional Materials* **2014**, *24* (43), 6751–6761.

(30) Idumah, C. I.; Obele, C. M.; Emmanuel, E. O.; Hassan, A. Recently Emerging Nanotechnological Advancements in Polymer Nanocomposite Coatings for Anti-Corrosion, Anti-Fouling and Self-Healing. *Surfaces and Interfaces* **2020**, *21* (May), 100734.

(31) Yanagisawa, Y.; Nan, Y.; Okuro, K.; Aida, T. Mechanically Robust, Readily Repairable Polymers via Tailored Noncovalent Cross-Linking. *Science* **2018**, *359* (6371), 72–76.

(32) Perera, M. M.; Ayres, N. Dynamic Covalent Bonds in Self-Healing, Shape Memory, and Controllable Stiffness Hydrogels. *Polymer Chemistry* **2020**, *11* (8), 1410–1423.

(33) M. Kushner, A.; D. Vossler, J.; A. Williams, G.; Guan, Z. A Biomimetic Modular Polymer with Tough and Adaptive Properties. *Journal of the American Chemical Society* **2009**, *131* (25), 8766–8768.

(34) Sun, J. Y.; Zhao, X.; Illeperuma, W. R. K.; Chaudhuri, O.; Oh, K. H.; Mooney, D. J.; Vlassak, J. J.; Suo, Z. Highly Stretchable and Tough Hydrogels. *Nature 2012 489:7414* **2012**, *489* (7414), 133–136.

(35) Qiu, W. Z.; Yang, H. C.; Xu, Z. K. Dopamine-Assisted Co-Deposition: An Emerging and Promising Strategy for Surface Modification. *Advances in Colloid and Interface Science*. 2018, pp 111–125.

(36) Asha, A. B.; Chen, Y.; Narain, R. Bioinspired Dopamine and Zwitterionic Polymers for Non-Fouling Surface Engineering. *Chemical Society Reviews* **2021**, *50* (20), 11668–11683.

(37) Menzies, D. J.; Ang, A.; Thissen, H.; Evans, R. A. Adhesive Prebiotic Chemistry Inspired Coatings for Bone Contacting Applications. *ACS Biomaterials Science and Engineering* **2017**, *3* (5), 793–806.

(38) Toh, R. J.; Evans, R.; Thissen, H.; Voelcker, N. H.; D'ischia, M.; Ball, V. Deposition of Aminomalononitrile-Based Films: Kinetics, Chemistry, and Morphology. *Langmuir* **2019**, *35* (30), 9896–9903.

(39) Chen, W. H.; Liao, T. Y.; Thissen, H.; Tsai, W. B. One-Step Aminomalononitrile-Based Coatings Containing Zwitterionic Copolymers for the Reduction of Biofouling and the Foreign Body Response. *ACS Biomaterials Science and Engineering* **2019**, *5* (12), 6454–6462.

(40) Liao, T. Y.; Easton, C. D.; Thissen, H.; Tsai, W. B. Aminomalononitrile-Assisted Multifunctional Antibacterial Coatings. *ACS Biomaterials Science and Engineering* **2020**, *6* (6), 3349–3360.

(41) Kabir, A.; Dunlop, M. J.; Acharya, B.; Bissessur, R.; Ahmed, M. Water Recycling Efficacies of Extremely Hygroscopic, Antifouling Hydrogels. *RSC Advances* **2018**, *8* (66), 38100–38107.

(42) Thissen, H.; Koegler, A.; Salwiczek, M.; Easton, C. D.; Qu, Y.; Lithgow, T.; Evans, R. A. Prebiotic-Chemistry Inspired Polymer Coatings for Biomedical and Material Science Applications. *NPG Asia Materials* **2015**, *7* (11), 1–9.

(43) Deng, Z.; Bouchékif, H.; Babooram, K.; Housni, A.; Choytun, N.; Narain, R. Facile Synthesis of Controlled-Structure Primary Amine-Based Methacrylamide Polymers via the Reversible Addition-Fragmentation Chain Transfer Process. *Journal of Polymer Science Part A: Polymer Chemistry* **2008**, *46* (15), 4984–4996.

(44) Ma, W.; Yang, P.; Li, J.; Li, S.; Li, P.; Zhao, Y.; Huang, N. Immobilization of Poly(MPC) Brushes onto Titanium Surface by Combining Dopamine Self-Polymerization and ATRP:

Preparation, Characterization and Evaluation of Hemocompatibility in Vitro. *Applied Surface Science* **2015**, *349*, 445–451.

(45) Cheng, Q.; Asha, A. B.; Liu, Y.; Peng, Y. Y.; Diaz-Dussan, D.; Shi, Z.; Cui, Z.; Narain, R. Antifouling and Antibacterial Polymer-Coated Surfaces Based on the Combined Effect of Zwitterions and the Natural Borneol. *ACS Applied Materials and Interfaces* **2021**, *13* (7), 9006–9014.

(46) Hwang, G.; Kang, S.; El-Din, M. G.; Liu, Y. Impact of an Extracellular Polymeric Substance (EPS) Precoating on the Initial Adhesion of Burkholderia Cepacia and Pseudomonas Aeruginosa. *Biofouling* **2012**, *28* (6), 525–538.

(47) Blair, J. M. A.; Richmond, G. E.; Piddock, L. J. V. Multidrug Efflux Pumps in Gram-Negative Bacteria and Their Role in Antibiotic Resistance. *Future microbiology* **2014**, *9* (10), 1165–1177.

(48) Graves, J. L.; Tajkarimi, M.; Cunningham, Q.; Campbell, A.; Nonga, H.; Harrison, S. H.; Barrick, J. E. Rapid Evolution of Silver Nanoparticle Resistance in Escherichia Coli. *Frontiers in Genetics* **2015**, *5* (FEB), 42.

(49) Liu, S.; Guo, W. Anti-Biofouling and Healable Materials: Preparation, Mechanisms, and Biomedical Applications. *Advanced Functional Materials* **2018**, *28* (41), 1800596.

(50) Zhuo, Y.; Xiao, S.; Håkonsen, V.; Li, T.; Wang, F.; He, J.; Zhang, Z. Ultrafast Self-Healing and Highly Transparent Coating with Mechanically Durable Icephobicity. *Applied Materials Today* **2020**, *19*, 100542.

Chapter 5 Conclusion

5.1 Major Findings

Infections caused by biofouling biofouling have become a serious concern in the health care sector. There is a significant need of developing novel antifouling and antibacterial biomaterial to resist biofouling due to nonspecific biomolecule adsorption on wet surfaces. Multifunctional surface with long-term stability and strong hydration layer is considered one of the best approaches to mitigate biofouling. The success of bacteria resistant materials depends on their ability to prevent initial adhesion of bacteria on the surface by reducing the interaction among them through maintaining a strong hydration layer. Compared to the polyhydrophilic materials, decorating the surface with polyzwitterionic materials is more promising for nonfouling application because of their stable interactions with a greater number of water molecules. To stably anchor these zwitterionic materials on the surface, a universal strong binding strategy is required which can be facilely applied to a wide range of surfaces regardless of different surface chemistry. In this regard, mussel-inspired dopamine chemistry has been widely used due to its surface independence and strong reactivity. In this thesis, along with dopamine chemistry, prebiotic chemistry inspired aminomalononitrile has been explored to successfully attach zwitterionic polymers onto the surface. While preparing dual functional antifouling and antibacterial material, most of the time biocompatibility of the developed material is overlooked. But in this thesis, for every project, to achieve enhanced biocompatibility, all the surfaces have been modified with cell membrane mimetic phosphorylcholine based zwitterionic material which is broadly considered as nontoxic biomaterial.

In this thesis work, three different surface modification techniques have been developed with antifouling and antibacterial properties. Different surface chemistry has been explored to achieve a stable hydrophilic coating for long-term biomedical applications. **In chapter 2,** a robust antifouling and antibacterial coating has been developed by utilizing dopamine chemistry. Synthesized zwitterionic copolymer poly (MPC-co-DMA) with adhesive DMA pendant was covalently grafted to amino rich PDA/PEI surfaces via amino-ene Michael addition reaction and superhydrophilic surface with 6.8° water contact angle was achieved. The incorporation of PEI into the PDA coating helped to decrease the surface roughness by reducing the PDA aggregates through destroying their non-covalent interactions. Successful grafting of zwitterionic copolymer onto the surface helped to achieve an outstanding antifouling surface with significantly less protein adhesion and less than 92% reduction in bacterial adhesion. This dual functional coating holds a great potential for biomedical application where long-term antifouling and antibacterial property is required.

In chapter 3 of this thesis, using dopamine chemistry, a self-cleaning dynamic surface has been developed based on benzoxaborole−catechol complexation. Zwitterionic polymer poly (MPC-*st*-MAABO) and quaternary ammonium (QA) containing cationic polymer poly (META-*st*-MAABO with different weight ratios were successfully grafted to the PDA coated surface by forming a strong cyclic boronic ester complex with a catechol group of the PDA layer. Due to the presence of QA biocides into the coating, bacteria cell viability went down to less than 10% which offered the coating as an excellent antibacterial surface for potential biomedical application. Additionally, MPC moiety helped to decrease the initial bacteria attachment on the surface with increased surface hydrophilicity. In the developed coating system, the dynamic boronate ester bond formed between PDA and polymers could be dissociated by introducing competitive cis diol containing

sugar molecule. Thus, it can help to remove both live and dead bacteria electrostatically attached to the polymer layer, avoiding biofouling related to the accumulation of dead bacteria. In this project, fructose was added as a sugar molecule which resulted in more than 85% release of attached bacteria and around 75% release of absorbed BSA protein. As the benzoxaborole−catechol complexation is reversible, after sugar treatment, the polymer modified PDA surface was regenerated by simply adding freshly prepared polymer solution onto the sugar treated surface to form the benzoxaborole−catechol complexation again at physiological pH 7.4, which is higher than the pKa value (∼7.2) of

benozoxaborole. Moreover, both the coating extracts and coated surface showed outstanding cell viability against MRC-5 human fibroblast cells demonstrating excellent biocompatibility. The developed sugar responsive dual functional self-cleaning surface with regeneration ability can be a potential candidate for many biomedical applications where antibacterial activity maintained overtime is required.

In chapter 4 of this thesis, a self-healing coating with antifouling and antibacterial properties has been developed utilizing the multiple hydrogen bond interaction between B5AMA and prebiotic chemistry inspired AMN coating. The presence of multiple polar functional groups into the B5AMA structure not only made it an excellent candidate for self-healing material but also the hygroscopic nature of B5AMA demonstrated exceptional antifouling property against bacteria adhesion and BSA protein adsorption. Along with antifouling property, B5AMA polymer coating also showed more than 100% MRC-5 cell viability proving similar biocompatibility as MPC based zwitterionic polymer. We found a complete closure of a scratch within a minute due to the presence of amide-amide and amide-hydroxyl multiple hydrogen bonds into the coating. As AMN has several electron donors such as amines and nitriles for metal coordination, this advantage was

utilized to reduce metallic silver from $AgNO_3$ solution and deposit on the modified surface. Thus, AgNPs incorporation into the coating showed more than 90% bacteria killing efficiency against both gram positive and gram-negative bacteria. This developed dual functional coating system with intrinsic self-healing property and superior biocompatibility has opened up a new era of functional coating for practical biomedical applications.

5.2 Future Work

Although in recent years significant achievements have been made in the rational design and fabrication of antifouling surfaces using dopamine chemistry, most of the proposed chemistries between dopamine and other molecules are still at the preliminary stage of exploration. The underlying theories and mechanisms of developing zwitterionic brush from PDA coated surface are still not clear. The polydopamine formation and zwitterionic polymer brush grafting and post-functionalization still need to be optimized. There should be more elaborative exploration on the proposed chemistries for antifouling surface development using dopamine and zwitterion conjugation. An obvious gap between fundamental research and industrial application with several major challenges need to be addressed such as the scale-up difficulty, high capital costs, uncertain durability and chemical stability in practical long-time operations. Finally, it should be emphasized that the ultimate goal for anti-fouling surface construction is to achieve high and durable performance to better meet the requirements of industrial or large-scale applications. With more insight on the polymerization mechanisms of dopamine and related catecholamine/polyphenol materials, new rationally designed materials with high functionality can be achieved, addressing the need for advanced antifouling materials for long-term applications in biomedical, agriculture, food industry and other sectors.

Another potential surface modification technique includes prebiotic chemistry-inspired AMN coating whose molecular structure still lacks proper investigation. A clear understanding of its reaction mechanism can lead to open options for many possible conjugations of organic molecules with an AMN coated surface for antifouling and antibacterial purposes.

Future work could focus on achieving precise control of grafting multifunctional polymer chains onto different types of substrates with different shapes, elucidating the relationship between specific biomedical functions and the polymeric architectures grafted onto a surface, and achieving multifunctionalities by simultaneous grafting of different macromolecules or multifunctional polymers.

The translation of these state-of-art functional coatings can make a valuable impact in clinical applications. Detailed *in vivo* studies should be conducted in large animal models to further investigate the medical outcome of the developed antifouling and antibacterial biomaterials with the collaboration of the clinical practitioners.

Bibliography:

(1) Park, J.; Gill, G. A.; Strivens, J. E.; Kuo, L. J.; Jeters, R. T.; Avila, A.; Wood, J. R.; Schlafer, N. J.; Janke, C. J.; Miller, E. A.; et al. Effect of Biofouling on the Performance of Amidoxime-Based Polymeric Uranium Adsorbents. *Ind. Eng. Chem. Res.* **2016**, *55* (15), 4328–4338.

(2) Harding, J. L.; Reynolds, M. M. Combating Medical Device Fouling. *Trends Biotechnol.* **2014**, *32* (3), 140–146.

(3) Lindner, E. A Low Surface Free Energy Approach in the Control of Marine Biofouling. *Biofouling* **1992**, *6* (2), 193–205.

(4) Bixler, G. D.; Bhushan, B. Review Article: Biofouling: Lessons from Nature. *Philosophical Transactions of the Royal Society A: Mathematical, Physical and Engineering Sciences*. **2012**, *270,* 2381–2417.

(5) Yu, Q.; Ista, L. K.; López, G. P. Nanopatterned Antimicrobial Enzymatic Surfaces Combining Biocidal and Fouling Release Properties. *Nanoscale* **2014**, *6* (9), 4750–4757.

(6) Magin, C. M.; Cooper, S. P.; Brennan, A. B. Non-Toxic Antifouling Strategies. *Materials Today*. **2010**, *13,* 36–44.

(7) O'Toole, G. A. A Resistance Switch. *Nature*. **2002**, *416,* 695–696.

(8) Yebra, D. M.; Kiil, S.; Dam-Johansen, K. Antifouling Technology - Past, Present and Future Steps towards Efficient and Environmentally Friendly Antifouling Coatings. *Progress in Organic Coatings*. **2004**, *50,* 75–104.

(9) Damodaran, V. B.; Murthy, S. N. Bio-Inspired Strategies for Designing Antifouling Biomaterials. *Biomater. Res.* **2016**, *20* (1).

(10) He, M.; Gao, K.; Zhou, L.; Jiao, Z.; Wu, M.; Cao, J.; You, X.; Cai, Z.; Su, Y.; Jiang, Z. Zwitterionic Materials for Antifouling Membrane Surface Construction. *Acta Biomaterialia*. **2016**, *40*, 142–152.

(11) Chen, S.; Li, L.; Zhao, C.; Zheng, J. Surface Hydration: Principles and Applications toward Low-Fouling/Nonfouling Biomaterials. *Polymer*. **2010**, *51*, 5283–5293.

(12) Zheng, J.; Li, L.; Tsao, H. K.; Sheng, Y. J.; Chen, S.; Jiang, S. Strong Repulsive Forces between Protein and Oligo (Ethylene Glycol) Self-Assembled Monolayers: A Molecular Simulation Study. *Biophys. J.* **2005**, *89* (1), 158–166.

(13) Zhao, J.; Shi, Q.; Luan, S.; Song, L.; Yang, H.; Shi, H.; Jin, J.; Li, X.; Yin, J.; Stagnaro, P. Improved Biocompatibility and Antifouling Property of Polypropylene Non-Woven Fabric Membrane by Surface Grafting Zwitterionic Polymer. *J. Memb. Sci.* **2011**, *369* (1–2), 5–12.

(14) Yu, Q.; Wu, Z.; Chen, H. Dual-Function Antibacterial Surfaces for Biomedical Applications. *Acta Biomaterialia*. **2015**, *16*, 1–13.

(15) Zhao, Y. H.; Zhu, X. Y.; Wee, K. H.; Bai, R. Achieving Highly Effective Non-Biofouling Performance for Polypropylene Membranes Modified by UV-Induced Surface Graft Polymerization of Two Oppositely Charged Monomers. *J. Phys. Chem. B* **2010**, *114* (7), 2422–2429.

(16) Shahkaramipour, N.; Tran, T. N.; Ramanan, S.; Lin, H. Membranes with Surface-Enhanced Antifouling Properties for Water Purification. *Membranes*. **2017,** *7*(1), 13.

(17) Jiang, S.; Cao, Z. Ultralow-Fouling, Functionalizable, and Hydrolyzable Zwitterionic Materials and Their Derivatives for Biological Applications. *Adv. Mater.* **2010**, *22* (9), 920–932.

(18) Bernards, M.; He, Y. Polyampholyte Polymers as a Versatile Zwitterionic Biomaterial Platform. *Journal of Biomaterials Science, Polymer Edition*. **2014**, *25*, 1479–1488.

(19) Zhang, L.; Tang, M.; Zhang, J.; Zhang, P.; Zhang, J.; Deng, L.; Lin, C.; Dong, A. One Simple and Stable Coating of Mixed-Charge Copolymers on Poly(Vinyl Chloride) Films to Improve Antifouling Efficiency. *J. Appl. Polym. Sci.* **2017**, *134* (12), 44632.

(20) Jhong, J. F.; Venault, A.; Liu, L.; Zheng, J.; Chen, S. H.; Higuchi, A.; Huang, J.; Chang, Y. Introducing Mixed-Charge Copolymers as Wound Dressing Biomaterials. *ACS Appl. Mater. Interfaces* **2014**, *6* (12), 9858–9870.

(21) Schlenoff, J. B. Zwitteration: Coating Surfaces with Zwitterionic Functionality to Reduce Nonspecific Adsorption. *Langmuir*. **2014**, *6,* 9625–9636.

(22) Lee, H.; Dellatore, S. M.; Miller, W. M.; Messersmith, P. B. Mussel-Inspired Surface Chemistry for Multifunctional Coatings. *Science (80-.).* **2007**, *318* (5849), 426–430.

(23) Park, J.; Brust, T. F.; Lee, H. J.; Lee, S. C.; Watts, V. J.; Yeo, Y. Polydopamine-Based Simple and Versatile Surface Modification of Polymeric Nano Drug Carriers. *ACS Nano* **2014**, *8* (4), 3347–3356.

(24) Chen, Y.; Feng, X.; Zhao, Y.; Zhao, X.; Zhang, X. Mussel-Inspired Polydopamine Coating Enhances the Intracutaneous Drug Delivery from Nanostructured Lipid Carriers Dependently on a Follicular Pathway. *Mol. Pharm.* **2020**, *17* (4), 1215–1225.

(25) Waite, J. H.; Tanzer, M. L. Polyphenolic Substance of Mytilus Edulis: Novel Adhesive Containing L-Dopa and Hydroxyproline. *Science (80-.).* **1981**, *212* (4498), 1038–1040.

(26) Waite, J. H.; Qin, X. Polyphosphoprotein from the Adhesive Pads of Mytilus Edulis. *Biochemistry* **2001**, *40* (9), 2887–2893.

(27) Silverman, H. G.; Roberto, F. F. Understanding Marine Mussel Adhesion. *Marine Biotechnology*. **2007**, pp 661–681.

(28) Yang, H. C.; Luo, J.; Lv, Y.; Shen, P.; Xu, Z. K. Surface Engineering of Polymer Membranes via Mussel-Inspired Chemistry. *J. Memb. Sci.* **2015**, *483*, 42–59.

(29) Lee, H. A.; Ma, Y.; Zhou, F.; Hong, S.; Lee, H. Material-Independent Surface Chemistry beyond Polydopamine Coating. *Acc. Chem. Res.* **2019**, *52* (3), 704–713.

(30) Jiang, J.; Zhu, L.; Zhu, L.; Zhu, B.; Xu, Y. Surface Characteristics of a Self-Polymerized Dopamine Coating Deposited on Hydrophobic Polymer Films. *Langmuir* **2011**, *27* (23), 14180–14187.

(31) Bernsmann, F.; Ball, V.; Addiego, F.; Ponche, A.; Michel, M.; Gracio, J. J. D. A.; Toniazzo, V.; Ruch, D. Dopamine-Melanin Film Deposition Depends on the Used Oxidant and Buffer Solution. *Langmuir* **2011**, *27* (6), 2819–2825.

(32) Hong, S.; Na, Y. S.; Choi, S.; Song, I. T.; Kim, W. Y.; Lee, H. Non-Covalent Self-Assembly and Covalent Polymerization Co-Contribute to Polydopamine Formation. *Adv. Funct. Mater.* **2012**, *22* (22), 4711–4717.

(33) Ryu, J. H.; Messersmith, P. B.; Lee, H. Polydopamine Surface Chemistry: A Decade of Discovery. *ACS Applied Materials and Interfaces*. **2018**, *10,* 7523–7540.

(34) Liebscher, J.; Mrówczyński, R.; Scheidt, H. A.; Filip, C.; Haìdade, N. D.; Turcu, R.; Bende, A.; Beck, S. Structure of Polydopamine: A Never-Ending Story? *Langmuir* **2013**, *29* (33), 10539–10548.

(35) Zeng, Y.; Liu, W.; Wang, Z.; Singamaneni, S.; Wang, R. Multifunctional Surface Modification of Nanodiamonds Based on Dopamine Polymerization. *Langmuir* **2018**, *34* (13), 4036–4042.

(36) Schanze, K. S.; Lee, H.; Messersmith, P. B. Ten Years of Polydopamine: Current Status and Future Directions. *ACS Applied Materials and Interfaces*. **2018**, *10,* 7521–7522.

(37) Nuzzo, R. G.; Allara, D. L. Adsorption of Bifunctional Organic Disulfides on Gold Surfaces. *Journal of the American Chemical Society*. **1983**, *105,* 4481–4483.

(38) Love, J. C.; Estroff, L. A.; Kriebel, J. K.; Nuzzo, R. G.; Whitesides, G. M. Self-Assembled Monolayers of Thiolates on Metals as a Form of Nanotechnology. *Chemical Reviews*. **2005**, *105,* 1103–1169.

(39) Ulman, A. Formation and Structure of Self-Assembled Monolayers. *Chem. Rev.* **1996**, *96* (4), 1533–1554.

(40) Kirkland, J. J. Porous Thin-Layer Modified Glass Bead Supports for Gas Liquid Chromatography. *Anal. Chem.* **1965**, *37* (12), 1458–1461.

(41) Iler, R. K. Multilayers of Colloidal Particles. *J. Colloid Interface Sci.* **1966**, *21* (6), 569–594.

(42) Richardson, J. J.; Cui, J.; Björnmalm, M.; Braunger, J. A.; Ejima, H.; Caruso, F. Innovation in Layer-by-Layer Assembly. *Chemical Reviews*. **2016**, *116,* 14828–14867.

(43) Liston, E. M.; Martinu, L.; Wertheimer, M. R. Plasma Surface Modification of Polymers for Improved Adhesion: A Critical Review. *J. Adhes. Sci. Technol.* **1993**, *7* (10), 1091–1127.

(44) Chu, P. K.; Chen, J. Y.; Wang, L. P.; Huang, N. Plasma-Surface Modification of Biomaterials. *Materials Science and Engineering: R: Reports*. **2002**, *36*(5-6), 143–206.

(45) Ball, V.; Del Frari, D.; Michel, M.; Buehler, M. J.; Toniazzo, V.; Singh, M. K.; Gracio, J.; Ruch, D. Deposition Mechanism and Properties of Thin Polydopamine Films for High Added Value Applications in Surface Science at the Nanoscale. *BioNanoScience*. **2012**, *2* 16–34.

(46) Tan, X.; Gao, P.; Li, Y.; Qi, P.; Liu, J.; Shen, R.; Wang, L.; Huang, N.; Xiong, K.; Tian, W.; et al. Poly-Dopamine, Poly-Levodopa, and Poly-Norepinephrine Coatings: Comparison of Physico-Chemical and Biological Properties with Focus on the Application for Blood-Contacting Devices. *Bioact. Mater.* **2021**, *6* (1), 285–296.

(47) Borges, J.; Mano, J. F. Molecular Interactions Driving the Layer-by-Layer Assembly of Multilayers. *Chemical Reviews*. **2014**, *114,* 8883–8942.

(48) Lynge, M. E.; Van Der Westen, R.; Postma, A.; Städler, B. Polydopamine - A Nature-Inspired Polymer Coating for Biomedical Science. *Nanoscale* **2011**, *3* (12), 4916–4928.

(49) Zhao, S.; Caruso, F.; Dahne, L.; Decher, G.; De Geest, B. G.; Fan, J.; Feliu, N.; Gogotsi, Y.; Hammond, P. T.; Hersam, M. C.; et al. The Future of Layer-by-Layer Assembly: A Tribute to ACS Nano Associate Editor Helmuth Mohwald. *ACS Nano* **2019**, *13* (6), 6151–6169.

(50) Zhou, R.; Ren, P. F.; Yang, H. C.; Xu, Z. K. Fabrication of Antifouling Membrane Surface by Poly(Sulfobetaine Methacrylate)/Polydopamine Co-Deposition. *J. Memb. Sci.* **2014**, *466*, 18–25.

(51) Yu, B. Y.; Zheng, J.; Chang, Y.; Sin, M. C.; Chang, C. H.; Higuchi, A.; Sun, Y. M. Surface Zwitterionization of Titanium for a General Bio-Inert Control of Plasma Proteins, Blood Cells, Tissue Cells, and Bacteria. *Langmuir* **2014**, *30* (25), 7502–7512.

(52) Liu, X.; Deng, J.; Ma, L.; Cheng, C.; Nie, C.; He, C.; Zhao, C. Catechol Chemistry Inspired Approach to Construct Self-Cross-Linked Polymer Nanolayers as Versatile Biointerfaces. *Langmuir* **2014**, *30* (49), 14905–14915.

(53) Li, G.; Cheng, G.; Xue, H.; Chen, S.; Zhang, F.; Jiang, S. Ultra Low Fouling Zwitterionic Polymers with a Biomimetic Adhesive Group. *Biomaterials* **2008**, *29* (35), 4592–4597.

(54) Sundaram, H. S.; Han, X.; Nowinski, A. K.; Ella-Menye, J. R.; Wimbish, C.; Marek, P.; Senecal, K.; Jiang, S. One-Step Dip Coating of Zwitterionic Sulfobetaine Polymers on Hydrophobic and Hydrophilic Surfaces. In *ACS Applied Materials and Interfaces*; **2014**; *6*, 6664–6671.

(55) Yang, W.; Sundaram, H. S.; Ella, J. R.; He, N.; Jiang, S. Low-Fouling Electrospun PLLA Films Modified with Zwitterionic Poly(Sulfobetaine Methacrylate)-Catechol Conjugates. *Acta Biomater.* **2016**, *40*, 92–99.

(56) Cheng, G.; Li, G.; Xue, H.; Chen, S.; Bryers, J. D.; Jiang, S. Zwitterionic Carboxybetaine Polymer Surfaces and Their Resistance to Long-Term Biofilm Formation. *Biomaterials* **2009**, *30* (28), 5234–5240.

(57) Gao, C.; Li, G.; Xue, H.; Yang, W.; Zhang, F.; Jiang, S. Functionalizable and Ultra-Low Fouling Zwitterionic Surfaces via Adhesive Mussel Mimetic Linkages. *Biomaterials* **2010**, *31* (7), 1486–1492.

(58) Amoako, K. A.; Sundaram, H. S.; Suhaib, A.; Jiang, S.; Cook, K. E. Multimodal, Biomaterial-Focused Anticoagulation via Superlow Fouling Zwitterionic Functional Groups Coupled with Anti-Platelet Nitric Oxide Release. *Adv. Mater. Interfaces* **2016**, *3* (6).

(59) Ye, G.; Lee, J.; Perreault, F.; Elimelech, M. Controlled Architecture of Dual-Functional Block Copolymer Brushes on Thin-Film Composite Membranes for Integrated "Defending" and "Attacking" Strategies against Biofouling. *ACS Appl. Mater. Interfaces* **2015**, *7* (41), 23069–23079.

(60) Wang, B. L.; Jin, T. W.; Han, Y. M.; Shen, C. H.; Li, Q.; Lin, Q. K.; Chen, H. Bio-Inspired Terpolymers Containing Dopamine, Cations and MPC: A Versatile Platform to Construct a Recycle Antibacterial and Antifouling Surface. *J. Mater. Chem. B* **2015**, *3* (27), 5501–5510.

(61) Zhang, C.; Ma, M. Q.; Chen, T. T.; Zhang, H.; Hu, D. F.; Wu, B. H.; Ji, J.; Xu, Z. K. Dopamine-Triggered One-Step Polymerization and Codeposition of Acrylate Monomers for Functional Coatings. *ACS Appl. Mater. Interfaces* **2017**, *9* (39), 34356–34366.

(62) Ren, P. F.; Yang, H. C.; Jin, Y. N.; Liang, H. Q.; Wan, L. S.; Xu, Z. K. Underwater Superoleophobic Meshes Fabricated by Poly(Sulfobetaine)/Polydopamine Co-Deposition. *RSC Adv.* **2015**, *5* (59), 47592–47598.

(63) Chang, C. C.; Kolewe, K. W.; Li, Y.; Kosif, I.; Freeman, B. D.; Carter, K. R.; Schiffman, J. D.; Emrick, T. Underwater Superoleophobic Surfaces Prepared from Polymer Zwitterion/Dopamine Composite Coatings. *Adv. Mater. Interfaces* **2016**, *3* (6), 1500521.

(64) Zhang, C.; Li, H. N.; Du, Y.; Ma, M. Q.; Xu, Z. K. CuSO4/H2O2-Triggered Polydopamine/Poly(Sulfobetaine Methacrylate) Coatings for Antifouling Membrane Surfaces. *Langmuir* **2017**, *33* (5), 1210–1216.

(65) Xu, G.; Liu, P.; Pranantyo, D.; Xu, L.; Neoh, K. G.; Kang, E. T. Antifouling and Antimicrobial Coatings from Zwitterionic and Cationic Binary Polymer Brushes Assembled via "Click" Reactions. *Ind. Eng. Chem. Res.* **2017**, *56* (49), 14479–14488.

(66) Shahkaramipour, N.; Lai, C. K.; Venna, S. R.; Sun, H.; Cheng, C.; Lin, H. Membrane Surface Modification Using Thiol-Containing Zwitterionic Polymers via Bioadhesive Polydopamine. *Ind. Eng. Chem. Res.* **2018**, *57* (6), 2336–2345.

(67) Kuang, J.; Messersmith, P. B. Universal Surface-Initiated Polymerization of Antifouling Zwitterionic Brushes Using a Mussel-Mimetic Peptide Initiator. *Langmuir* **2012**, *28* (18), 7258–7266.

(68) Sin, M. C.; Sun, Y. M.; Chang, Y. Zwitterionic-Based Stainless Steel with Well-Defined Polysulfobetaine Brushes for General Bioadhesive Control. *ACS Appl. Mater. Interfaces* **2014**, *6* (2), 861–873.

(69) Liu, C.; Lee, J.; Ma, J.; Elimelech, M. Antifouling Thin-Film Composite Membranes by Controlled Architecture of Zwitterionic Polymer Brush Layer. *Environ. Sci. Technol.* **2017**, *51* (4), 2161–2169.

(70) Sundaram, H. S.; Han, X.; Nowinski, A. K.; Brault, N. D.; Li, Y.; Ella-Menye, J. R.; Amoaka, K. A.; Cook, K. E.; Marek, P.; Senecal, K.; et al. Achieving One-Step Surface Coating of Highly Hydrophilic Poly(Carboxybetaine Methacrylate) Polymers on Hydrophobic and Hydrophilic Surfaces. *Adv. Mater. Interfaces* **2014**, *1* (6).

(71) Sun, F.; Wu, K.; Hung, H. C.; Zhang, P.; Che, X.; Smith, J.; Lin, X.; Li, B.; Jain, P.; Yu, Q.; et al. Paper Sensor Coated with a Poly(Carboxybetaine)-Multiple DOPA Conjugate via Dip-Coating for Biosensing in Complex Media. *Anal. Chem.* **2017**, *89* (20), 10999–11004.

(72) Ye, H.; Xia, Y.; Liu, Z.; Huang, R.; Su, R.; Qi, W.; Wang, L.; He, Z. Dopamine-Assisted Deposition and Zwitteration of Hyaluronic Acid for the Nanoscale Fabrication of Low-Fouling Surfaces. *J. Mater. Chem. B* **2016**, *4* (23), 4084–4091.

(73) Huang, C. J.; Wang, L. C.; Shyue, J. J.; Chang, Y. C. Developing Antifouling Biointerfaces Based on Bioinspired Zwitterionic Dopamine through PH-Modulated Assembly. *Langmuir* **2014**, *30* (42), 12638–12646.

(74) Kang, S. M.; Hwang, N. S.; Yeom, J.; Park, S. Y.; Messersmith, P. B.; Choi, I. S.; Langer, R.; Anderson, D. G.; Lee, H. One-Step Multipurpose Surface Functionalization by Adhesive Catecholamine. *Adv. Funct. Mater.* **2012**, *22* (14), 2949–2955.

(75) Qiu, W. Z.; Yang, H. C.; Xu, Z. K. Dopamine-Assisted Co-Deposition: An Emerging and Promising Strategy for Surface Modification. *Advances in Colloid and Interface Science*. **2018**, *256,* 111–125.

(76) Kolewe, K. W.; Dobosz, K. M.; Rieger, K. A.; Chang, C. C.; Emrick, T.; Schiffman, J. D. Antifouling Electrospun Nanofiber Mats Functionalized with Polymer Zwitterions. *ACS Appl. Mater. Interfaces* **2016**, *8* (41), 27585–27593.

(77) Kirschner, A. Y.; Chang, C. C.; Kasemset, S.; Emrick, T.; Freeman, B. D. Fouling-Resistant Ultrafiltration Membranes Prepared via Co-Deposition of Dopamine/Zwitterion Composite Coatings. *J. Memb. Sci.* **2017**, *541*, 300–311.

(78) Zhang, C.; Ou, Y.; Lei, W. X.; Wan, L. S.; Ji, J.; Xu, Z. K. CuSO4/H2O2-Induced Rapid Deposition of Polydopamine Coatings with High Uniformity and Enhanced Stability. *Angew. Chemie - Int. Ed.* **2016**, *55* (9), 3054–3057.

(79) Xie, Y.; Tang, C.; Wang, Z.; Xu, Y.; Zhao, W.; Sun, S.; Zhao, C. Co-Deposition towards Mussel-Inspired Antifouling and Antibacterial Membranes by Using Zwitterionic Polymers and Silver Nanoparticles. *J. Mater. Chem. B* **2017**, *5* (34), 7186–7193.

(80) Ding, Y. H.; Floren, M.; Tan, W. Mussel-Inspired Polydopamine for Bio-Surface Functionalization. *Biosurface and Biotribology* **2016**, *2* (4), 121–136.

(81) Yang, J.; Cohen Stuart, M. A.; Kamperman, M. Jack of All Trades: Versatile Catechol Crosslinking Mechanisms. *Chemical Society Reviews*. **2014**, 8271–8298.

(82) Li, P.; Cai, X.; Wang, D.; Chen, S.; Yuan, J.; Li, L.; Shen, J. Hemocompatibility and Anti-Biofouling Property Improvement of Poly(Ethylene Terephthalate) via Self-Polymerization of Dopamine and Covalent Graft of Zwitterionic Cysteine. *Colloids Surfaces B Biointerfaces* **2013**, *110*, 327–332.

(83) Shevate, R.; Kumar, M.; Karunakaran, M.; Hedhili, M. N.; Peinemann, K. V. Polydopamine/Cysteine Surface Modified Isoporous Membranes with Self-Cleaning Properties. *J. Memb. Sci.* **2017**, *529*, 185–194.

(84) Cui, J.; Ju, Y.; Liang, K.; Ejima, H.; Lörcher, S.; Gause, K. T.; Richardson, J. J.; Caruso, F. Nanoscale Engineering of Low-Fouling Surfaces through Polydopamine Immobilisation of Zwitterionic Peptides. *Soft Matter* **2014**, *10* (15), 2656–2663.

(85) Zhi, X.; Li, P.; Gan, X.; Zhang, W.; Shen, T.; Yuan, J.; Shen, J. Hemocompatibility and Anti-Biofouling Property Improvement of Poly(Ethylene Terephthalate) via Self-Polymerization of Dopamine and Covalent Graft of Lysine. *J. Biomater. Sci. Polym. Ed.* **2014**, *25* (14–15), 1619–1628.

(86) Chen, L.; Tan, L.; Liu, S.; Bai, L.; Wang, Y. Surface Modification by Grafting of Poly(SBMA-Co-AEMA)-g-PDA Coating and Its Application in CE. *J. Biomater. Sci. Polym. Ed.* **2014**, *25* (8), 766–785.

(87) Liu, C. Y.; Huang, C. J. Functionalization of Polydopamine via the Aza-Michael Reaction for Antimicrobial Interfaces. *Langmuir* **2016**, *32* (19), 5019–5028.

(88) Asha, A. B.; Chen, Y.; Zhang, H.; Ghaemi, S.; Ishihara, K.; Liu, Y.; Narain, R. Rapid Mussel-Inspired Surface Zwitteration for Enhanced Antifouling and Antibacterial Properties. *Langmuir* **2019**, *35* (5), 1621–1630.

(89) Gillich, T.; Benetti, E. M.; Rakhmatullina, E.; Konradi, R.; Li, W.; Zhang, A.; Schlüter, A. D.; Textor, M. Self-Assembly of Focal Point Oligo-Catechol Ethylene Glycol Dendrons on Titanium Oxide Surfaces: Adsorption Kinetics, Surface Characterization, and Nonfouling Properties. *J. Am. Chem. Soc.* **2011**, *133* (28), 10940–10950.

(90) Li, N.; Li, T.; Qiao, X. Y.; Li, R.; Yao, Y.; Gong, Y. K. Universal Strategy for Efficient Fabrication of Blood Compatible Surfaces via Polydopamine-Assisted Surface-Initiated Activators Regenerated by Electron Transfer Atom-Transfer Radical Polymerization of Zwitterions. *ACS Appl. Mater. Interfaces* **2020**, *12* (10), 12337–12344.

(91) Ma, H.; Hyun, J.; Stiller, P.; Chilkoti, A. "Non-Fouling" Oligo(Ethylene Glycol)-Functionalized Polymer Brushes Synthesized by Surface-Initiated Atom Transfer Radical Polymerization. *Adv. Mater.* **2004**, *16* (4), 338–341.

(92) Matyjaszewski, K.; Miller, P. J.; Shukla, N.; Immaraporn, B.; Gelman, A.; Luokala, B. B.; Siclovan, T. M.; Kickelbick, G.; Valiant, T.; Hoffmann, H.; et al. Polymers at Interfaces: Using Atom Transfer Radical Polymerization in the Controlled Growth of Homopolymers and Block

Copolymers from Silicon Surfaces in the Absence of Untethered Sacrificial Initiator. *Macromolecules* **1999**, *32* (26), 8716–8724.

(93) He, X.; Yang, W.; Pei, X. Preparation, Characterization, and Tunable Wettability of Poly(Ionic Liquid) Brushes via Surface-Initiated Atom Transfer Radical Polymerization. *Macromolecules* **2008**, *41* (13), 4615–4621.

(94) Edmondson, S.; Vo, C. D.; Armes, S. P.; Unali, G. F. Surface Polymerization from Planar Surfaces by Atom Transfer Radical Polymerization Using Polyelectrolytic Macroinitiators. *Macromolecules* **2007**, *40* (15), 5271–5278.

(95) Ma, W.; Yang, P.; Li, J.; Li, S.; Li, P.; Zhao, Y.; Huang, N. Immobilization of Poly(MPC) Brushes onto Titanium Surface by Combining Dopamine Self-Polymerization and ATRP: Preparation, Characterization and Evaluation of Hemocompatibility in Vitro. *Appl. Surf. Sci.* **2015**, *349*, 445–451.

(96) Wang, J.; Wei, J. Hydrogel Brushes Grafted from Stainless Steel via Surface-Initiated Atom Transfer Radical Polymerization for Marine Antifouling. *Appl. Surf. Sci.* **2016**, *382*, 202–216.

(97) Jiang, J.; Zhang, P.; Zhu, L.; Zhu, B.; Xu, Y. Improving Antifouling Ability and Hemocompatibility of Poly(Vinylidene Fluoride) Membranes by Polydopamine-Mediated ATRP. *J. Mater. Chem. B* **2015**, *3* (39), 7698–7706.

(98) Jin, X.; Yuan, J.; Shen, J. Zwitterionic Polymer Brushes via Dopamine-Initiated ATRP from PET Sheets for Improving Hemocompatible and Antifouling Properties. *Colloids Surfaces B Biointerfaces* **2016**, *145*, 275–284.

(99) Wang, W. C.; Wang, J.; Liao, Y.; Zhang, L.; Cao, B.; Song, G.; She, X. Surface Initiated ATRP of Acrylic Acid on Dopamine-Functionalized AAO Membranes. *J. Appl. Polym. Sci.* **2010**, *117* (1), 534–541.

(100) Li, G.; Xue, H.; Cheng, G.; Chen, S.; Zhang, F.; Jiang, S. Ultralow Fouling Zwitterionic Polymers Grafted from Surfaces Covered with an Initiator via an Adhesive Mussel Mimetic Linkage. *J. Phys. Chem. B* **2008**, *112* (48), 15269–15274.

(101) Ginic-Markovic, M.; Barclay, T.; Constantopoulos, K. T.; Al-Ghamdi, T.; Blok, A.; Markovic, E.; Ellis, A. V. A Versatile Approach to Grafting Biofouling Resistant Coatings from Polymeric Membrane Surfaces Using an Adhesive Macroinitiator. *RSC Adv.* **2015**, *5* (77), 63017–63024.

(102) Peng, B.; Lai, X.; Chen, L.; Lin, X.; Sun, C.; Liu, L.; Qi, S.; Chen, Y.; Leong, K. W. Scarless Wound Closure by a Mussel-Inspired Poly(Amidoamine) Tissue Adhesive with Tunable Degradability. *ACS Omega* **2017**, *2* (9), 6053–6062.

(103) Xing, C. M.; Meng, F. N.; Quan, M.; Ding, K.; Dang, Y.; Gong, Y. K. Quantitative Fabrication, Performance Optimization and Comparison of PEG and Zwitterionic Polymer Antifouling Coatings. *Acta Biomater.* **2017**, *59*, 129–138.

(104) Brault, N. D.; Gao, C.; Xue, H.; Piliarik, M.; Homola, J.; Jiang, S.; Yu, Q. Ultra-Low Fouling and Functionalizable Zwitterionic Coatings Grafted onto SiO2 via a Biomimetic Adhesive Group for Sensing and Detection in Complex Media. *Biosens. Bioelectron.* **2010**, *25* (10), 2276–2282.

(105) Zhao, J.; Mo, R.; Tian, L. M.; Song, L. J.; Luan, S. F.; Yin, J. H.; Ren, L. Q. Oriented Antibody Immobilization and Immunoassay Based on Boronic Acid-Containing Polymer Brush. *Chinese J. Polym. Sci. (English Ed.* **2018**, *36* (4), 472–478.

(106) Shahkaramipour, N.; Ramanan, S. N.; Fister, D.; Park, E.; Venna, S. R.; Sun, H.; Cheng, C.; Lin, H. Facile Grafting of Zwitterions onto the Membrane Surface to Enhance Antifouling Properties for Wastewater Reuse. *Ind. Eng. Chem. Res.* **2017**, *56* (32), 9202–9212.

(107) Barclay, T. G.; Hegab, H. M.; Michelmore, A.; Weeks, M.; Ginic-Markovic, M. Multidentate Polyzwitterion Attachment to Polydopamine Modified Ultrafiltration Membranes for Dairy Processing: Characterization, Performance and Durability. *J. Ind. Eng. Chem.* **2018**, *61*, 356–367.

(108) Meng, F. N.; Zhang, M. Q.; Ding, K.; Zhang, T.; Gong, Y. K. Cell Membrane Mimetic PVDF Microfiltration Membrane with Enhanced Antifouling and Separation Performance for Oil/Water Mixtures. *J. Mater. Chem. A* **2018**, *6* (7), 3231–3241.

(109) Zhu, L. J.; Liu, F.; Yu, X. M.; Gao, A. L.; Xue, L. X. Surface Zwitterionization of Hemocompatible Poly(Lactic Acid) Membranes for Hemodiafiltration. *J. Memb. Sci.* **2015**, *475*, 469–479.

(110) Zhu, Y.; Sundaram, H. S.; Liu, S.; Zhang, L.; Xu, X.; Yu, Q.; Xu, J.; Jiang, S. A Robust Graft-to Strategy to Form Multifunctional and Stealth Zwitterionic Polymer-Coated Mesoporous Silica Nanoparticles. *Biomacromolecules* **2014**, *15* (5), 1845–1851.

(111) Vatankhah-Varnosfaderani, M.; Hu, X.; Li, Q.; Adelnia, H.; Ina, M.; Sheiko, S. S. Universal Coatings Based on Zwitterionic-Dopamine Copolymer Microgels. *ACS Appl. Mater. Interfaces* **2018**.

(112) Thissen, H.; Koegler, A.; Salwiczek, M.; Easton, C. D.; Qu, Y.; Lithgow, T.; Evans, R. A. Prebiotic-Chemistry Inspired Polymer Coatings for Biomedical and Material Science Applications. *NPG Asia Mater.* **2015**, *7* (11), 1–9.

(113) Menzies, D. J.; Ang, A.; Thissen, H.; Evans, R. A. Adhesive Prebiotic Chemistry Inspired Coatings for Bone Contacting Applications. *ACS Biomater. Sci. Eng.* **2017**, *3* (5), 793–806.

(114) Toh, R. J.; Evans, R.; Thissen, H.; Voelcker, N. H.; D'ischia, M.; Ball, V. Deposition of Aminomalononitrile-Based Films: Kinetics, Chemistry, and Morphology. *Langmuir* **2019**, *35* (30), 9896–9903.

(115) Cheng, Q.; Asha, A. B.; Liu, Y.; Peng, Y. Y.; Diaz-Dussan, D.; Shi, Z.; Cui, Z.; Narain, R. Antifouling and Antibacterial Polymer-Coated Surfaces Based on the Combined Effect of Zwitterions and the Natural Borneol. *ACS Appl. Mater. Interfaces* **2021**, *13* (7), 9006–9014.

(116) Raulin, F.; Lussiana, J.-P. Prebiotic Formation of Iminothioesters. II: Addition of Thiophenols to Malonic Nitriles. *Orig. Life* **1984**, *14* (1), 157–162.

(117) Mittelman, M. W. *Marine Biotechnology*; **1999**.

(118) Harris, L. G. Microbial Cell Structure and Organization: Bacteria. *Encycl. Infect. Immun.* **2022**, *1*, 345–362.

(119) Ojkic, N.; Serbanescu, D.; Banerjee, S. Surface-to-Volume Scaling and Aspect Ratio Preservation in Rod-Shaped Bacteria. *Elife* **2019**, *8*, 1–11.

(120) O'Toole, G. A. Classic Spotlight: How the Gram Stain Works. *J. Bacteriol.* **2016**, *198* (23), 3128–3128.

(121) Bart Gottenbos, Dirk W. Grijpma, Henny C. van der Mei, J. F. and H. J. B. Antimicrobial Effects of Positively Charged Surfaces on Adhering Gram-Positive and Gram-Negative Bacteria. *J. Antimicrob. Chemother.* **2001**, *48*, 7–13.

(122) Vollmer, W.; Blanot, D.; De Pedro, M. A. Peptidoglycan Structure and Architecture. *FEMS Microbiol. Rev.* **2008**, *32* (2), 149–167.

(123) Wilson, W. W.; Wade, M. M.; Holman, S. C.; Champlin, F. R. Status of Methods for Assessing Bacterial Cell Surface Charge Properties Based on Zeta Potential Measurements. *J. Microbiol. Methods* **2001**, *43* (3), 153–164.

(124) Ayala-Torres, C.; Hernández, N.; Galeano, A.; Novoa-Aponte, L.; Soto, C. Y. Zeta Potential as a Measure of the Surface Charge of Mycobacterial Cells. *Ann. Microbiol.* **2014**, *64* (3), 1189–1195.

(125) Bixler, G. D.; Bhushan, B. Review Article: Biofouling: Lessons from Nature. *Philosophical Transactions of the Royal Society A: Mathematical, Physical and Engineering Sciences*. 2012, pp 2381–2417.

(126) Shahkaramipour, N.; Lai, C. K.; Venna, S. R.; Sun, H.; Cheng, C.; Lin, H. Membrane Surface Modification Using Thiol-Containing Zwitterionic Polymers via Bioadhesive Polydopamine. *Ind. Eng. Chem. Res.* **2018**, *57* (6), 2336–2345.

(127) Dang, Y.; Quan, M.; Xing, C. M.; Wang, Y. B.; Gong, Y. K. Biocompatible and Antifouling Coating of Cell Membrane Phosphorylcholine and Mussel Catechol Modified Multi-Arm PEGs. *J. Mater. Chem. B* **2015**, *3* (11), 2350–2361.

(128) Fu, Y.; Wang, Y.; Huang, L.; Xiao, S.; Chen, F.; Fan, P.; Zhong, M.; Tan, J.; Yang, J. Salt-Responsive “Killing and Release” Antibacterial Surfaces of Mixed Polymer Brushes. *Ind. Eng. Chem. Res.* **2018**, *57* (27), 8938–8945.

(129) Selim, M. S.; Yang, H.; Wang, F. Q.; Li, X.; Huang, Y.; Fatthallah, N. A. Silicone/Ag@SiO2core-Shell Nanocomposite as a Self-Cleaning Antifouling Coating Material. *RSC Adv.* **2018**, *8* (18), 9910–9921.

(130) Schlenoff, J. B. Zwitteration: Coating Surfaces with Zwitterionic Functionality to Reduce Nonspecific Adsorption. *Langmuir*. 2014, pp 9625–9636.

(131) Wu, J.; Lin, W.; Wang, Z.; Chen, S.; Chang, Y. Investigation of the Hydration of Nonfouling Material Poly(Sulfobetaine Methacrylate) by Low-Field Nuclear Magnetic Resonance. *Langmuir* **2012**, *28* (19), 7436–7441.

(132) Gao, C.; Li, G.; Xue, H.; Yang, W.; Zhang, F.; Jiang, S. Functionalizable and Ultra-Low Fouling Zwitterionic Surfaces via Adhesive Mussel Mimetic Linkages. *Biomaterials* **2010**, *31* (7), 1486–1492.

(133) Wang, B. L.; Jin, T. W.; Han, Y. M.; Shen, C. H.; Li, Q.; Lin, Q. K.; Chen, H. Bio-Inspired Terpolymers Containing Dopamine, Cations and MPC: A Versatile Platform to Construct a Recycle Antibacterial and Antifouling Surface. *J. Mater. Chem. B* **2015**, *3* (27), 5501–5510.

(134) Sin, M. C.; Sun, Y. M.; Chang, Y. Zwitterionic-Based Stainless Steel with Well-Defined Polysulfobetaine Brushes for General Bioadhesive Control. *ACS Appl. Mater. Interfaces* **2014**, *6* (2), 861–873.

(135) Kuang, J.; Messersmith, P. B. Universal Surface-Initiated Polymerization of Antifouling Zwitterionic Brushes Using a Mussel-Mimetic Peptide Initiator. *Langmuir* **2012**, *28* (18), 7258–7266.

(136) Guinn, K.; Fojtik, A.; Davis-Fields, N.; Poulson, R. L.; Krauss, S.; Webster, R. G.; Stallknecht, D. E. Antibodies to Influenza A Viruses in Gulls at Delaware Bay, USA. *Avian Diseases*. 2016, pp 341–345.

(137) Jiang, J.; Zhu, L.; Zhu, L.; Zhu, B.; Xu, Y. Surface Characteristics of a Self-Polymerized Dopamine Coating Deposited on Hydrophobic Polymer Films. *Langmuir* **2011**, *27* (23), 14180–14187.

(138) Bernsmann, F.; Ball, V.; Addiego, F.; Ponche, A.; Michel, M.; Gracio, J. J. D. A.; Toniazzo, V.; Ruch, D. Dopamine-Melanin Film Deposition Depends on the Used Oxidant and Buffer Solution. *Langmuir* **2011**, *27* (6), 2819–2825.

(139) Yang, H. C.; Waldman, R. Z.; Wu, M. B.; Hou, J.; Chen, L.; Darling, S. B.; Xu, Z. K. Dopamine: Just the Right Medicine for Membranes. *Adv. Funct. Mater.* **2018**, *28* (8).

(140) Li, L.; Zeng, H. Marine Mussel Adhesion and Bio-Inspired Wet Adhesives. *Biotribology* **2016**, *5*, 44–51.

(141) Lu, Z.; Xiao, J.; Wang, Y.; Meng, M. In Situ Synthesis of Silver Nanoparticles Uniformly Distributed on Polydopamine-Coated Silk Fibers for Antibacterial Application. *J. Colloid Interface Sci.* **2015**, *452*, 8–14.

(142) Sundaram, H. S.; Han, X.; Nowinski, A. K.; Ella-Menye, J. R.; Wimbish, C.; Marek, P.; Senecal, K.; Jiang, S. One-Step Dip Coating of Zwitterionic Sulfobetaine Polymers on

Hydrophobic and Hydrophilic Surfaces. In *ACS Applied Materials and Interfaces*; 2014; Vol. 6, pp 6664–6671.

(143) Amoako, K. A.; Sundaram, H. S.; Suhaib, A.; Jiang, S.; Cook, K. E. Multimodal, Biomaterial-Focused Anticoagulation via Superlow Fouling Zwitterionic Functional Groups Coupled with Anti-Platelet Nitric Oxide Release. *Adv. Mater. Interfaces* **2016**, *3* (6).

(144) Sundaram, H. S.; Han, X.; Nowinski, A. K.; Brault, N. D.; Li, Y.; Ella-Menye, J.-R.; Amoaka, K. A.; Cook, K. E.; Marek, P.; Senecal, K.; et al. Achieving One-Step Surface Coating of Highly Hydrophilic Poly(Carboxybetaine Methacrylate) Polymers on Hydrophobic and Hydrophilic Surfaces. *Adv. Mater. Interfaces* **2014**, *1* (6), 1400071.

(145) Li, G.; Xue, H.; Cheng, G.; Chen, S.; Zhang, F.; Jiang, S. Ultralow Fouling Zwitterionic Polymers Grafted from Surfaces Covered with an Initiator via an Adhesive Mussel Mimetic Linkage. *J. Phys. Chem. B* **2008**, *112* (48), 15269–15274.

(146) Zhang, C.; Ma, M. Q.; Chen, T. T.; Zhang, H.; Hu, D. F.; Wu, B. H.; Ji, J.; Xu, Z. K. Dopamine-Triggered One-Step Polymerization and Codeposition of Acrylate Monomers for Functional Coatings. *ACS Appl. Mater. Interfaces* **2017**, *9* (39), 34356–34366.

(147) Isohata, H.; Hanzawa, Y. Bridge Construction Technology and the Western Influence in Modern Japan. *Eng. Struct.* **1997**, *19* (9), 788–794.

(148) Zhang, C.; Li, H. N.; Du, Y.; Ma, M. Q.; Xu, Z. K. CuSO4/H2O2-Triggered Polydopamine/Poly(Sulfobetaine Methacrylate) Coatings for Antifouling Membrane Surfaces. *Langmuir* **2017**, *33* (5), 1210–1216.

(149) Chang, C. C.; Kolewe, K. W.; Li, Y.; Kosif, I.; Freeman, B. D.; Carter, K. R.; Schiffman, J. D.; Emrick, T. Underwater Superoleophobic Surfaces Prepared from Polymer Zwitterion/Dopamine Composite Coatings. *Adv. Mater. Interfaces* **2016**, *3* (6).

(150) An, Q.; Huang, T.; Shi, F. Correction: Covalent Layer-by-Layer Films: Chemistry, Design, and Multidisciplinary Applications (Chem. Soc. Rev., (2018) DOI: 10.1039/C7cs00406k). *Chem. Soc. Rev.* **2018**, *47* (14), 5529.

(151) Chen, Y.; Diaz-Dussan, D.; Wu, D.; Wang, W.; Peng, Y. Y.; Asha, A. B.; Hall, D. G.; Ishihara, K.; Narain, R. Bioinspired Self-Healing Hydrogel Based on Benzoxaborole-Catechol Dynamic Covalent Chemistry for 3D Cell Encapsulation. *ACS Macro Lett.* **2018**, *7* (8), 904–908.

(152) Jiang, J. H.; Zhu, L. P.; Li, X. L.; Xu, Y. Y.; Zhu, B. K. Surface Modification of PE Porous Membranes Based on the Strong Adhesion of Polydopamine and Covalent Immobilization of Heparin. *J. Memb. Sci.* **2010**, *364* (1–2), 194–202.

(153) Sun, X.; Shao, Y.; Boluk, Y.; Liu, Y. The Impact of Cellulose Nanocrystals on the Aggregation and Initial Adhesion to a Solid Surface of Escherichia Coli K12: Role of Solution Chemistry. *Colloids Surfaces B Biointerfaces* **2015**, *136*, 570–576.

(154) Liu, C.-Y.; Huang, C.-J. Functionalization of Polydopamine via the Aza-Michael Reaction for Antimicrobial Interfaces. *Langmuir* **2016**.

(155) Kruger, N. J. The Bradford Method for Protein Quantitation. In *The Protein Protocols Handbook*; 1996; pp 15–20.

(156) Leblanc, M.; Fischer, W. Gold and Platinum Group Elements in Cobaltarsenide Ores: Hydrothermal Concentration from a Serpentinite Source-Rock (Bou Azzer, Morocco). *Mineral. Petrol.* **1990**, *42* (1–4), 197–209.

(157) Yang, H. C.; Wu, M. B.; Li, Y. J.; Chen, Y. F.; Wan, L. S.; Xu, Z. K. Effects of Polyethyleneimine Molecular Weight and Proportion on the Membrane Hydrophilization by Codepositing with Dopamine. *J. Appl. Polym. Sci.* **2016**, *133* (32).

(158) Yang, H. C.; Liao, K. J.; Huang, H.; Wu, Q. Y.; Wan, L. S.; Xu, Z. K. Mussel-Inspired Modification of a Polymer Membrane for Ultra-High Water Permeability and Oil-in-Water Emulsion Separation. *J. Mater. Chem. A* **2014**, *2* (26), 10225–10230.

(159) Lee, H.; Scherer, N. F.; Messersmith, P. B. Single-Molecule Mechanics of Mussel Adhesion. *Proc. Natl. Acad. Sci.* **2006**, *103* (35), 12999–13003.

(160) Hwang, G.; Kang, S.; El-Din, M. G.; Liu, Y. Impact of an Extracellular Polymeric Substance (EPS) Precoating on the Initial Adhesion of Burkholderia Cepacia and Pseudomonas Aeruginosa. *Biofouling* **2012**, *28* (6), 525–538.

(161) Horbett Thomas, A.; Brash John, L. Proteins at Interfaces: Current Issues and Future Prospects. In *Proteins at Interfaces: Physicochemical and Biochemical Studies*; 1987; Vol. 343, pp 1–33.

(162) Ishihara, K. Bioinspired Phospholipid Polymer Biomaterials for Making High Performance Artificial Organs. *Sci. Technol. Adv. Mater.* **2000**, *1* (3), 131–138.

(163) Yang, Z.; Wu, Y.; Wang, J.; Cao, B.; Tang, C. Y. In Situ Reduction of Silver by Polydopamine: A Novel Antimicrobial Modification of a Thin-Film Composite Polyamide Membrane. *Environ. Sci. Technol.* **2016**, *50* (17), 9543–9550.

(164) Liu, Z.; Wang, Y.; Zu, Y.; Fu, Y.; Li, N.; Guo, N.; Liu, R.; Zhang, Y. Synthesis of Polyethylenimine (PEI) Functionalized Silver Nanoparticles by a Hydrothermal Method and Their Antibacterial Activity Study. *Mater. Sci. Eng. C* **2014**, *42*, 31–37.

(165) Donlan, R. M.; Costerton, J. W. Biofilms: Survival Mechanisms of Clinically Relevant Microorganisms. *Clinical Microbiology Reviews*. 2002, pp 167–193.

(166) Hall-Stoodley, L.; Costerton, J. W.; Stoodley, P. Bacterial Biofilms: From the Natural Environment to Infectious Diseases. *Nature Reviews Microbiology*. 2004, pp 95–108.

(167) Wang, B.; Ye, Z.; Xu, Q.; Liu, H.; Lin, Q.; Chen, H.; Nan, K. Construction of a Temperature-Responsive Terpolymer Coating with Recyclable Bactericidal and Self-Cleaning Antimicrobial Properties. *Biomater. Sci.* **2016**, *4* (12), 1731–1741.

(168) Hou, Z.; Wu, Y.; Xu, C.; Reghu, S.; Shang, Z.; Chen, J.; Pranantyo, D.; Marimuth, K.; De, P. P.; Ng, O. T.; et al. Precisely Structured Nitric-Oxide-Releasing Copolymer Brush Defeats Broad-Spectrum Catheter-Associated Biofilm Infections in Vivo. *ACS Cent. Sci.* **2020**, *6* (11), 2031–2045.

(169) Su, Y.; Feng, T.; Feng, W.; Pei, Y.; Li, Z.; Huo, J.; Xie, C.; Qu, X.; Li, P.; Huang, W. Mussel-Inspired, Surface-Attachable Initiator for Grafting of Antimicrobial and Antifouling Hydrogels. *Macromol. Rapid Commun.* **2019**, *40* (17), 1–8.

(170) Mitra, D.; Kang, E. T.; Neoh, K. G. Polymer-Based Coatings with Integrated Antifouling and Bactericidal Properties for Targeted Biomedical Applications. *ACS Appl. Polym. Mater.* **2021**, *3* (5), 2233–2263.

(171) Xue, C. H.; Guo, X. J.; Ma, J. Z.; Jia, S. T. Fabrication of Robust and Antifouling Superhydrophobic Surfaces via Surface-Initiated Atom Transfer Radical Polymerization. *ACS Appl. Mater. Interfaces* **2015**, *7* (15), 8251–8259.

(172) Ding, X.; Yang, C.; Lim, T. P.; Hsu, L. Y.; Engler, A. C.; Hedrick, J. L.; Yang, Y. Y. Antibacterial and Antifouling Catheter Coatings Using Surface Grafted PEG-b-Cationic Polycarbonate Diblock Copolymers. *Biomaterials* **2012**, *33* (28), 6593–6603.

(173) Zhi, Z.; Su, Y.; Xi, Y.; Tian, L.; Xu, M.; Wang, Q.; Padidan, S.; Li, P.; Huang, W. Dual-Functional Polyethylene Glycol-b-Polyhexanide Surface Coating with in Vitro and in Vivo Antimicrobial and Antifouling Activities. *ACS Appl. Mater. Interfaces* **2017**, *9* (12), 10383–10397.

(174) Yang, Q.; Strathmann, M.; Rumpf, A.; Schaule, G.; Ulbricht, M. Grafted Glycopolymer-Based Receptor Mimics on Polymer Support for Selective Adhesion of Bacteria. *ACS Appl. Mater. Interfaces* **2010**, *2* (12), 3555–3562.

(175) Gu, J. S.; Yu, H. Y.; Huang, L.; Tang, Z. Q.; Li, W.; Zhou, J.; Yan, M. G.; Wei, X. W. Chain-Length Dependence of the Antifouling Characteristics of the Glycopolymer-Modified Polypropylene Membrane in an SMBR. *J. Memb. Sci.* **2009**, *326* (1), 145–152.

(176) Tankhiwale, R.; Bajpai, S. K. Preparation, Characterization and Antibacterial Applications of ZnO-Nanoparticles Coated Polyethylene Films for Food Packaging. *Colloids Surfaces B Biointerfaces* **2012**, *90* (1), 16–20.

(177) Aumsuwan, N.; McConnell, M. S.; Urban, M. W. Tunable Antimicrobial Polypropylene Surfaces: Simultaneous Attachment of Penicillin (Gram +) and Gentamicin (Gram -). *Biomacromolecules* **2009**, *10* (3), 623–629.

(178) Caro, A.; Humblot, V.; Méthivier, C.; Minier, M.; Salmain, M.; Pradier, C. M. Grafting of Lysozyme and/or Poly(Ethylene Glycol) to Prevent Biofilm Growth on Stainless Steel Surfaces. *J. Phys. Chem. B* **2009**, *113* (7), 2101–2109.

(179) Schaer, T. P.; Stewart, S.; Hsu, B. B.; Klibanov, A. M. Hydrophobic Polycationic Coatings That Inhibit Biofilms and Support Bone Healing during Infection. *Biomaterials* **2012**, *33* (5), 1245–1254.

(180) Ye, W.; Leung, M. F.; Xin, J.; Kwong, T. L.; Lee, D. K. L.; Li, P. Novel Core-Shell Particles with Poly(n-Butyl Acrylate) Cores and Chitosan Shells as an Antibacterial Coating for Textiles. *Polymer (Guildf).* **2005**, *46* (23), 10538–10543.

(181) Li, R.; Mansukhani, N. D.; Guiney, L. M.; Ji, Z.; Zhao, Y.; Chang, C. H.; French, C. T.; Miller, J. F.; Hersam, M. C.; Nel, A. E.; et al. Identification and Optimization of Carbon Radicals on Hydrated Graphene Oxide for Ubiquitous Antibacterial Coatings. *ACS Nano* **2016**, *10* (12), 10966–10980.

(182) Wei, T.; Tang, Z.; Yu, Q.; Chen, H. Smart Antibacterial Surfaces with Switchable Bacteria-Killing and Bacteria-Releasing Capabilities. *ACS Applied Materials and Interfaces*. **2017**, 37511–37523.

(183) Mi, L.; Jiang, S. Integrated Antimicrobial and Nonfouling Zwitterionic Polymers. *Angewandte Chemie - International Edition*. **2014**, 1746–1754.

(184) Yu, Q.; Cho, J.; Shivapooja, P.; Ista, L. K.; López, G. P. Nanopatterned Smart Polymer Surfaces for Controlled Attachment, Killing, and Release of Bacteria. *ACS Appl. Mater. Interfaces* **2013**, *5* (19), 9295–9304.

(185) Cheng, G.; Xue, H.; Zhang, Z.; Chen, S.; Jiang, S. A Switchable Biocompatible Polymer Surface with Self-Sterilizing and Nonfouling Capabilities. *Angew. Chemie - Int. Ed.* **2008**, *47* (46), 8831–8834.

(186) Cao, Z.; Mi, L.; Mendiola, J.; Ella-Menye, J. R.; Zhang, L.; Xue, H.; Jiang, S. Reversibly Switching the Function of a Surface between Attacking and Defending against Bacteria. *Angew. Chemie - Int. Ed.* **2012**, *51* (11), 2602–2605.

(187) Děkanovský, L.; Elashnikov, R.; Kubiková, M.; Vokatá, B.; Švorčík, V.; Lyutakov, O. Dual-Action Flexible Antimicrobial Material: Switchable Self-Cleaning, Antifouling, and Smart Drug Release. *Adv. Funct. Mater.* **2019**, *29* (31).

(188) Wu, B.; Zhang, L.; Huang, L.; Xiao, S.; Yang, Y.; Zhong, M.; Yang, J. Salt-Induced Regenerative Surface for Bacteria Killing and Release. *Langmuir* **2017**, *33* (28), 7160–7168.

(189) Qian, W.; Qiu, J.; Su, J.; Liu, X. Minocycline Hydrochloride Loaded on Titanium by Graphene Oxide: An Excellent Antibacterial Platform with the Synergistic Effect of Contact-Killing and Release-Killing. *Biomater. Sci.* **2018**, *6* (2), 304–313.

(190) Zoppe, J. O.; Ataman, N. C.; Mocny, P.; Wang, J.; Moraes, J.; Klok, H. A. Surface-Initiated Controlled Radical Polymerization: State-of-the-Art, Opportunities, and Challenges in Surface and Interface Engineering with Polymer Brushes. *Chem. Rev.* **2017**, *117* (3), 1105–1318.

(191) Ista, L. K.; Yu, Q.; Parthasarathy, A.; Schanze, K. S.; López, G. P. Reusable Nanoengineered Surfaces for Bacterial Recruitment and Decontamination. *Biointerphases* **2016**.

(192) Zhao, Z.; Ma, X.; Chen, R.; Xue, H.; Lei, J.; Du, H.; Zhang, Z.; Chen, H. Universal Antibacterial Surfaces Fabricated from Quaternary Ammonium Salt-Based Pnipam Microgels. *ACS Appl. Mater. Interfaces* **2020**.

(193) He, L.; Fullenkamp, D. E.; Rivera, J. G.; Messersmith, P. B. PH Responsive Self-Healing Hydrogels Formed by Boronate-Catechol Complexation. *Chem. Commun.* **2011**, *47* (26), 7497–7499.

(194) Nakahata, M.; Mori, S.; Takashima, Y.; Hashidzume, A.; Yamaguchi, H.; Harada, A. PH- and Sugar-Responsive Gel Assemblies Based on Boronate-Catechol Interactions. *ACS Macro Lett.* **2014**, *3* (4), 337–340.

(195) Chen, Y.; Diaz-Dussan, D.; Wu, D.; Wang, W.; Peng, Y. Y.; Asha, A. B.; Hall, D. G.; Ishihara, K.; Narain, R. Bioinspired Self-Healing Hydrogel Based on Benzoxaborole-Catechol Dynamic Covalent Chemistry for 3D Cell Encapsulation. *ACS Macro Lett.* **2018**, *7* (8), 904–908.

(196) Wu, D.; Wang, W.; Diaz-dussan, D.; Peng, Y.; Chen, Y.; Narain, R.; Hall, D. G. In Situ Forming, Dual-Crosslink Network, Self-Healing Hydrogel Enabled by a Bioorthogonal Nopoldiol − Benzoxaborolate Click Reaction with a Wide PH Range. **2019**.

(197) Hung, T.; Fu, C.; Su, C.; Chen, J.; Wu, W.; Lin, Y. Enzyme and Microbial Technology Immobilization of Cellulase onto Electrospun Polyacrylonitrile (PAN) Nanofibrous Membranes and Its Application to the Reducing Sugar Production from Microalgae. *Enzyme Microb. Technol.* **2011**, *49* (1), 30–37.

(198) Yalcinkaya, F. Surface Modification of Electrospun Nanofibrous Membranes for Oily Wastewater Separation. *RSC Adv.* **2017**, 56704–56712.

(199) Zangmeister, R. A.; Morris, T. A.; Tarlov, M. J. Characterization of Polydopamine Thin Films Deposited at Short Times by Autoxidation of Dopamine. *Langmuir* **2013**, *29* (27), 8619–8628.

(200) Münch, A. S.; Adam, S.; Fritzsche, T.; Uhlmann, P. Tuning of Smart Multifunctional Polymer Coatings Made by Zwitterionic Phosphorylcholines. *Adv. Mater. Interfaces* **2020**, *1901422* (7), 1–10.

(201) Kozak, M.; Domka, L. Adsorption of the Quaternary Ammonium Salts on Montmorillonite. *J. Phys. Chem. Solids* **2004**, *65*, 441–445.

(202) Yang, G.; Zhao, J.; Cui, L.; Song, S.; Zhang, S.; Yu, L.; Zhang, P. Tribological Characteristic and Mechanism Analysis of Borate Ester as a Lubricant Additive in Di Ff Erent Base Oils. *RSC Adv.* **2017**, *7*, 7944–7953.

(203) Spitler, E. L.; Giovino, M. R.; White, S. L.; Dichtel, W. R. A Mechanistic Study of Lewis Acid-Catalyzed Covalent Organic Framework Formation. *Chem. Sci.* **2011**, *2*, 1588–1593.

(204) Faniran, J. A.; Shurvell, H. F. Infrared Spectra of Phenylboronic Acid (Normal and Deuterated) and Diphenyl Phenylboronate. *Can. J. Chem.* **1968**, *46* (12), 2089–2095.

(205) Gengenbach, T. R.; Major, G. H.; Linford, M. R.; Easton, C. D. Practical Guides for X-Ray Photoelectron Spectroscopy (XPS): Interpreting the Carbon 1s Spectrum. *J. Vac. Sci. Technol. A* **2021**, *39* (1), 013204.

(206) G. Beamson D. Briggs. High Resolution XPS of Organic Polymers: The Scienta ESCA300 Database (Beamson, G.; Briggs, D.). *J. Chem. Educ.* **1993**, *70* (1), A25.

(207) Wang, H.; Chen, M.; Jin, C.; Niu, B.; Jiang, S.; Li, X.; Jiang, S. Antibacterial [2-(Methacryloyloxy) Ethyl] Trimethylammonium Chloride Functionalized Reduced Graphene Oxide/Poly(Ethylene- Co - Vinyl Alcohol) Multilayer Barrier Film for Food Packaging. *J. Agric. Food Chem.* **2018**, *66* (3), 732–739.

(208) Asri, L. A. T. W.; Crismaru, M.; Roest, S.; Chen, Y.; Ivashenko, O.; Rudolf, P.; Tiller, J. C.; Mei, H. C. Van Der; Loontjens, T. J. A.; Busscher, H. J. A Shape-Adaptive , Antibacterial-Coating of Immobilized Quaternary-Ammonium Compounds Tethered on Hyperbranched Polyurea and Its Mechanism of Action. *Adv. Funct. Mater.* **2014**, *24*, 346–355.

(209) Chen, Y.; Wang, W.; Wu, D.; Nagao, M.; Hall, D. G.; Thundat, T.; Narain, R. Injectable Self-Healing Zwitterionic Hydrogels Based on Dynamic Benzoxaborole-Sugar Interactions with Tunable Mechanical Properties. *Biomacromolecules* **2018**, *19* (2), 596–605.

(210) Pettignano, A.; Grijalvo, S.; Häring, M.; Eritja, R.; Tanchoux, N.; Quignard, F.; Díaz Díaz, D. Boronic Acid-Modified Alginate Enables Direct Formation of Injectable, Self-Healing and Multistimuli-Responsive Hydrogels. *Chem. Commun.* **2017**, *53* (23), 3350–3353.

(211) Chen, Y.; Diaz-Dussan, D.; Wu, D.; Wang, W.; Peng, Y. Y.; Asha, A. B.; Hall, D. G.; Ishihara, K.; Narain, R. Bioinspired Self-Healing Hydrogel Based on Benzoxaborole-Catechol Dynamic Covalent Chemistry for 3D Cell Encapsulation. *ACS Macro Lett.* **2018**, *7* (8), 904–908.

(212) Sánchez-Clemente, R.; Igeño, M. I.; Población, A. G.; Guijo, M. I.; Merchán, F.; Blasco, R. Study of PH Changes in Media during Bacterial Growth of Several Environmental Strains. In *Multidisciplinary Digital Publishing Institute Proceedings*; 2018; Vol. 2, p 1297.

(213) Marsh, P. D. Dental Plaque as a Biofilm and a Microbial Community - Implications for Health and Disease. *BMC Oral Health* **2006**, *6* (SUPPL. 1), 1–7.

(214) Chen, Y.; Diaz-Dussan, D.; Wu, D.; Wang, W.; Peng, Y.-Y.; Benozir Asha, A.; G. Hall, D.; Ishihara, K.; Narain, R. Bioinspired Self-Healing Hydrogel Based on Benzoxaborole-Catechol Dynamic Covalent Chemistry for 3D Cell Encapsulation. *ACS Macro Lett.* **2018**, *7* (8), 904–908.

(215) Cross, M. C.; Toomey, R. G.; Gallant, N. D. Protein-Surface Interactions on Stimuli-Responsive Polymeric Biomaterials. *Biomed. Mater.* **2016**, *11* (2), 022002.

(216) Nagase, K.; Kobayashi, J.; Kikuchi, A.; Akiyama, Y.; Kanazawa, H.; Okano, T. Thermally-Modulated on/off-Adsorption Materials for Pharmaceutical Protein Purification. *Biomaterials* **2011**, *32* (2), 619–627.

(217) Matsuno, R.; Ishihara, K. Integrated Functional Nanocolloids Covered with Artificial Cell Membranes for Biomedical Applications. *Nano Today* **2011**, *6* (1), 61–74.

(218) Ishihara, K.; Chen, W.; Liu, Y.; Tsukamoto, Y.; Inoue, Y. Cytocompatible and Multifunctional Polymeric Nanoparticles for Transportation of Bioactive Molecules into and within Cells. *Sci. Technol. Adv. Mater.* **2016**, *17* (1), 300–312.

(219) Joondan, N.; Jhaumeer, S.; Caumul, P.; Marie, D. E. P.; Roy, P.; Hosten, E. Colloids and Surfaces A : Physicochemical and Engineering Aspects Synthesis , Physicochemical Properties and Membrane Interaction of Novel Quaternary Ammonium Surfactants Derived from l -Tyrosine and l -DOPA in Relation to Their Antimicrobial , Hemolytic. *Colloids Surfaces A Physicochem. Eng. Asp.* **2016**, *511*, 120–134.

(220) Elder, M. J.; Stapleton, F.; Evans, E.; Dart, J. K. G. Biofilm-Related Infections in Ophthalmology. *Eye (Basingstoke)* **1995**, *9* (1), 102–109.

(221) Donelli, G. Biofilm-Based Healthcare-Associated Infections: Volume II. *Advances in Experimental Medicine and Biology* **2015**, *831*, 137–146.

(222) Dai, G.; Ai, X.; Mei, L.; Ma, C.; Zhang, G. Kill-Resist-Renew Trinity: Hyperbranched Polymer with Self-Regenerating Attack and Defense for Antifouling Coatings. *ACS Applied Materials and Interfaces* **2021**, *13* (11), 13735–13743.

(223) Voo, Z. X.; Khan, M.; Xu, Q.; Narayanan, K.; Ng, B. W. J.; Bte Ahmad, R.; Hedrick, J. L.; Yang, Y. Y. Antimicrobial Coatings against Biofilm Formation: The Unexpected Balance between Antifouling and Bactericidal Behavior. *Polymer Chemistry* **2016**, *7* (3), 656–668.

(224) Ding, X.; Yang, C.; Lim, T. P.; Hsu, L. Y.; Engler, A. C.; Hedrick, J. L.; Yang, Y. Y. Antibacterial and Antifouling Catheter Coatings Using Surface Grafted PEG-b-Cationic Polycarbonate Diblock Copolymers. *Biomaterials* **2012**, *33* (28), 6593–6603.

(225) Vaishampayan, A.; de Jong, A.; Wight, D. J.; Kok, J.; Grohmann, E. A Novel Antimicrobial Coating Represses Biofilm and Virulence-Related Genes in Methicillin-Resistant Staphylococcus Aureus. *Frontiers in Microbiology* **2018**, *9* (FEB), 1–14.

(226) Jiao, Y.; Tay, F. R.; Niu, L. na; Chen, J. hua. Advancing Antimicrobial Strategies for Managing Oral Biofilm Infections. *International Journal of Oral Science* **2019**, *11* (3), 1–11.

(227) Francolini, I.; Vuotto, C.; Piozzi, A.; Donelli, G. Antifouling and Antimicrobial Biomaterials: An Overview. *Apmis* **2017**, *125* (4), 392–417.

(228) Chen, S.; Li, L.; Zhao, C.; Zheng, J. Surface Hydration: Principles and Applications toward Low-Fouling/Nonfouling Biomaterials. *Polymer*. 2010, pp 5283–5293.

(229) Maan, A. M. C.; Hofman, A. H.; de Vos, W. M.; Kamperman, M. Recent Developments and Practical Feasibility of Polymer-Based Antifouling Coatings. *Advanced Functional Materials* **2020**, *30* (32).

(230) Zhi, Z.; Su, Y.; Xi, Y.; Tian, L.; Xu, M.; Wang, Q.; Padidan, S.; Li, P.; Huang, W. Dual-Functional Polyethylene Glycol-b-Polyhexanide Surface Coating with in Vitro and in Vivo Antimicrobial and Antifouling Activities. *ACS Applied Materials and Interfaces* **2017**, *9* (12), 10383–10397.

(231) Gu, J. S.; Yu, H. Y.; Huang, L.; Tang, Z. Q.; Li, W.; Zhou, J.; Yan, M. G.; Wei, X. W. Chain-Length Dependence of the Antifouling Characteristics of the Glycopolymer-Modified Polypropylene Membrane in an SMBR. *Journal of Membrane Science* **2009**, *326* (1), 145–152.

(232) Liang, J.; She, J.; He, H.; Fan, Z.; Chen, S.; Li, J.; Liu, B. A New Approach to Fabricate Polyimidazolium Salt (PIMS) Coatings with Efficient Antifouling and Antibacterial Properties. *Applied Surface Science* **2019**, *478* (September 2018), 770–778.

(233) Xu, G.; Liu, P.; Pranantyo, D.; Xu, L.; Neoh, K. G.; Kang, E. T. Antifouling and Antimicrobial Coatings from Zwitterionic and Cationic Binary Polymer Brushes Assembled via "Click" Reactions. *Industrial and Engineering Chemistry Research* **2017**, *56* (49), 14479–14488.

(234) Cheng, G.; Xue, H.; Zhang, Z.; Chen, S.; Jiang, S. A Switchable Biocompatible Polymer Surface with Self-Sterilizing and Nonfouling Capabilities. *Angewandte Chemie - International Edition* **2008**, *47* (46), 8831–8834.

(235) Wei, T.; Zhan, W.; Yu, Q.; Chen, H. Smart Biointerface with Photoswitched Functions between Bactericidal Activity and Bacteria-Releasing Ability. *ACS Applied Materials and Interfaces* **2017**, *9* (31), 25767–25774.

(236) Mi, L.; Jiang, S. Integrated Antimicrobial and Nonfouling Zwitterionic Polymers. *Angewandte Chemie - International Edition*. 2014, pp 1746–1754.

(237) Tankhiwale, R.; Bajpai, S. K. Preparation, Characterization and Antibacterial Applications of ZnO-Nanoparticles Coated Polyethylene Films for Food Packaging. *Colloids and Surfaces B: Biointerfaces* **2012**, *90* (1), 16–20.

(238) Aumsuwan, N.; McConnell, M. S.; Urban, M. W. Tunable Antimicrobial Polypropylene Surfaces: Simultaneous Attachment of Penicillin (Gram +) and Gentamicin (Gram -). *Biomacromolecules* **2009**, *10* (3), 623–629.

(239) Caro, A.; Humblot, V.; Méthivier, C.; Minier, M.; Salmain, M.; Pradier, C. M. Grafting of Lysozyme and/or Poly(Ethylene Glycol) to Prevent Biofilm Growth on Stainless Steel Surfaces. *Journal of Physical Chemistry B* **2009**, *113* (7), 2101–2109.

(240) Schaer, T. P.; Stewart, S.; Hsu, B. B.; Klibanov, A. M. Hydrophobic Polycationic Coatings That Inhibit Biofilms and Support Bone Healing during Infection. *Biomaterials* **2012**, *33* (5), 1245–1254.

(241) Cado, G.; Aslam, R.; Séon, L.; Garnier, T.; Fabre, R.; Parat, A.; Chassepot, A.; Voegel, J. C.; Senger, B.; Schneider, F.; Frère, Y.; Jierry, L.; Schaaf, P.; Kerdjoudj, H.; Metz-Boutigue, M. H.; Boulmedais, F. Self-Defensive Biomaterial Coating against Bacteria and Yeasts: Polysaccharide Multilayer Film with Embedded Antimicrobial Peptide. *Advanced Functional Materials* **2013**, *23* (38), 4801–4809.

(242) Chen, D.; Wu, M.; Li, B.; Ren, K.; Cheng, Z.; Ji, J.; Li, Y.; Sun, J. Layer-by-Layer-Assembled Healable Antifouling Films. *Advanced Materials* **2015**, *27* (39), 5882–5888.

(243) Wang, Z.; Fei, G.; Xia, H.; Zuilhof, H. Dual Water-Healable Zwitterionic Polymer Coatings for Anti-Biofouling Surfaces. *Journal of Materials Chemistry B* **2018**, *6* (43), 6930–6935.

(244) Li, L.; Yan, B.; Yang, J.; Chen, L.; Zeng, H. Novel Mussel-Inspired Injectable Self-Healing Hydrogel with Anti-Biofouling Property. *Advanced Materials* **2015**, *27* (7), 1294–1299.

(245) Wang, Z.; Yi, B.; Wu, M.; Lv, D.; He, M. L.; Liu, M.; Yao, X. Bioinspired Supramolecular Slippery Organogels for Controlling Pathogen Spread by Respiratory Droplets. *Advanced Functional Materials* **2021**, *31* (34), 1–10.

(246) Sun, D.; Chong, Y. B.; Chen, K.; Yang, J. Chemically and Thermally Stable Isocyanate Microcapsules Having Good Self-Healing and Self-Lubricating Performances. *Chemical Engineering Journal* **2018**, *346* (April), 289–297.

(247) Wu, G.; An, J.; Tang, X. Z.; Xiang, Y.; Yang, J. A Versatile Approach towards Multifunctional Robust Microcapsules with Tunable, Restorable, and Solvent-Proof Superhydrophobicity for Self-Healing and Self-Cleaning Coatings. *Advanced Functional Materials* **2014**, *24* (43), 6751–6761.

(248) Idumah, C. I.; Obele, C. M.; Emmanuel, E. O.; Hassan, A. Recently Emerging Nanotechnological Advancements in Polymer Nanocomposite Coatings for Anti-Corrosion, Anti-Fouling and Self-Healing. *Surfaces and Interfaces* **2020**, *21* (May), 100734.

(249) Yanagisawa, Y.; Nan, Y.; Okuro, K.; Aida, T. Mechanically Robust, Readily Repairable Polymers via Tailored Noncovalent Cross-Linking. *Science* **2018**, *359* (6371), 72–76.

(250) Perera, M. M.; Ayres, N. Dynamic Covalent Bonds in Self-Healing, Shape Memory, and Controllable Stiffness Hydrogels. *Polymer Chemistry* **2020**, *11* (8), 1410–1423.

(251) M. Kushner, A.; D. Vossler, J.; A. Williams, G.; Guan, Z. A Biomimetic Modular Polymer with Tough and Adaptive Properties. *Journal of the American Chemical Society* **2009**, *131* (25), 8766–8768.

(252) Sun, J. Y.; Zhao, X.; Illeperuma, W. R. K.; Chaudhuri, O.; Oh, K. H.; Mooney, D. J.; Vlassak, J. J.; Suo, Z. Highly Stretchable and Tough Hydrogels. *Nature 2012 489:7414* **2012**, *489* (7414), 133–136.

(253) Asha, A. B.; Chen, Y.; Narain, R. Bioinspired Dopamine and Zwitterionic Polymers for Non-Fouling Surface Engineering. *Chemical Society Reviews* **2021**, *50* (20), 11668–11683.

(254) Menzies, D. J.; Ang, A.; Thissen, H.; Evans, R. A. Adhesive Prebiotic Chemistry Inspired Coatings for Bone Contacting Applications. *ACS Biomaterials Science and Engineering* **2017**, *3* (5), 793–806.

(255) Toh, R. J.; Evans, R.; Thissen, H.; Voelcker, N. H.; D'ischia, M.; Ball, V. Deposition of Aminomalononitrile-Based Films: Kinetics, Chemistry, and Morphology. *Langmuir* **2019**, *35* (30), 9896–9903.

(256) Chen, W. H.; Liao, T. Y.; Thissen, H.; Tsai, W. B. One-Step Aminomalononitrile-Based Coatings Containing Zwitterionic Copolymers for the Reduction of Biofouling and the Foreign Body Response. *ACS Biomaterials Science and Engineering* **2019**, *5* (12), 6454–6462.

(257) Liao, T. Y.; Easton, C. D.; Thissen, H.; Tsai, W. B. Aminomalononitrile-Assisted Multifunctional Antibacterial Coatings. *ACS Biomaterials Science and Engineering* **2020**, *6* (6), 3349–3360.

(258) Kabir, A.; Dunlop, M. J.; Acharya, B.; Bissessur, R.; Ahmed, M. Water Recycling Efficacies of Extremely Hygroscopic, Antifouling Hydrogels. *RSC Advances* **2018**, *8* (66), 38100–38107.

(259) Thissen, H.; Koegler, A.; Salwiczek, M.; Easton, C. D.; Qu, Y.; Lithgow, T.; Evans, R. A. Prebiotic-Chemistry Inspired Polymer Coatings for Biomedical and Material Science Applications. *NPG Asia Materials* **2015**, *7* (11), 1–9.

(260) Ma, W.; Yang, P.; Li, J.; Li, S.; Li, P.; Zhao, Y.; Huang, N. Immobilization of Poly(MPC) Brushes onto Titanium Surface by Combining Dopamine Self-Polymerization and ATRP: Preparation, Characterization and Evaluation of Hemocompatibility in Vitro. *Applied Surface Science* **2015**, *349*, 445–451.

(261) Cheng, Q.; Asha, A. B.; Liu, Y.; Peng, Y. Y.; Diaz-Dussan, D.; Shi, Z.; Cui, Z.; Narain, R. Antifouling and Antibacterial Polymer-Coated Surfaces Based on the Combined Effect of Zwitterions and the Natural Borneol. *ACS Applied Materials and Interfaces* **2021**, *13* (7), 9006–9014.

(262) Hwang, G.; Kang, S.; El-Din, M. G.; Liu, Y. Impact of an Extracellular Polymeric Substance (EPS) Precoating on the Initial Adhesion of Burkholderia Cepacia and Pseudomonas Aeruginosa. *Biofouling* **2012**, *28* (6), 525–538.

(263) Blair, J. M. A.; Richmond, G. E.; Piddock, L. J. V. Multidrug Efflux Pumps in Gram-Negative Bacteria and Their Role in Antibiotic Resistance. *Future microbiology* **2014**, *9* (10), 1165–1177.

(264) Graves, J. L.; Tajkarimi, M.; Cunningham, Q.; Campbell, A.; Nonga, H.; Harrison, S. H.; Barrick, J. E. Rapid Evolution of Silver Nanoparticle Resistance in Escherichia Coli. *Frontiers in Genetics* **2015**, *5* (FEB), 42.

(265) Liu, S.; Guo, W. Anti-Biofouling and Healable Materials: Preparation, Mechanisms, and Biomedical Applications. *Advanced Functional Materials* **2018**, *28* (41), 1800596.

(266) Zhuo, Y.; Xiao, S.; Håkonsen, V.; Li, T.; Wang, F.; He, J.; Zhang, Z. Ultrafast Self-Healing and Highly Transparent Coating with Mechanically Durable Icephobicity. *Applied Materials Today* **2020**, *19*, 100542.

(267) Deng, Z.; Bouchékif, H.; Babooram, K.; Housni, A.; Choytun, N.; Narain, R. Facile Synthesis of Controlled-Structure Primary Amine-Based Methacrylamide Polymers via the Reversible Addition-Fragmentation Chain Transfer Process. *Journal of Polymer Science Part A: Polymer Chemistry* **2008**, *46* (15), 4984–4996.